Copyright Warning & Restrictions

The copyright law of the United States (Title 17, United States Code) governs the making of photocopies or other reproductions of copyrighted material.

Under certain conditions specified in the law, libraries and archives are authorized to furnish a photocopy or other reproduction. One of these specified conditions is that the photocopy or reproduction is not to be "used for any purpose other than private study, scholarship, or research." If a, user makes a request for, or later uses, a photocopy or reproduction for purposes in excess of "fair use" that user may be liable for copyright infringement,

This institution reserves the right to refuse to accept a copying order if, in its judgment, fulfillment of the order would involve violation of copyright law.

Please Note: The author retains the copyright while the New Jersey Institute of Technology reserves the right to distribute this thesis or dissertation

Printing note: If you do not wish to print this page, then select "Pages from: first page # to: last page #" on the print dialog screen

ABSTRACT

SYNTHETIC APPROACHES TO THE UNDERSTANDING OF DNA NUCLEOBASE METHYLATION

By
Jagruti Rana

DNA methylation is a major source of genetic variation and cancer. Methylation occurs when nucleophilic DNA bases react with methylating agent methyl methanesulfonate (MMS), dimethyl sulfate (DMS), *N*-methyl-*N*-nitrosourea (MNU), *N*-methyl-*N*′-nitro-*N*-nitrosoguanidine (MNNG), etc. N7-methyl-2′-deoxyguanosine (N7-methyl-dG, or ^{7Me}dG) adduct is the most abundant DNA methylation products for most methylating agents. DNA polymerase actions on ^{7Me}dG are difficult to study due to its instability against ring-opening hydrolysis and deglycosylation. Oligonucleotides containing a single chemical adduct of ^{7Me}dG cannot be chemically synthesized. In addition, ^{7Me}dG is unstable in vivo due to the presence of DNA repair enzymes. This work explores the possibility of using stable analogues of N7-methyl-dG to study the polymerase bypass. The chemical synthesis of N7-methyl-9-deaza-dG (^{7Me9C}dG) has been developed and the nucleoside has been successfully incorporated into oligonucleotides. Thermal melting studies show that replacement of dG by ^{7Me9C}dG only slightly decreases DNA duplex stability. Replication of the DNA templates containing ^{7Me9C}dG and the related 7-methyl-7-deaza-dG (^{7Me7C}dG) and 7-deaza-dG (^{7C}dG) by Klenow fragment of *E. coli* DNA polymerase I is examined. The misincorporation frequencies on the ^{7Me9C}dG, ^{7Me7C}dG, and ^{7C}dG templates are comparable to the dG template, although the 7-methyl group slows down the turnover rate of the polymerase when dCTP is incorporated. The stability of ^{7Me9C}dG and ^{7Me7C}dG against the actions of formamidopyrimidine DNA *N*-glycosylase (Fpg) and human

alkyladenine DNA Glycosylase (hAAG) are also studied. ^{7Me9C}dG is stable in the presence of both enzymes. In contrast, ^{7Me7C}dG is cleaved by Fpg, and possibly by hAAG but in an extremely slow rate. This work demonstrates that ^{7Me9C}dG is a better analogue than ^{7Me7C}dG for future cellular studies.

Epigenetic mechanisms regulate the expression of genetic information. A major epigenetic event is DNA cytosine methylation, which is catalyzed by the DNA methyltransferases (DNMTs). Among different mammalian DNMTs, DNMT1 is the most abundant and active, and plays multiple roles in carcinogenesis, embryonic development, and several other biological functions. Reactivation of silenced tumor suppressor genes by DNMT inhibitors (DNMTi) is provides a relatively new approach to cancer therapy. A couple of irreversible nucleoside DNMT inhibitors have been developed clinically. However, due to their low specificity and high cellular toxicity, there is a clear need for the development of reversible inhibitors. S-adenosyl homocysteine (SAH) is a known strong inhibitor of DNA methyltransferases. Based on the crystal structure of SAH bound to human DNMT1-DNA complex, a series of transition state analogues have been designed to occupy the SAH binding site and the cytosine binding site simultaneously. These analogues have been successfully synthesized from adenosine using a modular approach. Inhibition of DNMT1 by these analogues will be studied in the future.

SYNTHETIC APPROACHES TO THE UNDERSTANDING OF DNA NUCLEOBASE METHYLATION

By
Jagruti Rana

A Dissertation
Submitted to the Faculty of
New Jersey Institute of Technology
in Partial Fulfillment of the Requirements for the Degree of
Doctor of Philosophy in Chemistry

Department of Chemistry and Environmental Science

January 2015

.

APPROVAL PAGE
SYNTHETIC APPROACHES TO THE UNDERSTANDING OF DNA NUCLEOBASE METHYLATION

Jagruti Rana

Dr. Haidong Huang, Dissertation Advisor — Date
Assistant Professor of Chemistry and Environmental Science, NJIT

Dr. Somenath Mitra, Committee Member — Date
Distinguished Professor of Chemistry and Environmental Science, NJIT

Dr. Edgardo Farinas, Committee Member — Date
Associate Professor of Chemistry and Environmental Science, NJIT

Dr. Tamara Gund, Committee Member — Date
Professor of Chemistry and Environmental Science, NJIT

Dr. Pradyot Patnaik, Committee Member — Date
Consultant, Radiance, Burlington, New Jersey

BIOGRAPHICAL SKETCH

Author: Jagruti Rana

Degree: Doctor of Philosophy

Date: January 2015

Undergraduate and Graduate Education:

- Doctor of Philosophy in Chemistry
  New Jersey Institute of Technology, Newark, NJ, 2015

- Bachelor of Education,
  South Gujarat University,Gujarat, India, 2006

- Master of Science in Chemistry,
  South Gujarat University,Gujarat, India, 2004

- Bachelor of Science in Chemistry,
  South Gujarat University, Gujarat, India, 2002

Major: Chemistry

Publications:

Rana, J., and Huang, H. (2013) Actions of the Klenow fragment of DNA polymerase I and Some DNA Glycosylases on Chemically Stable Analogues of N7-methyl-2′-deoxyguanosine, *Bioorganic & Medicinal Chemistry 21*, 6886-6892.

Patel, S., Rana, J., Roy, J., and Huang, H. (2012) Cleavage of Pyrene-Stabilized RNA Bulge Loops by Trans-(+/-)-cyclohexane-1,2-diamine, *Chemistry Central Journal 6*, 3.

Presentations:

Rana, J., and Huang, H. (April 2014) Chemically Stable Analogues of 7-Methyl-2'-Deoxyguanosine: Synthesis, Polymerase Replication, and Thermal Stability Studies , 59th Annual NJ Academy of Science Meeting, Raritan Valley Community College, Branchburg, NJ.

Rana, J., and Huang, H. (February 2014) Chemically Stable Analogues of 7-Methyl-2'-Deoxyguanosine: Synthesis, Polymerase Replication, and Thermal Stability Studies, Female Research Showcase hosted by Society of Women Engineers, New Jersey Institute of Technology, Newark, NJ.

Rana, J., Gao, X., and Huang, H. (November 2013) Polymerase Bypass of Chemically Stable Analogues of N7-Alkylguanine, the Most Abundant DNA Alkylation Damage Products, 9th Annual Graduate Student Research Day, New Jersey Institute of Technology, Newark,NJ.

Rana, J., and Huang, H. (June 2013) Chemically Stable Analogues of 7-Methyl-2'-Deoxyguanosine: Synthesis, Polymerase Replication, and Stability against Deglycosylation Action of Base-Excision-Repair Enzymes, The Chemical Biology Discussion Group Year-End Symposium, The New York Academy of sciences (NYAS), New York.

Rana, J., and Huang, H. (November 2012) Chemically Stable Analogues of 7-Methyl-2'-Deoxyguanosine : Synthesis, Polymerase Replication and Thermal Stability Studies, 8th Annual Graduate Student Research Day, New Jersey Institute of Technology, Newark,NJ.

Rana, J., Roy, J., Patel, M., and Huang, H. (April 2012) Rational Design of DNA Aptamer Sensors for Adenosine and 8-Oxoguanine, 57th Annual NJ Academy of Science, Meeting, Seton Hall University, South Orange, NJ.

Rana, J., Roy, J., Patel, M., and Huang, H. (March 2012) Rational Design of DNA Aptamer Sensors for Adenosine and 8-Oxoguanine., 243rd ACS National Meeting & Exposition, San Diego, CA.

This kept me going:

They all attain perfection when they find joy in their work.
In Hindi: जब वे अपने कार्य में आनंद खोज लेते हैं तब वे पूर्णता प्राप्त करते हैं
- Shrimad Bhagavad Gita

To my loving husband, Snehal
For his love, support, invaluable patience, and
encouragement throughout the process of my studies.
THANK YOU. You believed in me even when I did not believe in myself.

To my loving parents: Dhansukhbhai and Urmilaben
For their unconditional love and support.
Thanks for being a constant motivational source to me.

To my sweet sisters: Manisha, Hetal
For supporting me and encouraging me with their best wishes.

To my caring brother-in-law, Mayank
For standing up by our family through the good times and bad.

To my loving parents-in-law: Ishverbhai and Kusumben
For supporting me and being patient.

To my beautiful daughter, Prisha
For being my little cheerleader.
We did it!

This thesis is dedicated to all of you, for your motivation, love, and for keeping my life in balance.

ACKNOWLEDGMENT

A major research project like this is never the work of anyone alone. The contributions of many different people, in their different ways, have made this possible. I would like to extend my appreciation especially to the following.

This thesis would not have been possible without the invaluable guidance and support of my advisor Dr. Haidong Huang. I offer my sincerest gratitude to him for his patience, motivation, enthusiasm, and immense knowledge as well as his pain-staking effort in proof reading the drafts, are greatly appreciated. I could not have imagined having a better advisor and friendlier mentor for my doctoral study. I am also very grateful to Dr. Somenath Mitra, Dr. Edgardo Farinas, Dr. Tamara Gund and Dr. Pradyot Patnaik for their contributions as members of my dissertation committee and providing insightful comments.

My sincere thanks also go to Dr. Venanzi Carol for her valuable support as an academic advisor. My sincere thanks go to Prof. Willis B Hammond for allowing me to use Hydrogentaion apparatus in his lab. One more time I would like to thank Dr. Tamara Gund for allowing me to use her lab during course of my study.

I am also thankful to Ms. Clarisa Gonzalez-Lenahan, Associate Director of graduate studies, for her invaluable help in the thesis review.

My appreciation also goes to the Department of Chemistry and Environmental Science for offering me Teaching Assistantship. Additionally, I would like to give thanks Dr. Chaudhery Hussain, Dr. Pin Gu, Yogesh Gandhi, the Late Gayle Katz, Genti Price for their assistance during my study and Dr.Gulotta for her valuable guidance and support

during my teaching assistantship at NJIT. I am grateful for the financial, academic and technical support from New Jersey Institute of Technology.

Last, but by no means least I would thank my fellow labmates Peter, Xun and Rui, also my past labmates Shanshan, Jyoti, Rajni, Mayur, Meng and other lab members for their continual support and encouragement throughout my study. I owe a lot to my friends: Kajal, Megha, Jalpa, Hemant,Tripura for their help and emotional support. Finally, I would especially like to thank my beloved husband if it weren't for his continued love and support, I'm not so sure that I wouldn't be where I am today. Finally, thanks to my grandma, the Late Gajaraben Rana who taught me the important lessons of life, Sarojmashi, my babysitter Meenaben, my nieces, nephews, all my friends and family members for their undying love and support.

Thank God for the wisdom and perseverance that he has been bestowed upon me during this research project, and indeed, throughout my life: "I can do everything through him who gives me strength."

TABLE OF CONTENTS

TABLE OF CONTENTS
(Continued)

TABLE OF CONTENTS
(Continued)

LIST OF TABLES

LIST OF FIGURES

LIST OF FIGURES
(Continued)

LIST OF SCHEMES

LIST OF ABBREVIATIONS

DNA	Deoxyribonucleic acid
^{7C}dG	7-deaza-2'-deoxyguanosine
DNMT	DNA methyltransferase
MMS	Methyl methanesulfonate
DMS	Dimethyl sulfate
BER	Base Excision Repair
N7-Me-G	N7-methylguanine
^{7Me}dG	N7-methyl-deoxyguanine
O6-Me-G	O6-methylguanine
SAM	*S*-adenosylmethionine
DNMT	DNA methyltransferase
^{7Me9C}dG	N7-methyl-9-deaza-dG
^{7Me7C}dG	7-methyl-7-deaza-dG
DMF	N, N-dimethylformamide (Solvent)
dmf	N, N-dimethylformamide (Protecting group)
DBU	Diazabicyclo[5.4.0]undec-7-ene
DCM	Dichloromethane
MMS	Methyl methanesulfonate
DMS	Dimethyl sulfate

LIST OF ABBREVIATIONS
(Continued)

MNU	*N*-methyl-*N*-nitrosourea
MNNG	*N*-methyl-*N*′-nitro-*N*-nitrosoguanidine
Fpg	formamidopyrimidine DNA *N*-glycosylase
hAAG	human alkyladenine DNA Glycosylase
SAH	S-adenosyl homocysteine
DNMTi	DNMT inhibitors
MeC	5-methylcytosine
AP	Apurinic or abasic site
FAPY	Formamidopyrimidine
Kf	Klenow fragment
DBU	1,8-Diazabicyclo[5.4.0]undec-7-ene
THF	Tetrahydrofuran
dNTPs	deoxynucleoside 5′-triphosphates
Pol I	DNA polymerase I
Fam	Carboxyfluorescein
PAGE	Polyacrylamide gel electrophoresis
IBX	2-iodoxybenzoic acid
TEA	Triethylamine
DMAP	4-Dimethylaminopyridine
mCPBA	*meta*-Chloroperoxybenzoic acid

CHAPTER 1

GENERAL INTRODUCTION

1.1 DNA Damage and Mutation

Deoxyribonucleic acid (DNA) is a molecule that encodes the genetic instructions used in each living cell; its integrity and stability are essential to life. The sequence of bases in the interior of DNA double helix constitutes the genetic code that is critically important for all organisms. Each strand is comprised of a sugar-phosphate backbone and attached bases, and is bound to a complementary strand by non-covalent hydrogen bonding and stacking interactions. The bases are adenine (A), thymine (T), cytosine (C) and guanine (G), where A and T are paired together by two hydrogen bonds and G and C are paired together by three hydrogen bonds (Figure 1.1). The chemical view of DNA acknowledges the unique shape of each base and position of the functional groups that distinguish the four 'letters' of the alphabet. The twisting of the double helix results in the DNA having two distinct grooves, the major and minor grooves. The major groove is shallow and wide and this is where many proteins and enzymes interact with DNA. The minor groove is the deep and narrower groove. Chemical modifications on DNA can change the shape, electrostatics, or conformer distribution of the duplex. These changes enable enzymes to specifically recognize chemical modifications. This type of specific molecular recognition has a profound implication for DNA damage repair, gene mutation, and epigenetic control.

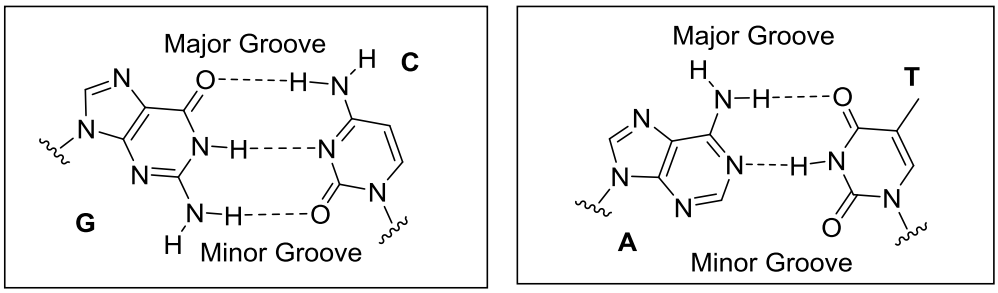

Figure 1.1 DNA base pairing (G with C and A with T), and the major and minor grooves.

Cellular DNA is constantly subjected to modifications by aging processes, environmental influences, and lifestyle factors such as smoking- or diet-induced biochemical alterations to DNA. Frequently, these lead to DNA lesions. Although DNA lesions play an essential role in the formation of cancer via carcinogens, it is also one of the major mechanisms used for the treatment of cancer via chemotherapeutic agents and radiation therapy. When chemotherapeutic agents are used for the treatment of cancer, the biological end points can lead to either a positive clinical outcome (killing the cancer cells) or a negative outcome (mutations leading to secondary cancers from the initial treatment). This mixed cytotoxic and genotoxic effects were observed in the early development of chemotherapeutic agents such as Dacarbazine and Procarbazine.[1] The determining factor on whether the damage will lead to cell death or mutations is the processing of the damage by the cell. DNA damages and mutations differ in fundamental ways. Damages are physical irregularities in the DNA, such as the formation of DNA adducts and single- and double-strand breaks. They also include the formation of mismatched nucleobases arising from erroneous replication of undamaged nucleosides. Because damage can be recognized enzymatically, they can be correctly repaired if redundant information is available. If damage remains in a gene, it can prevent

transcription of the gene, and thus production of a protein or it can be incorrectly replicated or transcribed, causing mutations. On the other hand, a mutation is a change in the base sequence of the genetic material and is not enzymatically recognizable at the DNA level once the base change is present in both strands. Mutations can be caused by poor replication of damaged DNA or undamaged DNA, although the error rate on damaged DNA is much higher. Mutations in a cell can cause alterations in protein function or regulation. They are replicated when the cell replicates. In a population of cells, mutant cells will increase or decrease in frequency according to the effects of the mutation on the ability of the cell to survive and reproduce.

Therefore, although distinctly different from each other, DNA damages and mutations are closely related. Numerous DNA lesions have been identified, including covalent modifications of nucleobases with chemicals, depurination from the backbone of DNA, oxidative damage on deoxyribose, and subsequent generation of DNA strand interruption resulting from depurination and sugar oxidative damage.[2] Naturally occurring DNA damages arise more than 60,000 times per day per mammalian cell.[2] Fortunately, our cells have evolved powerful mechanisms to detect and repair the various types of damage that can occur to DNA. Whether this damage is caused by chemical reactions or by errors in replication of undamaged nucleosides, it is repaired by one of the three excision repair pathways: nucleotide excision repair (NER), base excision repair (BER), and DNA mismatch repair (MMR). BER is responsible primarily for removing small, non-helix-distorting base lesions from the genome, for example, alkylation damage such as the formation of N7-methylguanine (N7-Me-G), N3-methyladenine (N3-Me-A) and O6-Methylguanine (O6-Me-G), oxidative damage such as 8-oxoguanine (OG)(Figure

1.2).[2] The related nucleotide excision repair pathway repairs bulky helix-distorting lesions. If remaining unrepaired, damaged bases could otherwise cause mutations by mispairing during replication or lead to strand breaks in DNA. DNA mismatch repair is a system for recognizing and repairing erroneous insertion, deletion, and mis-incorporation of bases that arise during DNA replication and recombination.

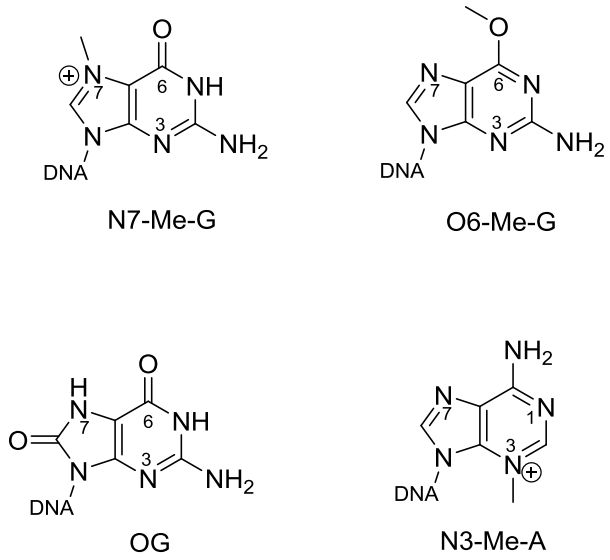

Figure 1.2 Structures of DNA base lesions.

During the cell cycle, checkpoint mechanisms ensure that cellular DNA is intact before permitting DNA replication and cell division to occur. Failures in these checkpoints can lead to an accumulation of damage, which in turn leads to mutations or epigenetic alterations.[3] Both of these types of alteration can be replicated and passed on to subsequent cell generations. These alterations can change gene function or regulation of gene expression and possibly contribute to progression to diseases such as cancer.

Among them, the biological effects of DNA methylation have long been an interest of researchers, especially those on the formation of cancers.

1.2 DNA Methylation

Humans are exposed to methylating agents in daily life.[4] The attack on DNA by these electrophilic methylating agents can lead to various types of lesions on the heterocyclic bases or backbone (Figure 1.3). Most of these resulting adducts are mutagenic or cytotoxic. The nucleophilicities of different reaction sites in DNA have been well studied. The exocyclic amino groups of guanine, cytosine, and adenine are poor nucleophiles in methylation reactions. Although each ring nitrogen and exocyclic oxygen is potentially capable of acting as a nucleophile, their reactivity towards electrophiles substantially varies by position and whether the DNA is single- or double-stranded. The most reactive sites of nonenzymatic DNA methylation (see next paragraph) are the ring nitrogen's of purine bases. Among them, the N7 position of guanine is the most nucleophilic site.[5] Molecular electrostatic potentials of the nucleophilic sites on the bases and base pairs showed that the N7 position of guanine possesses the highest negative electrostatic potential in DNA.[6] In double-stranded DNA, O6-guanine and N3-adenine have the next highest potential, followed by N3-guanine, O2-cytosine, N7-adenine, O4-thymine and O2-thymine.[6] The negative electrostatic potential is larger on the major groove for a guanine:cytosine base pair, whereas it is larger on the minor groove for an adenine: thymine base pair.

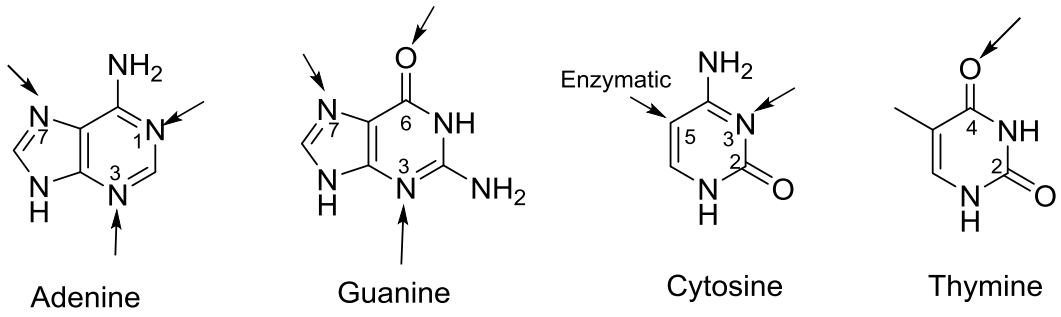

Figure 1.3 Methylation patterns of the DNA bases. (The arrows indicate methylation sites.[4])

In single-stranded DNA, it is worth noting that N3-cytosine has a similar negative electrostatic potential to that of N7-guanine, while N1-adenine has a similar potential to that of O6-guanine.[6] N1-adenine and N3-cytosine have a reactivity characteristic of amidine groups due to the adjacent amino groups on the neighboring carbons. These two positions are protected by hydrogen bonding in double-stranded DNA (dsDNA) but are quite nucleophilic in single stranded DNA (ssDNA) due to the absence of hydrogen bonding participation. The pKa's of these two nitrogen sites are 4.1 and 4.5 in ssDNA, which are higher than that of N7-guanine.[7]

Consideration of electrostatic potentials and steric hindrances help in part explains the reaction preferences seen with methylating agents, but the type of agents also influences the distribution of adducts. Methyl methanesulfonate (MMS), dimethyl sulfate (DMS), *N*-methyl-*N*-nitrosourea (MNU), and *N*-methyl-*N*′-nitro-*N*-nitrosoguanidine (MNNG) have been used extensively to study the chemical and biological effects of methylation. Understanding of the distribution is important for the evaluation of methylating outcome, as different lesions also have different mutagenic and cytotoxic effects. For example, it was observed that N7-methyl-dG (^{7Me}dG) was the major adduct

when DNA was exposed to all the above methylating agents.[8] However, the reactions occur through two different pathways: the S_N1 (unimolecular nucleophilic substitution) and the S_N2 (biomolecular nucleophilic substitution) pathways. (Figure 1.3); The S_N1 type methylating agents such as MNU and MNNG, also attack on the oxygen atoms on DNA bases to give a significant amount of O6-methylguanine (O6-Me-G) and a small amount of O4-methylthymine (O4-Me-T).[9] The S_N2 type methylating agents such as MMS and DMS generate overwhelmingly N7-Me-G.[9] Experimental data show that treating dsDNA with MMS (S_N2 type methylating agent) produced 83 % of N7-Me-G whereas MNU (S_N1 type methylating agent) produced 67 % of N7-Me-G.[4] The more significant difference in reactivity between MMS and MNU lies in the proportion of oxygen adducts. In addition to N7-Me-G, MMS produced 11% N3-methyladenine (N3-Me-A) and 0.3% O6-Me-G, whereas MNU produced 12% N3-Me-A and 7% O6-Me-G.[10] The remaining base positions N1-adenine, N7-adenine, N1-guanine, N3-guanine, N3-cytosine, O2-cytosine, N3-thymine, O2-thymine, and O4-thymine combined comprise <5% of the adduct burden in dsDNA produced by MMS or MNU.[10]

The events of human DNA methylation in daily lives originate from a wide variety of sources, including foods, beverages, tobacco, cosmetics, and industrial products.[11] Detailed understanding of the biochemical fate of methylation adducts becomes extremely important. Although the N7-position is the major site of methylation, compared to many other DNA adducts, N7-guanine adducts are chemically unstable with half lives in dsDNA ranging from as little as 2 h to 150 h.[12] The instability of N7-guanine adducts is created by the formal placement of an additional positive charge on the guanine ring system.[4] Although this instability can eventually result in DNA strand break,

which leads to cytotoxicity, numerous studies have suggested that N-methyl-G itself is not very mutagenic. In contrast, O-alkylations (e.g., O6-alkylguanine and O4-alkylthymidine) are highly mutagenic based on a variety of solid evidence.[13] Nevertheless, we chose to study N7-methyl-dG (^{7Me}dG) since direct observation of the nonmutagencity of N7-methyl-dG is lacking at the molecular level in vitro due to its instability. N7-guanine adducts have been classified as nonmutagenic based on the speculation that the N7-position does not participate in Watson-Crick base pairing.[14] However, this information can only be verified experimentally by the study of how DNA polymerases process the damage which is an essential step in the eventual biological endpoint of the damage. Because of its inherent instability ^{7Me}dG has been unable to be chemically synthesized and incorporated into oligonucleotide substrates suitable for DNA polymerase assays. Using the stable analogues of ^{7Me}dG, we have developed a strategy to generate models of ^{7Me}dG-containing substrates, which are suitable for the study of their interactions with DNA polymerases. This is the focus of my first project.

1.3 DNA Methylation and Epigenetics

In contrast to exogeneous agents, methylating agents also exist endogenously inside cells; for instance, *S*-adenosylmethionine(SAM), a methyl donor for many cellular reactions, has been shown to produce methylation products such as epigenetic DNA modification 5-methylcytosine (MeC). There are over 200 different types of cells in the human body. Each type maintains a unique cellular identity represented by the specific sets of genes they transcribe. Because the genetic material in each of these cells is essentially identical, there must be strict regulation of gene expression in each cell within

the human body. This transcriptional regulation is carried out by controlling the accessibility to genes. This layer of control is achieved by the packaging of DNA into particular arrangements. DNA is wrapped around proteins called histones, which are structurally organized and condensed into chromatin. Histone proteins can be modified, and these modifications serve as important regulators in the transcription of necessary genes throughout the life cycle of an organism. In mammals, the methylation on specific sites of DNA called CpG islands is an additional method of transcriptional control. In nucleic acid chemistry, adjacent nucleotide pairings are sometimes referred to in an NpN fashion, where N is the base and p is the phosphodiester bond; thus, CpG is the designation given to cytosine phospho guanine. The frequency of the CpG dinucleotide is very low (or rather, sporadic) in the human genome. It has been estimated that genomic DNA consists of about 10% CpG dinucleotides, which are unevenly distributed between bulk DNA and CpG islands.[15] Histone modifications and CpG island methylation are collectively called epigenetic; a term defined as heritable changes in gene expression that occur without a change in the DNA sequence.

Previously, scientists have attributed a person phenotype's characteristics based solely on the composition of the persons genomic DNA. It is through the genetic composition and alterations that we have studied the neoplastic evolution and were confounded to the idea that cancer was mainly a disease of genetics. Recently, the study of external influences on the DNA has come to question this idea in favor of a much larger complex mechanism which involves the abnormal epigenetic control. Epigenetic control at the chromatin level is essential for all eukaryotic organisms, and is especially important in multicellular organisms to organize key biological processes such as

differentiation, imprinting, X-chromosome inactivation and aging. Cellular differentiation is the best example of epigenetic changes. All multi-cellular organisms, including animals originate from a single cell after fertilization of an egg by a sperm. Therefore all cells in a given organism will have the same genome, but during fetal development each cell will gain a specific set of epigenetic marks. DNA methylation is such an epigenetic mark that stably regulates cell differentiation. While uncontrolled cell differentiation is a character of cancer cells, understanding of the relationship between DNA methylation regulation and cancer formation becomes critical in elucidating this complex mechanism.

Uncontrolled differentiation is often a result of silenced cancer-suppressor genes. CpG islands are normally not methylated, however, if a CpG island within a promoter becomes methylated, the gene associated with the promoter is permanently silenced, and this silencing can be transmitted through mitosis. This means that CpG island methylation is an epigenetic means of inheritance. So far, the generally accepted mechanism of DNA methylation in regulating gene expression and gene silencing can be classified into two mechanisms. The first is that CpG methylation alters the secondary conformation of DNA from the B form to the Z form, a much more compact form with a deeper groove. This disrupts the interactions between specific transcription factors and gene promoters, consequently resulting in the direct inhibition of gene transcription.[16] The second mechanism is that CpG methylation leads gene regulation regions near the 5′ end to complex with methyl CpG-binding protein (MBD).[17] Under the network of mCpG-MBD complexes, histones become more positively charged and bind more tightly with DNA, making chromatin more compact. Thus, the binding of transcription factors with DNA is limited and transcription is inhibited.

1.4 DNA Methylation and Cancer

Early studies using global measurement of 5-methylcytosine content in normal and neoplastic tissues suggested that decreased DNA methylation levels is a common feature of cancer.[18] However, a more recent study by Costello et al. (2000) suggested that relationship between the global methylation levels and cancer formation is dependent on the type of cancer cells., Certain tumor types, like breast, head and neck, and testicular, displayed a relatively low frequency of aberrant methylation while other tumors such as colon, glioma, and acute myeloid leukemia, displayed a significantly higher frequency of aberrant methylation events. It was estimated that an average of 608 (up to as many as 4500) CpG islands were aberrantly hypermethylated in tumors.[19] Methylation abnormalities were detectable in both low and high-grade malignancies, supporting the notion that methylation changes can be an early event in tumor progression. Furthermore, CpG island methylation was not random indicating that certain CpG islands may be more susceptible to de novo methylation than others or that selective loss of expression from certain CpG island associated genes may be favored if loss of that gene provides the cell with a growth advantage.

The reaction of CpG island methylation features the addition of a methyl group at the carbon-5 (C5) position of cytosine residues. The level of CpG island methylation is controlled by DNA methyltransferase (DNMT), an enzyme that catalyzes the transfer of a methyl moiety from SAM to the C5 position. All DNMTS are essential for normal development, as it was shown that mice lacking any of the DNMTs died at fetal development stage or early after birth.[20] The mammalian DNMTs family encompasses DNMT1, DNMT3A and DNMT3B.

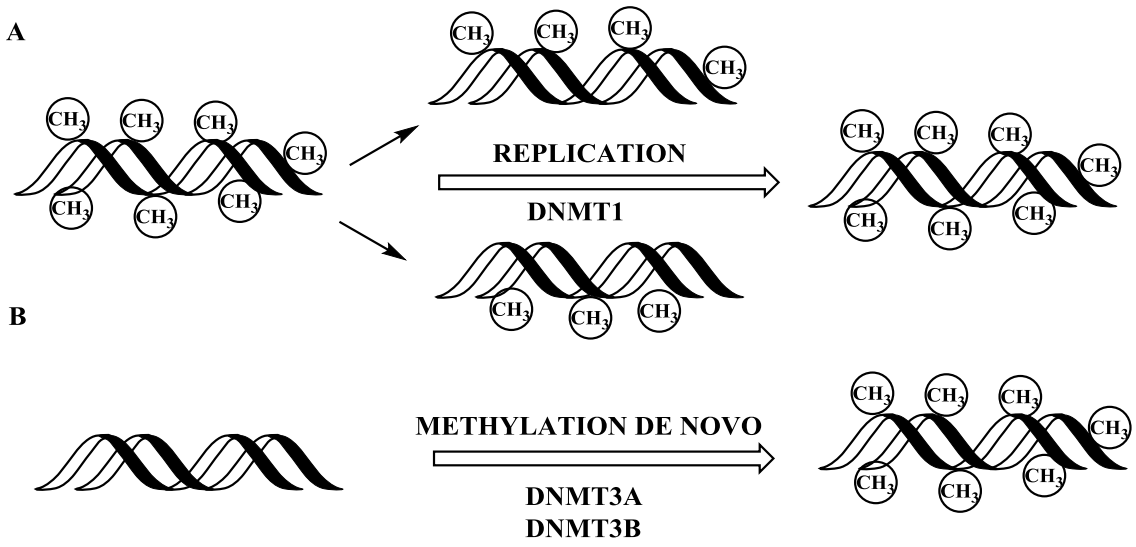

Figure 1.4 Methylation pattern in genomic DNA.[21, 22]

The maintenance DNMT1 is the most abundant methyltransferase in mammalian cells. It transfers methyl groups to the hemimethylated DNA during replication, whereas the de novo DNMT3A and DNMT3B add methyl groups to CpG dinucleotides of unmethylated DNA (Figure.1.3). Hemimethylated DNA is referred to as a duplex DNA where only one of two (complementary) strands is methylated (Figure.1.4). A hemimethylated site is a single CpG that is methylated on one strand, but not on the other. Hemimethylation is important because it directly identifies de novo methylation events, allowing differentiation between de novo vs. maintenance factors. The structure of mammalian DNMTs can be divided into two major parts, a large N-terminal regulatory domain of variable size, which has regulatory functions, and a C-terminal catalytic domain which is conserved in eukaryotic and prokaryotic carbon-5 DNMTs (Figure 1.5).

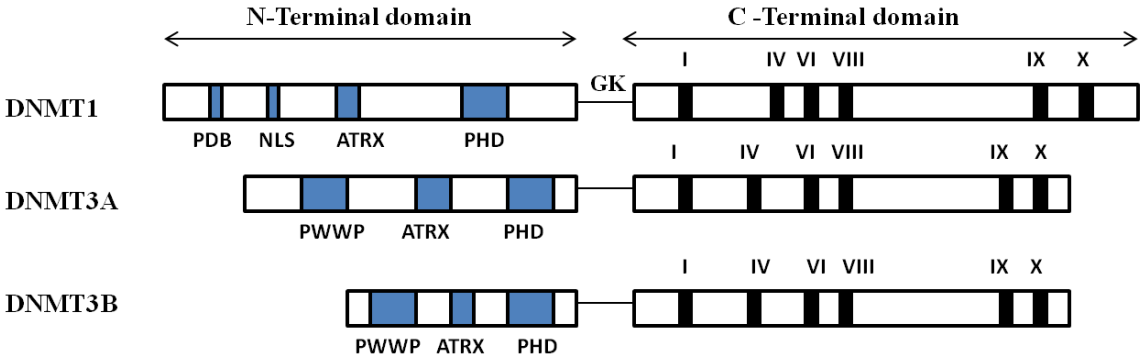

Figure 1.5 Members of mammalian DNMTs family. The N-terminus of DNMT1 includes a proliferating cell nuclear antigen binding domain (PDB), nuclear localization signal sequence (NLS), a cysteine rich zinc finger DNA binding motif (ATRX), polybromo homology domain (PHD); while Dnmt3a and Dnmt3b consist of a tryptophan-rich region (PWWP), ATRX and PHD.[23, 24]

The N-terminal regulatory and the C-terminal catalytic domains are linked by a short fragment of repeated GK dipeptides. The N-terminal domain possesses nuclear localization signal sequence (NLS) responsible for localization of DNMTs in the nucleus. The N-fragment of DNMTs also contains proliferating cell nuclear antigen binding domain (PDB), a cysteine rich zinc finger DNA binding motif (ATRX), and polybromo homology domain (PHD) targeting DNMTs to the replication foci. However, PWWP, a tetrapeptide that interacts with histones, is only present in N-terminal domains of DNMT3A and DNMT3B.[25] The C-terminal domain contains six conservative motifs I, IV, VI, VIII, IX and X. Motifs I and X form SAM binding site, motif IV binds cytosine at the active site, motif VI possesses glutamyl residue donating protons, and motif IX maintains the structure of the target recognition domain (TRD) usually located between motifs VIII and IX, that makes base-specific contacts in the major groove of DNA.[26] In contrast to DNMT1, C-terminal domain of DNMT3A and DNMT3B is active without interaction with their N-regulatory regions. These differences between DNMT1 and de

novo DNMTs may provide the structural basis for the design of selective DNMT1 inhibitors.

Since many tumors suppressor genes are silenced by DNA methylation during carcinogenesis, Reexpression of methylation silenced tumor suppressor genes by inhibiting the DNMT can lead to suppression of tumor growth or provide novel opportunities for anticancer therapy. Inhibition of the activity of these proteins will therefore result in progressive reduction of DNA methylation in newly dividing cells. My second project is focused on the development of DNA methyltransferase inhibitors.

CHAPTER 2

CHEMICALLY STABLE ANALOGUES OF 7-METHYL-2′-DEOXYGUANOSINE

2.1 Introduction

N7-methylated guanine adducts are the most abundant products when DNA is exposed to many methylating agents found in industrial products, food substances, and tobacco smoke. Methylating agents constitute one of the best studied groups of model genotoxic chemicals, represented by such laboratory classics as, *N*-methyl-*N*-nitrosourea (MNU), methyl-*N*′-nitro-*N*-nitrosoguanidine (MNNG) and methyl methanesulfonate (MMS). In addition to their wide use in experimental genetic toxicology, methylating agents are of interest in view of the known human exposure to them and the possible genetic risks associated with it. Relatively small population subgroups suffer limited workplace exposure to weakly genotoxic methylating chemicals such as dimethyl sulfate (DMS) and methylbromide.[27] On the other hand, of potentially greater public health significance is the exposure of the general population to strongly carcinogenic methylating agents such as N-nitrosodimethylamine (NDMA) and 4-methylnitrosamino-1-3-pyridyl-1-butanone (NNK). These nitrosamines are present in significant quantities in tobacco smoke, while, in addition, NDMA is also found in nitrate- or nitrite-treated foods, certain beverages, and certain occupational settings.[11, 28] Although neither NDMA nor NNK is reactive toward DNA, they can be converted by liver cytochrome P450 enzymes to the highly reactive N-nitrosomethylamine (Figure 2.1).

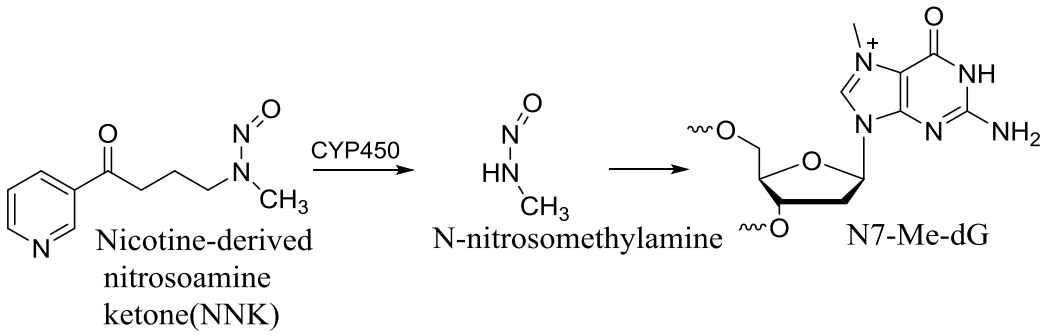

Figure 2.1 Formation of N7-Methyl-dG (^{7Me}dG) adduct from NNK.

DNA methylation can occur "naturally" as well. There are also endogenous methylating agents such as SAM, which is required for the enzymatic conversion of cytosine into 5-MeC as part of the DNA methylation pathway that helps regulate gene expression**.** Alternatively, SAM can act as a weak DNA methylating agent through nonenzymetic reactions.[29] Human can also be exposed to methylating agents during chemotherapy. Dacarbazine and Procarbazine are two known anti-cancer agents that produce DNA methylation on N7 position of guanine.[1]

However, N7-Me-dG is difficult to study due to its short lifetime. This low stability presents a challenge for chemists to prepare oligonucleotides containing N7-Me-dG using the standard phosphoramidite chemistry. The cationic base would have been cleaved by nucleophiles at various stages if the standard phosphoramidite of 7-MeG were to be synthesized. In addition, the N7-Me-G would not survive the oligonucleotide deprotection conditions after the solid phase synthesis. On the other side, the fact that these adducts are converted to more mutagenic products in cells makes the interpretation

of in vivo mutagenic data problematic. Precise understanding of the mutagenic effects of N7-Me-G is an important task for chemists and biochemists. This chapter describes the chemical synthesis of stable analogues of N7-Me-G.

2.1.1 Biological Significance of N-Methyl and O-Methyl Adducts

Exposure of mammalian cells to methylating agents causes transfer of methyl groups to N- as well as O-atoms of DNA bases. The structural and biological consequences of the different N- and O-methyl adducts have been studied to various extents. Methylation at oxygen atoms results in DNA lesions, especially O6-Me-G which has been shown to be strong inducers of gene mutations.[30] Yet many methylating agents react much more frequently with nitrogen atoms than with oxygen atoms in the DNA, resulting in high proportions of N7-Me-G and N3-Me-A in DNA adduct. Studies using DNA templates treated with methylating agents and purified polymerases established the dogma that N7-Me-G does not block replication and is perhaps not miscoding, but its depurination produces an apurinic (AP) site, which if not repaired can be mutagenic and cytotoxic, whereas N3-Me-A has been predicted as a replication fork blocking lesion. Structural studies of DNA polymerases suggest that minor groove N3-purine and O2-pyrimidine contacts are important during extension from newly synthesized base pairs, thus providing an explanation as to why methyl groups at these positions would impede polymerases.[31]

Methylation at the N3 site of adenine, which lies in the minor groove, has been shown to result in cytotoxicity, but not mutations by high-fidelity polymerases.[32] N3-Me-A is cytotoxic by virtue of its ability to block replication and by virtue of its ability to

give rise to a chemically or enzymatically generated AP site. Thus, compounds that can generate exclusively N3-Me-A adducts can be used to destroy cells without any risk of mutagenicity. For example, minor groove specific methylation reagent such as Me-Lex has been suggested to play such a role.[32] N3-Me-A is a quantitatively significant DNA adduct formed from the reaction of many methylating agents. However, it is also in combination with a large number of other DNA lesions, including N7-Me-G, O6-Me-G, and N1-Me-A. In a previous study on the potential effect of N3-Me-A on DNA replication, MMS and DMS, which predominantly react with DNA to produce N7-Me-G, were used to methylate poly(dA-dT).[33] Under these conditions, the heteropolymer contained a mixture of N3-Me-A, N1-Me-A, and N7-Me-A adducts in a ratio of 16: 3: 1. Replication of this template by *E. coli* DNA polymerase I decreased proportionally to the level of total methyl lesions and/or abasic sites. The reduction of DNA polymerization is likely to be caused by the N3-Me-A lesions.[34] In contrast to error-free polymerases, in vitro bypass study on a stable analogue of N3-Me-A showed that bypass polymerases such as eukaryotic Y-family polymerases can efficiently replicate N3-Me-A, although with significantly higher error rates.[35]

Unlike adenine, guanine methylation occurs mainly at the N7-position. Initially N7-Me-dG (^{7Me}dG) was thought to be responsible for the high G→A transition rate observed for the methylation of DNA. This assumption was indirectly supported by the fact that ^{7Me}dG has a low pK_a and should form a mispair with dT as a zwitterions.[36] However, this became questionable when O6-methyl-dG, another guanine adduct that induces G→A transitions, was discovered (see the next paragraph).[37] Another complication that N7-Me-dG brings is the secondary lesions. Ever since identification of

the first N7-guanine adduct, several hundred studies on DNA adducts have been reported. The instability of N7 purine adducts has prevented more through studies of these adducts via site-specific approaches. Two hydrolysis pathways contribute to the instability of N7-Me-dG (Figure 2.2). Hydrolysis of the imidazole ring gives FAPY (Formamidopyrimidine) products which are weakly mutagenic. Studies have shown that the ring opened methyl-formamidopyrimidine adduct of N7-Me-G can block *E. coli* DNA polymerase Klenow fragment (Kf polymerase) in vitro,[38, 39] However, the misincorporation frequencies are significantly higher when error-prone polymerases are used. Significant misincorporation of T was observed when N7-Me-FAPY-G was bypassed by human polymerases η and pol κ.[40] Hydrolysis of the glycosidic bond either by a spontaneous process or an enzymatic repair mechanism gives AP site which is known to have mutagenic and toxic consequences. Replication of AP sites by translesion synthesis polymerases finishes with predominately deoxyadenosine incorporated.[41] These misinsertion events are responsible for the G→T transversions, the major mutations observed for N7-Me-G adducts.

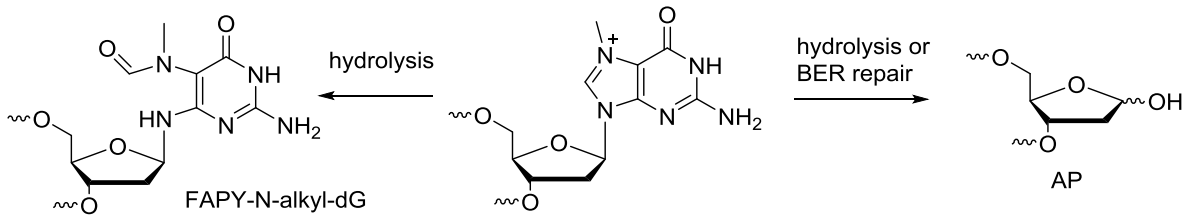

Figure 2.2 Hydrolysis pathways of N7-Alkyl-dG.

On the other hand, oxygen-centered base methylation adducts are directly mutagenic and much current evidence suggests that the most abundant of these, O6-Me-G, plays a major role in mutagenesis and carcinogenesis. O6-Me-G mispairs with thymine during DNA replication, which gives rise to a transition mutation of G:C to A:T.[37] The structure of O6-Me-G:T base pair was recently observed in a crystallography study. Although O6-Me-G is readily replicated and does not produce secondary lesions, it can be cytotoxic by being processed by MMR. This process results in long single-strand patches; if that overlaps another O6-Me-G site of repair on the opposite strand, MMR can generate double-strand disruptions or breaks.[42] Other than O6-Me-G, O2-cytosine and O4-thymine (Figure 2.3) can also react with methylation agents presumably because they are not blocked by hydrogen bonding, and the extra pair of electrons available at oxygen is free to react, even in a double-stranded form. O4-Me-T has been examined as a site-specific adducts in mammalian vectors and appears to be more mutagenic than O6-Me-G.[43]

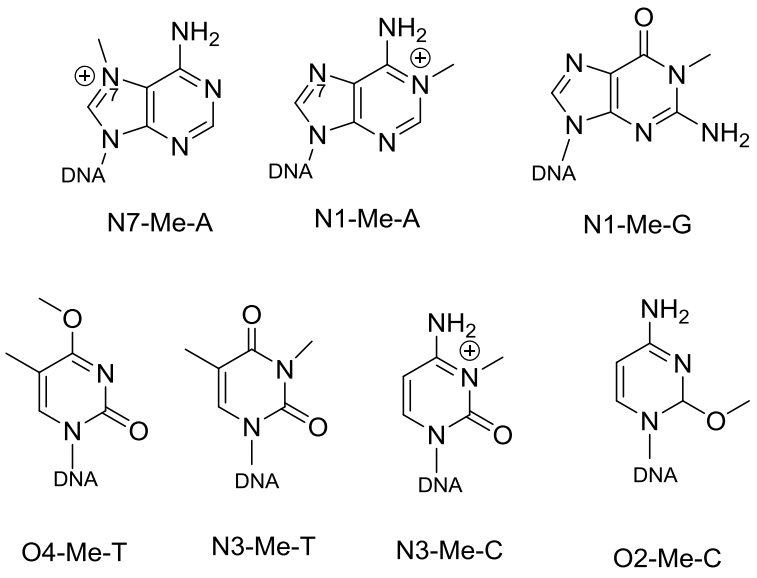

Figure 2.3 Structures of DNA methylation lesions.

In contrast, N1-adenine and N3-cytosine (Figure 2.3) are not very reactive toward methylation reagents due to the hydrogen bonding participation, although these two sites are much more susceptible to methylation in single stranded DNA. A more recent study using site specific adducts in vectors passed through *E. coli* found that N3-Me-C was more mutagenic than N1-Me-A, whereas both adducts blocked replication.[20] The N1-guanine and N3-thymine are secondary amines that have adjacent carbonyl groups and are thus less reactive, the rare N1-Me-G and N3- Me-T (Figure 2.3) adducts were also shown to be mutagenic and replication blocking.[44]

In summary, O-methylation products (e.g., O6-Me-G and O4-Me-T) are highly mutagenic, whereas the mutagenicity of N-methylation products (e.g., N3-Me-A and N7-Me-G) are weak but not clearly understood because of the possibilities of generating secondary DNA lesions or recruiting error-prone polymerases. In general, the studies of mutagenicity of DNA methylation adducts are challenging questions due to the uncontrolled product distribution, the presence of secondary lesions, and the involvement of multiple polymerases and repair enzymes.

2.2 Need for Stable Analogues of N7-Methyl-Guanine

The best way to precisely understand the mutagenic potential of a DNA lesion resulting from misincorporation is to study the relative rate of dNTP incorporation by each polymerase (See chapter 3). The low stability of N7-methylguanine becomes an obstacle to synthesize oligonucleotides containing a single N7-methylguanine for the analysis of DNA polymerase bypass. In fact, the only N7-alkylguanine that has been synthesized and used for such a bypass study is the aflatoxin B_1 (AFB_1) N7-guanine adduct.[45] Reaction between guanine and AFB_1 generates only one guanine adduct. Thus the method is not

applicable to N7-methylguanines. Other reported synthetic N7-methylguanines were only produced as randomly distributed mixtures, and more often together with other types of low-abundance guanine adducts.[46] The results were typically analyzed by looking into the in vivo mutation map on a certain gene, or the composition percentage of digested nucleotides after in vitro polymerase reactions. A problem of interpreting these data is that many low-abundance guanine adducts are in fact much more mutagenic than N7-methylguanines. Their contribution to the observed mutation is difficult to estimate. For example, when methylation reagents such as NDMA and MMS react with guanine, O6-methylguanine is also observed. Therefore researchers often attribute all observed G→A transitions in vivo to the formation of O6-Me-G. This attribution is strongly backed by the result of an in vivo study which showed the amount of O6-Me-G, not N7- Me-G, correlated with the G→A transition events.[37, 47, 48] However, the recent discovery that N7-Me-FAPY-G, which is generated from N7-Me-G, may also causes G→A transitions has made the interpretation more complicated.[39, 40] In contrast to the well studied G→A transitions, other guanine mutation were often overlooked or explained only by speculations. For example, G→T transversions were explained by the formation of abasic sites from N7-Me-G, although repair-enzyme knockout experiment results were contradictory.[49] Alternatively, G→T transversions were explained by the potential mutagenic effect of N3-Me-G, which in fact was as poorly understood as N7-Me-G.[50] In addition, G→C transversions observed in Chinese hamster ovary cells were overlooked.[51] Despite the ambiguity of the in vivo mutagenesis data, other indirect evidence does support that N7-Me-G is non-mutagenic. First, thermal stability and structural studies of a duplex DNA containing N7-Me-dG revealed that alkylation at the N7 position did not

disrupt normal duplex formation.[52, 53] This DNA duplex was synthesized by incorporating the triphosphate of N7-Me-G. Similar single-stranded DNA containing N7-Me-G was not reported, probably due to the difficulty to separate the two strands without the risk of hydrolyzing the N7-Me-G. Second, nucleotide composition analysis of the replication products of an RNA template containing randomly formed N7-methylguanosine showed that N7-Me-rG did not increase the amount of UTP incorporated by RNA-dependent RNA polymerase,[46] although the margin of error determined that the best conclusion one can draw is that N7-Me-rG is not very mutagenic on RNA replication.

In summary, N7-Me-G does not appear to have the tendency to incorporate mismatched nucleosides at abnormally high frequencies. The N7 cationic charge does not have significant impact on the ionic state of the base as was first proposed in the 1950's. However, the exact misincorporation frequencies opposite N7-Me-G would never be determined if the technologies in synthesizing and handling unstable nucleosides remain restricted.

2.3 Design of the Analogue N7-Methyl-Guanine

A stable analogue of an unstable DNA lesion can provide a good model to study its various biophysical and biochemical properties. Huang and Greenberg[54] previously made structural analogues of oxidized abasic site and discovered that the analogues were replicated in a way similar to the natural lesion. Verdine [55] reported N7-Me-2'-F-dG as a stable analogue of N7-Me-dG and used it to trap 3-methyladenine DNA glycosylase II (AlkA), the repair enzyme of N7-Me-G and N3-Me-A. However, the 2'-F group is known to affect the polymerase activity and is not the best replacement in bypass studies.[56] Schärer[57] recently used 7-deaza-dG as a stable analogue to study nitrogen mustard interstrand cross-link. A similar strategy was used to replace N3-Me-dA by 3-

Me-3-deaza-dA to study the bypass.[35] The result showed 3-Me-3-deaza-dA was a stronger blocker of error-free DNA polymerases. The same analogue was recently used to trap AlkA for structural determination.[58] These neutral isosteres of alkylated purines should serve as the general replacement for structural or bypass studies. However, the N-glycosidic bond of these isosteres could be repaired by BER enzymes. For example, 7-Me-7-deaza-G, a chemically stable analogue of N7-Me-G, can be removed by *E. coli* BER enzyme Formamidopyrimidine [fapy]-DNA glycosylase (Fpg) (See chapter 4). It was also discovered that 3-Me-3-deaza-A can be removed by AlkA.[59]

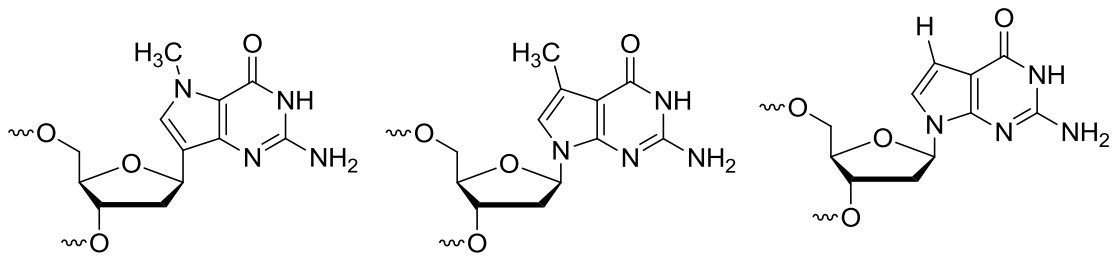

^{7Me9C}dG ^{7Me7C}dG ^{7C}dG

Figure 2.4 N7-Methyl-dG Analogues: N7-Methyl-9-deaza-dG (^{7Me9C}dG), 7-Methyl-7-deaza-dG (^{7Me7C}dG), 7-deaza-dG (^{7C}dG).

Hence, the best structural analogues of N7-methylguanine should fulfill the following requirements.

1. The structure is stable and can be synthesized via the phosphoramidite chemistry.
2. The structure is stable against the actions of BER enzymes.
3. The structure is modular for the preparation of other N7-alkylG adducts for future studies.

Finally, N7-methyl-9-deaza-dG (^{7Me9C}dG) was selected as the analogue.7-Methyl-7-deaza-dG (^{7Me7C}dG) was also studied for the purpose of comparison (Figure 2.4).

2.4 Synthesis of ^{7Me9C}dG Phosphoramidite

This synthesis requires preparation of 9-deazaguanine which was originally prepared by Gibson[60] et al (Scheme 2.1). In their study, the synthesis of 9-deazaguanine was synthesized by using the commercially available 2-amino-6-methylpyrimidin-4(3H)-one as a starting material. The 9-deazaguanine was prepared in 5 steps. Nitration of starting material afforded in compound **2**. Treatment of **2** with N, N-dimethylformamide (DMF) - dimethylacetal at room temperatures afforded the corresponding derivative **3**. The exocyclic amino group of **3** was protected with dmf (Dimethylformamide). The N1 Position of derivative **3** was protected with a benzyl group by treatment of benzyl bromide in the presence of 1,8-Diazabicyclo[5.4.0]undec-7-ene (DBU), giving derivative **4**. The 6-amino group of **4** was further protected with dmf at elevated temperature and converted to derivative **5**. Derivative **5** upon reductive cyclization was converted to N1-benzyl-9-deazaguanine (**6)** in an 89% yield (Scheme 2.1).

The same strategy, with slight modifications, was used to synthesize our target molecule (**7**) (Scheme 2.2). However, we experienced some difficulties in converting **5** to **6**. All our attempts resulted in recovery of the starting material. In contrast to the original synthesis in which they used a saturated solution of $Na_2S_2O_4$ mixed with tetrahydrofuran (THF) ,we found that the solubility of compound **5** was very low in the aqueous-THF mixture, so we synthesized compound **6** using DMF as the co-solvent and at an elevated temperature (65^o C). Compound **6** was subjected to a methylation reaction using methyl iodide as the reagent. The reaction initially proceeded poorly. Careful analysis of the 1H NMR of the starting material suggested that it might have been difficult to remove residual water from the previous reaction. However, even after drying compound **6** under

high vacuum overnight, the reaction still suffer from low yields. Finally, it was proved that this reaction was very sensitive to water and thus the solvent THF needs to be dried under vigorous conditions. The yield was improved to 45% when THF was treated with $LiAlH_4$ under reflux conditions for more than 16 hours.

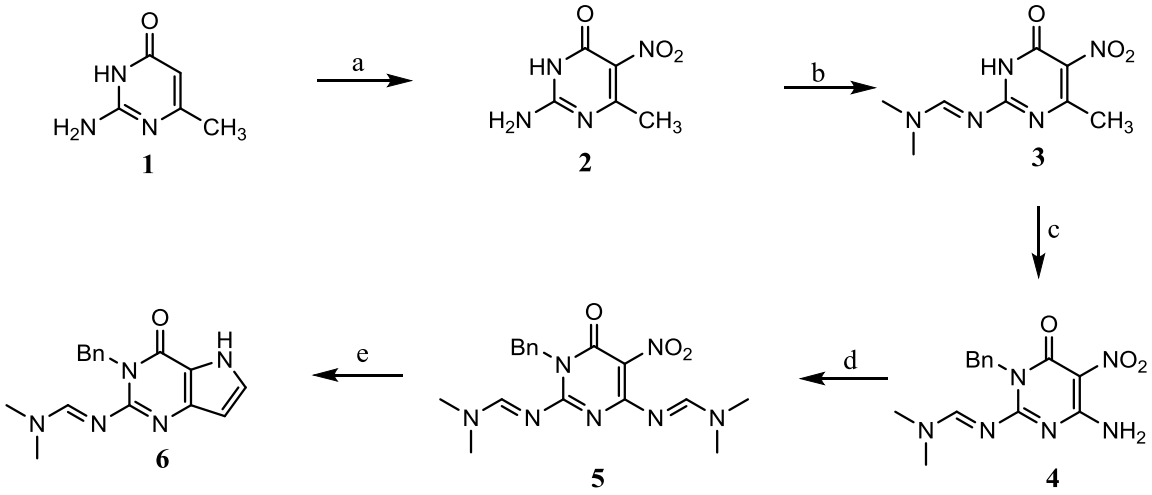

Scheme 2.1 Reported Synthesis of the Nucleobase ^{9C}G.*60* (a) H_2SO_4, HNO_3, 50°C, 1 h,80%; (b) DMF-dimethylacetal,CH_2Cl_2, rt, 1 h,92%; (c) DMF , DBU, Benzyl bromide, rt, 2 h,QY; (d) dry DMF, DMF-dimethylacetal 80^{o}C, 8 h,93% (e) THF, $Na_2S_2O_4$, rt, 1 h,89%.

Scheme 2.2: Synthesis of the Nucleobase ^{7Me9C}G

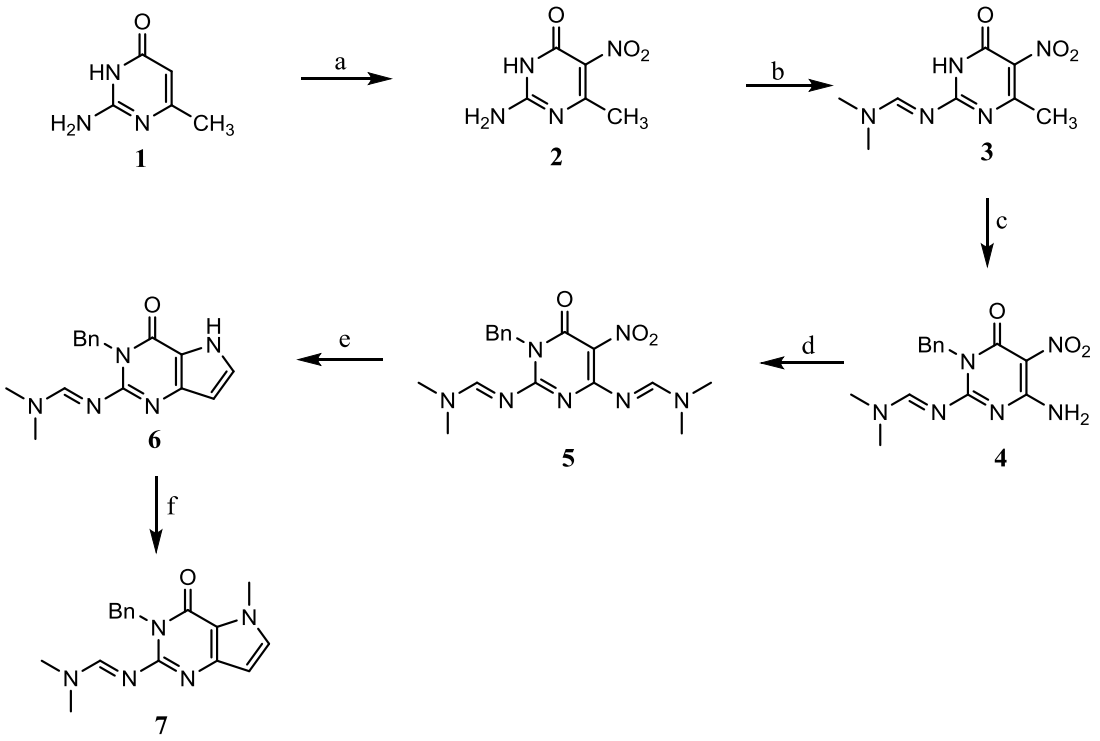

Scheme 2.2 Synthesis of the Nucleobase ^{7Me9C}G. (a) H_2SO_4, HNO_3, 0°C, 3 h,88%; (b) DMF-dimethylacetal,CH_2Cl_2, rt, 2 h,74%; (c) DMF , DIPEA, Benzyl bromide, r.t., 16 h,85%; (d) DMF, DMF-DMAC, 65^{o}C, 4 h,70% (e) DMF, $Na_2S_2O_4$, 65^{o}C, 2 h,84%; (f) NaH, methyl iodide, dry THF, rt, 16 h, 45%.

The glycosyl donor 1-(a,b)-O-Methyl-3,5-di-(O-*p*-toluoyl)-2′-deoxyribose was prepared according to a reported procedure (Scheme 2.3).[61] The commercially available D-2-deoxyribose was treated with methanoic HCl which was generated in situ from acetyl chloride and methanol. This reaction gave the O-methyl acetal of 2′-deoxyribose. The 5′- and 3′-hydroxyl groups of 2′-deoxyribose were then protected with O-toluate by the reaction with p-toluoyl chloride using DMAP as a catalyst.

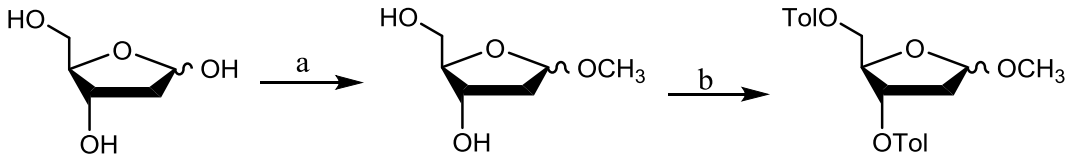

8

Scheme 2.3 Synthesis of Protected Methyl Glycoside of 2′-deoxyribose. (a) D-2-deoxyribose, CH_3COCl, MeOH, rt, 4.5 h (b) DMAP, p-Toluoyl chloride, dry pyridine, rt, 16 h, 43% overall.

The C-glycosidic bond of N7-methyl-9-deaza-dG was formed via condensation of **7** and **8**. $SnCl_4$ was used as the Lewis acid to activate the O-glycosidic bond of **8**, leading to the formation of oxycarbenium ion, which underwent a Friedel-Crafts reaction with the electron-rich C9 position of N7-methyl-9-deazaguanine. This reaction was affected by a variety of factors (Table 2.1). In general, a 1:1 mixture of methylene chloride and acetonitrile is a better solvent system than nitromethane, which was the solvent that Gibson used to prepare 2′-deoxy-9-deazaguanosine. The inclusion of methylene chloride is critical as it increases the solubility of the starting material. The molecular ratio of $SnCl_4$ to the base also affected the yield. Larger amount of $SnCl_4$ afforded significantly higher yields. The optimal yield obtained in this reaction was 40%, much higher than that reported by Gibson for the 2′-deoxy-9-deazaguanine synthesis. This difference may be a result of the electron-donating effect of the N7-methyl group. However, it is more likely that reaction optimization contributed to the higher yield in our experiments. After compound **9** was synthesized, the remaining steps were all protection and deprotection reactions. Initially, we planned to use dmf as the protecting group for the exocyclic amine for oligonucleotide synthesis, as it was already installed in the early stage of the synthesis. Later, we found that dmf on compound **9** was very robust and could not be removed even in 1:1 ethanol/concentrated ammonia at 80 °C for 48 h. Therefore

deprotection of dmf would likely be problematic, if it were used for oligonucleotide synthesis, although it was also possible that the adjacent benzyl group blocked the hydrolysis. Incorporation of non-methylated 9-deaza-dG (^{9C}dG) into oligonucleotides has previously been reported on several occasions. Based on earlier studies we have changed our synthesis route and thought of replacing dmf with an isobutyryl group to protect the exocyclic amine. On the other hand, it was reported that C1 epimerization occurred during the deprotection of isobutyramide of 9-deaza-dG in concentrated aqueous ammonia at 55 °C for 12 h.[62] One alternative solution was to use isopropylphenoxyacetyl (iPac), a more base-labile protecting group, allowing deprotection in ammonia at room temperature. However, another study on the deprotection of isobutyramide of a 2′,3′-didehydro-2′,3′-deoxy nucleoside of 9-deazaguanine did not report obvious epimerization even if the reaction was carried out in saturated ammonia in ethanol at 80 °C for 20 h.[63] Therefore we decided to first try isobutyryl group for the protection of the exocyclic amine of ^{7Me9C}dG. (See later paragraph)

Table 2.1 Factors that Affected the Synthesis of 7-methyl-9-deaza-dG

Entry	**$SnCl_4$ (eqn.)**	**Solvent**	**Time(hr)**	**Temp.**	**% Yield**
1	1.5	dry Nitromethane	16 h	60°C	0
2	4	dry Nitromethane	16 h	60°C	10
3	4	dry DMF	4 h	65°C	0
4	4	dry DCM	4 h	reflux	0
5	4	dry CH_3CN	4 h	reflux	0
6	4	dry CH_3CN :dry DCM	4 h	reflux	44

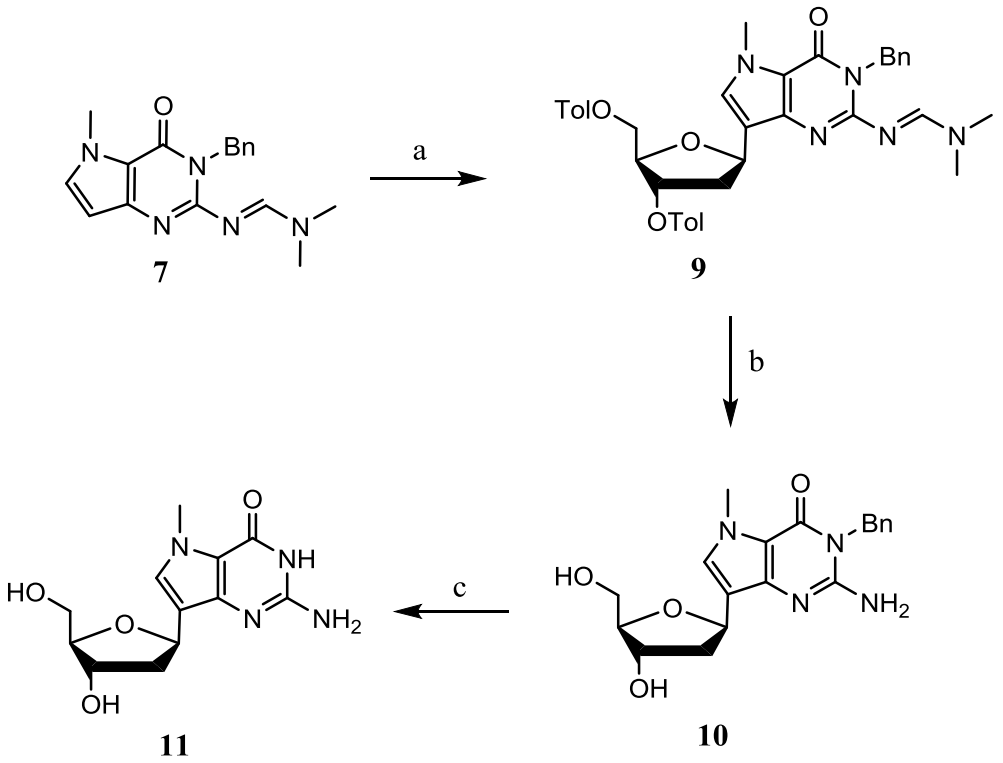

Scheme 2.4 Synthesis of ^{7Me9C}dG Nucleoside. (a) Compound **8** $SnCl_4$, 1:1 (v/v) dry CH_2Cl_2–CH_3CN, reflux, 4 h, 44%; (b)0.4 M KOH in 1:1 (v/v) H_2O–EtOH, reflux, 16 h, 89%; (c) HCO_2NH_4, Pd/C, EtOH, reflux, 16 h, 46%.

The dmf group of **9** was successfully removed in 0.4 M methanoic KOH under reflux conditions. No evidence for epimerization during deprotection was found. In the next step, cleavage of the benzyl group under catalytic hydrogenation conditions with Pd/C at 50 psi did not proceed. Substitution of Pd/C with the more reactive Pd $(OH)_2$ /C showed no improvement. A literature survey showed that the benzyl protecting on the N1 positions of hypoxanthine and guanine and the N3 positions of uracil and thymine [64, 65] is difficult to remove under normal hydrogenolysis conditions. Successful transformation requires a large amount of Pd[34] catalyst or high temperature (over 100°C)[66]. Concerned upon the safety risks of using large quantities of Pd/C or higher temperature, we decided to adopt catalytic transfer hydrogenation conditions. The first attempt to use 1, 4-

cyclohexadiene as the hydrogen source was unsuccessful.[67] Then ammonium formate was used as the hydrogen source, which successfully removed the benzyl group. The debenzylated compound **11** was obtained in 46% yield. TLC showed that starting material was not completely consumed. Ultimately, extension of the reaction time or adding more ammonium formate did not help improve the yield.

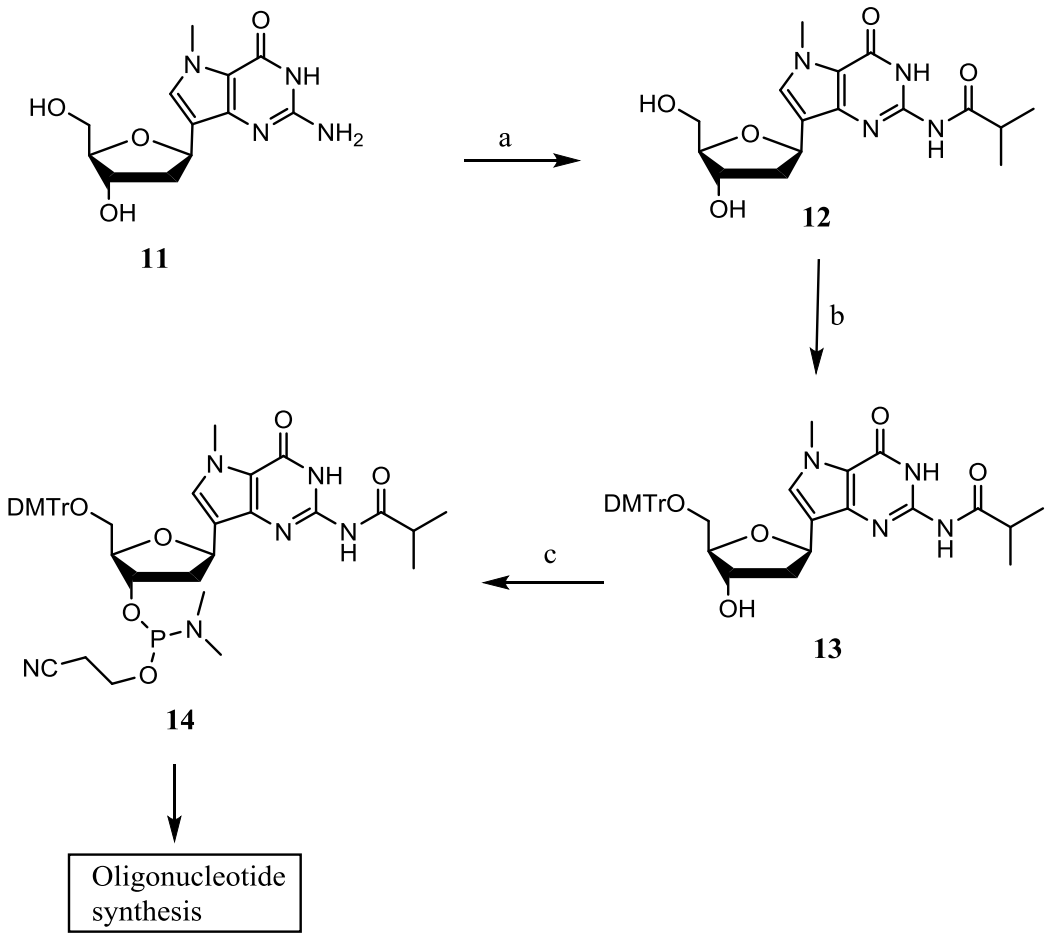

Scheme 2.5 Synthesis of ^{7Me9C}dG Phosphoramidite. (a) TMSCl, Et_3N, CH_2Cl_2, 0.5 h, then isobutyric anhydride, dry pyridine, rt, 2 h, 68% (b) Dimethoxytrityl chloride, Et_3N, DMAP, dry CH_2Cl_2, rt, 16 h, 60%; (c) 2-cyanoethyl N,N-diisopropylchlorophosphoramidite, DIPEA, dry CH_2Cl_2, rt, 2 h, 48%.

The phosphoramide of ^{7Me9C}dG (**7**) was then prepared using standard protocols from **6**.[68] According to previous discussion, the exocyclic amine of the ^{9C}dG was protected with an isobutyryl group. The compound **11** was converted to compound **12** via transient protection. When we tested our methylated nucleoside **12**, we also found that it was fully deprotected and converted back to **11** in concentrated ammonia at 55 °C for 12 hours with no evidence of epimerization.

The 5′-hydroxyl of **12** was protected as dimethoxytrityl (DMTr) ether. Initially we used pyridine as the solvent. However, the pyridinium salts generated in the reaction co-migrated with the starting material on the silica gel column, making recovery of unreacted starting material difficult. Later we changed the solvent to methylene chloride. This change was reproducible and unreacted starting material can be easily recycled for same reaction. We found that the amount of DMAP and TEA has impact on the reaction yield. Increase of the amount of TEA from 1.5 eq. to 2 eq. and DMAP from 0.05 eq. to 0.2 eq. resulted in improved yield (60%). The 3′-hydroxyl was then activated as a phosphoramidite through standard chemistry to yield the solid phase synthesis-ready nucleotide **14**. The commercially available phosphoramidites of ^{7Me7C}dG and ^{7C}dG, along with **7**, were incorporated into oligonucleotides: oligonucleotide **15, 16 (**3′- ACT CTG TXC TTC GAT G-5′, where X = dG, ^{7Me9C}dG respectively), oligonucleotide **17, 18, 19** (3'-TAC CCT GCA CGA CAX AGT TTC AGC GGC ATG-5' where X = ^{7C}dG , ^{7Me9C}dG, ^{7Me7C}dG respectively) and 5′-Fam labeled oligonucleotide **21, 22, 23** (3′- TAC CTC TCT TCC XTC CTA CGA ATG C-FAM-5′ where X = ^{7C}dG , ^{7Me9C}dG, ^{7Me7C}dG respectively). These oligonucleotides were used for the subsequent studies on thermal stability, polymerase replication fidelity, and stability against enzymatic deglycosylation.

2.4.1 Materials and Methods

All chemicals were purchased from Sigma-Aldrich or Fisher Scientific unless specified. THF was dried over $LiAlH_4$ and then distilled under Ar. CH_2Cl_2, pyridine, and acetonitrile were distilled over CaH. Compound **7** was synthesized from 6-methylisocytosine in five steps according to a reported procedure.[60] The only modification of the procedure was the last cyclization step where the solvent was changed from THF to DMF due to the limited solubility of the starting material. NMR spectra were recorded on a 300 MHz Bruker spectrometer. High resolution ESI-MS spectra were obtained in the mass facility at Rutgers University (Newark, NJ).

Compound 2: To a mixture of 2-amino-6-methylpyrimidine-4(3H)-one (5 g, 40 mmol) in 25 mL of H_2SO_4 at 0°C was added 4 mL HNO_3 with an additional funnel. After being stirred at room temperature for 3 hr, the reaction mixture was slowly poured into 360 mL of diethyl ether and stirred for 15min.The liquid was decanted and the remaining solid was mixed 100 mL of ethyl acetate and was stirred for 10 h. The solid (6 g, 88% yield) was filtered and used for next step without any further purification. ^{1}H NMR (300 MHz, DMSO-d_6) δ ppm 2.26 (d, J=1.40 Hz, 3 H).

Compound 3: To a suspension of **2** (6 g, 35 mmol) in methylene chloride (106 mL) DMF-dimethylacetal (12.1 mL) was added and the mixture was stirred at room temperature for 1.5 hour. The precipitated product was removed by filtration to give **3** (5.86 g, 74%). ^{1}H NMR (300 MHz, DMSO-d_6) δ ppm 2.27 (s, 3 H) 3.08 (s, 3 H) 3.21 (s, 3 H) 8.73 (s, 1 H).

Compound 4: To a suspension of compound **3** (6.55 g, 29 mmol) in DMF (143 mL), N, N-diisopropylethylamine (DIPEA) (4.70 g, 36.4 mmol) was added and the reaction mixture became clear. To this solution was added benzyl bromide (15.66 g, 92 mmol, over 1 h) and the mixture was stirred at room temperature overnight. The residue was dissolved in methylene chloride (200 mL). The solution was washed with sat. solution of $NaHCO_3$ (3 x 100 mL), dried $MgSO_4$ and concentrated. Trituration with methanol (150-200 ml) to give **4** (7.72 g, 85%). ^{1}H NMR (300 MHz, CHLOROFORM-*d*) δ ppm 2.43 (s, 2 H) 3.22 (s, 3 H) 3.30 (s, 3 H) 5.44 (s, 2 H) 7.23 - 7.36 (m, 3 H) 7.42 - 7.50 (m, 2 H) 8.78 (s, 1 H).

Compound 5: To a suspension of compound **4** (7.72 g, 25 mmol) in DMF (30 mL) at 65°C DMF-DMAC (4.41mL) was added and the mixture was stirred at this temperature for 3-4 h until TLC analysis showed disappearance of the substrate. Concentration and trituration of the residue with methanol (150 mL) resulted in **5** (6.57 g, 70%). ^{1}H NMR (300 MHz, CHLOROFORM-*d*) δ ppm 3.06-3.21 (m, 12 H) 5.36 (s, 2 H) 5.66 (d, *J*=12.21 Hz, 1 H) 7.18 - 7.29 (m, 3 H) 7.40 (d, *J*=6.68 Hz, 2 H) 7.90 (d, *J*=12.21 Hz, 1 H) 8.57 (s, 1 H).

Compound 6: To a stirring solution of **5** (3.2 g, 8.6 mmol) in DMF (66 mL) maintained at 60-65°C was added sodium dithionite ($Na_2S_2O_4$, 23 g). Distilled water was added (180 mL) gradually portion wise to this solution during a period of 30 min, until an orange yellowish solution was obtained and color lightened. The reaction mixture was cooled to

room temperature and the yellowish white precipitate was collected by filtration and then washed with water to give **6** (2.11 g, 84%). ^{1}H NMR (300 MHz, CHLOROFORM-*d*) δ ppm 3.06 (s, 3 H) 3.11 (s, 3 H) 5.61 (s, 2 H) 6.28 (t, *J*=2.50 Hz, 1 H) 7.10 (t, *J*=2.93 Hz, 1 H) 7.17 - 7.32 (m, 4 H) 7.38 - 7.44 (m, 2 H) 8.48 (s, 1 H).

Compound 7. To a stirring solution of compound **6** (0.610 g, 2 mmol) in dry THF (40 mL) was added sodium hydride (83mg, 2 mmol). The reaction was stirred for 10 min before iodomethane (2.90 g, 20 mmol) was added at 0°C. The mixture was stirred at room temperature overnight. The reaction was diluted with methylene chloride and washed successively with sat.$NaHCO_3$ and brine. The organic layer was separated, dried over $MgSO_4$, and filtered. The filtrate was concentrated. The residue was chromatographed on a column of silica gel eluted with 3:2 hexane/ethyl acetate to give compound **7** (275 mg, 45%). ^{1}H NMR (300 MHz, $CDCl_3$) δ ppm 3.03 (s, 3 H), 3.09 (s, 3 H), 4.04 (s, 3 H), 5.52 (s, 2 H), 6.20 (d, *J*=3 Hz, 1 H), 6.93 (d, *J*=3 Hz, 1 H), 7.15-7.30 (m, 3 H), 7.38 (d, *J*=7 Hz, 2 H), 8.47 (s, 1 H). ^{13}C NMR (75 MHz, $CDCl_3$) δ ppm 34.9, 35.6, 40.7, 45.1, 100.7, 115.0, 126.6, 127.8, 128.0, 131.3, 139.0, 144.3, 154.1, 156.1. ESI-MS (M+ H^+) for $C_{17}H_{19}N_5O$: expected 310.1662, found 310.1662.

Compound 9. To a suspension of compound **7** (0.914 g, 2.95 mmol) and 1-(α, β)-O-methyl-3,5-di-(O-*p*-toluoyl)-2′-deoxy-D-ribose(compound **8)** (1.36 g, 3.54 mmol) in a mixture of methylene chloride (12 mL) and acetonitrile (12 mL) was added a solution of $SnCl_4$ in methylene chloride (1 M, 11.82 mL, 11.82 mmol). The reaction mixture was heated at reflux for 3-4 h until TLC analysis showed disappearance of the nucleobase.

The reaction mixture was diluted with methylene chloride and washed successively with sat.$NaHCO_3$ and brine. The organic layer was separated, dried over $MgSO_4$, and filtered. The filtrate was concentrated. The residue was chromatographed on a column of silica gel eluted with 1:1 hexane/ethyl acetate to give compound **9** (0.840 g, 44 %). ^{1}H NMR (300 MHz, $CDCl_3$) δ ppm 2.37-2.51 (m, 8 H), 3.01-3.07 (m, 3 H), 3.11 (s, 3 H), 3.99 (s, 3H), 4.49-4.62 (m, 2 H), 4.65-4.74 (m, 1 H), 5.48-5.58 (m, 2 H), 5.75-5.81 (m, 1 H), 6.95 (s, 1 H), 7.17-7.33 (m, 8 H), 7.39 (d, *J*=7 Hz, 2 H), 7.98 (dd, *J*=17, 8 Hz, 4 H), 8.56 (s, 1 H). ^{13}C NMR (75 MHz, $CDCl_3$) δ ppm 21.1, 34.4, 35.0, 37.5, 40.2, 44.5, 64.0, 72.9, 76.5, 81.2, 112.6, 115.0, 126.1, 126.5, 127.0, 127.2, 128.5, 129.1, 129.6, 138.4, 141.7, 143.1, 143.4, 153.4, 155.6, 156.0, 165.6, 165.8. ESI-MS (M+ $H^{+)}$ for $C_{38}H_{39}N_5O_{6:}$ expected 661.2900, found 662.2919.

Compound 10. A suspension of **9** (0.430 g, 0.66 mmol) in 0.4 M potassium hydroxide in a mixture of ethanol and water (1:1, 10 ml) was heated under reflux overnight and allowed to cool to room temperature. The reaction mixture was evaporated to dryness. The residue was chromatographed on a column of silica gel with 5% methanol in ethyl acetate to give **10** (220 mg, 89%). ^{1}H NMR (300 MHz, CD_3OD) δ ppm 2.03 (dd, *J*=13, 6 Hz, 1 H), 2.36-2.52 (m, 1 H), 3.62-3.71 (m, 1 H), 3.74-3.83 (m, 1 H), 3.93 (s, 3 H), 3.99 (br, 1 H), 4.43 (d, *J*=5 Hz, 1 H), 5.20-5.32 (m, 3 H), 7.13-7.37 (m, 6 H). The ^{1}H NMR in $CDCl_3$ showed a different spectrum which indicates the formation of an intramolecular hydrogen bond between the benzyl C-H and the exocyclic amine. ^{13}C NMR (75 MHz, CD_3OD) δ ppm 35.9, 43.7, 45.2, 64.9, 75.9, 76.3, 89.5, 114.4, 114.7, 127.7, 128.7, 129.9,

133.1, 137.4, 144.2, 152.6, 156.6. ESI-MS ($M+H^+$) for $C_{19}H_{24}N_4O_4$: expected 371.1714, found 371.1729.

Compound 12. To compound **10** (304 mg, 0.82 mmol) and 10% palladium on carbon (600 mg) in ethanol was added ammonium formate (504 mg, 8 mmol) under Ar. The reaction mixture was heated under reflux overnight and then filtered through Celite. The filtrate was evaporated to dryness. The residue was chromatographed on a column of silica gel with 12% methanol in ethyl acetate to give **5** (106 mg, 46%). ^{1}H NMR (300 MHz, CD_3OD) δ (ppm) 1.89- 2.02 (m, 2H), 2.35 (ddd, *J*=13, 11, 5 Hz, 1H), 3.60-3.68 (m, 1H), 3.71-3.78 (m, 1H), 3.86 (s, 3H), 3.94 (d, *J*=1 Hz, 1 H), 4.04 (q, *J*=7 Hz, 1H), 4.38 (d, *J*=5 Hz, 1H), 5.19 (dd, *J*=11, 5 Hz, 1H), 7.05 (s, 1 H). Compound **11** (144 mg, 0.54 mmol) was co-evaporated with anhydrous pyridine (6 mL) three times and dried under vacuum overnight. It was then dissolved in pyridine (4 mL). TMSCl (0.7 mL, 5.4 mmol) was added slowly to the suspension in an ice bath. After 30 min, Isobutyric anhydride (0.45 ml, 2.7mmol) was added and the mixture was stirred for 2.5 h at room temperature. The reaction mixture was then chilled in an ice bath; 5 mL of cold water was added and the mixture was stirred for 15 min before con. aqueous ammonia (5 mL) was added. The reaction was stirred for another 30 min and the volatiles were the removed under reduced pressure. The residue was re-dissolved in dichloromethane and purified by column chromatography using 2% MeOH in ethyl acetate as the eluent to give **12** (111 mg, 58%). ^{1}H NMR (300 MHz, $CDCl_3$) δ ppm 1.16-1.32 (m, 6H), 1.16-1.21 (m, 2H), 2.02-2.13 (m, 1H), 2.43-2.76 (m, 2H), 3.70-3.79 (m, 1H), 3.87-3.96 (m, 1H), 3.98-4.07 (m, 3H), 4.12 (s, 1H), 4.60 (d, *J*=5 Hz, 1H), 5.27 (dd, *J*=11, 5 Hz, 1H), 6.97 (s, 1H). ^{13}C NMR (75

MHz, $CDCl_3$) δ ppm 19.0,19.1, 35.7, 36.3, 36.3, 43.4, 64.1, 74.8, 75.6, 88.2, 114.6, 116.5, 130.4, 140.8, 144.5, 153.2, 178.6. ESI-MS ($M+H^+$) for $C_{16}H_{22}N_4O_5$: expected 351.1663, found 351.1604.

Compound 13. Compound **12** (104 mg, 0.3 mmol) was dried by coevaporation with anhydrous pyridine. The residue was suspended in anhydrous dichloromethane (6 mL), followed by the addition of dry triethylamine (80 μL, 0.6 mmol). A solution of 4, 4'-dimethoxytrityl chloride (121 mg, 0.36 mmol) and DMAP (7 mg, 60 μmol) in dichloromethane was added and the reaction mixture was stirred at room temperature overnight before it was quenched by adding 0.1 mL MeOH. The reaction was diluted with dichloromethane and washed successively with sat.$NaHCO_3$ and brine. The organic layer was dried over anhydrous $MgSO_4$ and filtered. The solvent was removed in vacuo. The crude product was purified via flash silica gel column chromatography eluted with hexane/ethyl acetate/triethylamine (10%:88%:2%) to give the dimethoxytrityl ether of **13** (123 mg, 60%) as a white foam. ^{1}H NMR (300 MHz, $CDCl_3$) δ ppm 0.84-1.03 (m, 3H), 1.09-1.31 (m, 3H), 1.91-2.11 (m, 3H), 2.19 (dd, *J*=13, 5 Hz, 1H), 3.08-3.20 (m, 1H), 3.23-3.40 (m, 2H), 3.72-3.82 (m, 6H), 3.99 (s, 3H), 4.04-4.17 (m, 1H), 4.58 (d, *J*=5 Hz, 1H), 5.35 (dd, *J*=11, 5 Hz, 1H), 6.78 (dd, *J*=9, 4 Hz, 4H), 6.98 (s, 1H), 7.15-7.31 (m, 4H), 7.34- 7.44 (m, 3H), 7.52 (d, *J*=7 Hz, 2H). ^{13}C NMR (75 MHz, $CDCl_3$) δ ppm 18.6, 18.7, 35.7, 36.1, 41.0, 55.2, 72.7, 74.7, 86.0, 113.1, 115.0, 115.9, 126.8, 127.8, 128.2, 130.1, 130.4, 136.1, 136.4, 142.4, 143.9, 145.2, 153.5, 158.5, 178.2, 178.17. ESI-MS ($M+Li^+$) for $C_{37}H_{40}N_4O_7Li$: expected 659.3052, found 659.3114.

Compound 14. A solution compound **13** (86 mg, 0.13 mmol), diisopropylethylamine (91 µL, 0.52 mmol), and 2-cyanoethyl N,N'-diisopropylchloro phosphoramidite was stirred for 2 h at room temperature under argon. The reaction was quenched with 0.1 mL MeOH and concentrated in vacuo. The crude material was purified by silica gel chromatography using hexane/ethyl acetate (1:1) as the eluent to yield **14** (54 mg, 48%) as a white foam. ^{1}H NMR (300 MHz, $CDCl_3$) δ ppm 1.08 (d, *J*=7 Hz, 1H), 1.12-1.21 (m, 12H), 1.49 (d, *J*=7 Hz, 6H), 1.65 (s, 4H), 2.45 (t, *J*=7 Hz, 1H), 2.68 (d, *J*=7 Hz, 1H), 3.70 (d, *J*=7 Hz, 1H), 3.77 (br, 9H), 4.02 (s, 4H), 4.05-4.17 (m, 4H), 6.78 (m, 4H), 7.03 (s, 1H), 7.16-7.30 (m, 8H), 7.44 (s, 1H). ^{31}P NMR (121 MHz, $CDCl_3$) δ ppm 148.4, 149.0. ESI-MS ($M+Li^+$) for $C_{37}H_{40}N_4O_7Li$: expected 859.4131, found 859.4237.

2.4.1.1 DNA Synthesis and Purification

Oligonucleotide **20** was purchased from Integrated DNA Technologies (Coralville, IA). Other oligonucleotides were synthesized on an ABI 394 DNA synthesizer. The phosphoramidites of Bz-A, dmf-G, Ac-C, T, ^{7C}dG, and 5'-FAM were purchased from Glen Research Corporation (Sterling, VA). The phosphoramidite of ^{7Me7C}dG was purchased from Berry and Associates, Inc. (Dexter, MI). The coupling time of modified phosphoramidites was extended to 15 min. Oligonucleotides were deprotected in concentrated ammonia at 55 °C for 12 h. The crude oligonucleotides were purified by 20% denaturing PAGE. The gel band that contained the desired oligonucleotide was cut, crushed, and soaked in a solution of 100 mM NaCl and 1 mM EDTA overnight. The extract was centrifuged and the supernatant was desalted using a C-18 Sep-Pak cartridge (Waters). The concentrations of DNA were quantified using UV absorbance at 260 nm on

a Shimadzu UV-1700 spectrometer. High-resolution ESI-MS spectra of oligonucleotides were obtained in Rutgers University (Newark) mass facility after precipitation in 2.5 M ammonium acetate solution.

Oligonucleotide **18** (3'-TAC CCT GCA CGA CAX AGT TTC AGC GGC ATG-5'**),** calculated, 9198.5396 (M+H), found, 9198.7096;

Oligonucleotide **16 (**3'- ACT CTG TXC TTC GAT G-5'), calculated, 4871.8264 (M+H), found, 4875.9163;

5'-Fam labeled oligonucleotide **22 (**3'- TAC CTC TCT TCC XTC CTA CGA ATG C-FAM-5'), calculated, 8072.7111 (M+Na), found, 8073.5228.

2.5 Thermal Stability of Duplex DNA Containing N7-methyl-9-deaza-dG

2.5.1 UV Melting Temperatures

Duplex DNAs (50 μM for each strand) were hybridized in 100 mM NaCl, 10 mM $MgCl_2$, and 10 mM piperazine-N,N′-bis(2-ethanesulfonic acid) (PIPES) buffer (pH 7.5). A solutions of the DNA duplex (1-5 μM) containing 20 mM NaCl, 2 mM $MgCl_2$, and 10 mM PIPES (pH 7.5) in a total volume of 100 μL was heated from 15 to 85°C at 1°C/min. UV absorbance at 260 nm was taken every 1°C. The melting temperatures were calculated from the first derivative of the curve using the LabSolution software. Experiments were performed in triplicate. ΔH and ΔS were derived from Van't Hoff plots using the equation $1/T_m = (R/\Delta H)\ln[C]_{total} + (\Delta S\text{-}R\ln 4)/\Delta H$. $[C]_{total}$ is the total concentration of the two DNA strands.

2.5.2 Results and Discussion

The melting temperatures of duplex DNA **15-16** were measured to study the impact of ^{7Me9C}dG on the thermal stability of duplex DNA. The results showed that the duplex melting temperature (T_m) was lowered slightly by 1.3 °C in the presence of ^{7M9C}dG when the duplex concentration was 5 μM. This small difference of T_m (^{7M9C}dG) is unlikely to affects the polymerase fidelity significantly. Previous study by Verdine et al. on duplex DNA containing ^{7Me}dG showed that ^{7Me}dG also lowered melting temperature of duplex DNA.[53] In that study, the melting temperature drop was mainly caused by the entropy effect. In fact, ^{7Me}dG contributes to a stronger duplex in the enthalpy change. Study on duplex DNA containing ^{7Me7C}dG, on the other hand by Seela et al. showed that ^{7Me7C}dG contributes to a slightly weaker duplex in the enthalpy change.[69] Replacement of dG with ^{7Me7C}dG caused a decrease of 0-0.5 kcal/mol in ΔH per substitution, depending on the sequence.

To get a deeper understanding of thermal denaturation experiment, we obtained the thermodynamic parameters of the duplex formation (Table 2.1). The enthalpy change (ΔH°) of duplex formation was made significantly more favorable by the presence of ^{7Me9C}dG. The base pairing stability of ^{7Me9C}dG:dC showed an increase of 5.7 kcal/mol in enthalpy change. The different influences of base pairing of ^{7Me7C}dG: dC and ^{7Me9C}dG:dC on the enthalpy change of duplex formation could result from a variety of reasons. Structurally both bases contain a 7-methyl group and lack the N7 lone pair which is important for water binding. The 7-methyl group positively contributes to the stacking energy and should increase the stability of the duplex to a similar extent. However, The loss of the N7 binding site is expected to decrease the stability of the duplex,[70] but the

amount of decrease should also be similar. Other differences between the two structures might be that the two base pairs may be different in hydrogen bonding energies or sugar ring conformations. The hydrogen bonding energy between 7,9-dimethyl-9-deazaguanine and 1-methylcytosine is 2.1 kcal/mol smaller than that between 7,9-dimethyl-7-deazaguanine and 1-methylcytosine, according to a computational study conducted by our group. Therefore hydrogen bonding energy predicted a result opposite to the experimental observation. The other explanation based on sugar ring pucker is more reasonable due to the fact that C-nucleosides prefer the 3'-endo conformation, as opposed to the 2'-endo conformation expected for N-nucleosides.[64]

Despite the favored sugar ring conformation for duplex formation, the less favorable entropy change ($\Delta S°$**)** contributed predominantly to destabilize duplex DNA. This observation is similar to the result of ^{7Me}dG[52], although the impact of entropy change observed for ^{7Me}dG was more dramatic. At room temperature, replacement of dG by ^{7Me}dG resulted in an increase in duplex stability ($-\Delta G_{298}$), while replacement by ^{7M9C}dG rendered the duplex less stable.

Table 2.2 Thermodynamics of the Formation of Duplex DNA Containing ^{7M9C}dG[a]

5’- TGA GAC A**C**G AAG CTA C-3’

3’- ACT CTG T**X**C TTC GAT G-5’

15, X = dG

16, X = ^{7Me9C}dG

Duplex	T_m (°C)[b]	ΔH (kcal/mol)	ΔS (cal/mol K)	ΔG_{298} (kcal/mol)
15	61.1	-116.2	-322	-20.3
16	58.8	-121.9	-345	-19.2

a. Buffer conditions: 20 mM NaCl, 2 mM $MgCl_2$, 10 mM PIPES (pH 7.5).

b. Measured at 5 μM duplex concentrations.

CHAPTER 3

REPLICATION OF N7-METHYL-9-DEAZA-DG AND 7-METHYL-7-DEAZA-DG BY KLENOW FRAGMENT (EXO$^-$) OF *E. COLI* DNA POLYMERASE I.

3.1 Background Information

DNA is considered to be "the molecule of life" since it contains the genetic blueprint for all organisms. The ability to accurately and efficiently duplicate DNA is essential for the survival and proliferation of any organism. The process of replicating an organism's genomic material is complex and requires the coordinated efforts of an ensemble of proteins to initiate, propagate, and terminate each biochemical event in a timely and orderly fashion.[71] At the core of the replication process is the DNA polymerase, the enzyme that catalyzes the incorporation of mononucleotides into a growing polymer (primer) using a DNA template as a guide for directing each incorporation event. The newly-polymerized molecule is complementary to the template strand and identical to the template's original partner strand. During this process, the polymerase maintains an incredible degree of selectivity to insert only one of four potential deoxynucleoside 5′-triphosphates (dNTPs) opposite a template base while possessing an extraordinary degree of flexibility to recognize four distinct pairing partners. DNA polymerases strictly follow the Watson-Crick base-pairing rules, with cytosine and guanine always forming a pair and thymine and adenine always forming a pair. The fidelity of a DNA polymerase is the result of accurate replication of a desired template. Specifically, this involves multiple steps, including the ability to read a template strand, select the appropriate nucleoside triphosphate and insert the correct nucleotide at the 3′ primer terminus, such that Watson-

Crick base pairing is maintained. In addition to effective discrimination of correct versus incorrect nucleotide incorporation, some DNA polymerases possess a 3′→5′ exonuclease activity. This activity, known as “proofreading”, is used to excise incorrectly incorporated mononucleotides that are then replaced with the correct nucleotide. The function of DNA polymerase is not quite perfect, with the enzyme making about one mistake for every billion base pairs copied, even with the assist of proof-reading ability.

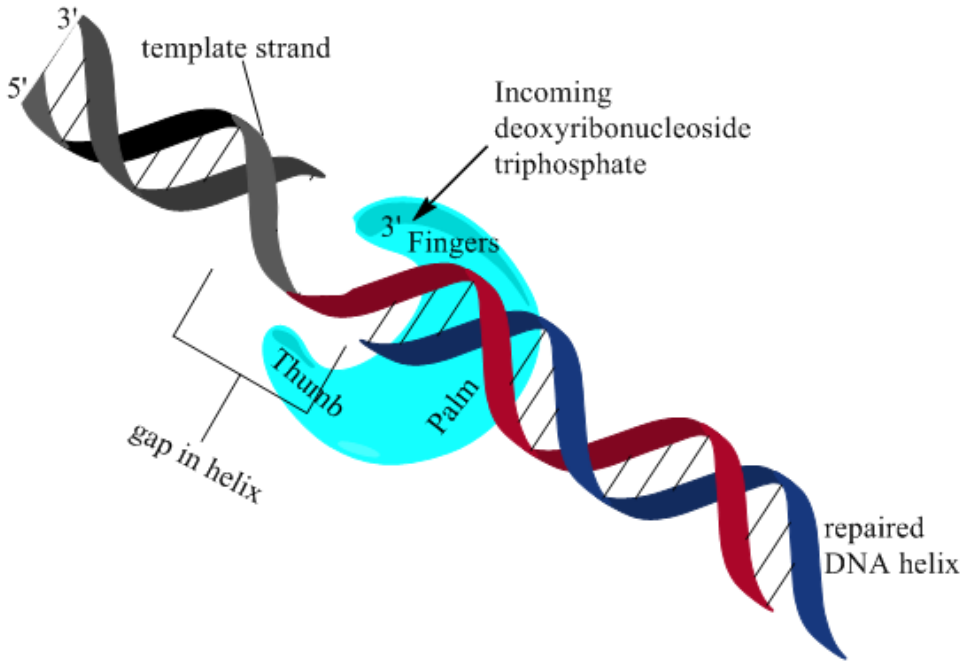

Figure 3.1 Cartoon depiction of DNA Polymerase Structure.

The known DNA polymerases have highly conserved structures. The shape can be described as resembling a right hand with thumb, finger, and palm domains (Figure 3.1). The palm domain appears to function in catalyzing the transfer of phosphoryl groups in the phosphoryl transfer reaction. DNA is in the palm when the enzyme is active. The finger domain functions to bind the nucleotide triphosphate with the template base. The

thumb domain plays a potential role in the processivity, translocation, and positioning of the DNA.[72] DNA polymerase can add free nucleotides to only the 3′ end of the newly-forming strand. This results in elongation of the new strand in a 5′→3′ direction. No known DNA polymerase is able to begin a new chain (“de novo”); therefore replication requires a primer at which it can add the first nucleotide (Figure 3.2). The 3′-OH group forms a bond to the phosphorous atom of the free nucleotide closet to the 5′-O atom. A new phosphodiester bond now joins the two nucleotides. A pyrophosphate group (PPi) is

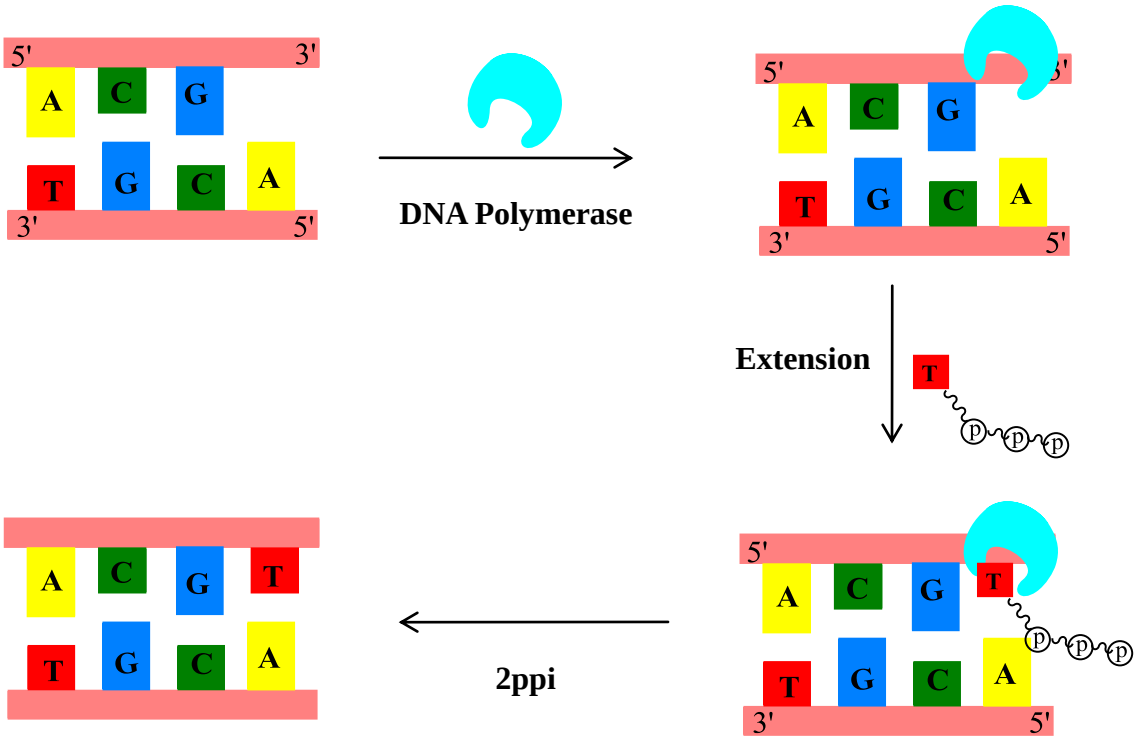

Figure 3.2 Cartoon depiction of DNA Polymerase Processivity.

liberated during the formation of the phosphodiester bond. The pyrophosphate is hydrolyzed, releasing a great deal of energy and driving the reaction forward to completion. Otherwise the pyrophosphate can inhibit the enzyme turnover.

DNA polymerases are divided into seven families based on their sequence homology and crystal structure analysis. These include families A, B, C, D, X, Y and RT. Error-free (high-fidelity) lesion bypass and error-prone (low-fidelity) lesion bypass are important cellular responses to DNA damage during replication, both of which require a DNA polymerase. A high fidelity DNA polymerase, such as those in the A, B, and C families, has a very low error rate in incorporating correct nucleotides into the newly synthesized DNA strand. It follows the mechanism contributes to the selection of correct dNTP by Watson–Crick base pairing. While the low fidelity DNA polymerase, such as those in the X and Y families, incorporates non-Watson-Crick base-paired nucleotides into a growing DNA strand with relatively high frequency. High fidelity DNA synthesis is beneficial for maintaining genetic information. When a DNA lesion disallows a high-fidelity polymerase to incorporate the correct nucleotide, replication stalls to avoid mutations. However, this may lead to cytotoxicity. In case of emergency, low-fidelity polymerases can be recruited to bypass the lesion, with a compromise of losing fidelity.

In this work, DNA polymerase I (Pol I), a high-fidelity polymerase in prokaryotic cells, was used to examine the effects of the N7-methyl group of N7-Me-dG. DNA pol I obtained from *E. coli* is used extensively for molecular biology research. Discovered by Arthur Kornberg in 1956,[73] pol I possesses following enzymatic activities : the 5'→3' (Polymerase) activity, and both the 3'→5' exonuclease (Proofreading) and the 5'→3' exonuclease activities (RNA Primer removal). However, the 5'→3' exonuclease activity

makes it unsuitable for many applications. Fortunately this undesirable enzymatic activity can be simply removed from the holoenzyme to leave a useful molecule called the Klenow fragment, widely used in molecular biology. The Klenow fragment is a large protein fragment produced when DNA polymerase I from *E. coli*. It retains the 5'→ 3' polymerase activity and the 3′→5′ exonuclease activity for removal of precoding nucleotides and proofreading, but loses its 5'→ 3' exonuclease activity. Just as the 5' →3' exonuclease activity of DNA polymerase I from *E.coli* can be undesirable, the 3' → 5' exonuclease activity of Klenow fragment can also be undesirable for certain applications. This problem can be overcome by introducing mutations in the gene that encodes Klenow. These results in forms of the enzyme being expressed that retain 5' → 3' polymerase activity but lack any exonuclease activity (5' → 3' or 3' → 5'). This form of the enzyme is called the exo- Klenow fragment (Kf (exo$^-$)).

3.1.1 Mechanism of DNA Polymerization and Methods in the Measurement of DNA Polymerization Efficiency and Fidelity

Kinetic mechanism for most DNA polymerases follows these steps (Figure 3.2). Step 1 is the binding of polymerase (E) to DNA substrate. Step 2 involves dNTP binding to the polymerase/DNA complex. Step 3 represents a conformational change in the polymerase: DNA complex that is followed by phosphoryl transfer (Step 4). After the nucleotide is covalently added to the growing primer, there is a conformational change step in the polymerase that relaxes the E′:DNAn+1:PPi to the E:DNAn+1:PPi species (Step 5). Following this step, PPi is released as the first product from the polymerase (Step 6). At this stage, the polymerase can remain bound to the product DNA (DNA_{n+1}) to continue

synthesis on the same nucleic acid substrate or dissociate from the DNA_{n+1} to renew polymerization on another substrate.

Maintaining fidelity during DNA replication is challenging since the changing nature of the heteropolymeric DNA template places strain on the unusually high demand for substrate specificity. The hydrogen bonding interactions explain how each incorporation event occurs efficiently and selectively. The molecular events underlying

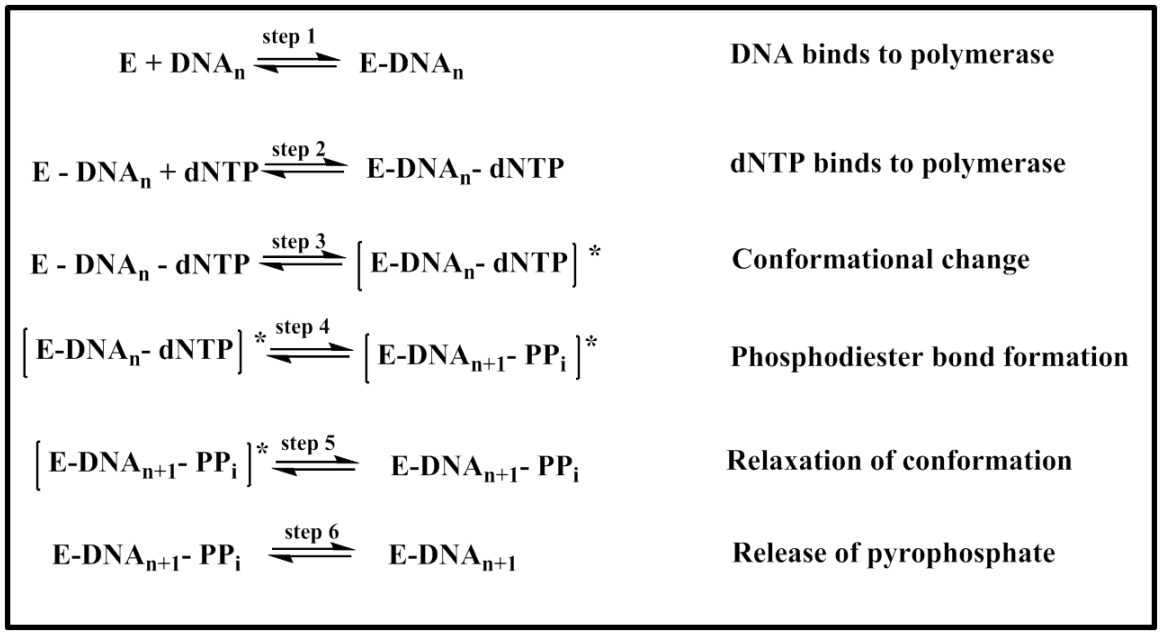

Figure 3.3 Kinetic mechanisms for most DNA Polymerases.[74]

reductions in misincorporation rates are typically interpreted with respect to perturbations in the formation of correct hydrogen bonds between the incoming dNTP and its mismatched partner. Simply put, the rates for misincorporating a dNTP are slow since the functional groups required for proper Watson-Crick interactions do not line up properly. Unfortunately, the nucleobases that provide favorable hydrogen bonding interactions are reactive and thus, susceptible to modifications that can influence the mechanism and

fidelity of DNA polymerases. Methylating agents such as MMS and MNNG preferentially react with the N3 and N7 positions of adenine and the O6 and N7 position of guanine.[2] Methylation at the O6 position of guanine changes the hydrogen bonding capabilities, which increases the frequency of misincorporation events. In addition, methylation at the N7 position destabilizes the N-glycosidic bond leading to spontaneous depurination of this lesion and result abasic sites by nonenzymatically or via the actions of various DNA glycosylases (Discussed in next chapter). The abasic sites are strong blockers of high-fidelity DNA polymerases due to the lack of hydrogen-bond-forming nucleobases.

It is well-established that a cancer cell is genetically different from its normal counterpart. Changes in genetic composition and context can occur by mutagenic events that are caused by inappropriate and/or dysfunctional DNA replication. To understand these mutagenic events, we need to examine how defects in DNA affect the activity and fidelity of polymerases, which contributes to the initiation and progression of cancer. A powerful approach toward understanding the mechanism of mutagenesis is to compare the catalytic efficiency of DNA polymerases for the incorporation of a correct (e.g., dGTP opposite cytosine) versus an incorrect (e.g., dGTP opposite thymine) nucleotide triphosphate.

In this chapter, the study of in-vitro mutagenesis on modified bases can be achieved from steady-state enzyme kinetic analyses. In these assays, a primer template complex is mixed with a polymerase and a dNTP. The primer is end-labeled with a fluorophore (5'-Fam). The reaction is run for a fixed amount of time (to keep the amount of product $\leq$ 30% to avoid "multiple hits", i.e., that each primer-template associates with

and dissociates from polymerase multiple times). The nucleotide insertion velocity (v_0) at the lesion site, given by the ratio of the integrated intensities of primers extended to the target site (and beyond) compared with the integrated intensity of primers extended to a site just prior to the target, was calculated for each [dNTP]. Velocities were calculated by using the equation[75] $v_0 = I/ (I_0+0.5I)\ t$, where I_0 (DNA_n) and I (DNA_{n+1}) (Figure 3.3a) are gel band intensities after t sec of reaction time. I is the amount of product formed, I_0 is the amount of starting material. The maximum magnitude of I was controlled by adjusting the concentrations of dNTPs in the reactions and the reaction times. The velocity reflects the slowest step among polymerase association with primer-template, substrate-initiated conformational change, formation of the phosphodieseter bond, dissociation of pyrophosphate, and dissociation and reassociation with a different primer-template. Treatment of the reaction with inorganic pyrophosphatase guarantees that pyrophosphate release is not the rate-determining step. The most likely rate determining step is the nucleotide incorporation step, particularly when mismatched nucleotide triphosphates are involved. The velocities for the incorporation of one nucleotide at a time vs dNTP concentration can be fit into the Michaelis-Menten equation (Equation 1).

$$\left(v_0 = \frac{V_{max}\ [\ dNTP]}{K_m + [\ dNTP]} \right) \qquad (3.1)$$

The apparent steady-state kinetic parameters (K_m and V_{max}) for the incorporation of the correct and incorrect nucleotides can be determined by the fitting. The k_{cat} values were

then calculated by dividing the V_{max} values with the concentration of the polymerase used. The efficiency of nucleotide incorporation was determined by the ratio of k_{cat}/K_m.

$$f_{mis} = \frac{(k_{cat}/K_m)_{incorrect}}{(k_{cat}/K_m)_{correct}} \quad (3.2)$$

The fidelity of nucleotide incorporation f_{mis} (misinsertion efficiency) was determined by the taking ratios of (Equation 3.2) incorrect to correct insertions i.e., the base normally pairing with the base that was modified (e.g. C with, N7-Me-G) for each of the four dNTPs.

3.2 Experimental

(a)

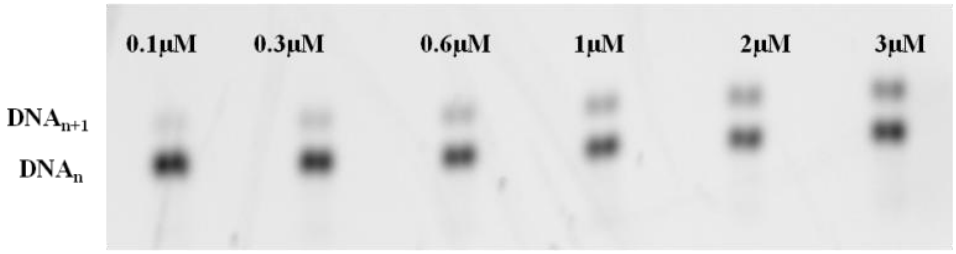

(b)

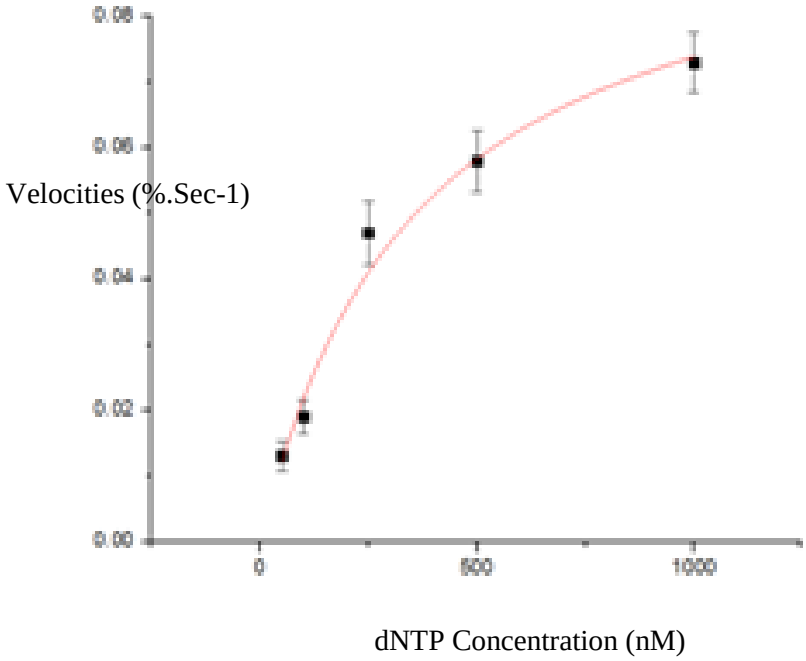

Figure 3.4 Polymerase assays. (a) PAGE analysis of Gel band intensity versus dNTP substrate concentration. The colors of the gel images were inversed for clarity. (b) Michaelis-Menten curves were obtained by using Origin 8.1.Reactions and product analyses were performed as described in 3.2"Polymerase Assays". All values are the averages of three independent experiments.

DNA templates 17-19 (50 μM) were hybridized in equal molar ratio with the 5'-Fam labeled primer in a solution of 12.5 mM NaCl and 12.5 mM Tris-HCl (pH 7.5). Kf (exo$^-$) (New England Biolab, 0.320–20 nM) was incubated with inorganic pyrophosphatase (New England Biolab, 1.5 mole equiv.) in a 80 μL solution containing 1 mg/mL BSA, 5 mM NaCl, 1 mM Tris-HCl, 1 mM $MgCl_2$, and 100 nM DTT (pH 7.9) at 25°C for 10 min. the enzyme solution was mixed with 80 μL of dNTP of different concentrations, which range from about $0.3K_m$ to $3K_m$. After an appropriate amount of time (3-15 min, depending on the type of dNTP), the reaction were stopped by adding 40 μL of 90% formamide loading buffer. The mixture was concentrated and loaded to 20% denaturing PAGE (Figure 3.4).

The gel was visualized using AlphaImager® EP with a liner dynamic range of 4096 gray scale. The intensities of the primer and extension bands were quantified using Alphaview 3.0. When dTTP was used, multiple extension bands were observed. The total intensity of these bands was used for calculation. The reaction rates were calculated according to $v_0 = I/(I_0+0.5I)t$. Michaelis-Menten curves were generated using values obtained from the averaging of at least three replicates using Origin 8.1 (Figure 3.4).

3.3 Results and Discussion of Polymerase Assays

Bypass of ^{7Me9C}dG by the Klenow fragment of *E. coli* Pol I together with ^{7C}dG and ^{7Me7C}dG was studied in vitro. Single-nucleotide insertion experiments were performed using the standing start kinetic study of dNTP incorporation on a DNA template containing a single ^{7Me9C}dG or ^{7Me7C}dG. In a crystal structure of Kf (exo$^-$)/duplex DNA cocrystallized with ddCTP (PDB 2HVI) (Figure 3.4), hydrogen bond was observed

between the N7-position of guanine in the template. Hydrogen bonding plays crucial role in the process of DNA polymerization. The N7 nitrogen of dG is very different from all the N7-methyl compounds[61, 76-84] due to its ability of bind water molecule or divalent metal ions. Hence, we have used ^{7C}dG instead of dG for comparison in order to separately investigate the influences of the additional methyl group and the loss of the N7 binding site. We have performed single-nucleotide insertion experiments under steady-state conditions and oligonucleotides **17-19** were used as the templates.

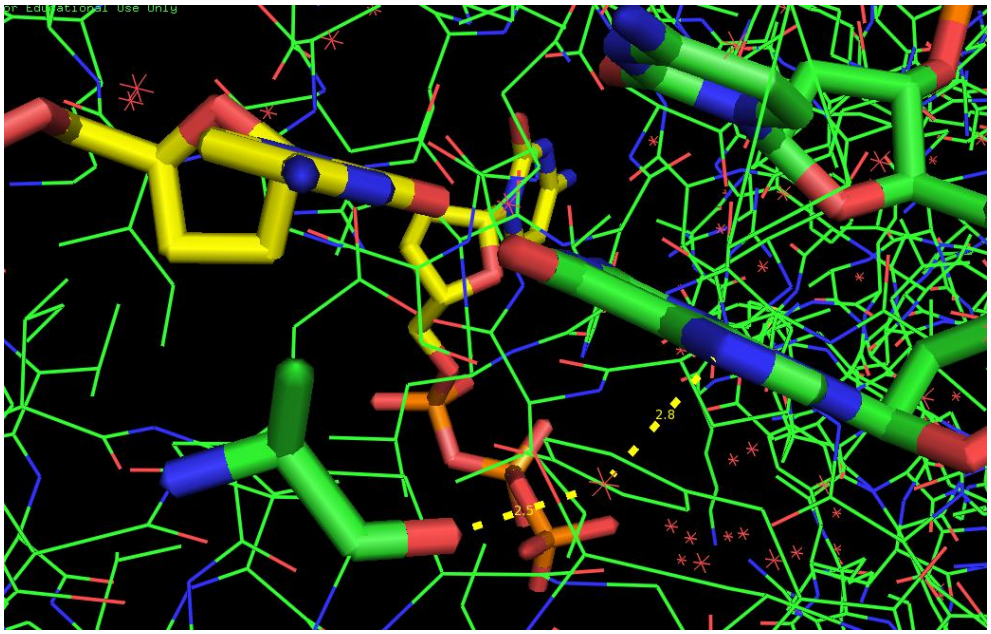

Figure 3.5 A Crystal structure of Kf (exo$^-$)/duplex DNA cocrystallized with ddCTP (PDB 2HVI).

The kinetics of the insertion of dATP, dCTP, dGTP, and dTTP opposite the ^{7C}dG, ^{7Me7C}dG, and ^{7Me9C}dG catalyzed by Klenow Fragment (Kf) (exo$^-$) of *E. coli* DNA pol I were followed by PAGE. Initial rates were determined in reactions in which the extent of reaction was less than 30% completion.[79] The kinetic parameters for all reactions are shown in Table 3.1.

Replacing dG with the methyl did not significantly affect the binding of the DNA to the polymerase and the K_m's of dCTP incorporation opposite all three templates were similar. However, they were much higher than a typical K_m of dCTP incorporation opposite dG (1-10 nM).[80] We have observed the next higher Km of dTTP incorporation opposite all three templates, which may simply occur as a consequence of the geometric constraints imposed by the tight binding pocket in a high-fidelity polymerase. dCTP incorporation with ^{7C}dG, ^{7Me7C}dG and ^{7Me9C}dG significantly decreases the binding efficiency (90-900 fold) compared to dG. Because the only similarity between ^{7C}dG, ^{7Me7C}dG, and ^{7Me9C}dG that differs from dG is their nonexistent hydrogen bond-accepting ability at N7, these results suggest that there may be an important major groove hydrogen bond to the N7 of dG during dCTP incorporation. The difference in K_m indicates that the N7-position of guanine may be important for efficient dNTP binding. This result is consistent with the crystal structure of Kf (exo$^-$)/duplex DNA cocrystallized with ddCTP, which shows a direct hydrogen bond between a water molecule and the N7 of dG opposite the ddCTP.[85] The same water molecule is also hydrogen-bonded to the amide backbone of the protein. Thus, the loss the N7 lone pair disrupts the normal hydration in the polymerase binding pocket, which may be crucial in the conformational change certainly affects the binding of the DNA and the dNTP. Furthermore, dCTP was incorporation opposite ^{7C}dG, ^{7Me7C}dG and ^{7Me9C}dG with 2, 5 and 8-fold (Table 3.1) lower k_{cat} than opposite dG, which indicates that the loss of the N7 lone pair slowed down the enzyme turnover slightly, whereas the size of the methyl group further amplified this effect. The catalytic efficiencies for Kf (exo$^-$) incorporating the correct dCTP opposite ^{7C}dG, ^{7Me7C}dG and ^{7Me9C}dG were reduced, with the k_{cat}/K_m values being 150, 68, and

55(%.μM^{-1} sec^{-1}), compared to the order of 10^4 (%.μM^{-1} sec^{-1}) for unmodified dG template. Thus, the methylgroup in the ^{7Me7C}dG and ^{7Me9C}dG confers a reduction in efficiency for dCTP insertion by approximately 2 and 3-fold, respectively. The major contributor to the reduction of catalytic efficiency is the weak binding resulting from the loss of the N7 lone pair. Overall, this result suggested that substitution of dG with the methyl group significantly slowed down polymerase replication; however, this catalytic efficiency reduction seems unlikely to induce the recruitment of low-fidelity polymerases in cells. The misinsertion frequencies (f_{mis}) for dATP and dTTP opposite all three templates were similar. However, The misinsertion frequency for dGTP opposite ^{7Me9C}dG was only slightly faster than those opposite ^{7Me7C}dG and ^{7C}dG. Overall, these three synthetic bases can be considered nonmutagenic for misinsertion events, because the misinsertion frequencies are still considered low compared to other known mutagenic DNA lesions. This result is consistent with other studies that support 7-methylguanine being non-mutagenic.

Table 3.1 Steady-State Kinetics of dNTP Incorporation Opposite ^{7c}dG, ^{7Me7C}dG, and ^{7Me9C}dG by Kf (Exo$^-$)

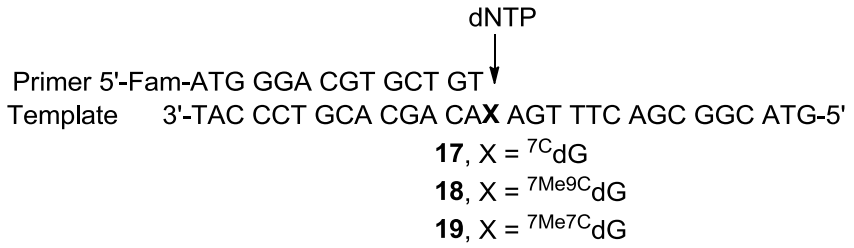

Template	dNTP	K_m (μM)	k_{cat} (%.sec^{-1})	k_{cat}/K_m (%.μM^{-1} sec^{-1})	f_{mis}
dG	dCTP	-	294 ± 2.1	-	-
^{7C}dG	dCTP	1.152 ± 0.186	170 ± 10	150	1
^{7C}dG	dATP	308.1 ± 80.5	99 ± 13	0.32	2.1 x 10^{-3}
^{7C}dG	dGTP	87.17 ± 15.71	3.7 ± 0.2	0.042	3.0 x 10^{-4}
^{7C}dG	dTTP	40.27 ± 14.79	8.4 ± 0.8	0.21	1.4 x 10^{-3}
^{7Me9C}dG	dCTP	1.180 ± 0.427	65 ± 8	55	1
^{7Me9C}dG	dATP	196.9 ± 120.9	47 ± 10	0.24	4.3 x 10^{-3}
^{7Me9C}dG	dGTP	74.87 ± 26.58	10 ± 1	0.14	2.5 x 10^{-3}
^{7Me9C}dG	dTTP	46.05 ± 25.62	6.4 ± 0.9	0.14	2.5 x 10^{-3}
^{7Me7C}dG	dCTP	0.562 ± 0.129	38 ± 2	68	1
^{7Me7C}dG	dATP	64.85 ± 30.78	9.5 ± 0.8	0.15	2.2 x 10^{-3}
^{7Me7C}dG	dGTP	56.89 ± 19.54	2.6 ± 0.2	0.046	6.6 x 10^{-4}
^{7Me7C}dG	dTTP	49.59 ± 10.57	7.2 ± 0.3	0.15	2.2 x 10^{-3}

3.4 Conclusion

For the first time, the influence of the methyl group of ^{7Me9C}dG on polymerase action was investigated by using chemically stable analogues. We found two important results. First,

the Km of dCTP binding observed for all three templates were comparable (Table 3.1), but much higher than the typical dG template (in the low nM range). An apparent explanation is the loss of the metal-binding or hydration site provided by the N7 lone pair. This loss might have caused distorted structure of the polymerase-template-primer-dNTP quaternary complex. The second important result is that the k_{cat} of dNTP incorporation opposite ^{7C}dG is similar to dG, but significantly higher than ^{7Me7C}dG and ^{7Me9C}dG. This demonstrated that methyl group slowed down the turnover of the enzyme although it was originally expected to play minor roles in affecting polymerase actions. The f_{mis} of the three templates were similar. They were about 2 orders of magnitude higher than a typical dG template, but still considered low compared to other DNA lesions. The methyl group itself does not cause significant misincorporation in high-fidelity polymerases. It will also be important to expand these studies to additional polymerases, including Dpo4 a (low fidelity Y-family polymerase).

CHAPTER 4

STABILITIES OF THE GLYCOSIDIC BONDS OF N7-METHYL-9-DEAZA-DG- AND 7-METHYL-7-DEAZA-DG IN THE PRESENCE OF BASE EXCISION REPAIR (BER) ENZYMES

4.1 Background Information

Cellular DNA is susceptible to chemical modifications when exposed to a wide spectrum of exogenous and endogenous DNA damaging agents. These agents can lead to a wide variety of nucleobase modifications that can occur by oxidation or alkylation. Persistence of some of these DNA lesions can be mutagenic and/or cytotoxic. Genotoxicity and cytotoxicity cause altered gene expression and cellular apoptosis, leading to aging, cancer, and various neurological disorders. To combat the deleterious effects of DNA lesions, cells have a variety of DNA repair pathways responsible for restoring damaged DNA to its canonical form. Therefore studies of the mutagenicity of DNA lesions in vivo have to be conducted on the basis of understanding what repair systems might have been involved in attenuate the influence of the damage. On the other hand, unsuccessful repair results in missing base information or DNA strand breaks, which leads to the formation of secondary lesions. In this chapter, we have examined the base excision repair (BER) pathway to confirm the stability of our modified nucleotide ^{7Me9C}dG. The base excision repair pathway is a highly regulated network. The following are types of damages repaired by BER pathway: alkylated bases, oxidized bases, deaminated bases, bases with open rings, and AP sites.[1] Incorporation of correct base in the BER pathway is essential for the preservation chromosomal stability by protecting the cells from DNA strand

breaks. The first enzyme to initiate the repair pathway is the DNA glycosylase, which is responsible for the excision of the damaged base. There are two kinds of DNA glycosylases; the monofunctional (MF) and the bifunctional (BF) DNA glycosylases. The MF glycosylases only have the glycosylase activity that enables them to excise the damaged base. They are hydrolase enzymes that simply use a water molecule to attack the anomeric carbon of the damaged nucleotide. The resulting abasic site can be efficiently excised in the base replacement segment of BER (Figure 4.1). The resulting single-stranded and nicked AP sites are processed by AP endonuclease 1 (APE1), which hydrolyzes the phosphodiester bond 5′ to the AP site. This generates a 3′ hydroxyl substrate for replacement synthesis by DNA polymerase β, followed by sealing of the resulting nick by DNA ligase complete the repair process. BF glycosylases differ from their MF counterparts by their using an active site amine nucleophile rather than water (Figure 4.1). This amine nucleophile also serves as a Schiff base electron sink to facilitate subsequent β elimination. β-Elimination of an AP site by a glycosylase-lyase yields a 3' α,β-unsaturated aldehyde adjacent to a 5' phosphate, which differs from the AP endonuclease cleavage product.[86] Some glycosylase-lyases can further perform δ-elimination, which converts the 3' aldehyde to a 3' phosphate. In addition, the BF DNA glycosylases possess the AP lyase activity, and thus they are capable of cutting the phosphodiester bond of the DNA, which creates the single strand break without the need for the AP endonuclease activity.

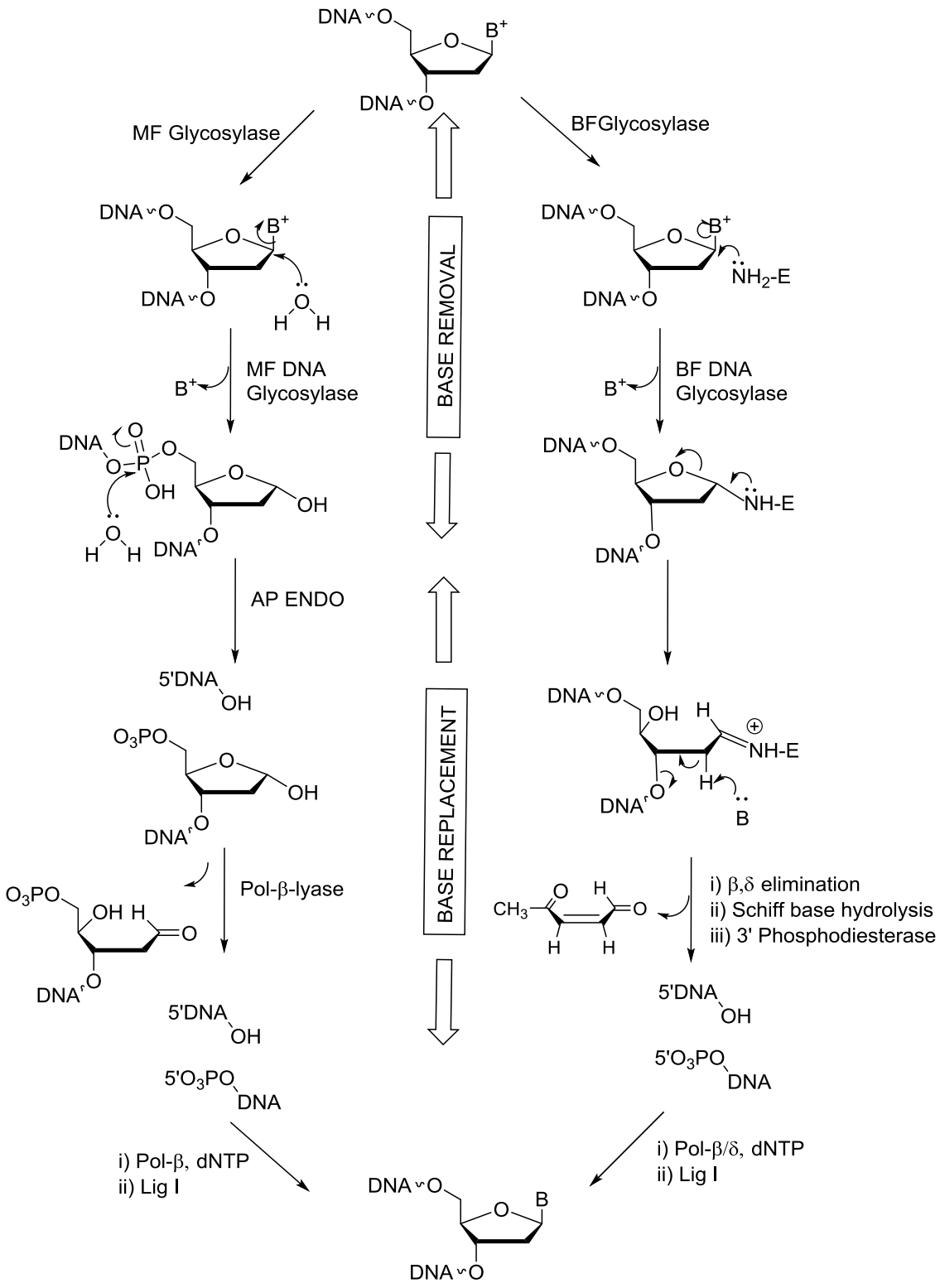

Figure 4.1 Two pathways for base excision repair of damaged bases in human DNA.[87]

In the BER pathway, the *N*-glycosyl bond of the damaged base is cleaved by a specific DNA glycosylase, releasing the damaged base. A wide variety of glycosylases have evolved to recognize different damaged bases and can be grouped into the different categories based on their substrates. To fulfill our motive to examine the stability of the glycosidic bonds of ^{7Me9C}dG and ^{7Me7C}dG against the actions of DNA glycosylase, we have used formamidopyrimidine DNA glycosylase (Fpg) and human alkyladenine DNA glycosylase (hAAG) because ^{7C}dG is a known substrate of Fpg and ^{7Me}dG is a known substrate of hAAG.[81, 82] hAAG catalyzes the hydrolysis of the N-glycosidic bond to release the damaged base via MF repair pathway and generate AP site, whereas Fpg is a BF DNA glycosylase (N-glycosylase and AP-lyase). The N-glycosylase activity releases damaged purines from double stranded DNA, generating AP site. The AP-lyase activity cleaves both 3´ and 5´ to the AP site thereby removing the AP site and leaving a one-base gap.

4.2 Experimental

5'-FAM labeled duplex DNAs (50 μM for each strand) were hybridized in 10 mM Tris-HCl (pH 7.5) and 100 mM NaCl. A solution containing the DNA duplex (10 μM), 1 mg/mL BSA, 1 mM bis-tris-propane-HCl (pH 7.0), 1 mM $MgCl_2$, 1 μM DTT, and the enzyme (8 units) in a total volume of 10 μL was incubated at 37 ºC for 2 hours. For the Fpg reaction, 10 μL of 90% formamide loading buffer was added to stop the reaction. For the hAAG reactions, 1 μL of 3 M NaOH was added and the reaction was incubated for another 15 min before neutralized with acetic acid. Then 10 μL of 90% formamide loading buffer was added. Both reactions were heated at 90 ºC for 10 minutes before

cooled on ice. The samples were analyzed by 20% denaturing PAGE. The gel was visualized using AlphaImager® EP. The intensities of the bands were quantified using Alphaview 3.0.

4.3 Results and Discussion of Glycosylase Assays

The stability of the glycosidic bonds of ^{7Me9C}dG and ^{7Me7C}dG against the actions of Fpg and hAAG was studied. 5'-FAM-labeled duplex DNAs containing ^{7C}dG (**21**), ^{7Me9C}dG (**22**), and ^{7Me7C}dG (**23**) were incubated with 1.67 μM (8 units in 10 μL) Fpg for 2 hours (Figure 4.2a). Faster moving bands in the gel corresponded to the cleaved single-stranded DNA generated via the AP lyase reactions and the deglycosylasation reactions catalyzed by Fpg. Quantification of the bands showed that Fpg cleaved over 95% of the duplex containing ^{7C}dG while we observed 10% cleavage of the duplex containing ^{7Me7C}dG. The k_{cat} of the cleavage of 7-deazaguanine is estimated to be 0.005 min^{-1}, based on the fact that the duplex DNA concentration (10 μM) used in this study was much higher than the typical K_m of an Fpg substrate. The duplex containing ^{7Me9C}dG was stable and remained intact after 2 hours of incubation.

The same experiment was repeated for duplex DNAs containing 2'-deoxyinosine (dI, **20**), ^{7Me9C}dG (**21**), and ^{7Me7C}dG (**22**) with 67 nM (8 units in 10 μL) of hAAG for 2 hours (Figure 4.2b). hAAG does not have the AP lyase activity and thus the reaction was further incubated with 0.3 M NaOH for 15 min to facilitate the cleavage of the AP site. The base treatment was expected to generate a β-elimination product as well as a δ-elimination product. The total amount of cleavage of the duplex containing the dI:dC base pair (**20**) was 59% and we have also observed weak cleaved bands (<3% in total) in

lanes 11 and 12. To confirm that these bands were in fact caused by NaOH, we extended the incubation time of **23** solely with NaOH to 18 h. We have observed that the percent cleavage was increased to 55%. To further confirm the hAAG action in lane 12, we extended the incubation time of **23** with hAAG to 18 hours and doubled the amount of enzyme while maintaining the NaOH incubation time of 15 min. We have observed only weak cleaved bands (Figure 4.3). Surprisingly, ^{7Me9C}dG did not show any sign of cleavage, whether with NaOH alone or with hAAG followed by NaOH treatment. These results demonstrated that ^{7Me9C}dG was remained intact in the presence of hAAG whereas hAAG is likely to cut ^{7Me7C}dG due to the broad substrate specificity (see later discussions) would be at very low rate.

As a DNA glycosylase with broad substrate specificity, Fpg was previously reported to remove N7-methyl-8-oxoguanine with much lower activity compared to the removal of 8-oxoguanine (OG).[5] The OG result in fact can help to explain that Fpg also removed ^{7Me7C}dG but with much lower activity than ^{7C}dG. The hydrogen bond between the backbone oxygen of a serine residue and the N7H of OG is responsible for the selectivity of Fpg for OG over undamaged guanine.[88] A similar CH-N hydrogen bond can possibly form between the serine residue and the C7-H of ^{7C}dG and when a methyl group is added to the N7 position of OG or the C7 position of ^{7C}dG, the enzyme activity is severely affected.

5'- ATG GAG AGA AGG CAG GAT GCT ATC G-3'
3'- TAC CTC TCT TCC **X**TC CTA CGA ATG C-FAM-5'
Substrate **20**, X= dI
21, X= ^{7C}dG
22, X = ^{7Me9C}dG
23, X = ^{7Me7C}dG

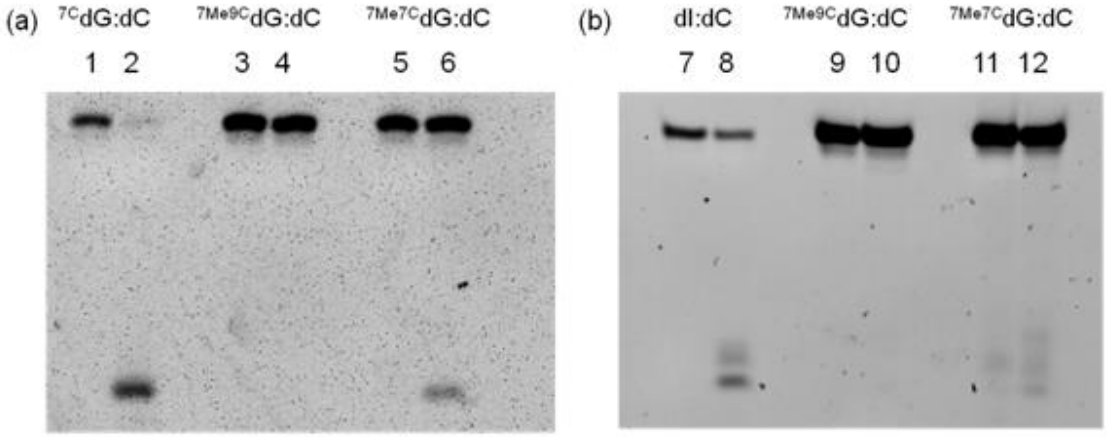

Figure 4.2 PAGE analysis of cleavage of duplex DNA containing damaged Nucleobases or Nucleobase Analogues. (a) Incubation with Fpg. Lane 1 and 2, substrate **21**; lane 3 and 4, substrate **22**; lane 5 and 6, substrate **23**. Conditions of lane 1, 3, and 5: 10 μM duplex, 1 mg/mL BSA, 1 mM bis-tris-propane-HCl (pH 7), 1 mM $MgCl_2$, 1 μM DTT, 37°C, 2 h; Conditions of lane 2, 4, and 6: same as lane 1, 3, and 5 except that Fpg (1.67 μM) was added. (b) Incubation with hAAG. Lane 7 and 8, substrate **20**; lane 9 and 10, substrate **22**; lane 11 and 12, substrate **23**. Conditions of lane 7, 9, and 11: 10 μM duplex, 1 mg/mL BSA, 2 mM tris-HCl (pH 8.8), 1 mM $(NH_4)_2SO_4$, 1 mM KCl, 200 μM $MgSO_4$, 37°C, 2h, then 0.3 M NaOH, 37°C, 15 min. Conditions of lane 8, 10, and 12: same as lane 7, 9, and 11 except that hAAG (62 nM) was added.

Human AAG, excises a variety of substrates including alkylated purines and hypoxanthine (Hx), the deamination product of adenine. hAAG also act on undamaged purines but the activities of hAAG on dI and alkylated purine nucleosides are significantly higher.[89] In our experiment, we extended the reaction time for ^{7Me7C}dG to 18h and doubled the enzyme concentration. However, the results showed no obvious cleavage other than the cleavage caused by NaOH.

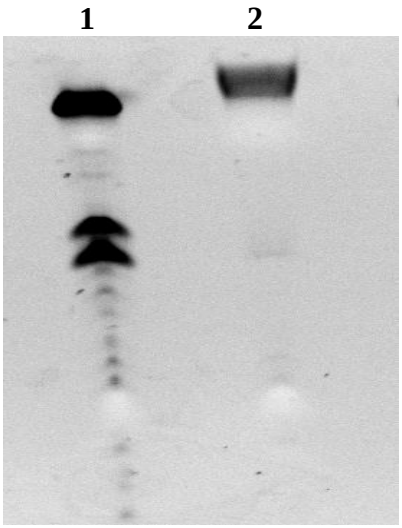

Figure 4.3 Incubation of duplex DNA **23** with NaOH. Conditions of lane 1, 2: 10 μM duplex. Lane 1, in 0.3 M NaOH, 37°C, 18 h. Lane 2, in 124 nM hAAG, 1 mg/mL BSA, 2 mM tris-HCl (pH 8.8), 1 mM $(NH_4)_2SO_4$, 1 mM KCl, and 200 μM $MgSO_4$, 37°C, 18h, followed by 0.3 M NaOH, 37°C, 15 min.

hAAG may still cut $^{7Me7C}G$ at an extremely slow rate, which is similar to the cleavage of undamaged purines. Although, the exact k_{cat} cannot be measured under our experiment conditions, the value must be lower than 3×10^{-4} min^{-1} if the amount of cleavage after 18 h is considered less than 0.5%. This slow rate of cleavage should not affect normal cellular studies.

4.4 BER Repair Inhibition Assay for Inosine in the Presence of ^{7Me9C}dG

^{7Me9C}dG was stable against both enzymes, which opens up the possibilities that it can be an inhibitor of BER enzymes. Since many anticancer drugs act by damaging DNA, thereby arresting cells in the act of DNA replication. Thus, in this context, DNA repair is undesirable and drugs that block repair of drug-induced lesions may synergistically enhance the chemotherapeutic effect of some anticancer drugs. In this kind of therapy, an artificial nucleotide within a duplex DNA strand that binds to BER enzymes but is not

cleaved by them may serve as an inhibitor. By keeping this in our mind, we have investigated the role of ^{7Me9C}dG as an inhibitor for hAAG. The hAAG assay for dI cleavage was repeated in the presence of **22** in various concentrations (1-5 μM) to check the inhibition effect of ^{7Me9C}dG. Percent inhibition of the enzyme activity was plotted against the inhibitor concentrations. The result showed only a small effect of inhibition, around 75% inhibition was observed at 5 μM of **22** (Figure 4.4). The inhibition constant (K_i) was estimated to be around 75 nM based on the reported K_m on a dI substrate.[82,89]

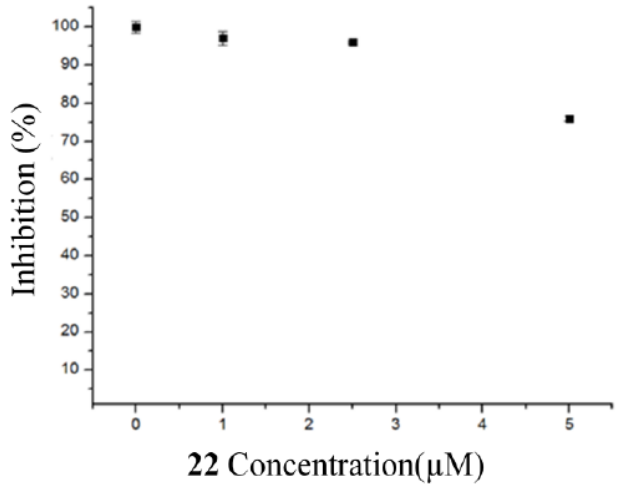

Figure 4.4 Inhibition of hAAG on a dI Substrate by duplex DNA containing ^{7Me9C}dG. The experiments were performed in triplicates.

4.5 Conclusion

We have examined the stability of ^{7Me9C}dG and ^{7Me7C}dG in the presence of BER enzymes Fpg and hAAG. A difficulty to study the biological effects of N7-methyl-dG adducts in cells is due to their low stabilities. In contrast to the in vitro conditions where N7-methyl-dG can survive through a reasonable amount of time at ambient temperature and pH conditions, cells contain a variety of BER enzymes that could potentially remove some of

the N7-methylated bases quickly. The advantage of using a stable analogue of N7-methyl-dG is not only to generate a single adduct through oligonucleotide synthesis, but ensure that the chemical structure of interest remains intact if additional studies are to be carried out in cells. Our studies showed that the glycosydic bond of ^{7Me7C}dG 7 was cut by Fpg at the k_{cat} of 0.005 min^{-1}. Although it is much lower than the values for OG (4.0 min^{-1}) and ^{7C}dG (3.2 min^{-1}), the cleavage will be significant if a study is to be carried out in cells and last 1-2 days. 7-Me-7-deaza-dG was stable in the presence of hAAG for at least 18 h. Obviously, the reaction catalyzed by hAAG is slow, it is prudent to avoid the structure of ^{7Me7C}dG if cellular studies are necessary. In contrast, its analogue ^{7Me9C}dG was stable against both enzymes. Therefore, ^{7Me9C}dG is a more versatile analogue of N7-Me-dG than ^{7Me9C}dG, especially when in vivo study is needed. Inhibition studies of hAAG on a dI substrate in the presence of duplex DNA containing ^{7Me9C}dG demonstrated that hAAG binds the inhibitor with a similar affinity to its substrate. This study has generated a hypothesis that can guide future experimental and theoretical studies directed to increase current knowledge of the mechanism of inhibition.

CHAPTER 5

DESIGN AND SYNTHESIS OF DNA METHYL TRANSFERASE INHIBITORS

5.1 Introduction

5.1.1 DNA Methylation

DNA methylation is a crucial biochemical reaction responsible for epigenetic regulation, which greatly influences gene activation, chromatin stability, and so on.

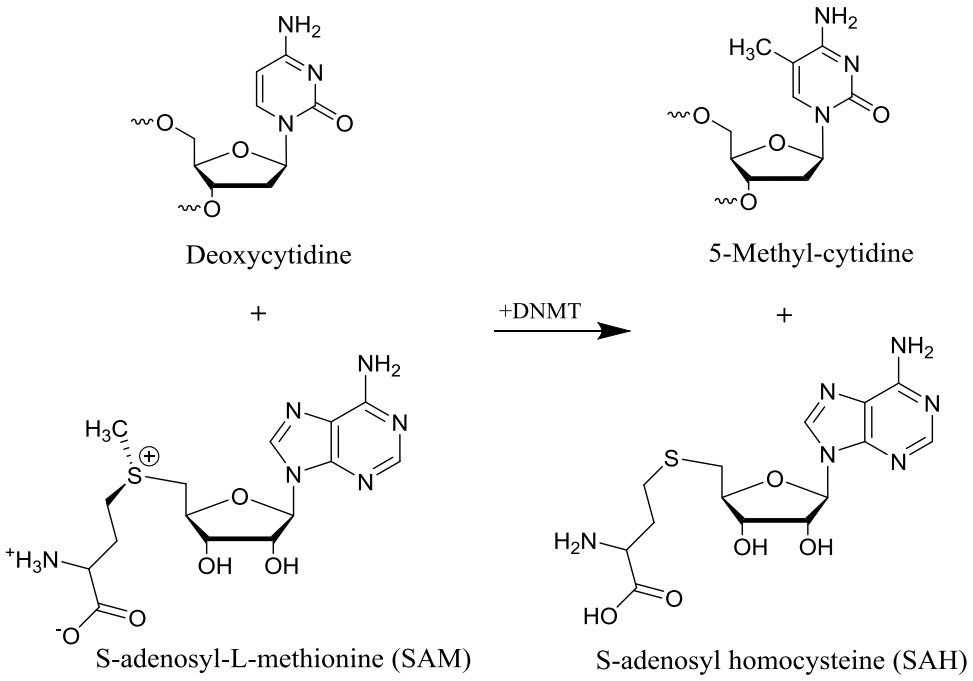

Figure 5.1 Methylation of cytosine catalyzed by DNMTs.

In mammals, normal DNA methylation is controlled by DNA methyltransferase (DNMT), an enzyme that catalyzes the transfer of a methyl group from S-adenosyl-l-methionine (SAM) to the C5-postion of cytosine (Figure 5.1). SAM is a common cofactor in cells. The methyl group attached to the cationic sulfur atom in SAM is chemically reactive. This allows donation of this active methyl group from the sulfur center to a specific position in a variety of substrates, e.g., DNA, RNA, proteins, and secondary metabolites catalyzed by methyltransferases (MTs). More than 40 metabolic reactions share this mechanism, and the product is S-adenosyl homocysteine (SAH) (Figure 5.1), which is an inhibitor of the most methylases.

5.1.2 The Catalytic Mechanism of DNA Methylation

The catalytic mechanism of DNA cytosine-C5 methylation[90] is shown as Figure 5.2. DNMT forms a complex with DNA, and the cytosine to be methylated flips out from the DNA. The thiol group of a cysteine residue in the active site of DNMTs serves as a nucleophile that attacks the 6-position of the target cytosine to generate a covalent intermediate. The 5-position of the cytosine is activated and conducts a nucleophilic attack on the SAM to form the 5-methyl covalent adduct and SAH. The attack on the 6-position is assisted by a transient protonation of the cytosine ring at the endocyclic nitrogen atom N3. The proton is provided by a nearby a glutamic acid residue. The same Glu residue is also in contact with the exocyclic N4 amino group. The extremely electron negative O-2 may also be stabilized by an arginine residue. Following the methyl transfer, the deprotonation at the 5-position generates elimination products: the methylated cytosine and the free cysteine of the enzyme. If this C5 proton is absent,

elimination does not occur and the enzyme becomes permanently bound to DNA. That is how DNA methyltransferases are inhibited by many suicide inhibitors.

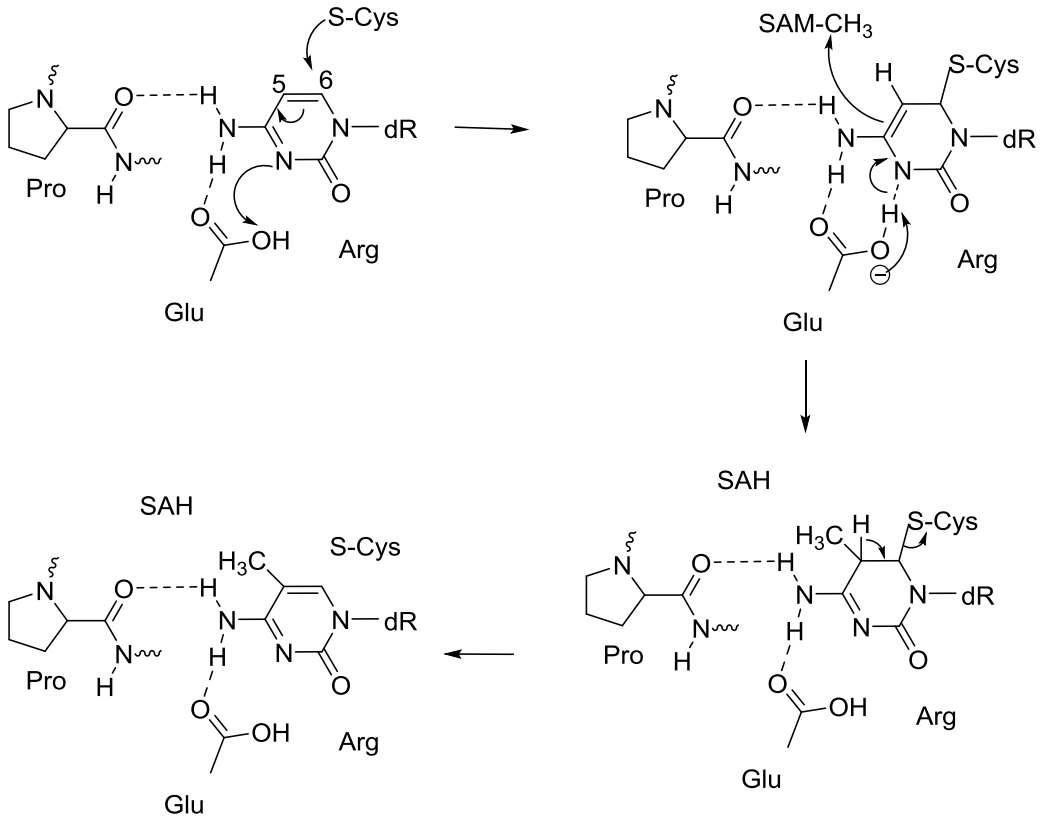

Figure 5.2 The proposed mechanism of DNA cytosine-C5 methylation.

5.1.3 Biological Importance of DNA Methylatransferase (DNMT)

All the known DNA methyltransferases use SAM as the methyl donor. There are four different DNMTs known in mammals: DNMT1, DNMT3a, DNMT3b and DNMT3L. DNMT1 (DNA cytosine-5-methyltransferase1) is responsible for the maintenance of methylated DNA by copying DNA methylation patterns from the parental strand to the newly synthesized daughter strand during the DNA replication process. DNMT1 is

ubiquitous; it is highly expressed in fetal tissues, heart, kidney, placenta, peripheral blood mononuclear cells, and less expressed in spleen, lung, brain, small intestine, colon, liver, and skeletal muscle.[91, 92] Differently, de novo methyltransferase DNMT3A is only present in low amounts in somatic cells and shows no preference for hemi- or unmethylated DNA.[93] It is widely accepted that DNMTs play a causal role in cancer formation through their DNA methylation activity on tumor suppressor genes, which makes them suitable candidates for anticancer targets.[94]

5.2 Developed DNMT Inhibitors

DNMT inhibitors (DNMTi) can be classified into two broad categories. One category includes nucleosides inhibitors, which are incorporated into DNA and act as suicide inhibitors via a covalent adduct formation. The second category is the non-nucleoside inhibitors.[95] To date, only two nucleoside analogs, 5-azacytidine (Vidaza) and 5-aza-2'-deoxycytidine (also known as Decitabine, Dacogen), have been used clinically. These drugs, after incorporation into DNA, cause covalent trapping and subsequent depletion of DNMTs. Azacitidine and Decitabine are approved by the FDA for the treatment of myelodysplastic syndrome.[96] These 5-azanucleoside analogues can be incorporated into DNA to replace cytosine. The absence of a hydrogen atom at the C5 position hinders DNMT release by β–elimination, with the consequence of DNMT trapping and degradation (Figure 5.4). Because of the nitrogen substituted base forms a stable covalent complex with DNMT, the cytotoxicity associated with aza-nuclosides increased

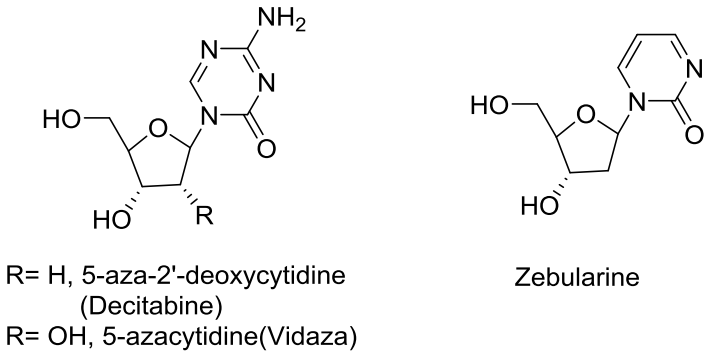

Figure 5.3 Nucleoside DNMTi.

the demand for more effective and selective DNMTi. Zebularine (Figure 5.3) is a novel DNMT inhibiting drug which offers much promise due to low toxicity, stability and effective bioavailability when administered orally. It also has high selectivity for tumor cells. The downfall of this drug has been the requirement for high doses (1 g/kg in mouse) which may pose problems in clinical trials.[97]

To avoid the toxicity and stability problems associated with nucleoside DNMTi, efforts have focused on the development of non-nucleoside reversible inhibitors. Generally, they inhibit DNA methylation by binding directly to DNMTs without incorporation into DNA. Some of the reversible DNMTi's (Figure 5.5a) are approved drugs for other indications, e.g., the anti-hypertensive drug Hydralazine, the local anesthetic Procaine, the anti-arrhythmic drug Procainamide,[98] and the methylene disalicylic acid NSC14778[99] (Figure 5.5b). Some DNMT inhibitors have been identified by docking-based virtual screening. Examples include the L-tryptophan derivative RG108 (Figure 5.5b), RG108 (NSC401077) was first characterized by Brueckner et al.[100] in 2005 and was conceived to interact with the catalytic domain of DNMT1.[101] This compound inhibits DNMT in human cancer cells. DNMT inhibitor MG98 (Structure has

not been disclosed yet) can safely and effectively lead to reactivation of methylation silence tumor suppressor genes. This has been shown in patients with RCC, a disease associated with hypermethylation and silencing of cell growth control and tumor suppressor genes.[102] MG98 seemed promising and was used in a Phase I study in solid tumors.[103] Because of current preclinical and clinical evidence, further phase II development of MG98 would be of interest. Recently, a non-nucleoside inhibitor, SGI-1027, (Figure 5.5c) and its analogues were developed which showed high potency in the anticancer activities.[104, 105]

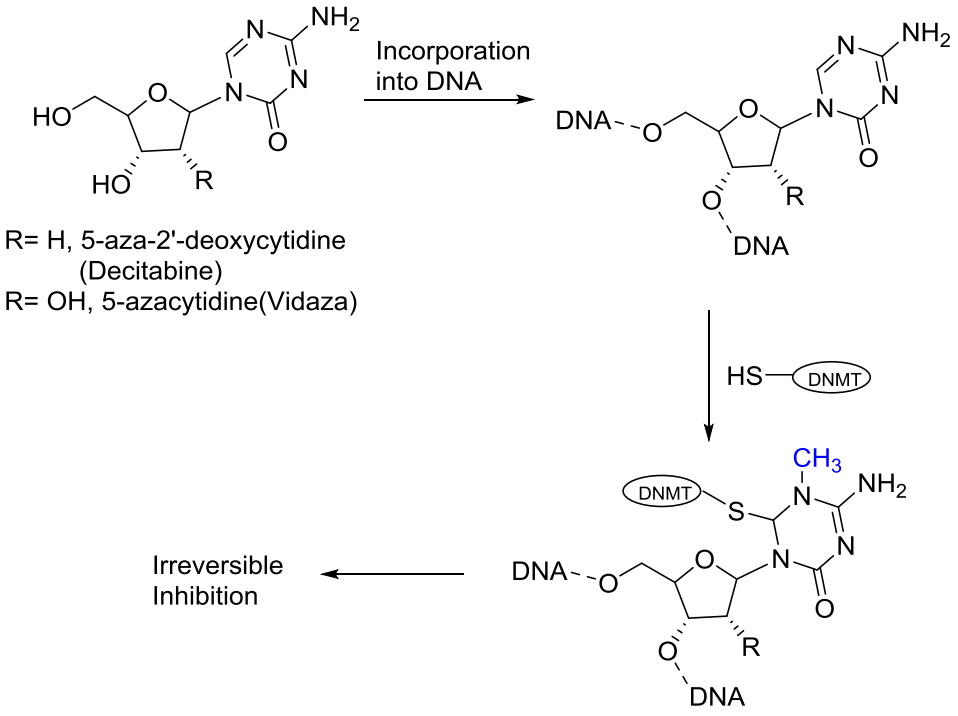

Figure 5.4 The mechanism of 5-azanucleoside analogues induced degradation of DNMTs.

Unlike genetic changes, epigenetic changes can be modified by the environment, diet, or pharmacological intervention. There are many bioactive dietary compounds that

can modulate the DNMT enzyme activities and thus promoter methylation pattern of genes in cancer. Apigenin in Parsley (Petroselinum), curcumin (1,7-bis (4-hydroxy- 3-methoxyphenyl)-1,6-heptadiene-3,5-dione) in turmeric (Curcuma longa), EGCG in green tea (Camellia sinensis), genistein in soybean (Glycine max), resveratrol (3,40,5-trihydroxytrans- stilbene) in red grapes (Vitis vinifera), sulforaphane (SFN) in cruciferous vegetables (Brassicacaae), and the caffeic acid and chlorogenic acid as coffee polyphenols were reported to inhibit DNMT enzyme activity in various cancer models.[106, 107]

SAH can bind to DNMTs and inhibit their catalytic reaction and has an important role in the regulation of biological DNA methylation. SAH analogs presumably binding in the co-factor binding pocket have also been reported as selective inhibitors against DNMT1 over DNMT3b2 by using rational design approach.[108] According to previous data (Figure 5.5 d (a)), replacement of the homocysteine side chain by the five membered (2S,4S)-4-mercaptopyrrolidine-2-carboxylic acid was a good replacement, while the corresponding six-membered counterpart was less active. It was also found that deletion of the carboxylic group (Figure 5.5 d (d)) eliminating the zwitter-ionic character was less active against enzymes. In addition, another SAH analogue (Figure 5.5e), which contains a shorter carboxyl side chain, was reported[109] to be a strong inhibitor for DNMTs, although a natural compound Sinefungin(figure 5.5f) is more potent.[110]

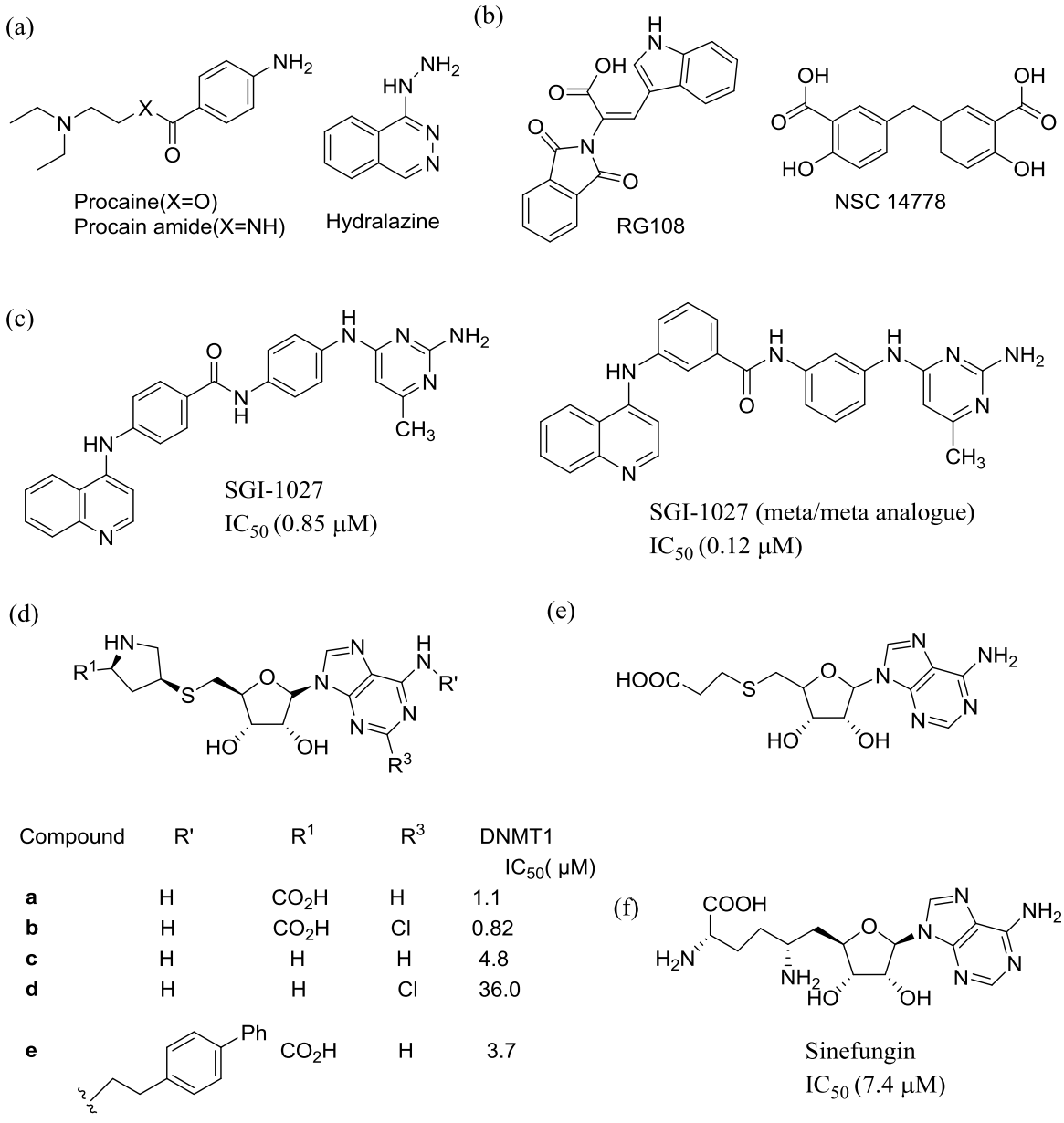

Figure 5.5 Chemical structures of non nucleoside DNMT inhibitors and other selected compounds with proposed demethylating activity. (a) Drugs used for other indications, (b) Compounds identified using virtual screening, (c) SGI-1027 and its analogue[105] (d) and (e) SAH analogs (f) Sinefungin.[104]

5.3 Crystal Structure Study and Design Concept for DNMTi

SAH is a known strong inhibitor of DNA methyltransferases at the SAM binding site, although the biological roles of SAH on the inhibition of DNMTs are not completely understood. Furthermore, SAH-binding proteins are widely found in cells and it is unlikely to use SAH to selectively inhibit DNMTs. The ideal inhibition should fill the following requirements. First, they can specifically inhibit cytosine DNA methyltransferases vs. other methyltransferases, and second, as mentioned earlier, they should bind DNMTs reversibly. The crystallographic structure of human DNMT1 is a very important tool to guide the design. There is more than one binding site within DNMT1. The one for SAM and the one for the extra helical cytosine of the duplex DNA are close to each other. It can be expected that an SAH analogue that occupies both pockets at the same time would selectively bind DNMTs. However, there is a concern whether this SAH analogue would bind differently in the absence of the DNA, as a study on a prokaryotic DNMT suggested that binding of SAM occurred after DNA binding, therefore it is likely that the SAM binding pocket is shaped through DNA binding. A superposition study of a bound SAH in DNA-free mDNMT1 and the productive covalent mDNMT1-DNA complex was performed by Wu[111] to evaluate the significance of the change. The results showed that SAH undergoes a slight positional shift from the DNA-free state to its productive covalent complex with DNA. Although the overall structural change is so small that the SAH analogue would bind the protein in its active conformation in the absence of the DNA shown as Figure 5.6.[112]

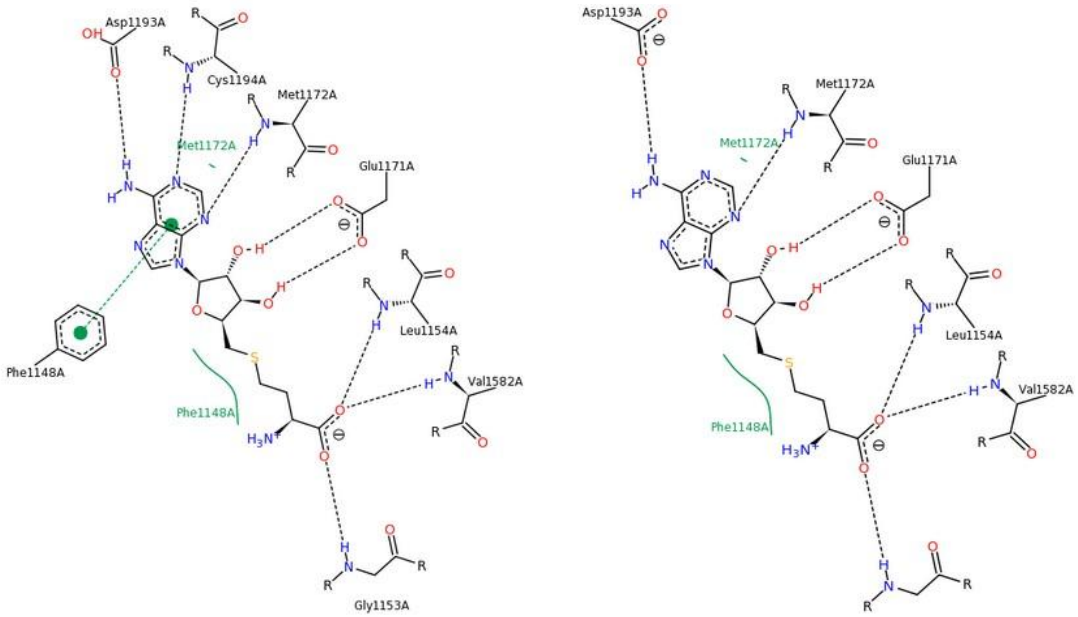

Figure 5.6 Interactions between SAH mDNMT1-DNA complex. Left: Interactions between SAH and binding pocket residues in free mDNMT1. Right: Bound SAH in the productive covalent mDNMT1-DNA complex is stabilized. Hydrogen bonds: black dashed lines; hydrophobic interactions: green dashed lines. [112]

The crystal structure of SAH and human DNMT1-DNA complex (figure 5.7) provided additional detailed information on the relative geometric locations of these two binding sites. The flipped out cytosine adopts an extra helical position to insert into a cytosine binding site that is in close proximity to the sulfur of SAH (Figure 5.7). The distance between the carbon at 5 position of cytosine and the sulfur atom of SAH is 4.5 Å. The flipped-out cytosine was stabilized by surrounding residues in the active site of the enzyme. (Figure 5.8) The carbonyl of the cytosine forms two hydrogen bonds with Arg 1313 and Arg 1315, and the 3-nitrogen forms a hydrogen bond with Glu 1269. The 4-amino group forms a hydrogen bond with the backbone of Pro 1227. This result indicates that the carbonyl group, the 3-position nitrogen and the 4-position amino group

of cytosine may play vital roles in binding. The 3-nitrogen may be less important when Glu1269 is deprotonated.

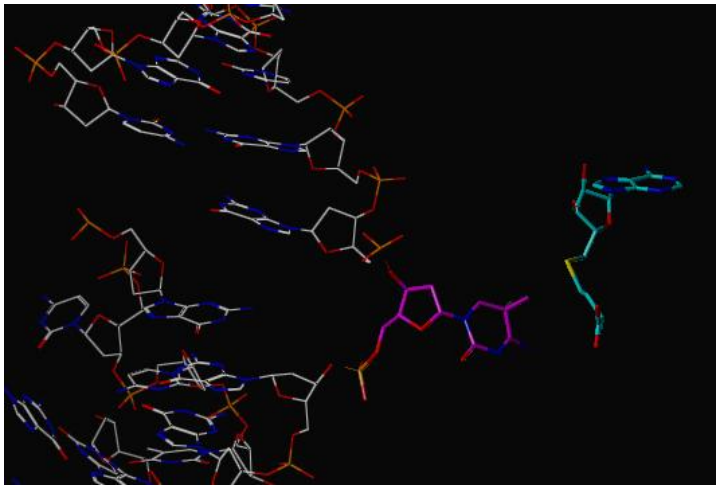

Figure 5.7 The crystal structure of SAH and human DNMT1-DNA complex (PDB: 4DA4). SAH1701 in chain A, Cytosine4918 in chain D, and parts of the DNA sequences in chain D were selected and shown only.[111]

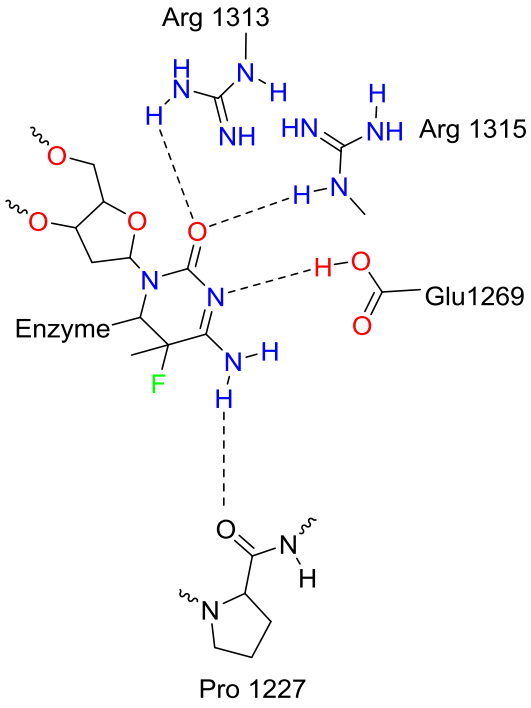

Figure 5.8 The flipped-out cytosine is stabilized by surrounding residues in the active site of the enzyme.[112]

A transition state analogue was designed to occupy the SAM binding site and the cytosine binding site simultaneously. It was decided that part of the SAM core structure was to be kept and part to be deleted. First, adenosine and the long chain should be kept. As Figure 5.6 shows, SAH can form several hydrogen bonds with the amino acid residues at the binding site of DNMT1, such as Glu 1171, Met 1172, Leu 1154, Val 1582, Gly 1153. Therefore, to maintain these interactions between DNMT1 and SAM analogues, the adenosine and carboxyl group with the long chain should be kept. Second, to be a selective inhibitor, extra binding interactions other than the ones involving SAH are required. The process of DNA cytosine methylation involves the addition of a methyl group to cytosine at the C5 position. Therefore, introducing a cytosine to the SAM analogue may enhance binding by taking advantages of the interactions between cytosine and cytosine-binding side chains. To simplify the synthesis, it was decided to use other functionalized aromatic rings (benzene or heterocyclic rings) to replace cytosine. Third, the sulfur atom with positive charge can be changed to a nitrogen atom, which is expected to be protonated under physiological conditions. Fourth, the α-amino group of SAM can be removed because it is not involved in any interaction with the protein, and it may affect the protonation state of the adjacent tertiary amine.

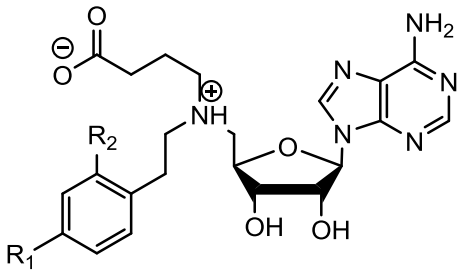

24: R_1=H, R_2=H
25: R_1=NO_2, R_2=H
26: R_1=H, R_2=OH

Figure 5.9 Design of a transition state inhibitor of DNMT.

In summary, the design of SAM analogues was inspired by the catalytic mechanism of DNMT and the study of the crystal structure of DNMT/DNA/SAH complex. The distance between the branching nitrogen and the aromatic ring is set to be 2 C-C bond-long to reflect the distance during the methyl transfer in the catalytic mechanism. A series of compounds were designed that contained different aromatic derivatives. These derivatives were expected to interact with the amino acid side chains mimicking the flipped cytosine in the catalytic mechanism. Among these compounds, **24** was previously prepared by Wu.[111] The preparation of **25** and **26** is described below.

5.4 Synthesis of DNMT Inhibitors

5.4.1 Retrosynthetic Analysis

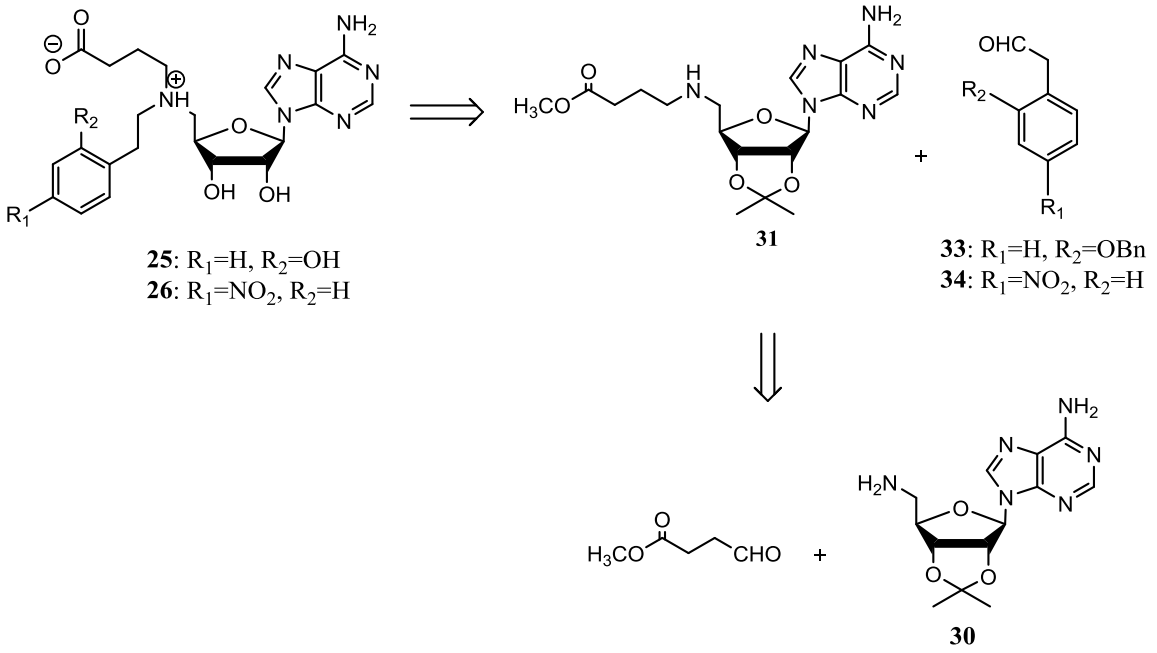

Scheme 5.1 Retrosynthetic Analysis of Target Compounds.

Compound **24-26** can be generated from three parts according to our retrosynthetic analysis (Scheme 5.1): the phenylacetaldehydes (**33, 34**), methyl 4-oxobutanoate, and 5'-amine-modified adenosine **31**. The three parts will be joined together by two successive reductive amination reactions.

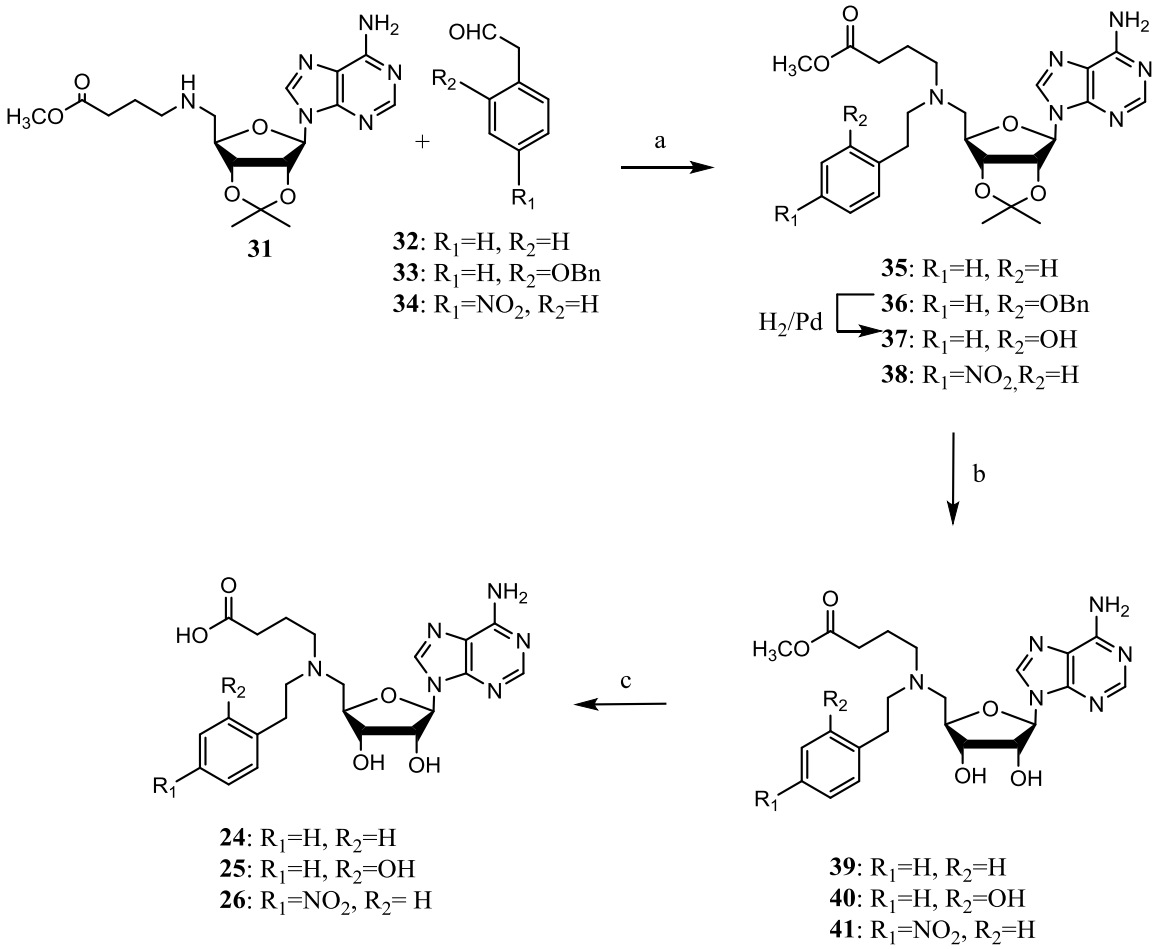

Scheme 5.2 General Synthesis Route. (a) $NaBH_3CN$, AcOH, (b) p-TsOH.H_2O (2equiv.), MeOH, (c) KOH.

The general synthetic strategy after the first reductive amination reaction is shown in scheme 5.2. In the case of the synthesis of **25**, the O-Bn group was removed by hydrogenolysis. The acetonide protection on the 2′- and 3′ hydroxyl groups was removed

via acid-catalysis methanolysis. The methyl esters were hydrolyzed under strong alkaline conditions.

5.4.2 Synthesis of the Common Precursor 31

The synthesis started from commercially available adenosine. The 2′-and 3′-hydroxyl groups were protected using acetonide. The reaction initially finished in nearly 60% yield. The reaction conditions included 11 mol equivalents of *p*-toluenesulfonic acid (*p*-TsOH) and a large excess of acetone, which was both a reactant and a solvent. The product was isolated by organic extraction. Several conditions have been examined to improve the reaction yields. We changed the amount of *p*-TsOH to 4.3 mol equivalents and decreased the solvent volume by 10 folds (Scheme 5.3). This change increased the acid catalyst concentration although the total amount of catalyst became less. In addition, extremely dry acetone was successfully prepared by fractional distillation over Drierite®. Potassium carbonate pellets were added directly to the reaction mixture to neutralize *p*-TsOH. This workup procedure avoided aqueous conditions which could convert some of the product back to the starting material due to the slow neutralization process. The yield was improved to 93% yield, higher than reported in most literatures.[113, 114] After the acetonide was installed, a leaving group was introduced by transforming the free 5′-hydroxy group of the 2′, 3′-O-isopropylideneadenosine (**27**) into a mesylate ester (**28**) using MsCl (Methanesulfonyl chloride) in the presence of triethylamine (TEA). Increasing mol. equivalence of MsCl from 1.2 to 1.6 and lowering solvent volume by 9 fold improved product yield. Compound **28** was very unstable and it was initially directly converted to an azide by adding sodium azide to the crude product in DMF without further purification. Later we found that purification of compound **28** using oven-dried

silica gel chromatography gave high recovery and the subsequent reaction with azide could be completed in much improved yield. Reduction of compound **29** was achieved by hydrogenolysis on Pd/C at 50 psi, which gave 5′-aminoadenosine derivative **30**

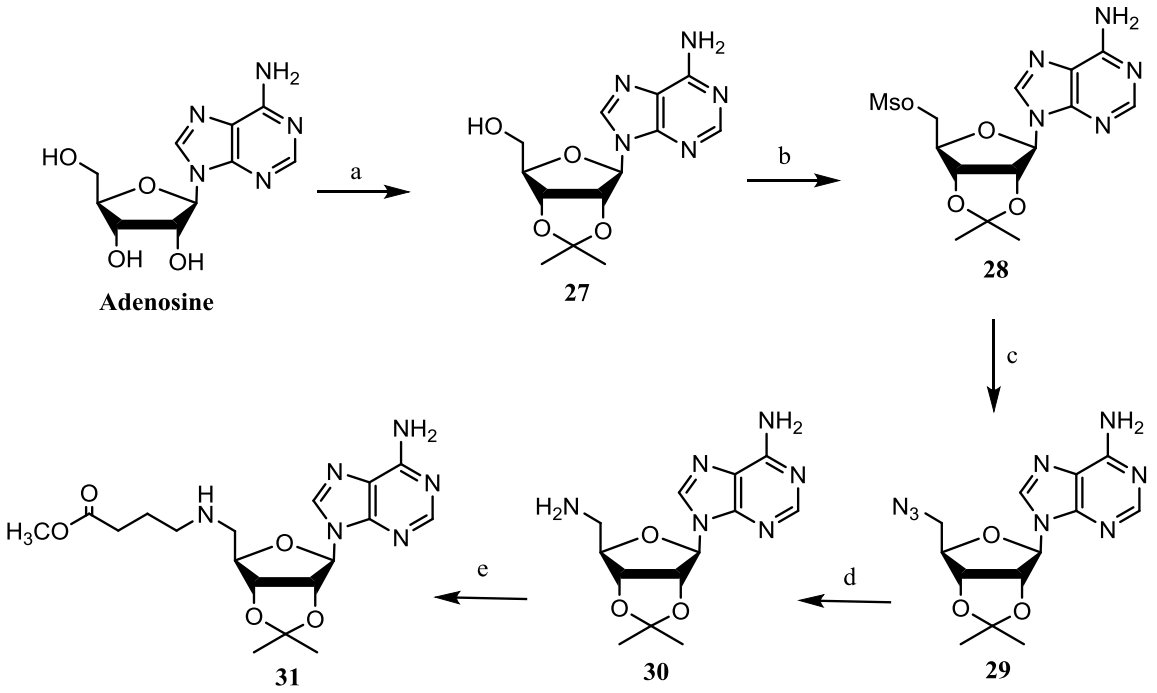

Scheme 5.3 Synthesis of Compound **31** (a) Acetone, p-TsOH, rt, 2 h, 93%. (b) CH_2Cl_2, EtN_3, MsCl, rt, 1.5 h, 89%. (c) NaN_3, DMF, 70°C, 48 h, 60%. (d) H_2, 10% Pd/C, MeOH, 50 psi, 16 h, 70%. (e) $NaBH_3CN$, AcOH, methyl-4-oxobutanoate, rt, 1.5 h, 12%.

Reductive amination of compound **30** with methyl 4-oxobutanoate was hard to control. As a result, disubstituted byproduct was formed: the mono- and di-substituted products could not be completely separated (Scheme 5.4.). Reducing the amount of methyl 4-oxobutanoate by 3 folds gave better selectivity, however, with a comprised low yield. The desired product was obtained in pure form in 12% yield from the amine (Scheme 5.1).

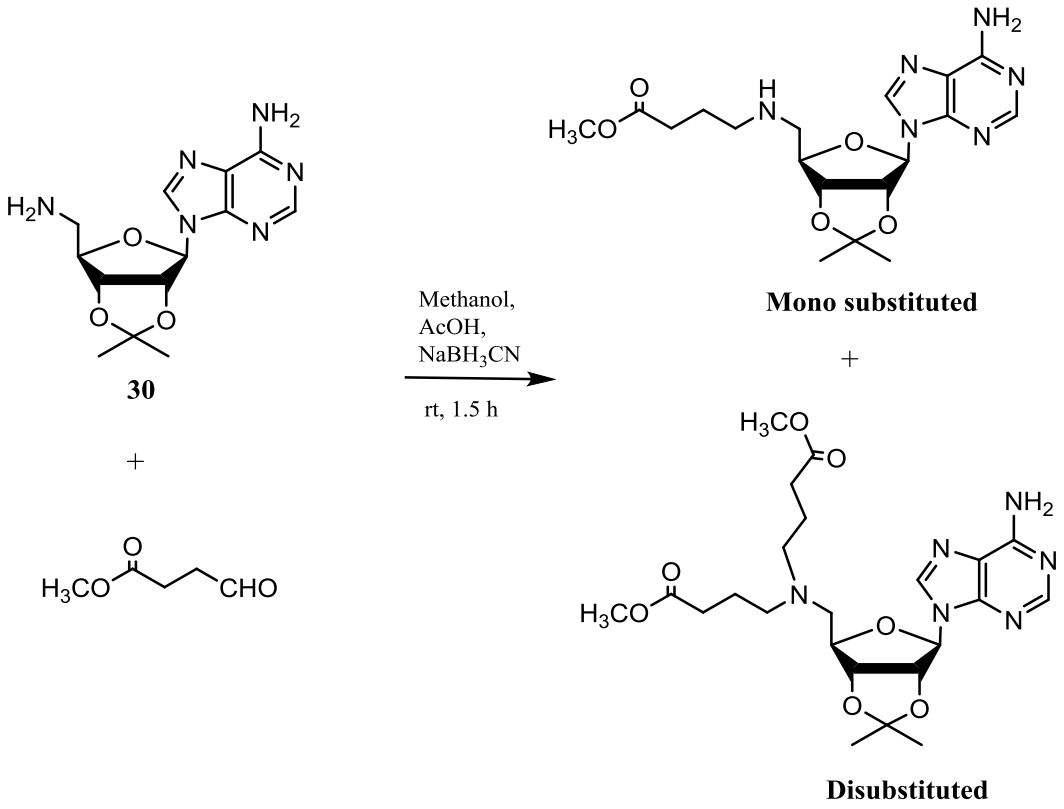

Scheme 5.4 Reductive Amination of Compound **30.**

5.4.3 Synthesis of 2-(*o*-Benzyloxy)phenylacetaldehyde (33)

The benzyl protected 2-(*o*-benzyloxy)phenylacetaldehyde can be synthesized from the commercially available 2-(*o*-hydroxyphenyl)ethanol. First, the 2-hydroxyl group was protected with a benzyl group (scheme 5.5) to prevent oxidation in next step. The next step is the oxidation of (2-(*o*-benzyloxyphenyl)ethanol. IBX (2-iodoxybenzoic acid) was used to oxidize the starting material to generate the desired compound **33** in 33% yields (Scheme 5.5).

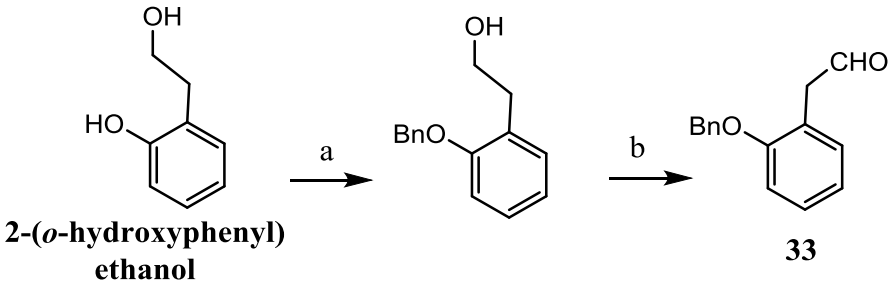

2-(*o*-hydroxyphenyl) ethanol **33**

Scheme 5.5 Synthesis of 2-(*o*-Benzyloxy)phenylacetaldehyde (**33**) (a) K_2CO_3,BnBr, DMF, 60°C, 16 h, 52%. (b) IBX, THF, 60°C, 16 h, 33%.

5.4.4 Synthesis of Compound 25

Compound **33** was reacted with **31** via reductive amination and the product **36** was purified by column chromatography (Scheme 5.6). The product formation was confirmed by Mass analysis (Figure 5.10a). The benzyl group was removed by hydrogenolysis. The product was subjected to acid methanolysis to remove the acetonide (Scheme 5.7). The product was used directly for next base hydrolysis reaction. After base hydrolysis, the final compound **25** was obtained. The yield of compound **25** was too low for column chromatography purification. Therefore, it was purified by HPLC and the collected fractions were analyzed by Mass spectroscopy (Figure 5.10b).

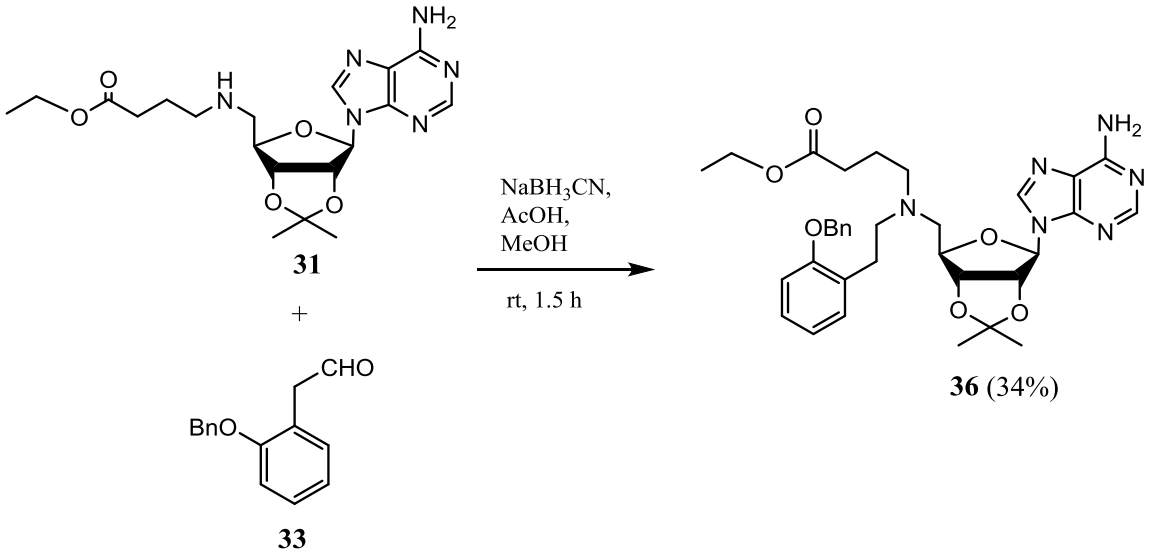

Scheme 5.6 Synthesis of Methyl Ester Compound **36**.

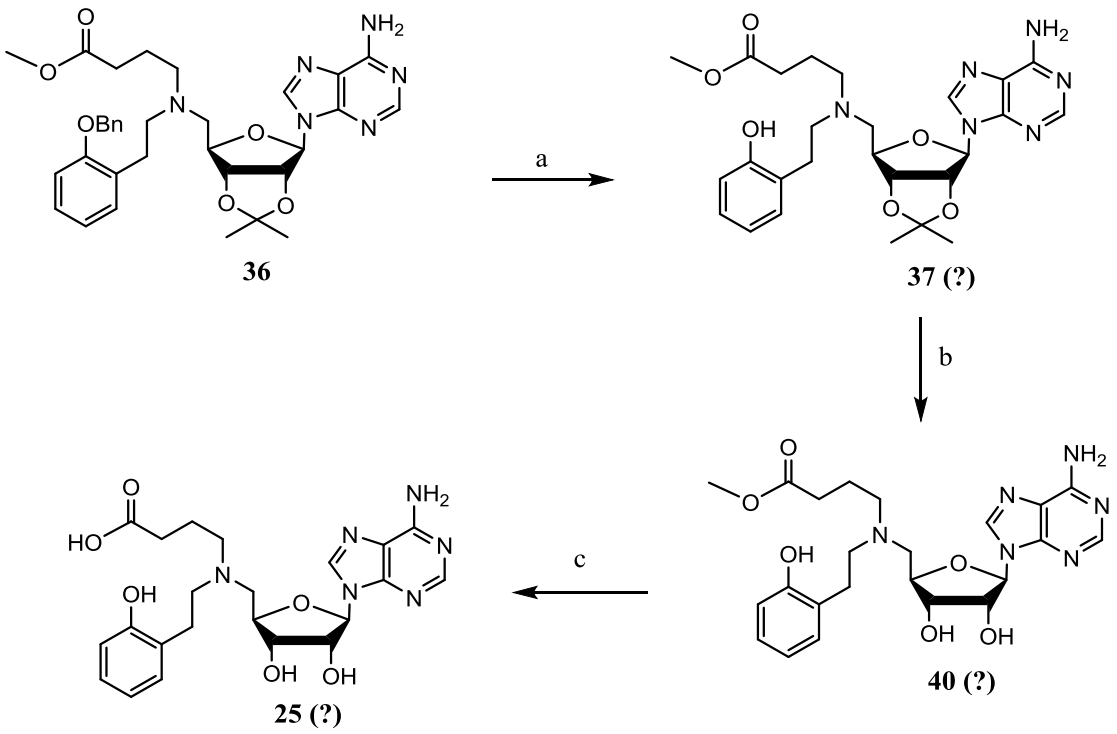

Scheme 5.7 Synthesis of Compound **25**. (a) H_2, 10% Pd/C, MeOH, 50 psi, 4 h (b) 0.2M HCl,MeOH:H_2O (10:1),rt, 16 h(c) 0.4M KOH, MeOH:H_2O (10:1),rt,16 h.

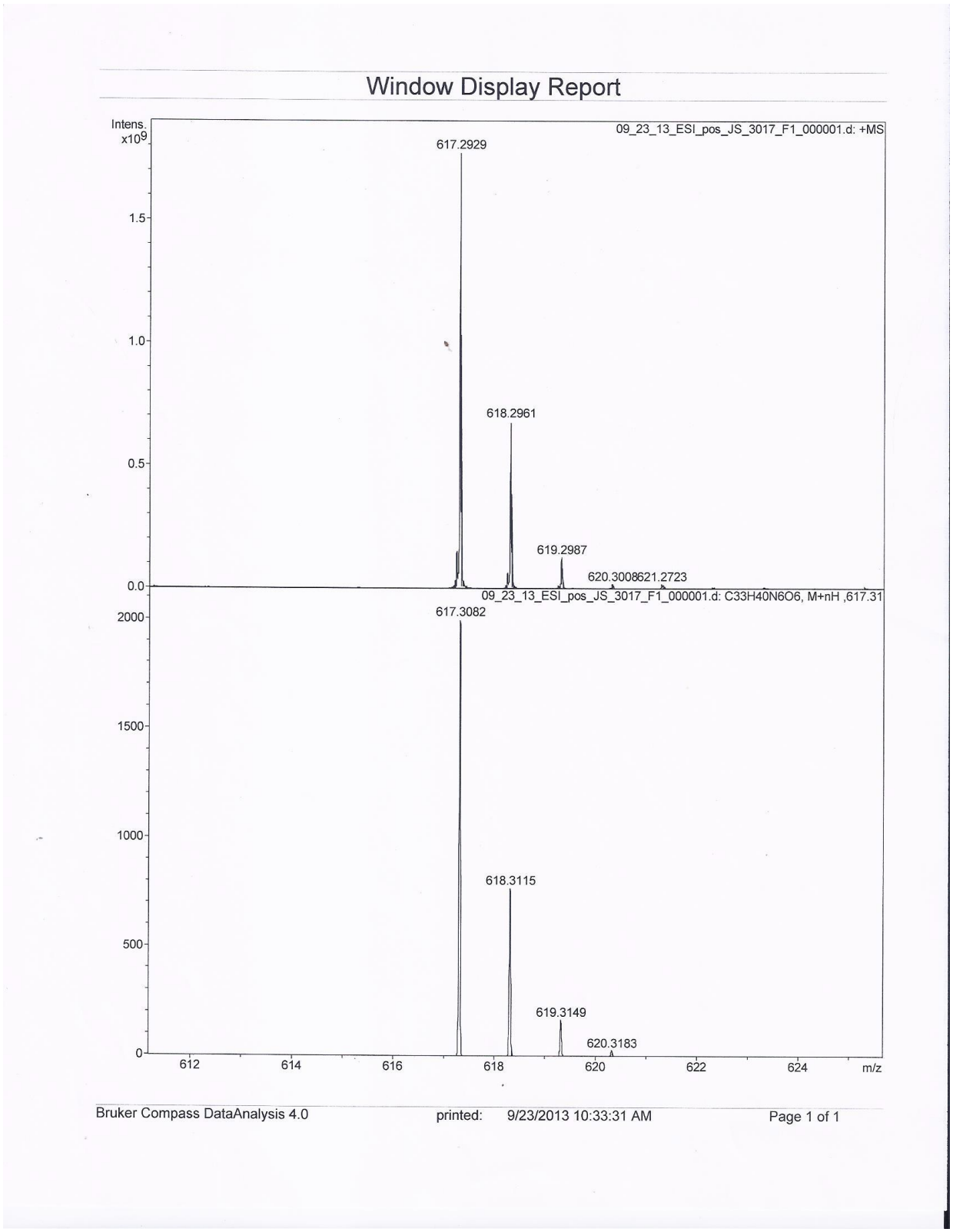

Figure 5.10a Mass Spectra of Compound **36**. (Bottom: ESI-MS ($M+H^+$) for $C_{33}H_{40}N_6O_6$, expected 617.3082, found (on top) 617.2929)

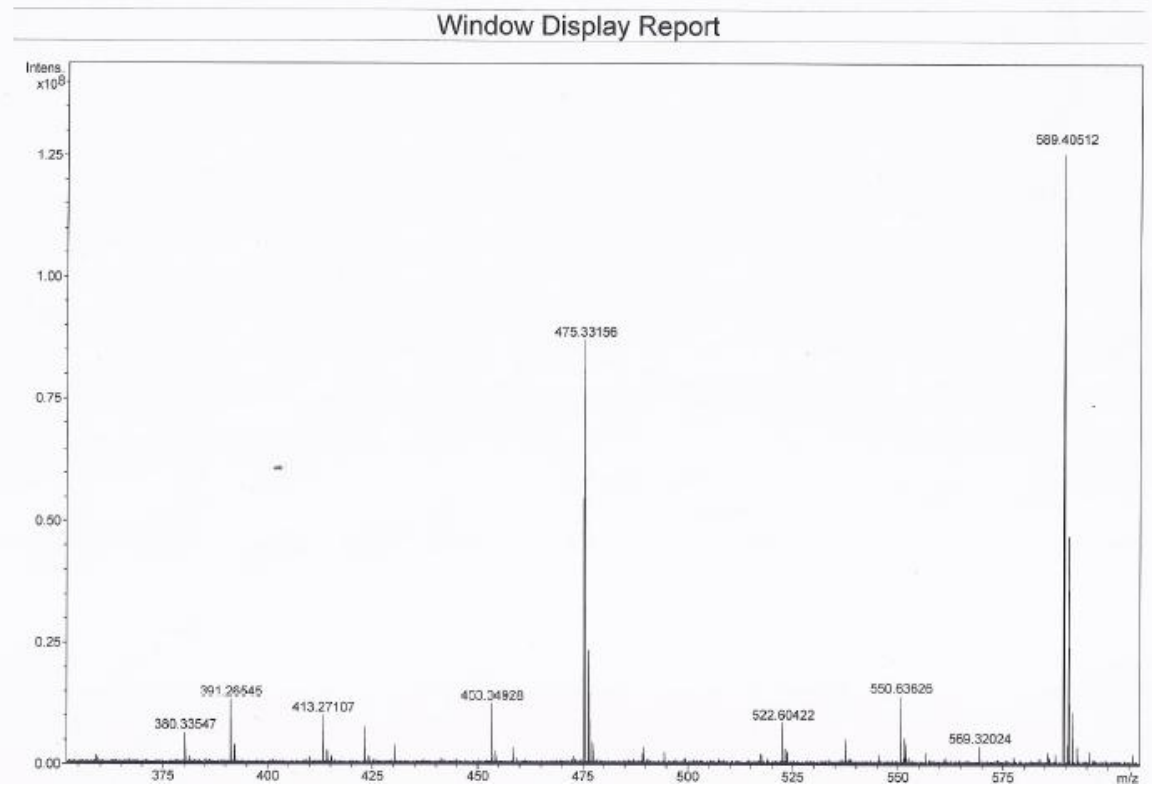

Figure 5.10b Mass Spectra of Final Compound **25**. Observed ESI-MS ($M+H^+$) 475.3316($C_{22}H_{31}N_6O_6$).

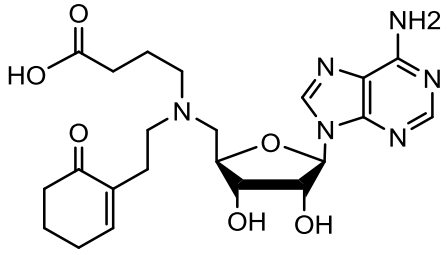

Figure 5.11 Cyclohexanone Derivative of Compound **25**

However, the Mass spectrum of the expected fraction showed a molecular ion with higher m/z than expected: ESI-MS ($M+H^+$) for $C_{22}H_{29}N_6O_6$, expected 473.2065, Observed ESI-MS ($M+H^+$) 475.3316($C_{22}H_{31}N_6O_6$) (Figure 6.1b). One possible explanation for this observation is that the phenol product was further reduced in the

hydrogenolysis conditions and the cyclohexanone derivative of compound **25** was generated (Figure 5.11).

5.4.5 Synthesis of 4-Nitrophenylacetaldehyde (34)

Compound **34** needs to be synthesized by oxidation from 4-nitrophenylethanol. PCC oxidation was tried at the beginning. To our surprise, ^{1}H NMR study of the product showed that despite the presence of the aldehyde peak, the expected CH_2 peak was missing at around 3-4 ppm (Figure 5.12). The spectrum agreed with the formation of 4-nitrobenzaldehyde (Scheme 5.8 (a)), which implied that this oxidation condition was too strong. The C-C bond of the possibly formed 4-nitrophenylacetaldehyde was cleaved in such conditions. Later, we decided to tried milder oxidation reaction. Neither Swern oxidation nor TEMPO-NaClO oxidation gave the desired product. Therefore DMP was selected as the oxidant.

We planned to use DMP (Dess–Martin periodinane) because DMP is mainly used as an oxidant for complex, sensitive and multifunctional alcohols. According to reported procedure, we synthesized DMP from IBX (2-iodoxybenzoic acid) and acetic anhydride.[54, 115] The product was directly precipitated from the reaction mixture when the temperature was cooled to room temperature. The resulting white solid was not soluble in methylene chloride, suggesting that DMP was not completely formed and the precipitate contained a large amount of IBX. Reaction with this self-prepared DMP proceeded but generated poor yields even with extended time. Later we used pure IBX to replace DMP and increased the temperature for the reaction and obtained final compound **34** in 34% yield (Scheme 5.8 (b)).[116]

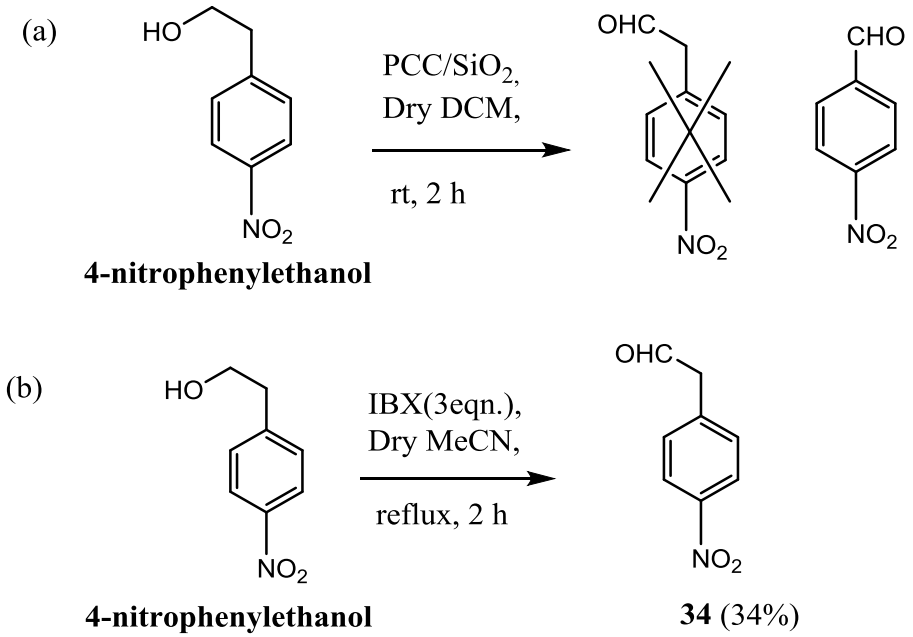

Scheme 5.8 Synthesis of Compound 4-Nitrophenylacetaldehyde **(34)**.

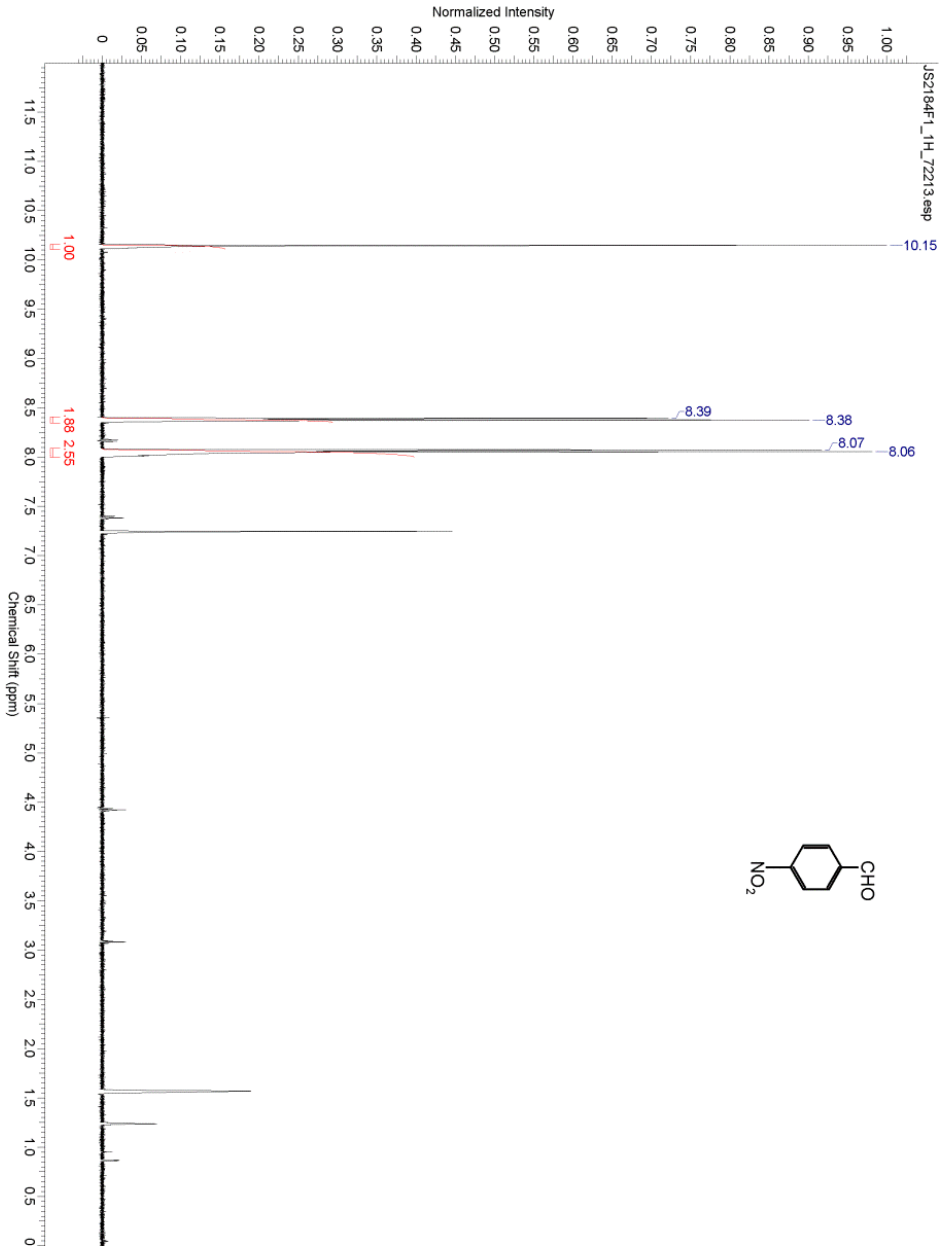

Figure 5.12 ^{1}H NMR Spectrum of 4-nitrobenzaldehyde.

5.4.6 Synthesis of Compound 26

During the synthesis of **36**, we found through NMR study that methyl 4-oxobutanoate was oxidizing slowly in air, which could impact the yield and the purity of the reductive amination product. Methyl 4-oxobutanoate is expensive and it is unlikely to purchase a new batch for each reaction. Therefore we have decided to prepare the material in our lab. Ethyl 4-bromobutyrate was identified as the commercial precursor to ethyl 4-oxobutanoate. Several efforts were made to realize this transformation. The first attempt was the direct oxidation of the alkyl bromide to generate the aliphatic aldehyde. Oxidation of alkyl halides with pyridine N-oxide has been known as a unique method to obtain carbonyl compounds.[117] N-oxide is the oxidized product of a tertiary amine, which finds wider application as an oxidants.[118] It can be prepared using a variety of oxidants including m-chloroperoxybenzoic acid (mCPBA) and hydrogen peroxide.

Accordingly, 4-dimethylaminopyridine N-oxide (DMAP N-oxide) was synthesized using m-CPBA.[119] IR spectrum showed complete conversion to DMAP N-Oxide. The resulting DMAP N-Oxide was used directly for the oxidation of ethyl 4-bromobutyrate (Scheme 5.9 (a)). However, crude NMR of the reaction showed no peak at around 9-10 ppm, indicating no aldehyde product was formed. It was also reported[120] that oxidation of primary, secondary, and tertiary amines with basic permanganate and rapid isolation of the reaction products result in an advantageous method for degrading amines to aldehydes and ketones. Accordantly, we tested the reaction using ethyl 4-aminobutyrate hydrochloride as a staring material to synthesize ethyl 4-oxobutanoate (Scheme 5.9 (b)).[121] Unfortunately, this reaction did not afford the desired product either. Finally, oxidation of ethyl 4-bromobutanoate was made successful by using commercial

pyridine N-Oxide (Scheme 5.9 (c)). The reaction was completed in 16 h and purified by column chromatography, giving ethyl 4-oxobutanoate in 9.6% yield. This low yield became a problem for the next steps when the synthesis was scaled up.

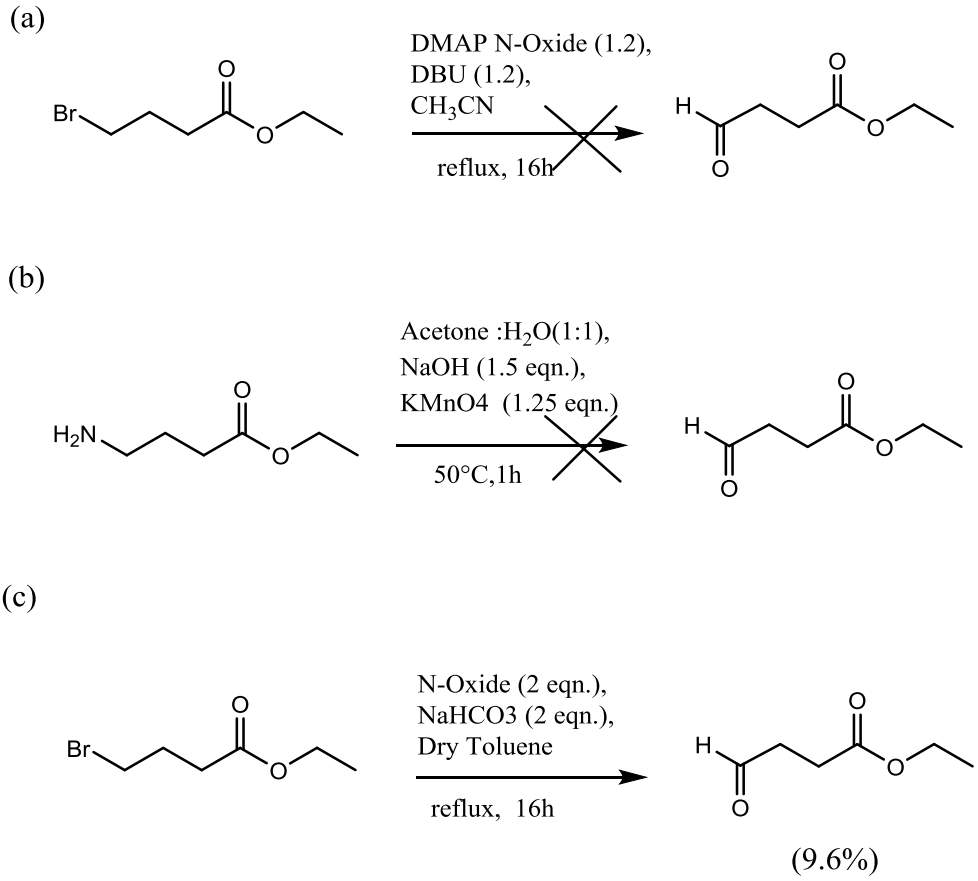

Scheme 5.9 Synthesis of Ethyl 4-Oxobutanoate.

Compound **30** was reacted with ethyl 4-oxobutanoate via reductive amination (Scheme 5.10). However, even with this freshly-made highly pure aldehyde, we still could not improve the yield. This suggests that the selectivity of N-alkylation of primary amine is inherently difficult to control. Later, we have changed our reaction route. Since compound **34** was less costly than ethyl 4-oxobutanoate, we tried the first reductive

amination with compound **34** and **30** in hope that the monoalkylated product can be obtained in higher selectivity. Unfortunately, the improvement was minimal (Scheme 5.11).

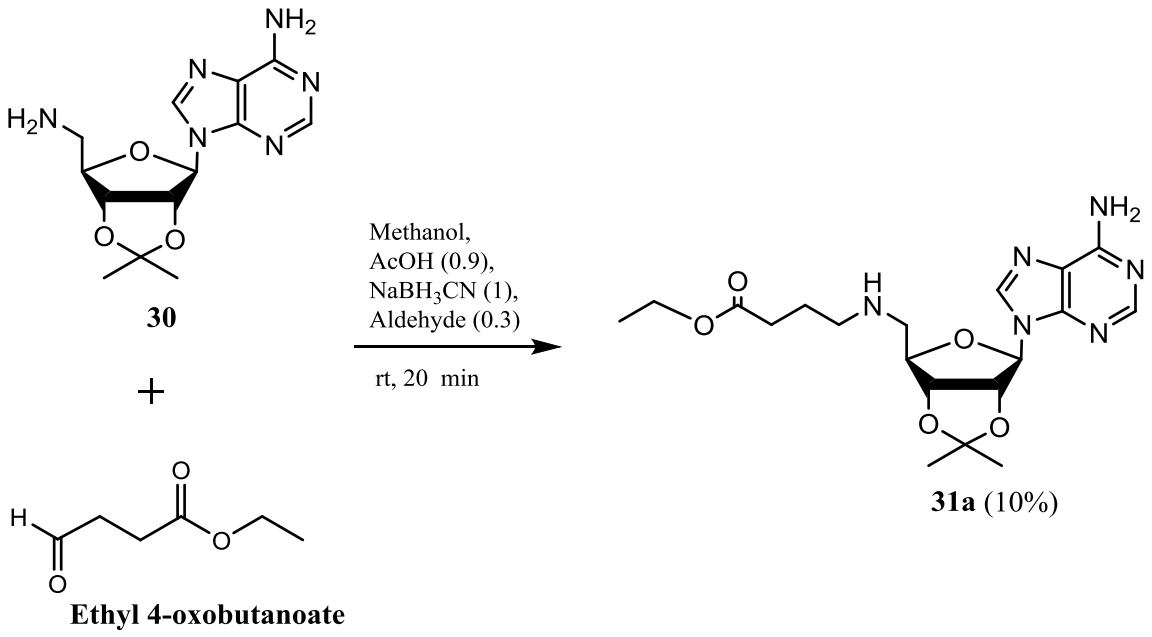

Scheme 5.10 Modified Synthesis of Compound **31a** (by reductive amination).

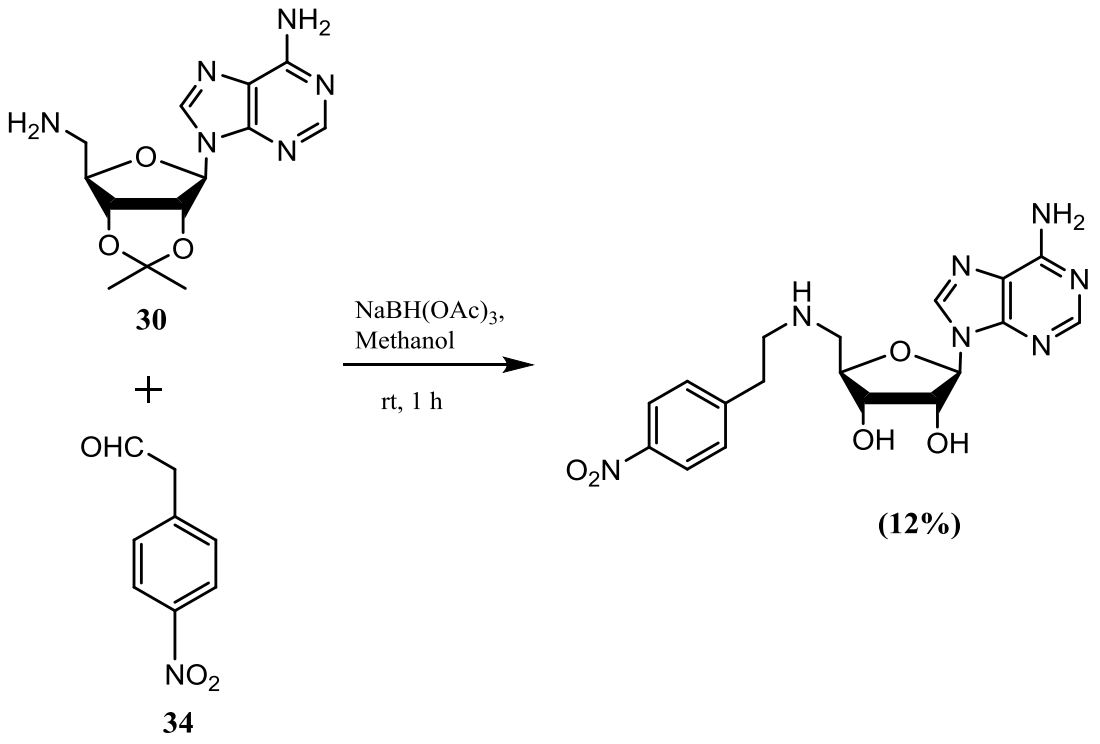

Scheme 5.11 Reductive Amination of Compound **30** and Compound **34**.

Discouraged by the failures to obtain pure compound **31** via reductive amination, we decided to directly synthesize **31** with S_N2 reaction of ethyl 4-bromobutyrate. However, this N-alkylation reaction appears deceptively simple but it is often unselective due to the concomitant overalkylations which give rise to mixtures of primary, secondary, and tertiary amines, as well as quaternary ammonium salts. Although, by careful adjustment of reaction parameters such as the relative proportions of the reactants, reaction temperature, and the use of additives, one can tune conditions accordingly, so that the secondary amine becomes predominant. The common protocol includes the most conventional conditions utilize an alkali metal carbonate (e.g. K_2CO_3) in a polar aprotic solvent (DMF,DMSO,or MeCN) at room temperature or under heating, depending on the nature of the starting materials.[121] It was also observed that the course of the alkylation

was strongly dependent on the number of carbon atoms present in the alkyl bromide; longer chain underwent alkylation more efficiently to afford monoalkylation product. Conversely, use of smaller chain lengths(<5 carbons) reversed the selectivity, giving rise to dialkylamines.[121]

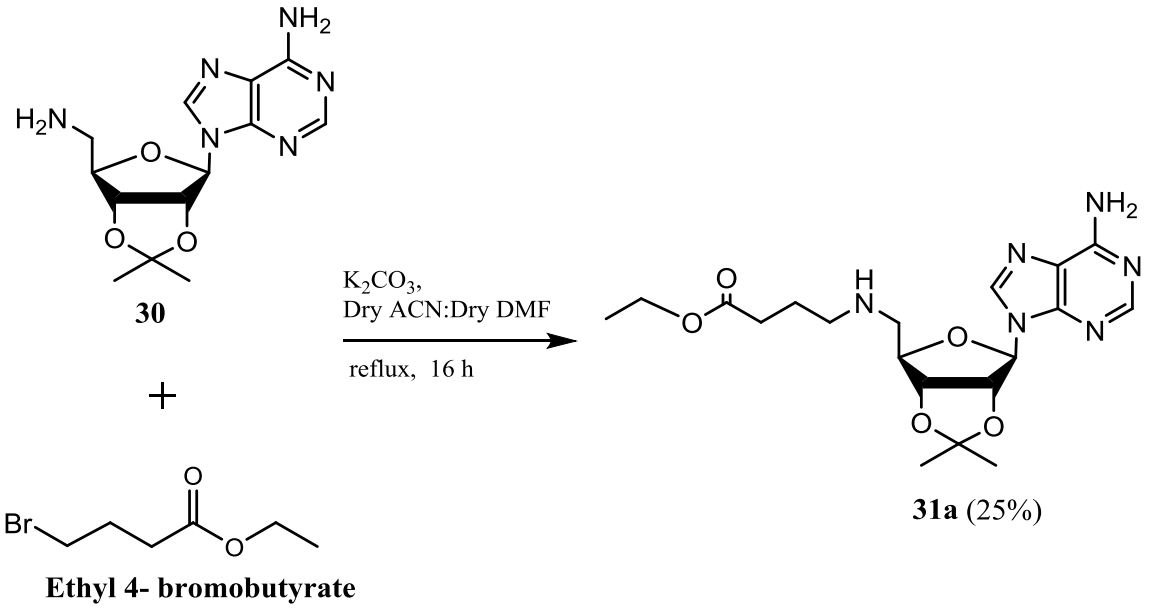

Scheme 5.12 Synthesis of Compound **31a** (by N-alkylation).

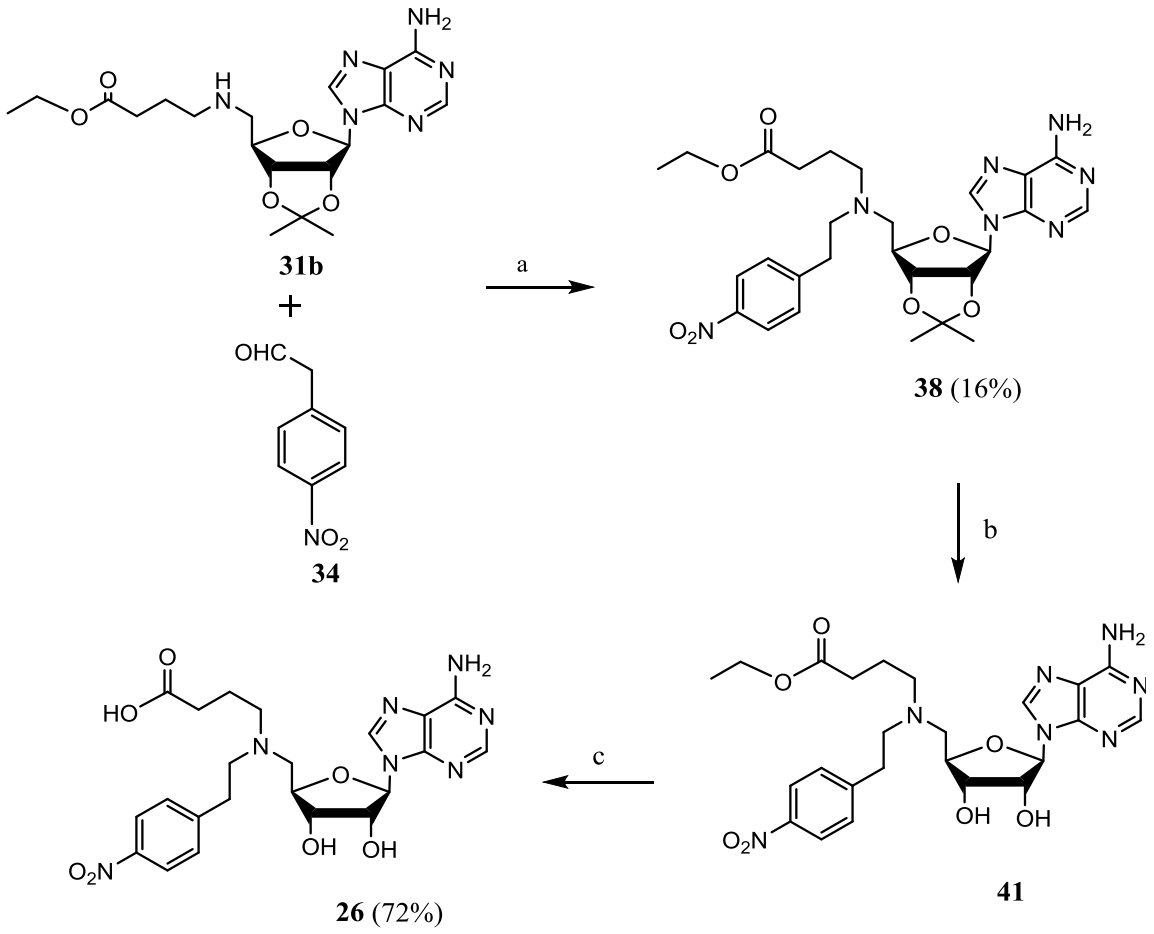

Scheme 5.13 Synthesis of Compound **26** (a) $NaBH(OAC)_3$,Methanol, rt, 1h, 16%. (b) 0.5M HCl, MeOH: H_2O (1:0.2), rt, 16 h. (c) 0.1M KOH, MeOH: H_2O (1:0.3), rt, 42 h, 72%.

To synthesize compound **31b,** ethyl 4-bromobutyrate was added in portion and DMF was added as co-solvent to increase the solubility of K_2CO_3. These efforts contributed to the formation of desired product **31**. (Scheme 5.12).[122] The product was purified by column chromatography in 25% yield. The second reductive amination was

performed as shown as scheme 6.21, giving compound **38** in 13 % yield. After acid and base hydrolysis, the final compound **26** was obtained (Scheme 5.13).

5.5 Materials and Methods

5.5.1 Organic Synthesis

All chemicals were purchased from Sigma-Aldrich or Fisher Scientific unless specified. Acetone was dried over Drierite® and then distilled under Ar. CH_2Cl_2 and DMF were distilled over CaH. NMR spectra were recorded on a 300 MHz Bruker spectrometer or 500 MHz Varian spectrometer. A liquid chromatography Model SIL-10 A (Shimadzu Crop.) was used. A LC real time analysis computer integrator was used for retetion time mesurements. The UV-Vis detector SPD-20A (Shimadzu Corp.) was used as follows detector 1= 260 nm and detector 2= 260 nm. A C-18 reversed phase (7.8 X 150mm) column filled with 10 μm (average particle size) was also used.

Compound 27: To a suspension of adenosine (2.0 g, 7.5 mmol) in dry acetone (20 mL) was added 36.5 mmol of dry p-TsOH (6.3 g, 4.2 equiv.) in one portion. The mixture was stirred under an atmosphere of Ar at room temperature for 2 h. The mixture was stirred with 100 mL 0.5M K_2CO_3 solution for 10 min and then extracted with methylene chloride till no spot from the organic extract can be observed on TLC. The organic layer was dried over $MgSO_4$ and then filtered. The solvent was evaporated. The product was directly used for the next reaction without purification. The white solid was obtained (2.14 g, 93%):^{1}H NMR (300 MHz, $CDCl_3$) δ ppm 1.39 (s, 3 H) 1.66 (s, 3 H) 3.97 (s, 1 H)

4.57 (s, 1 H) 5.12 (s, 1 H) 5.19 (s, 1 H) 5.83 (s, 1 H) 5.91 (s, 1 H) 6.52 (s, 1 H) 7.99 (s, 1 H) 8.33 (s, 1 H).

Compond 28: A solution of 4.88 mmol of 2′,3′-*O*-isopropylideneadenosine (1.5 g) in 20 mL of dry dichloromethane was flushed with Ar before 1.71 mL of triethylamine (11.7 mmol, 2.4 equiv.) and 0.57 mL methanesulfonyl chloride (7.32 mmol, 1.5 equiv.) were added.[123] Solution was stirred at room temperature for 1.5 hr and then 20 mL of saturated $NaHCO_3$ solution was added. The layers were separated and the organic layer was washed with 20 mL sat. solution of NaCl. The combined organic layers were dried over $MgSO_4$ and the solvent was evaporated. The crude product was purified by silica gel chromatography (Ethyl acetate/ Hexane 9:1) to give the mesylate ester (1.8 g, 89 %) as colourless foam. The product was directly used for the next reaction without NMR identification.

Compound 29: A mixture of **28**, (1.70 g, 40 mmol) and sodium azide (2.60 g, 0.04 mmol, 10 equiv.) was suspended in anhydrous DMF (18 ml). The reaction was heated at 70 °C for 48 hr.[124] The mixture was filtered, and evaporated under reduced pressure. DMF was removed in vacuo. The residue was purified by silica gel chromatography (Ethyl acetate/Hexane 1:9). A Light yellow syrup (818 mg, 60%) was obtained. ^{1}H NMR (500 MHz, METHANOL-d_4) δ ppm 1.33 - 1.41 (m, 3 H) 1.57 - 1.64 (m, 3 H) 3.67 - 3.82 (m, 2 H) 4.37 (br. s., 1 H) 5.04 (d, *J*=6 Hz, 1 H) 5.27 (br. s., 1 H) 6.09 - 6.18 (m, 1 H) 8.15 - 8.22 (m, 1 H) 8.29 - 8.35 (m, 1 H).

Compound 30: Compound **3** (428 mg) was dissolved in 10 mL methanol; 21.4 mg of 10% Pd/C was added. The reaction mixture was placed under Ar and then under an atmosphere of H_2 at 50 psi and the reaction was stirred at r.t for 16 h. The mixture was filtered, and evaporated under reduced pressure. The residue was purified by silica gel chromatography (15% MeOH in DCM) Compound **30** (282 mg) was obtained in 70% yield. ^{1}H NMR (300 MHz, CD_3OD) δ ppm 1.27 - 1.35 (m, 3 H) 1.49 - 1.57 (m, 3 H) 2.86 (d, *J*=6 Hz, 2 H) 4.14 - 4.21 (m, 1 H) 4.96 (d, *J*=9 Hz, 1 H) 5.38 - 5.45 (m, 1 H) 6.09 (1 H) 8.11 - 8.17 (m, 1 H) 8.22 (s, 1 H)

Compound 31: $NaBH_3CN$ 37 mg (0.58 mmol, 1 equiv.) and AcOH 91.7 μL were added to a solution of 180 mg of compound **30** (0.58 mmol, 1 equiv.) and 18 μL of methyl 4-oxobutanoate (0.18 mmol, 0.3 equiv.) in 1.5 mL MeOH. The reaction mixture was stirred at room temperature for 1.5 h. After diluting the reaction with ethyl acetate, the organic layer was washed with $NaHCO_3$, dried over $MgSO_4$, and then evaporated under reduced pressure. The residue was purified by silica gel chromatography (dichloromethane/ methanol 50:3). Compound **5** (28 mg) was obtained in 12% yield. ^{1}H NMR (300 MHz, CD_3OD) δ ppm 1.41 (s, 3 H) 1.58 - 1.64 (m, 3 H) 2.30 (td, *J*=7, 2 Hz, 2 H) 2.42 - 2.84 (m, 6 H) 3.65 (s, 3 H) 4.29 - 4.41 (m, 1 H) 5.03 (dd, *J*= 6, 3 Hz, 1 H) 5.54 (d, *J*=6, 2 Hz, 1 H) 6.20 (d, *J*=2 Hz, 1 H) 8.26 (s, 1 H) 8.29 (s, 1 H)

Ethyl 4-oxobutanoate: A mixture of 0.54 mL of ethyl 4-bromobutyrate, 800 mg of pyridine oxide and 673 mg NaHCO3 in 10 mL of toluene was refluxed for 16 hours. After return to ambient temperature, the reaction medium is diluted with 100 mL of EA

and then wash with Brine. The crude product was dried on Na_2SO_4, evaporated under reduced pressure and purified by silica gel chromatography. Compound Ethyl 4-oxobutanoate (50 mg) was obtained in 9.6 % yield. ^{1}H NMR (300 MHz, $CDCl_3$) δ ppm 1.27 (s, 3 H) 2.63 (s, 2 H) 2.80 (s, 2 H) 4.14 (s, 3 H) 9.82 (s, 1 H)

Compound 31a(by reductive amination): $NaBH_3CN$ 12.56 mg (0.2 mmol, 1 equiv.) and AcOH 13 μL were added to a solution of 60 mg of compound **4** (0.2 mmol, 1 equiv.) and Ethyl-4-oxobutanoate (0.06 mmol, 0.3 equiv.) in 1.0 mL MeOH. The reaction mixture was stirred at room temperature for 20 min. After diluting the reaction with ethyl acetate and sat. $NaHCO_3$ (aq.), the organic layer was washed with $NaHCO_3$, dried over $MgSO_4$, and then evaporated under reduced pressure. The residue was purified by silica gel chromatography (dichloromethane/methanol 50:6). Compound **31a** (8.3 mg) was obtained in 10% yield. ^{1}H NMR (300 MHz, $CDCl_3$) δ ppm 1.17 - 1.31 (m, 3 H) 1.38 (s, 3H) 1.62 (3 H) 2.11 (s, 1 H) 2.21 - 2.60 (m, 4 H) 2.98 - 3.54 (m, 3 H) 4.02 - 4.20 (m, 3 H) 5.10 (br. s., 1 H) 5.29 - 5.54 (m, 1 H) 6.02 - 6.27 (m, 2 H) 7.95 (br. s., 1 H) 8.26 - 8.39 (m, 1 H)

Compound 31a (by N-alkylation): To a solution of compound **30** in CH_3CN: DMF (80:1) was addded Ethyl 4-bromobutyrate (114 mg, 0.84 ml) and K_2CO_3 (100 mg). The mixture was heated to 80°C 16 h. After cooling, the mixture was filtered. The filtrate was concentrated and purified with column chromatography (DCM/ methanol 100:6) to yield **31b** as a white foam (77 mg, 25%). ^{1}H NMR (300 MHz, $CDCl_3$) δ ppm 1.17 - 1.29 (m, 3

H) 1.33 - 1.45 (m, 3 H) 1.62 (s, 3 H) 1.86 (t, *J*=7 Hz, 2 H) 2.28 - 2.43 (m, 2 H) 2.73 (d, *J*=9 Hz, 1 H) 2.90 - 3.08 (m, 1 H) 4.03 - 4.17 (m, 2 H) 4.43 (d, *J*=2 Hz, 1 H) 5.10 (dd, *J*=6, 3.03 Hz, 1 H) 5.44 (dd, *J*=6, 3.19 Hz, 1 H) 6.00 (d, *J*=3 Hz, 2 H) 7.93 (s, 1 H) 8.32 (s, 1 H)

Compound 33: To a suspension of compound 2-hydroxyphenethyl alcohol (220 mg, 1.6 mmol) in DMF (5 ml), K_2CO_3 (240 mg) was added. To this solution was added benzyl bromide (220 µl) and the mixture was stirred at 60°C temperature for 16 h. The residue was dissolved in ethyl acetate (100 mL); the solution was washed with H_2O and brine, dried over $MgSO_4$, and concentrated. The crude product was purified by column chromatography (1:19 Hexane: DCM) to yield **(2-(*o*-benzyloxy) phenyl) ethanol** (190 mg, 52%).

A solution of **2-(*o*-benzyloxy)phenylethanol** (23 mg, 0.10 mmol) and IBX(42 mg, 0.15 mmol) was stirred at 60°C in THF (3 mL) for 16 h. The reaction was diluted with diethyl ether (5 mL) and washed with sodium thiosulfate (5 mL) followed by saturated sodium bicarbonate (5 mL). The aqueous layer was back-washed with diethyl ether (10 mL). The organic layers were combined, washed with brine, and dried over magnesium sulfate. The solvent was evaporated, and the crude was purified with column chromatography (30:20 hexanes/DCM) to yield **7** (7.5 mg, 0.33 mmol, 33%). ^{1}H NMR (500 MHz, $CDCl_3$) δ ppm 3.72 (2 H) 5.11 (s, 2 H) 6.99 (d, *J*=7 Hz, 2 H) 7.16 - 7.46 (m, 7 H) 9.74 (d, *J*=1 Hz, 1 H).

Compound 34: To a stirred solution of 4-nitrophenyl alcohol (0.36 mmol) in acetonitrile (3 mL) was added at once 2-iodoxybenzoic acid (IBX, 0.36 mmol). The mixture was heated at 80 °C for 2 h and then cooled to rt. The mixture was then filtered through Celite® and the solvent was evaporated, giving the expected crude material as a yellow oil. The crude was purified with column chromatography (90:10 hexanes: ethyl acetate) to yield **34** (20 mg, 34%). ^{1}H NMR (300 MHz, $CDCl_3$) δ ppm 3.88 (d, *J*=1 Hz, 2 H) 7.40 (d, *J*=8 Hz, 2 H) 8.20 - 8.28 (m, 2 H) 9.83 (t, *J*=1 Hz, 1 H)

Compound 36: $NaBH_3CN$ 10.2 mg (0.162 mmol, 2 equiv.) and AcOH 4.7µL were added to a solution of 33 mg of compound **31** (0.081 mmol) and 7.5 mg (0.33mmol, 1 equiv.) compound **7** in 1 mL MeOH. The reaction mixture was stirred at room temperature for 16 h. After diluting the reaction with ethyl acetate, the organic layer was washed with $NaHCO_3$, dried over $MgSO_4$, and then evaporated under reduced pressure. The residue was purified by silica gel chromatography (DCM/methanol 95:5). Compound **36** (17 mg) was obtained in 34% yield. ^{1}H NMR (500 MHz, $CDCl_3$) δ ppm 1.16 - 1.43 (m, 8 H) 1.66 (d, *J*=11 Hz, 3 H) 2.11 (s, 2 H) 2.36 (t, *J*=7 Hz, 3 H) 3.16 (br. s., 3 H) 3.65 (dd, *J*=13, 5 Hz, 3 H) 4.89 - 5.34 (m, 2 H) 6.23 (br. s., 1 H) 6.94 (br. s., 2 H) 7.43 (br. s., 6 H) 8.45 - 8.60 (m, 2 H).

Compound 38: $NaBH(OAc)_3$ (35 mg ,0.165 mmol, 1.5equiv.) was added to a solution of **31b** (45 mg, 0.11 mmol) and **34** (18 mg, 0.11 mmol, 1 equiv.) in 1 mL DCM. The reaction mixture was stirred at room temperature for 30 min. MeOH (0.1 ml) was added and the mixture was concentrated. The residue was purified by silica gel chromatography

(DCM/methanol 100:3). Compound **38** (10 mg) was obtained in16% yield. ^{1}H NMR (300 MHz, $CDCl_3$) δ ppm 1.25 (t, *J*=7 Hz, 3 H) 1.38 (s, 3 H) 1.64 (s, 3H) 1.95 (br. s., 2 H) 2.31 (d, *J*=6 Hz, 2 H) 2.85 - 3.17 (m, 6 H) 4.12 (q, *J*=7 Hz, 2 H) 5.11 (br. s., 1 H) 5.38 (br. s., 1 H) 5.97 - 6.17 (m, 3 H) 7.07 (br. s., 2 H) 7.94 (s, 1 H) 8.01 - 8.11 (m, 2 H) 8.33 (s, 2 H).

Compound 25: Compound **36** (17 mg) was dissolved in 2 mL methanol; 8.5 mg of 10% Pd/C was added. The reaction mixture was placed under an atmosphere of H_2 (50 Psi) at room temperature for 4 h. The mixture was filtered, and evaporated under a reduced pressure. The crude product was directly used for the next reaction without purification. Compound **37** (12 mg) was obtained in 81.3% yield. A suspension of compound **37** (12 mg) in a mixture of 0.2 M methanolic HCl (1ml) and H_2O (0.1 ml) was stirred at room temperature for 16 h. After adjusting the pH 7.0, the reaction mixture of compound **40** was directly used for the next reaction without purification. To a suspension of compound **40** (15 mg), in a mixture of MeOH/H_2O (10:1, 1 ml: 0.1 ml), was added 22 mg of KOH in one portion. The mixture was stirred at room temperature for 16 h and then concentrated under reduced pressure. The residue was purified by HPLC. The flow rate was 3 ml/min. The mobile phase consisted of a mixture of MeCN-H_2O, (started from 15:0 V/V till 15: 90 V/V)). The retention time was 1.2 min.

Compound 26: A suspension of compound **38** (8.6 mg) in a mixture of 0.5 M methanolic HCl (1mL) and H_2O (0.2 mL) was stirred at room temperature for 6 h. After adjusting the pH to 7.0, the reaction mixture of compound **41** was directly used for the next reaction

without purification. To a suspension of compound **41** (8.6 mg) in a mixture of MeOH: H_2O (1 ml: 0.3 ml) was added 9.6 mg of KOH. The mixture was stirred at room temperature for 42 h and then neutralized by acetic acid. The solvent is evaporated at a reduced pressure and the residue was purified by silica gel chromatography (DCM / methanol 1:1). A yellow foam (5.8 mg, 72%) from **26** was obtained. ^{1}H NMR (500 MHz, CD_3OD) δ ppm 1.79 (br. s., 3 H) 2.18 (d, *J*=5 Hz, 3 H) 2.59 - 2.74 (m, 2 H) 2.88 - 3.08 (m, 3 H) 4.07 (d, *J*=6 Hz, 1 H) 4.14 - 4.33 (m, 2 H) 4.78 (d, *J*=4 Hz, 1 H) 5.99 (d, *J*=5 Hz, 1 H) 7.29 (d, *J*=8 Hz, 2 H) 7.99 - 8.08 (m, 2 H) 8.21 (s, 1 H) 8.32 (br. s., 1 H)

5.6 Conclusions and Future Studies

DNA methylation inhibition is an emerging area. Although the first inhibitors were discovered in the sixties, there are still a lot of demands to develop more potent and less toxic inhibitors, opening a promising road ahead to future therapies. A series of SAH-derived DNMT inhibitors was designed using a combination of mechanism-based design (transition state inhibitor) and structure-based modifications. The inhibition activities will be tested in vitro using human DNMT1 assays in future studies. The future perspectives lie in developing more similar compounds and elucidating their mechanisms of action in order to develop more effective DNMT1 inhibitors.

APPENDIX

SPECTROSCOPIC DATA

A.1 ^{1}H NMR Spectra

Compound 2

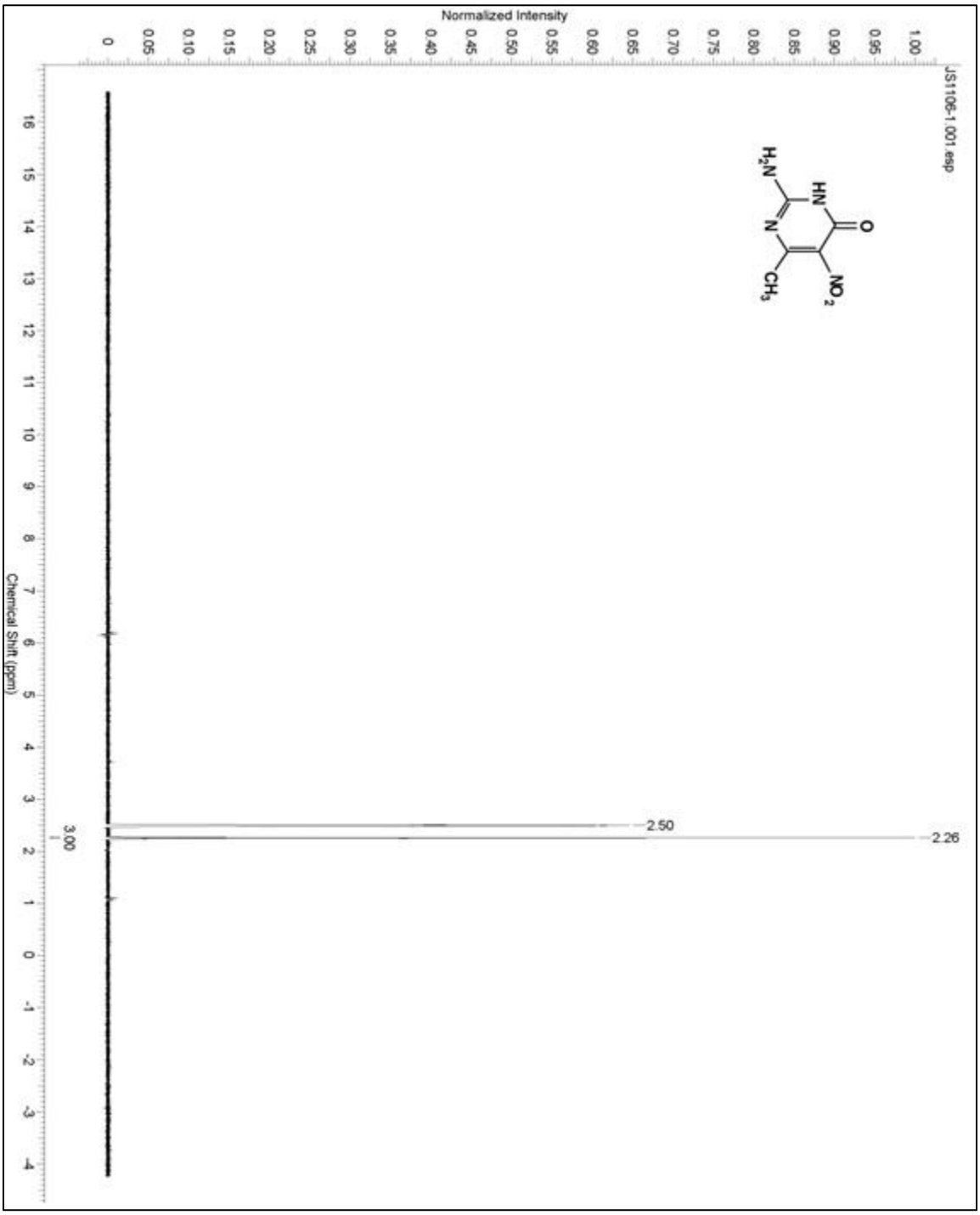

Compound 3

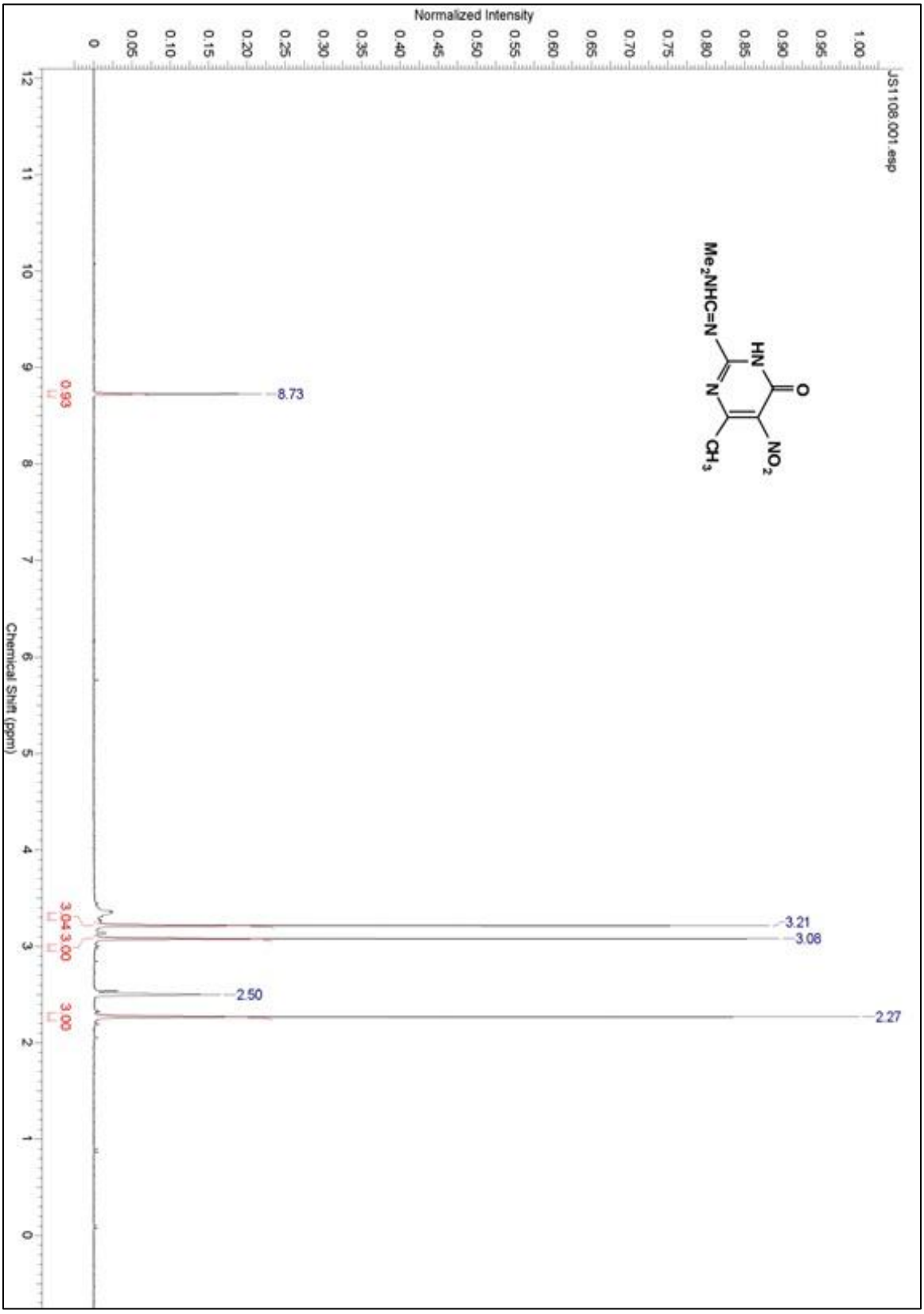
Normalized Intensity
JS1108.001.esp
Chemical Shift (ppm)
Me2NHC=N
HN
O
N
CH3
NO2
8.73
3.21
3.08
2.50
2.27
0.93
3.04
3.00
3.00

Compound 4

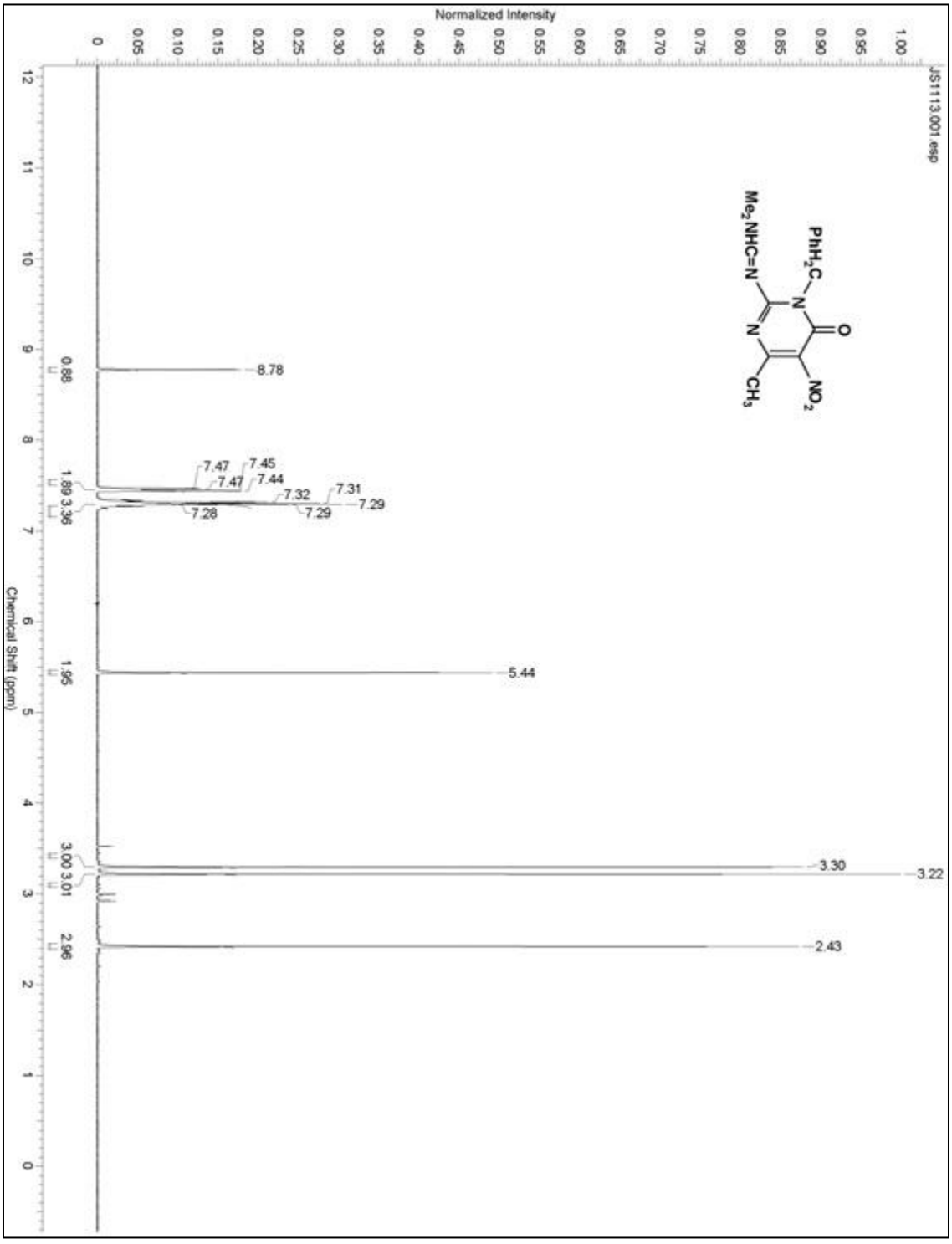
Normalized Intensity
JS1113.001.esp
Chemical Shift (ppm)
8.78
7.47
7.45
7.47
7.44
7.32
7.31
7.29
7.28
7.29
5.44
3.30
3.22
2.43
0.88
1.89
3.36
1.95
3.00
3.01
2.96
Me2NHC=N
PhH2C
CH3
NO2
O

Compound 5

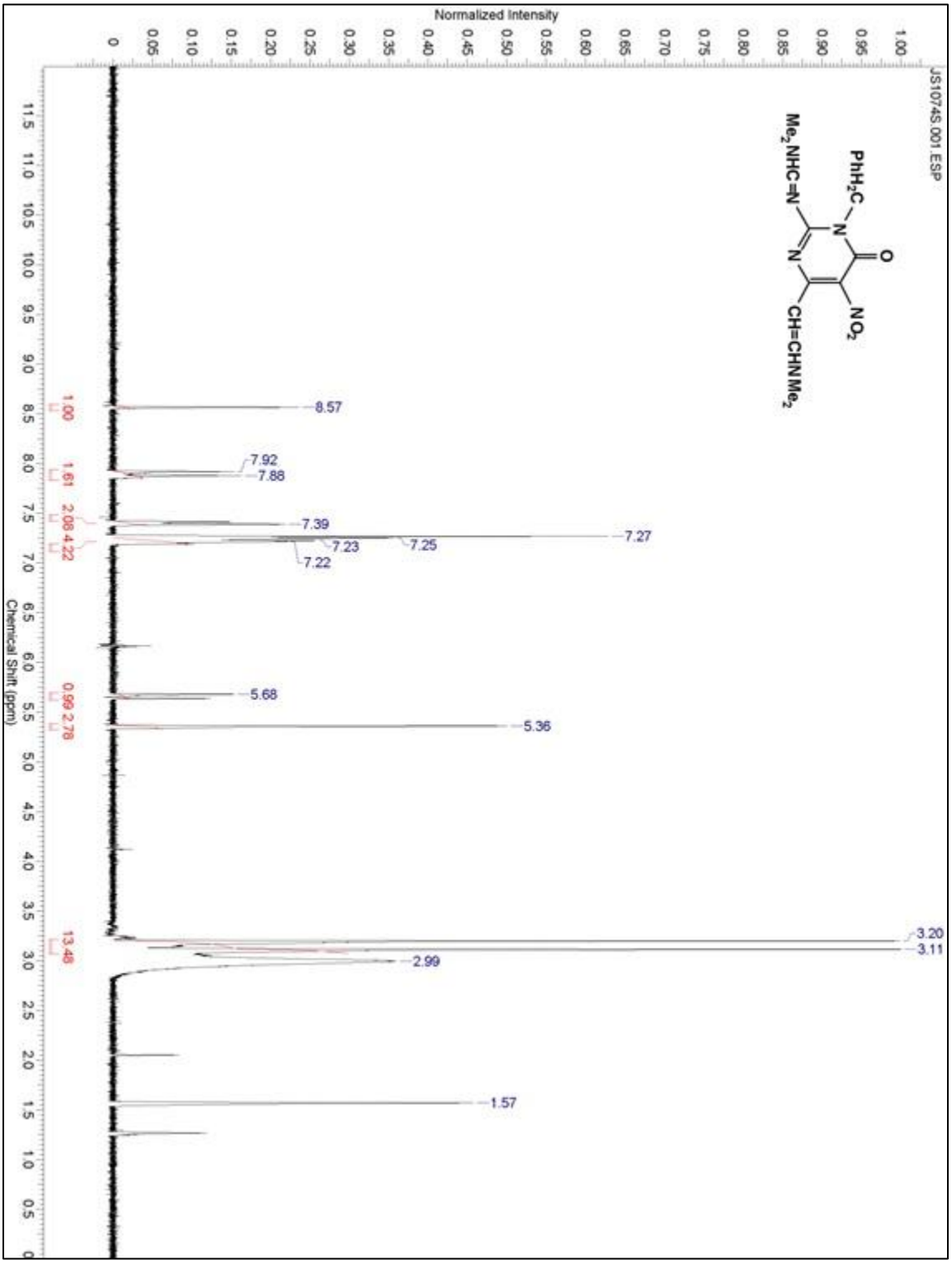
Normalized Intensity
JS1074S.001.ESP
Chemical Shift (ppm)
Me2NHC=N
PhH2C
O
NO2
CH=CHNMe2
8.57
7.92
7.88
7.39
7.27
7.25
7.23
7.22
5.68
5.36
3.20
3.11
2.99
1.57
1.00
1.61
2.08
4.22
0.99
2.78
13.48

Compound 6

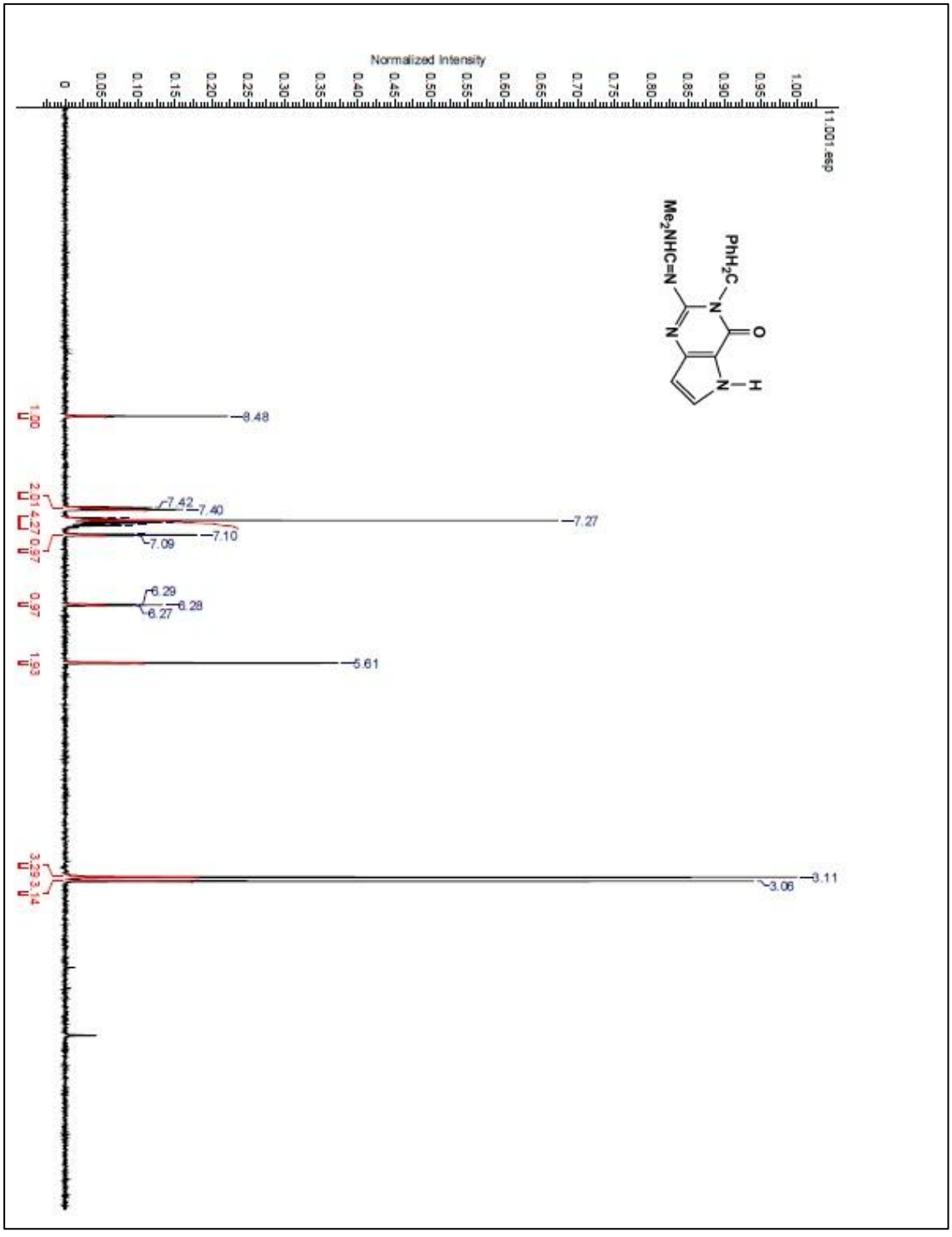
Normalized Intensity
11.001.esp
Me2NHC=N
PhH2C
8.48
7.42
7.40
7.27
7.10
7.09
6.29
6.28
6.27
5.61
3.11
3.06
1.00
2.01
4.27
0.97
0.97
1.93
3.29
3.14

Compound 7

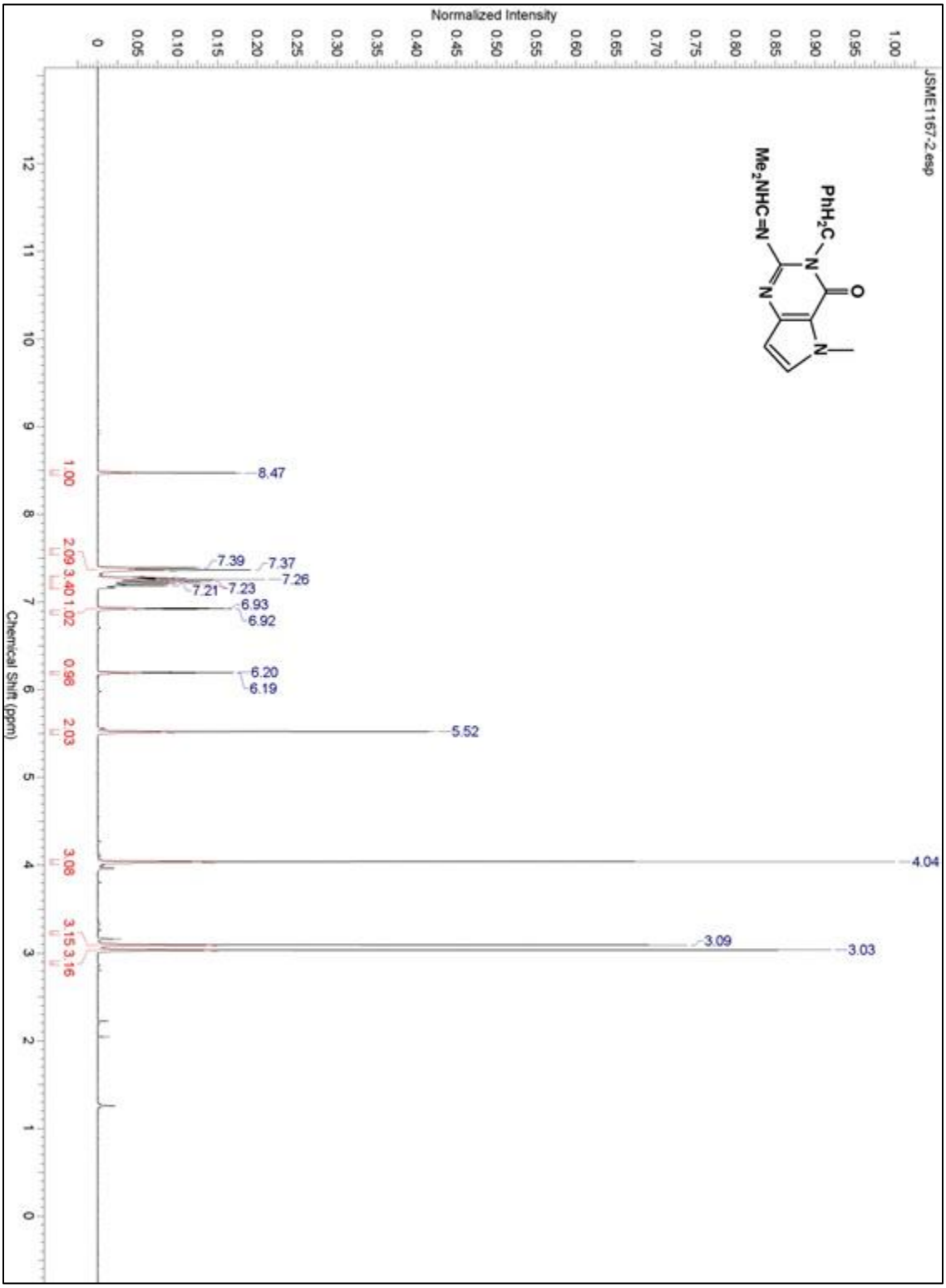
Normalized Intensity
JSME1167-2.esp
Me2NHC=N
PhH2C
Chemical Shift (ppm)
8.47
7.39
7.37
7.26
7.21
7.23
6.93
6.92
6.20
6.19
5.52
4.04
3.09
3.03
1.00
2.09
3.40
1.02
0.96
2.03
3.08
3.15
3.16

Compound 8

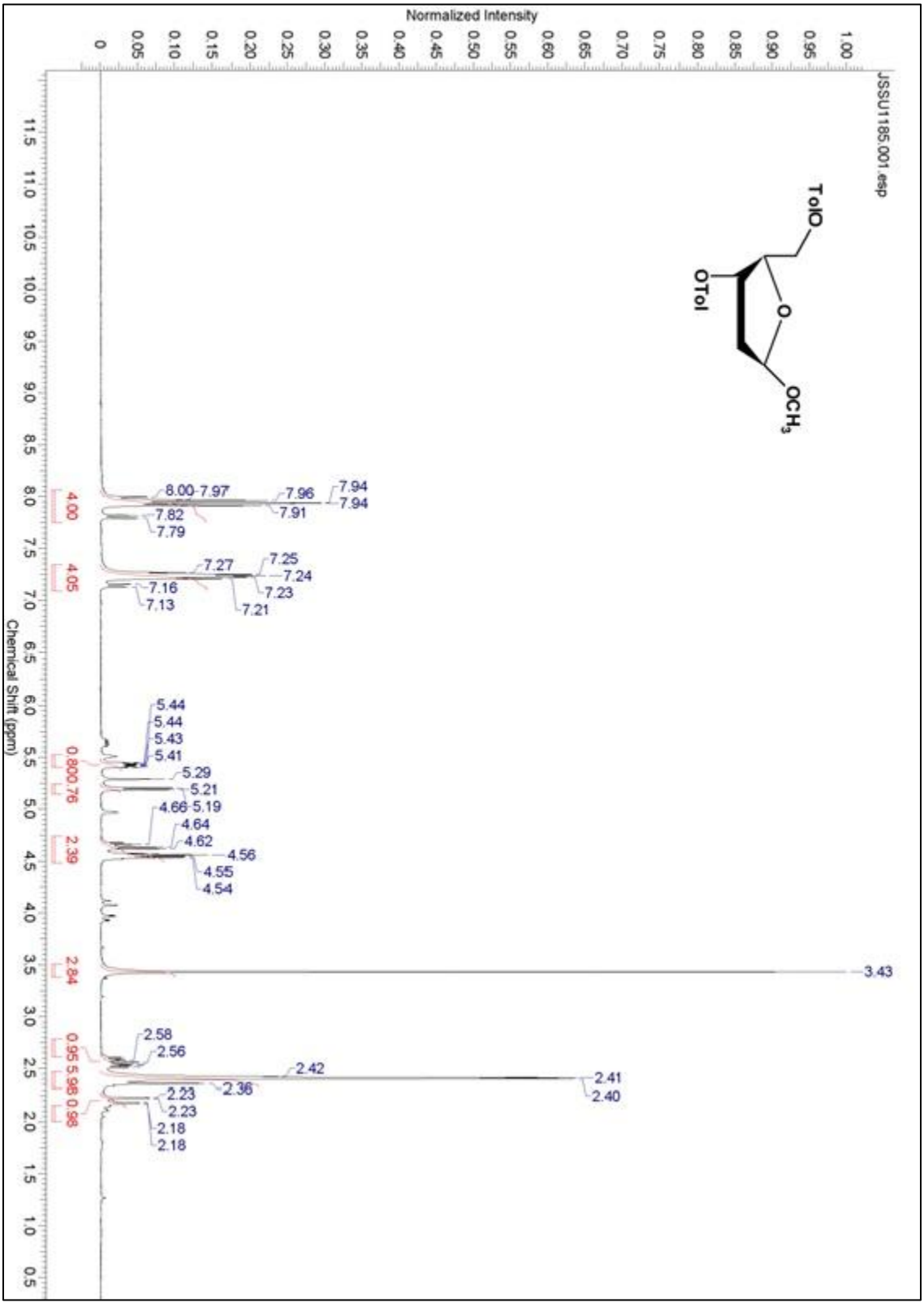
Normalized Intensity
JSSU1185.001.esp
TolO
OTol
O
OCH3
Chemical Shift (ppm)
8.00 7.97
7.96
7.94
7.94
7.91
7.82
7.79
7.27
7.25
7.24
7.23
7.21
7.16
7.13
5.44
5.44
5.43
5.41
5.29
5.21
4.66 5.19
4.64
4.62
4.56
4.55
4.54
3.43
2.58
2.56
2.42
2.41
2.40
2.36
2.23
2.23
2.18
2.18
4.00
4.05
0.80 0.76
2.39
2.84
0.95 5.98 0.98

Compound 9

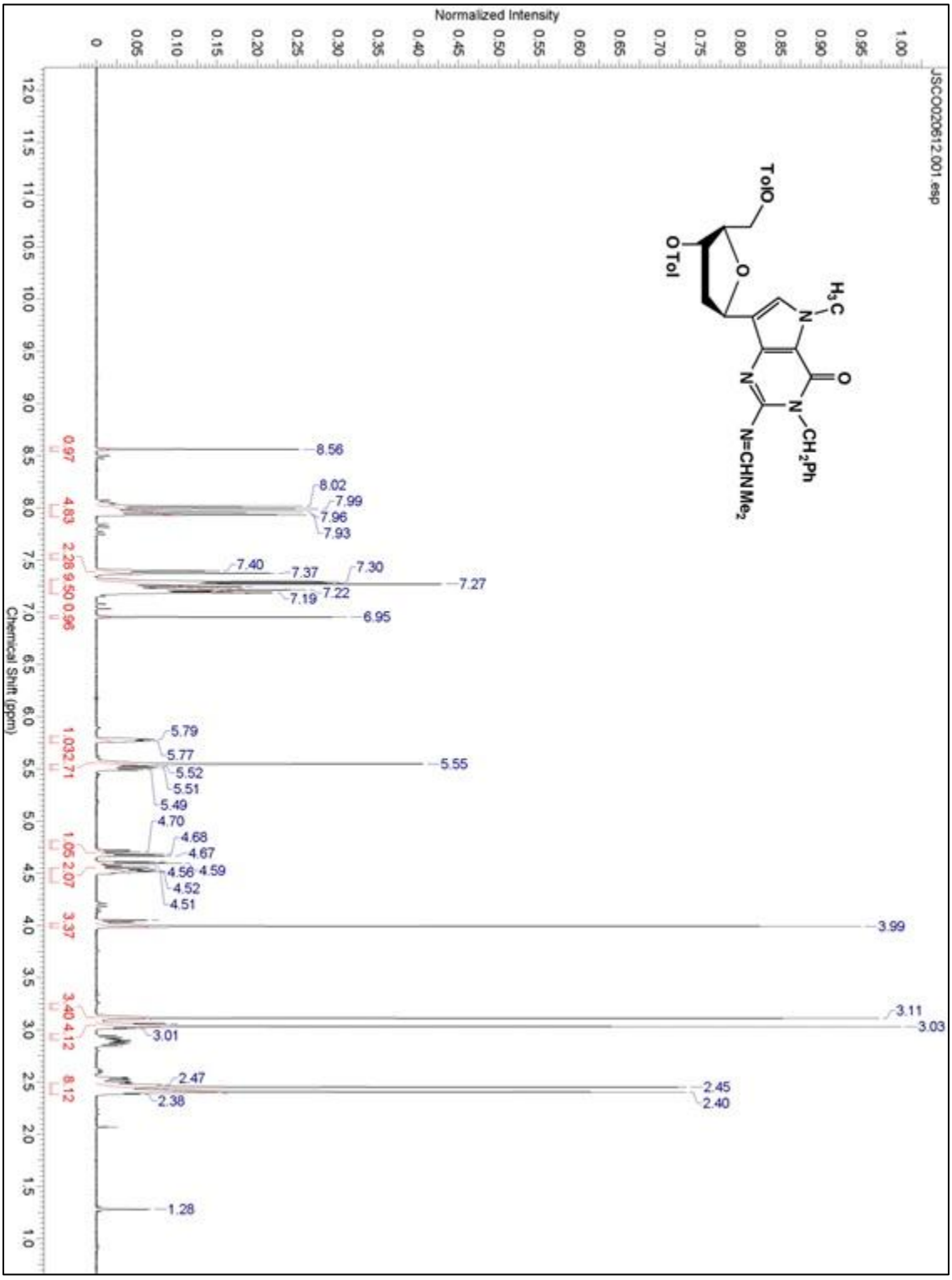
Normalized Intensity
Chemical Shift (ppm)
JSCO020612.001.esp
TolO
OTol
O
H3C
N
O
N
N
N=CHNMe2
CH2Ph
8.56
8.02
7.99
7.96
7.93
7.40
7.37
7.30
7.27
7.22
7.19
6.95
5.79
5.77
5.55
5.52
5.51
5.49
4.70
4.68
4.67
4.59
4.56
4.52
4.51
3.99
3.11
3.03
3.01
2.47
2.45
2.40
2.38
1.28
0.97
4.83
2.28
9.50
0.96
1.03
2.71
1.05
2.07
3.37
3.40
4.12
8.12

Compound 10

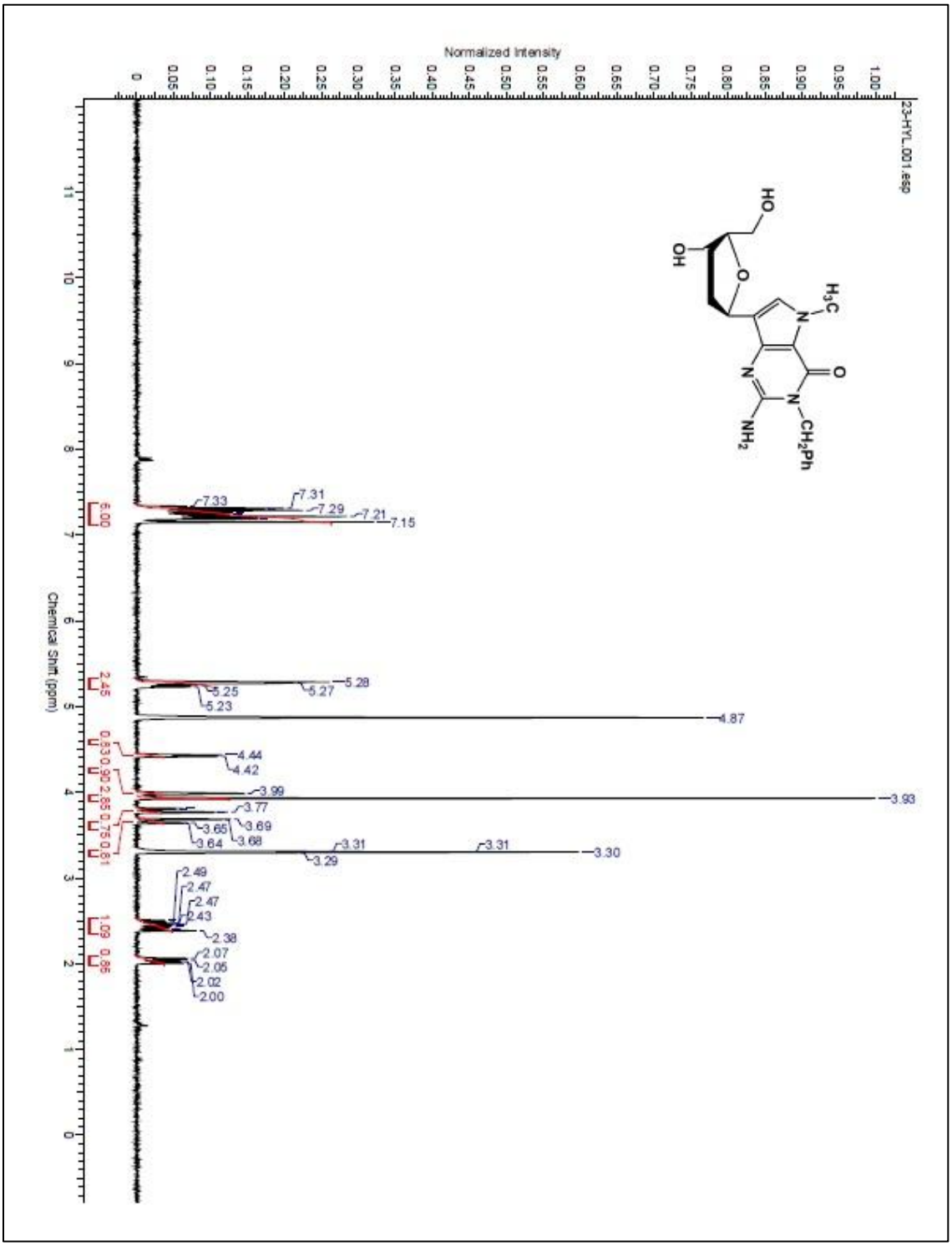
Normalized Intensity
23-HYL.001.esp
Chemical Shift (ppm)
HO
OH
O
H_3C
N
N
O
N
NH_2
CH_2Ph
7.33
7.31
7.29
7.21
7.15
6.00
5.28
5.27
5.25
5.23
2.45
4.87
4.44
4.42
0.83
0.90
2.85
0.76
0.81
3.99
3.93
3.77
3.65
3.64
3.69
3.68
3.31
3.29
3.31
3.30
2.49
2.47
2.47
2.43
2.38
1.09
0.86
2.07
2.05
2.02
2.00

Compound 11

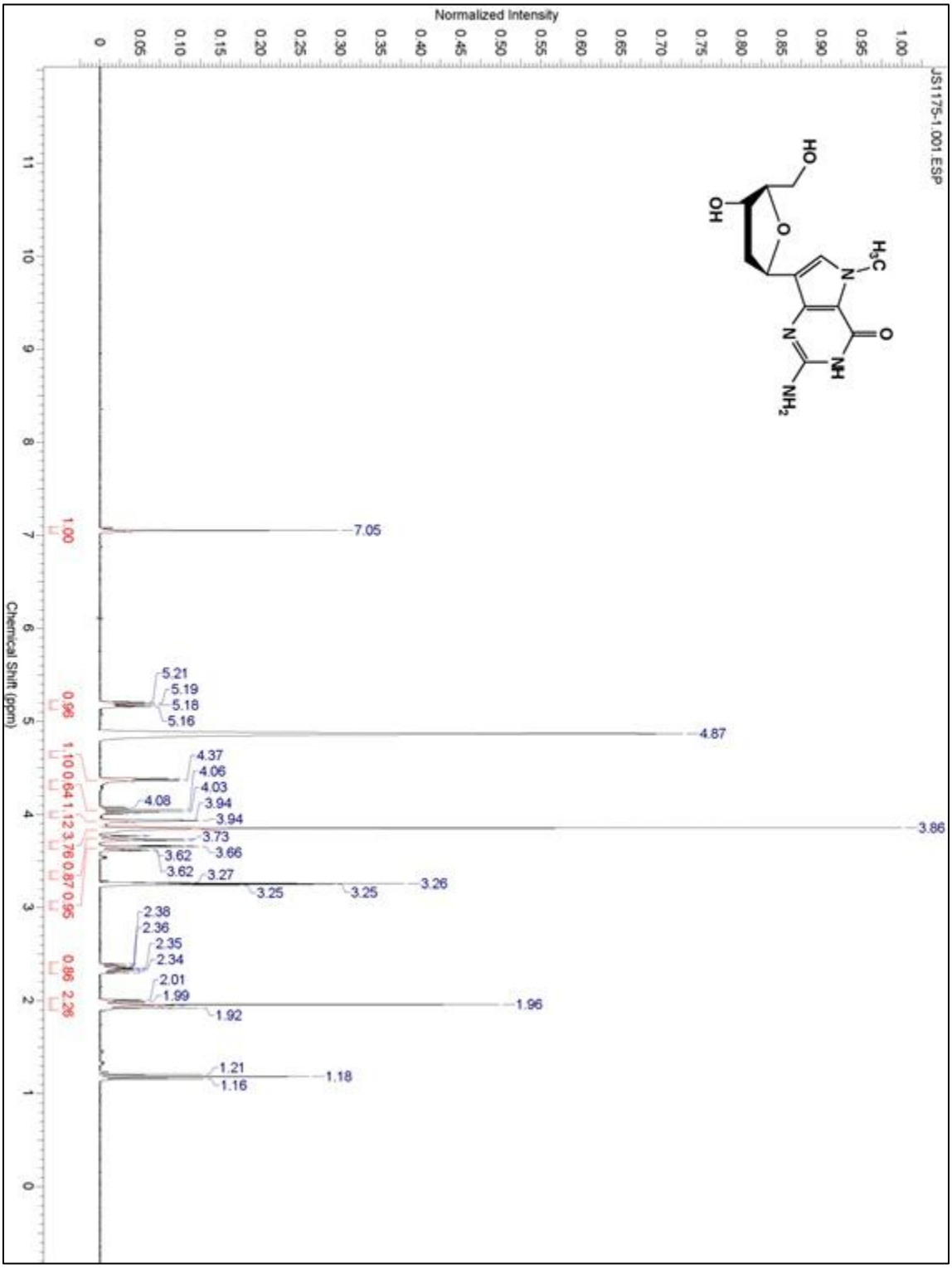
Normalized Intensity
JS1175-1.001.ESP
Chemical Shift (ppm)
7.05
5.21
5.19
5.18
5.16
4.87
4.37
4.06
4.03
4.08
3.94
3.94
3.86
3.73
3.62
3.66
3.62
3.27
3.25
3.25
3.26
2.38
2.36
2.35
2.34
2.01
1.99
1.96
1.92
1.21
1.16
1.18
1.00
0.96
1.10
0.64
1.12
3.76
0.87
0.95
0.86
2.26

Compound 12

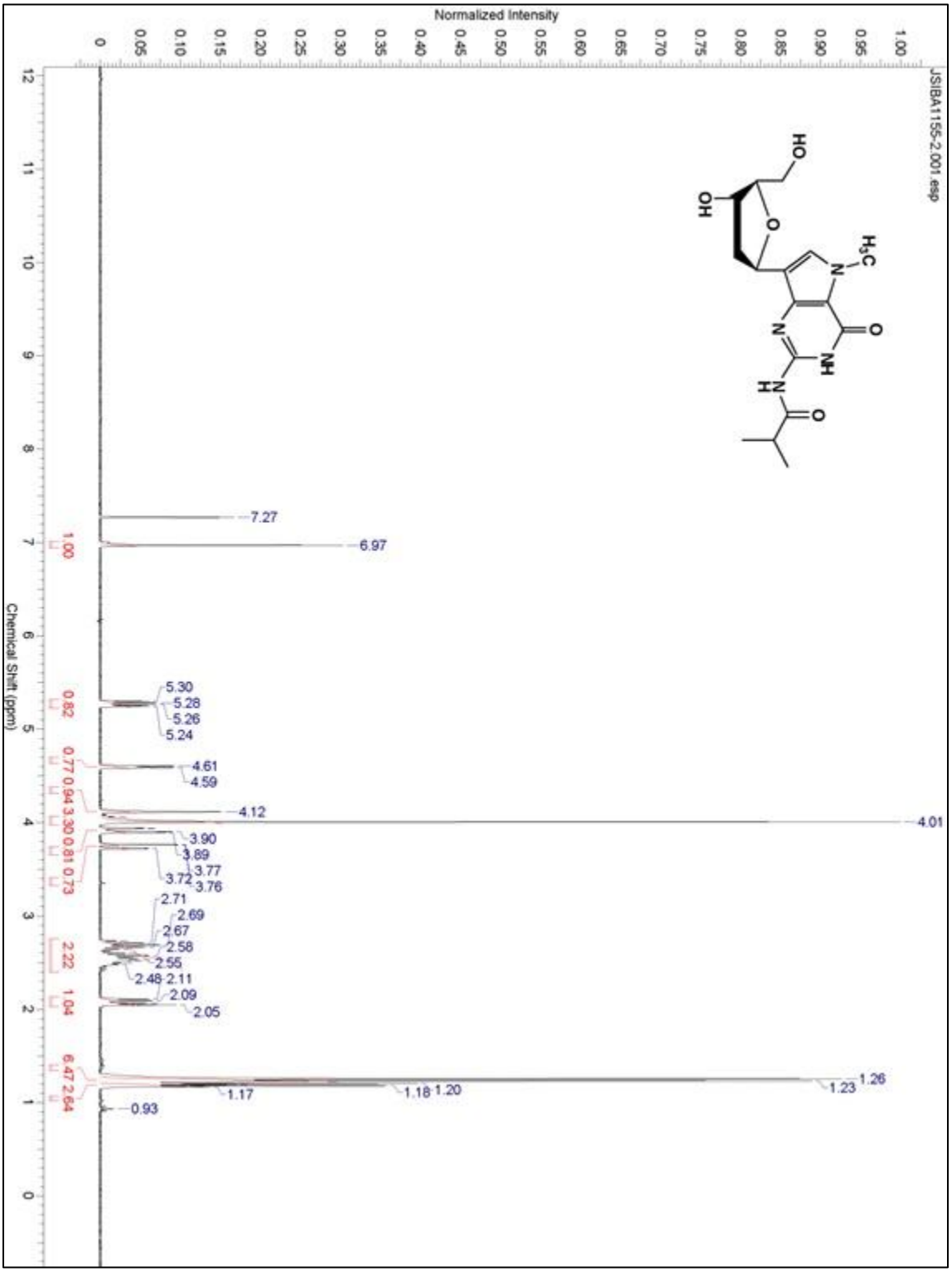
Normalized Intensity
JSIBA1155-2-001.esp
Chemical Shift (ppm)
7.27
6.97
5.30
5.28
5.26
5.24
4.61
4.59
4.12
4.01
3.90
3.89
3.77
3.76
3.72
2.71
2.69
2.67
2.58
2.55
2.48
2.11
2.09
2.05
1.26
1.23
1.20
1.18
1.17
0.93
1.00
0.82
0.77
0.94
3.30
0.81
0.73
2.22
1.04
6.47
2.64

Compound 13

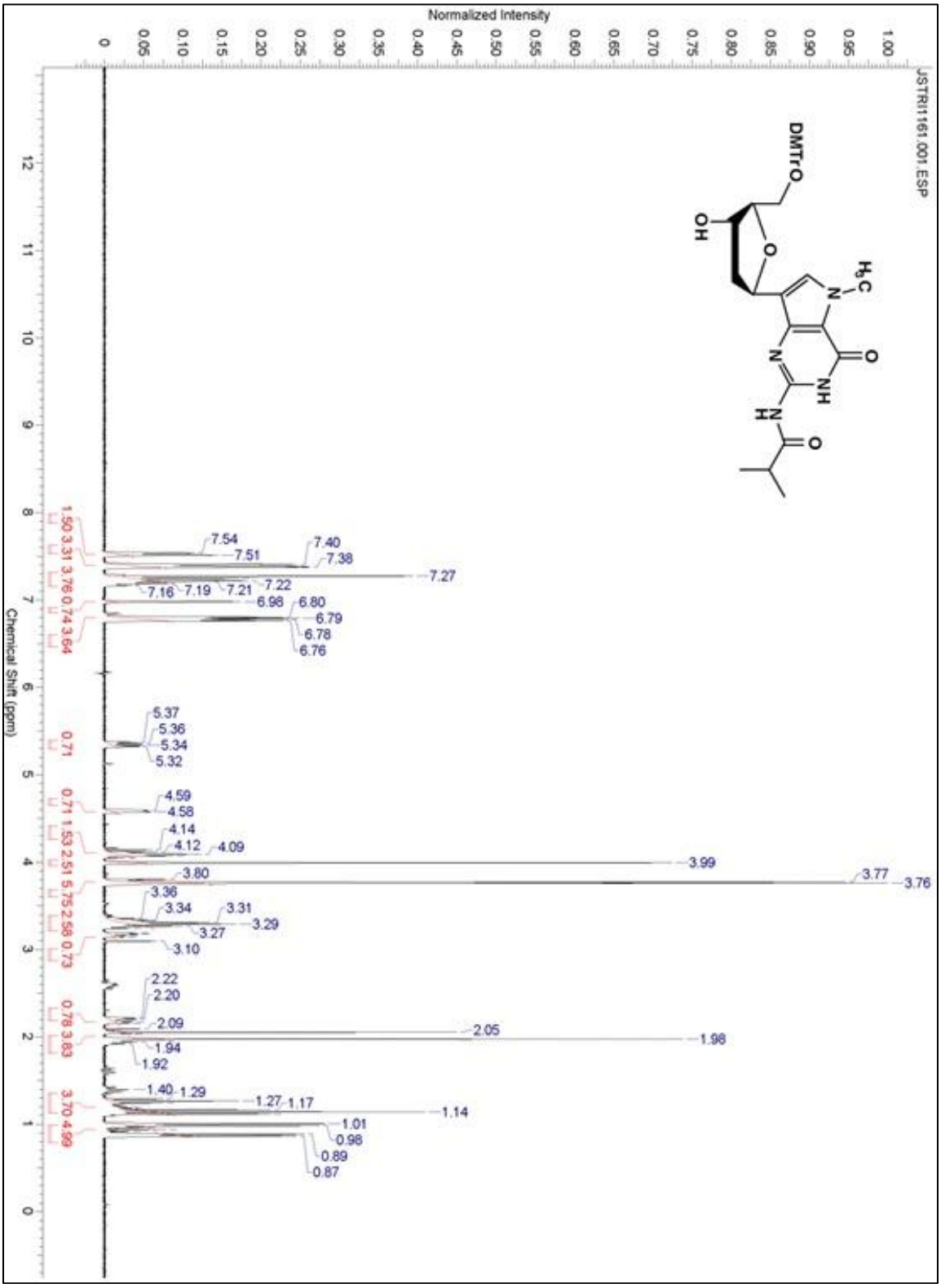
Normalized Intensity
JSTRI1161.001.ESP
Chemical Shift (ppm)
DMTrO
OH
O
N
H3C
O
N
NH
HN
O
7.54
7.51
7.40
7.38
7.27
7.16
7.19
7.21
7.22
6.98
6.80
6.79
6.78
6.76
5.37
5.36
5.34
5.32
4.59
4.58
4.14
4.12
4.09
3.99
3.80
3.77
3.76
3.36
3.34
3.31
3.29
3.27
3.10
2.22
2.20
2.09
2.05
1.98
1.94
1.92
1.40
1.29
1.27
1.17
1.14
1.01
0.98
0.89
0.87
1.50 3.31 3.76 0.74 3.64
0.71
0.71 1.53 2.51 5.75 2.58 0.73
0.78 3.83
3.70 4.99

Compound 14

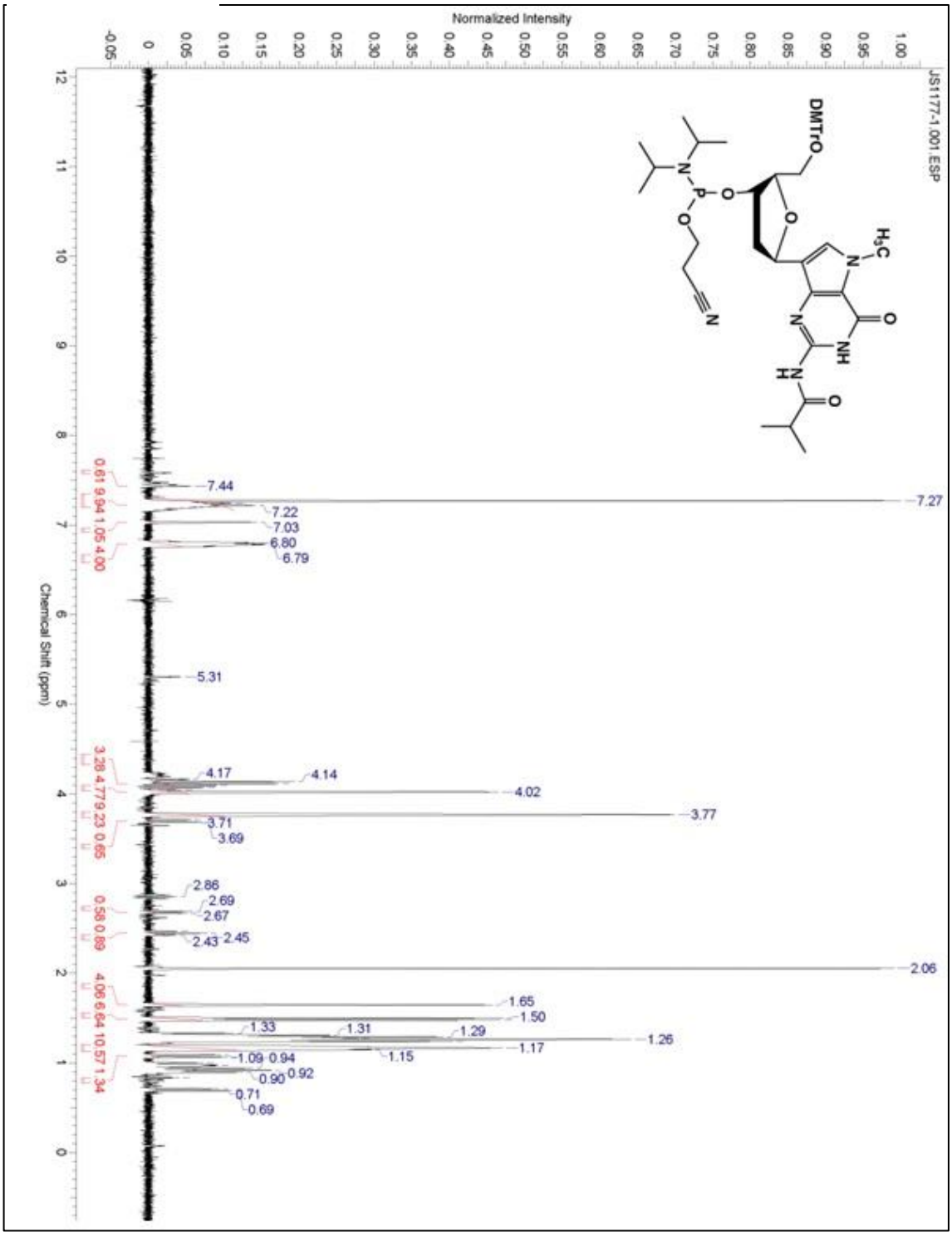
Normalized Intensity
JS1177-1.001.ESP
Chemical Shift (ppm)
DMTrO
H_3C
7.44
7.27
7.22
7.03
6.80
6.79
5.31
4.17
4.14
4.02
3.77
3.71
3.69
2.86
2.69
2.67
2.43
2.45
2.06
1.65
1.50
1.33
1.31
1.29
1.26
1.17
1.15
1.09
0.94
0.90
0.92
0.71
0.69
0.61 9.94 1.05 4.00
3.28 4.77 9.23 0.65
0.58 0.89
4.06 6.64 10.57 1.34

Compound 27

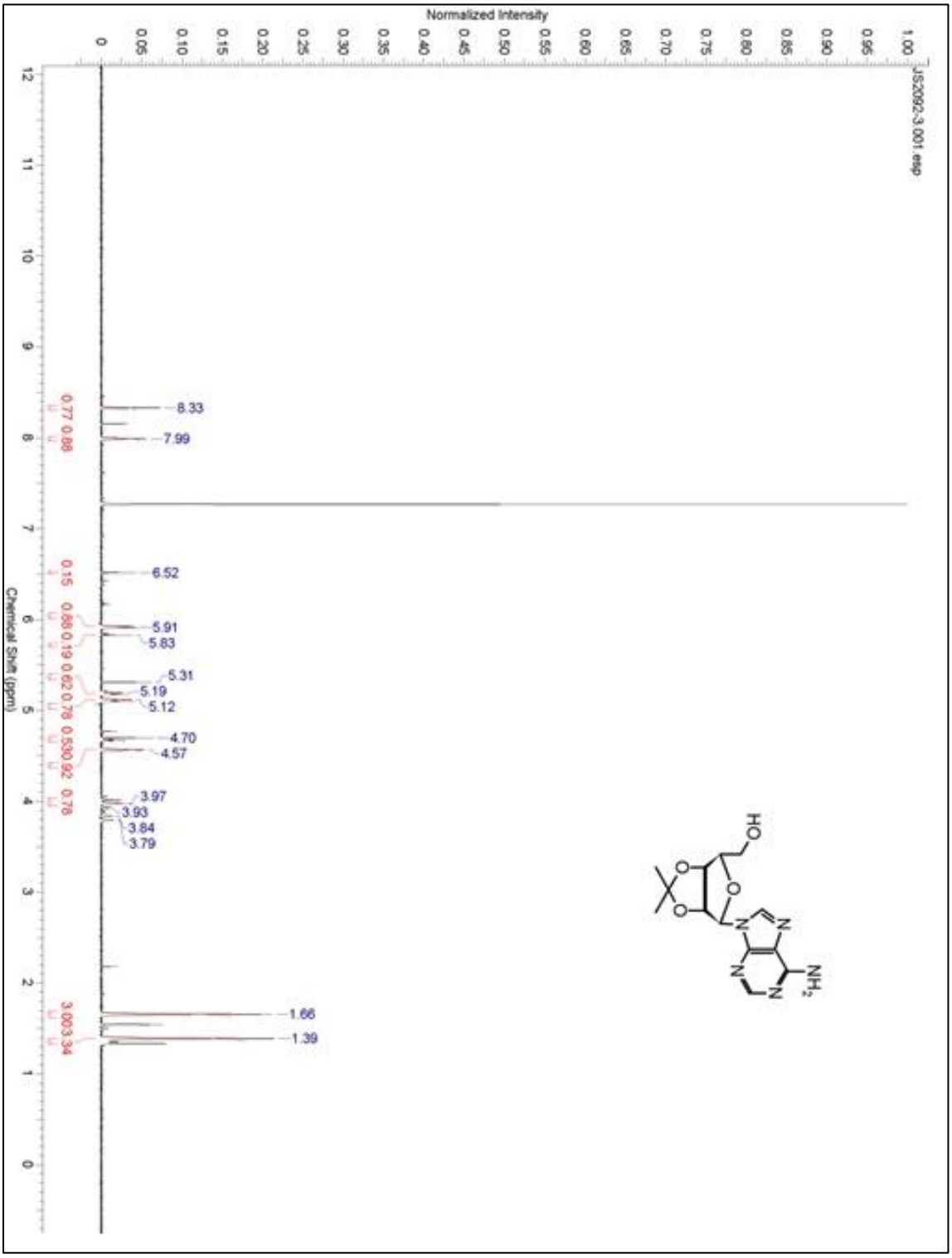
Normalized Intensity
JS2092-3-001.esp
Chemical Shift (ppm)
8.33
7.99
6.52
5.91
5.83
5.31
5.19
5.12
4.70
4.57
3.97
3.93
3.84
3.79
1.66
1.39
0.77
0.89
0.15
0.88
0.19
0.62
0.78
0.53
0.92
0.78
3.00
3.34
HO
O
O
O
N
N
N
N
NH2

Compound 29

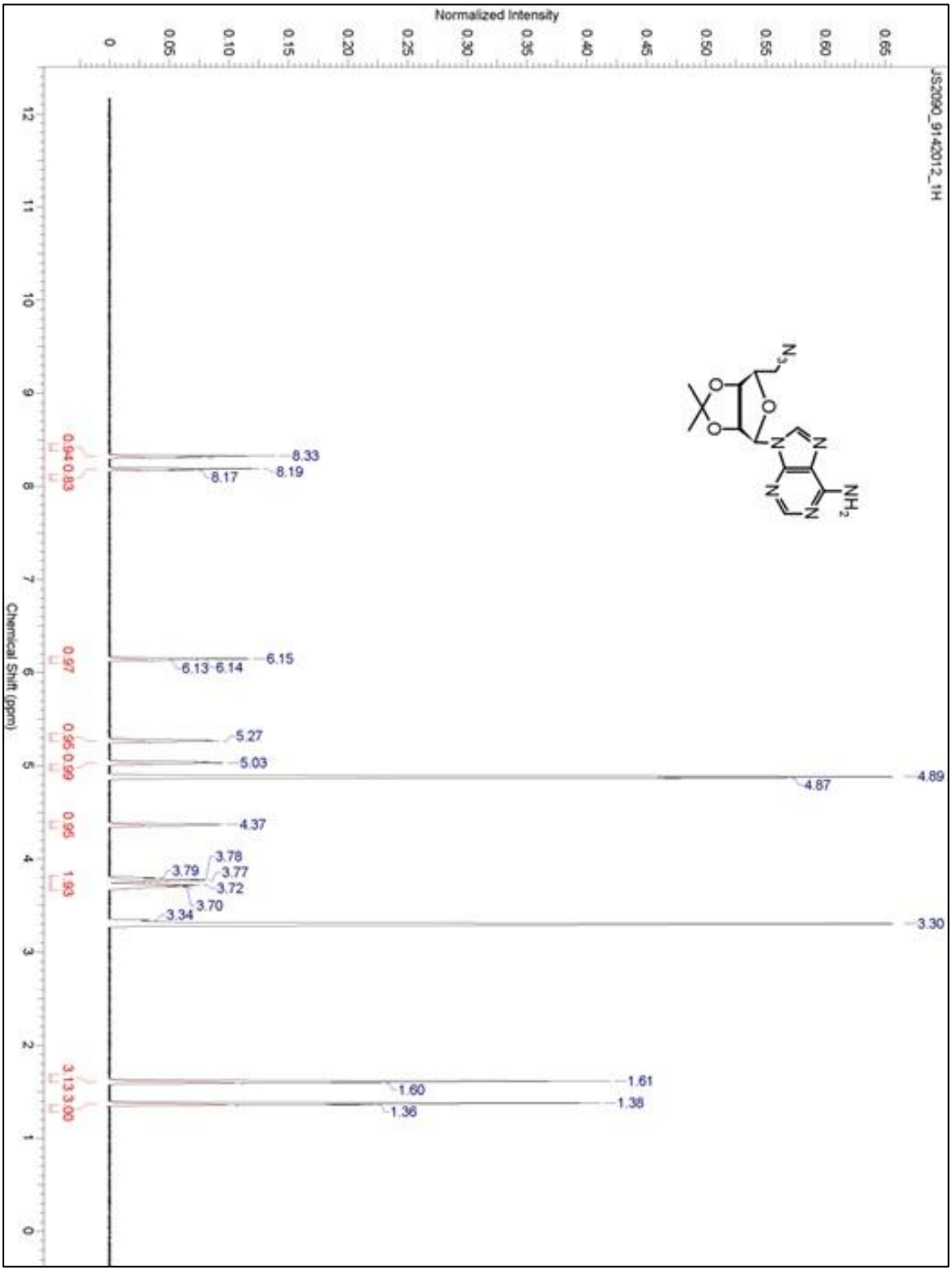
Normalized Intensity
JS2090_9142012_1H
Chemical Shift (ppm)
8.33
8.19
8.17
6.15
6.14
6.13
5.27
5.03
4.89
4.87
4.37
3.78
3.79
3.77
3.72
3.70
3.34
3.30
1.61
1.60
1.38
1.36
0.94
0.83
0.97
0.96
0.99
0.95
1.93
3.13
3.00
NH2

Compound 30

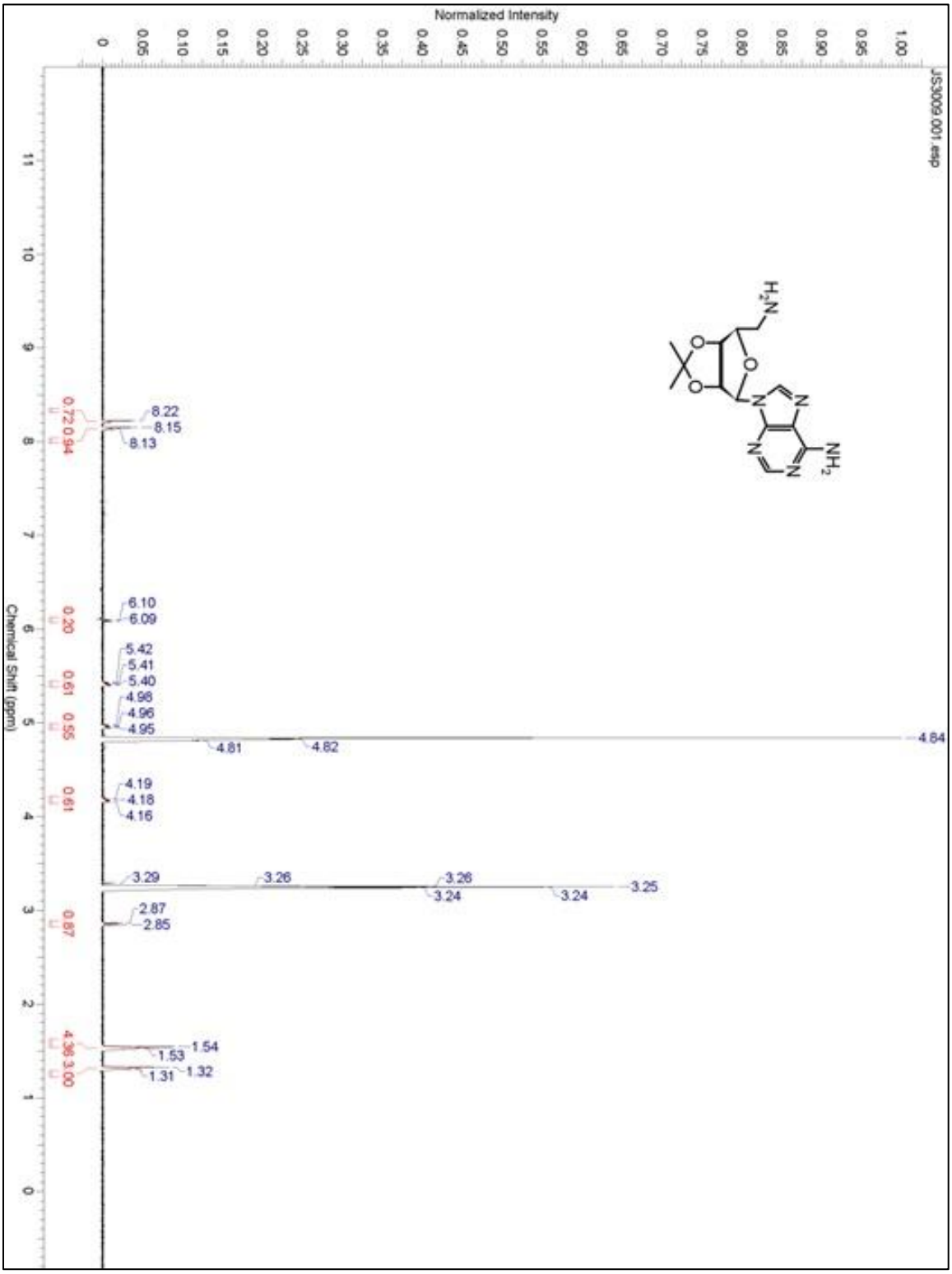
Normalized Intensity
JS3009.001.esp
Chemical Shift (ppm)
8.22
8.15
8.13
6.10
6.09
5.42
5.41
5.40
4.98
4.96
4.95
4.81
4.82
4.84
4.19
4.18
4.16
3.29
3.26
3.26
3.24
3.24
3.25
2.87
2.85
1.54
1.53
1.31
1.32
0.72
0.94
0.20
0.61
0.55
0.61
0.87
4.36
3.00

Compound 31

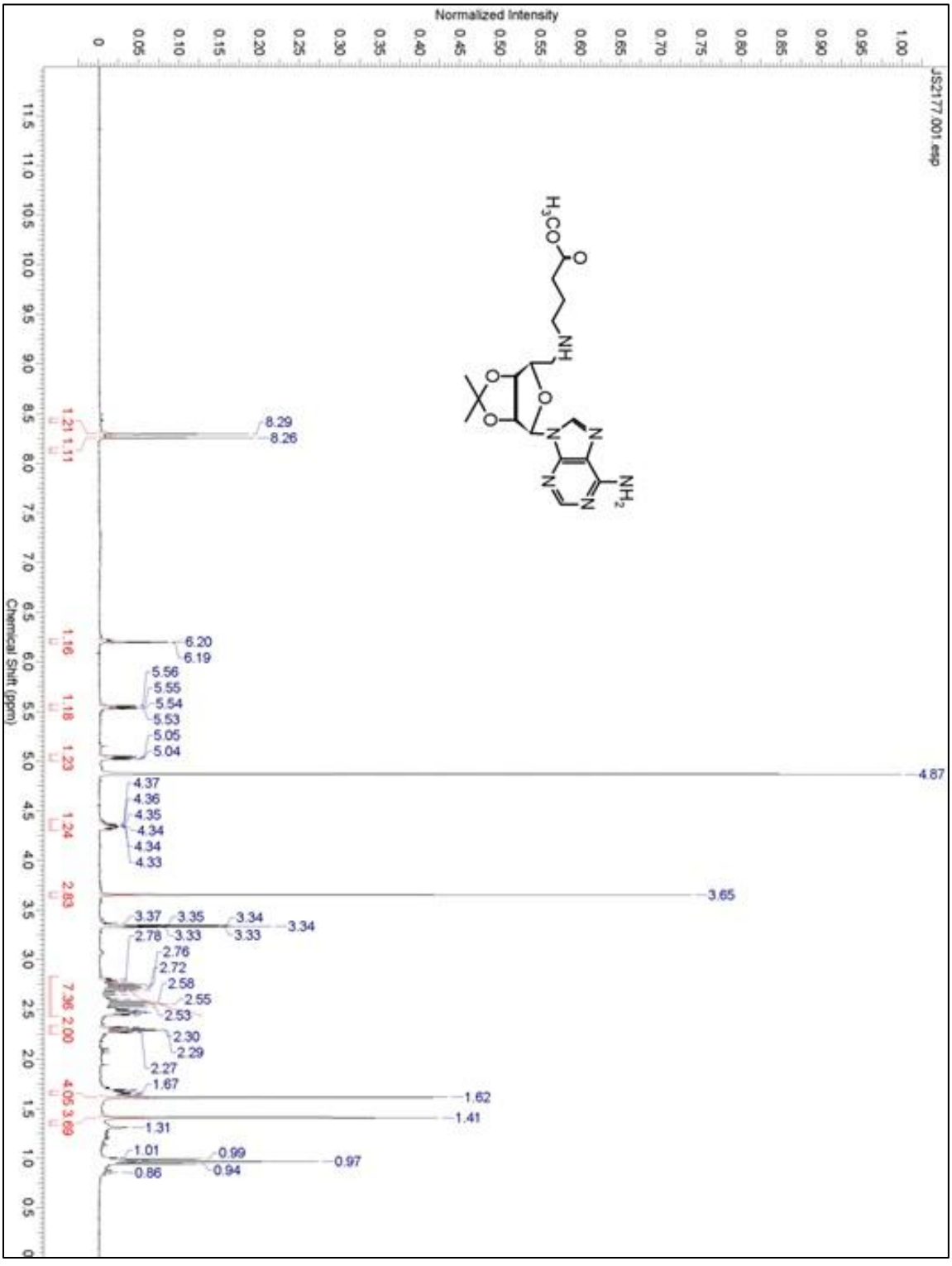
Normalized Intensity
JS2177.001.esp
Chemical Shift (ppm)
8.29
8.26
6.20
6.19
5.56
5.55
5.54
5.53
5.05
5.04
4.87
4.37
4.36
4.35
4.34
4.34
4.33
3.65
3.37
3.35
3.34
3.34
3.33
3.33
2.78
2.76
2.72
2.58
2.55
2.53
2.30
2.29
2.27
1.67
1.62
1.41
1.31
1.01
0.99
0.97
0.94
0.86
1.21
1.11
1.16
1.18
1.23
1.24
2.83
7.36
2.00
4.05
3.69

Compound 31a

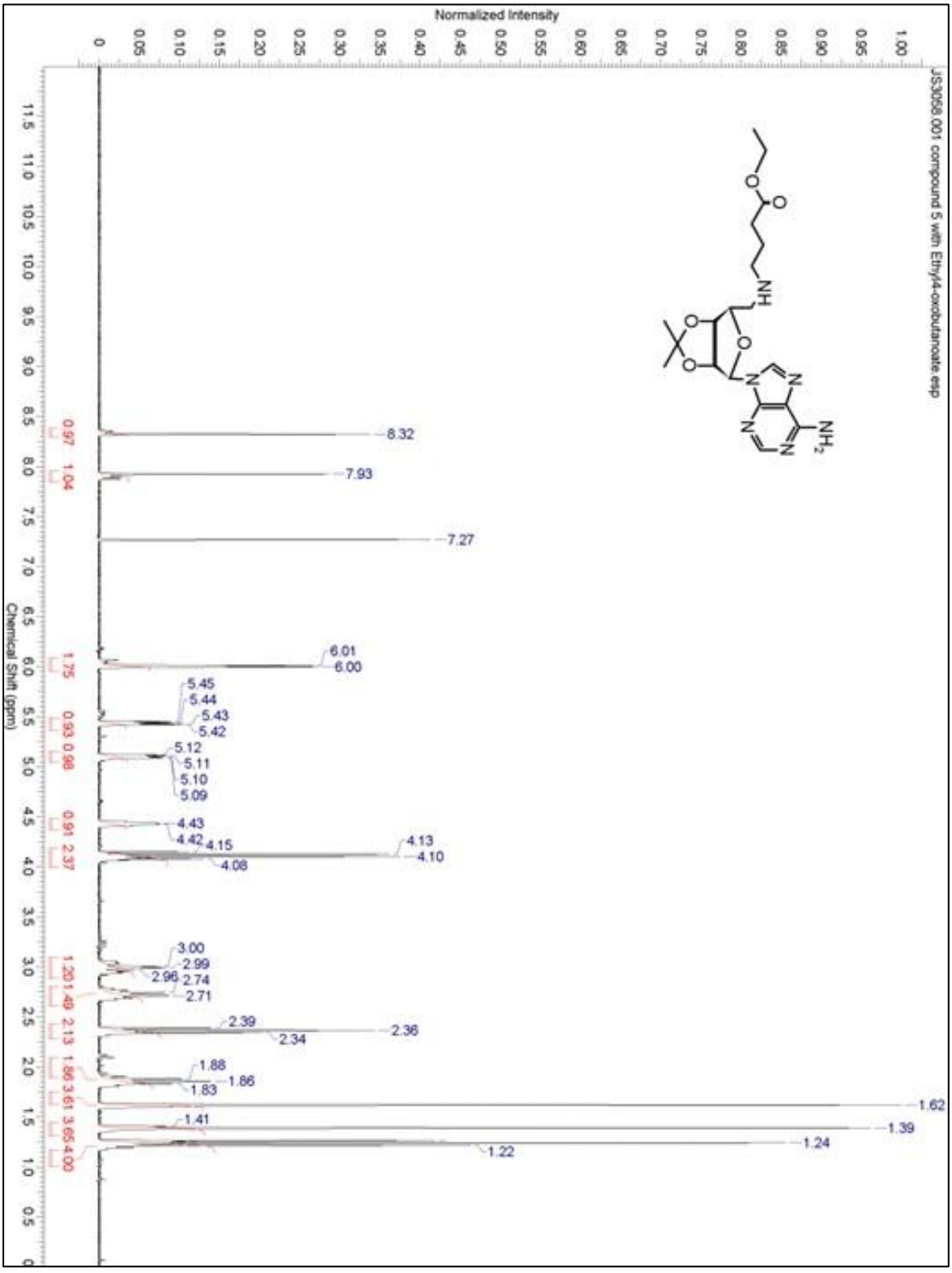

Ethyl 4-oxobutanoate

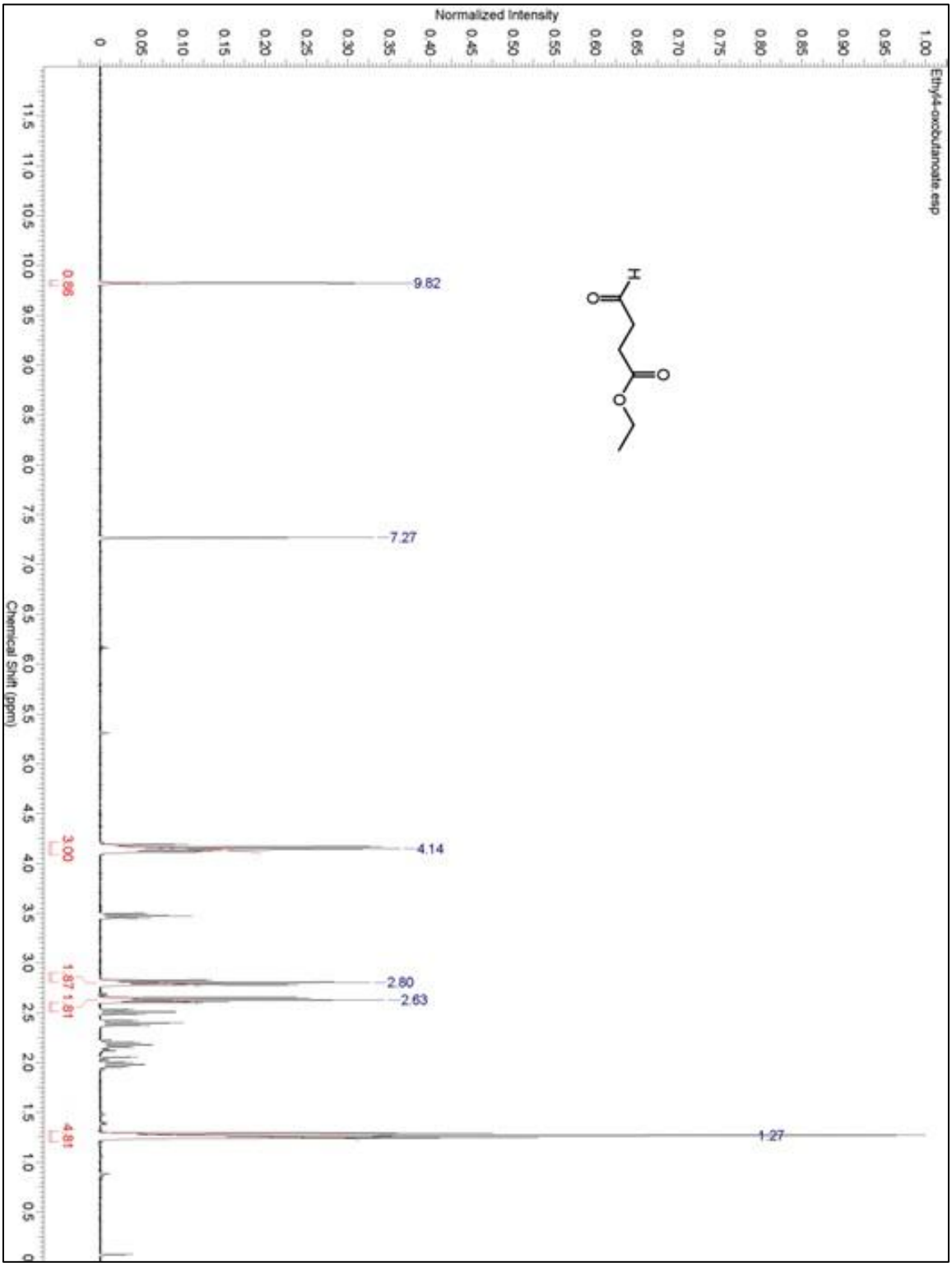

Compound 33

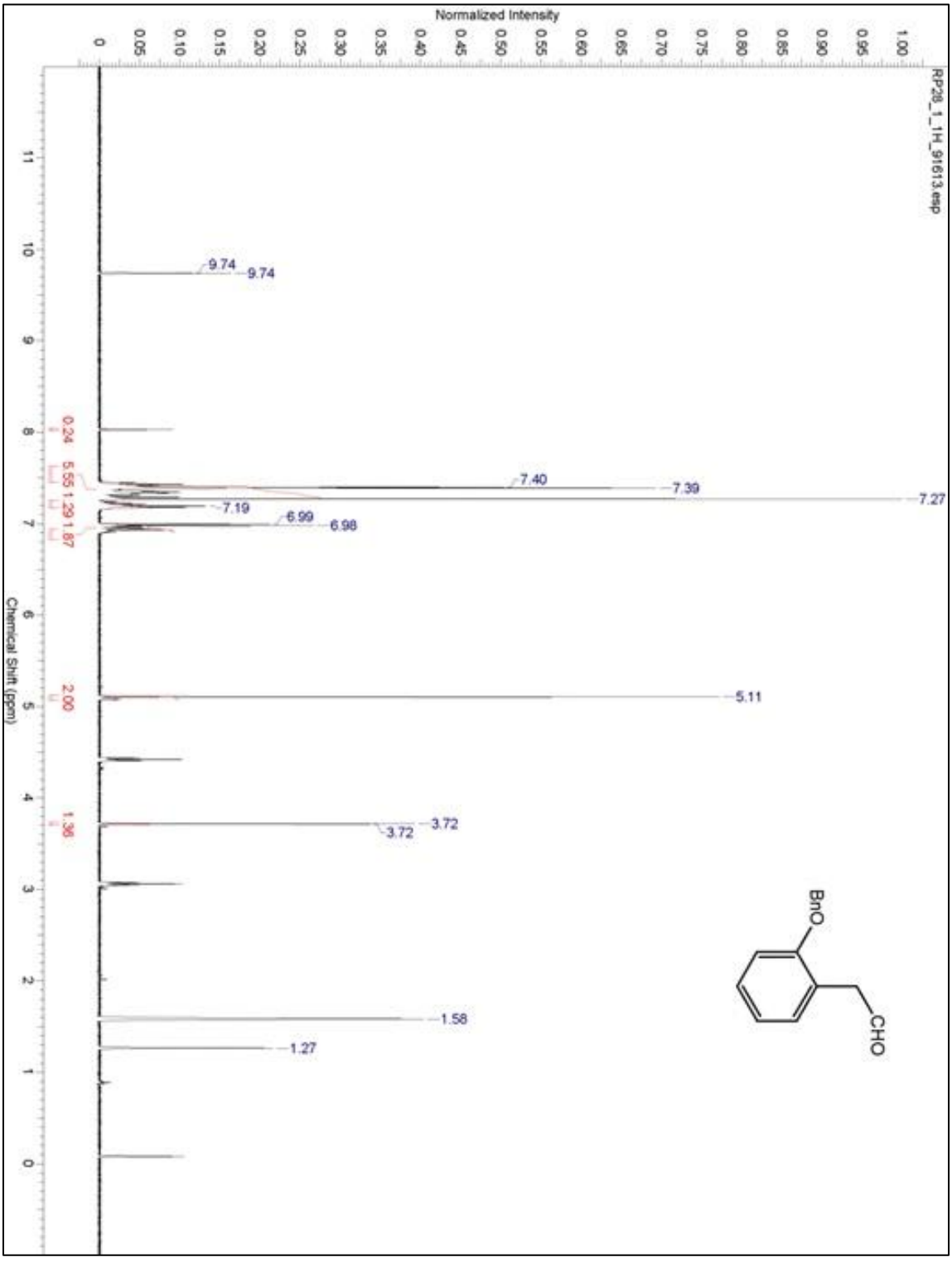
Normalized Intensity
RP28_1_1H_91613.esp
Chemical Shift (ppm)
9.74
9.74
7.40
7.39
7.27
7.19
6.99
6.98
5.11
3.72
3.72
1.58
1.27
0.24
5.55
1.29
1.87
2.00
1.36
BnO
CHO

Compound 34

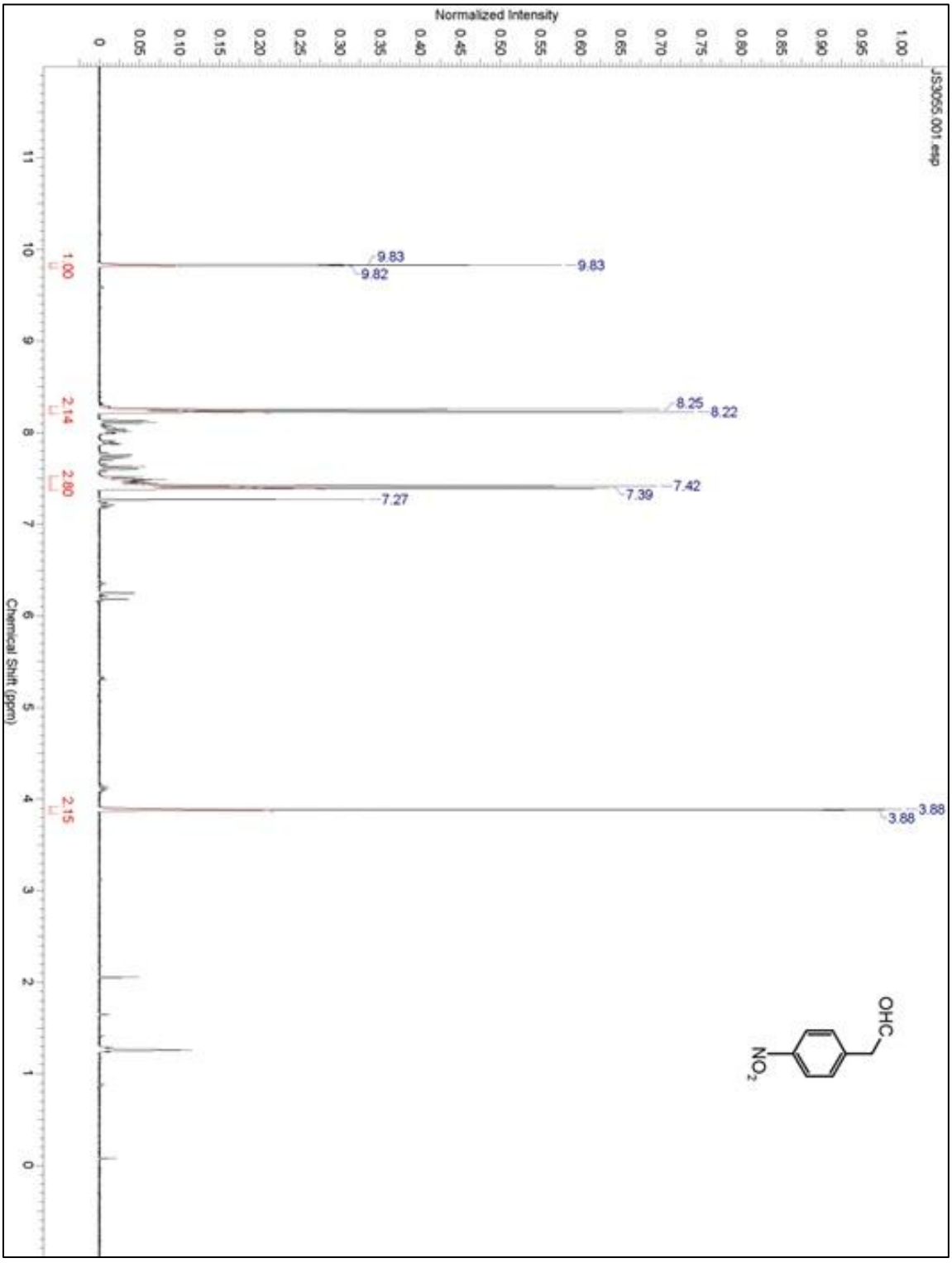
Normalized Intensity
JS3065.001.esp
Chemical Shift (ppm)
9.83
9.82
9.83
8.25
8.22
7.42
7.39
7.27
3.88
3.88
1.00
2.14
2.80
2.15
OHC
NO2

Compound 38

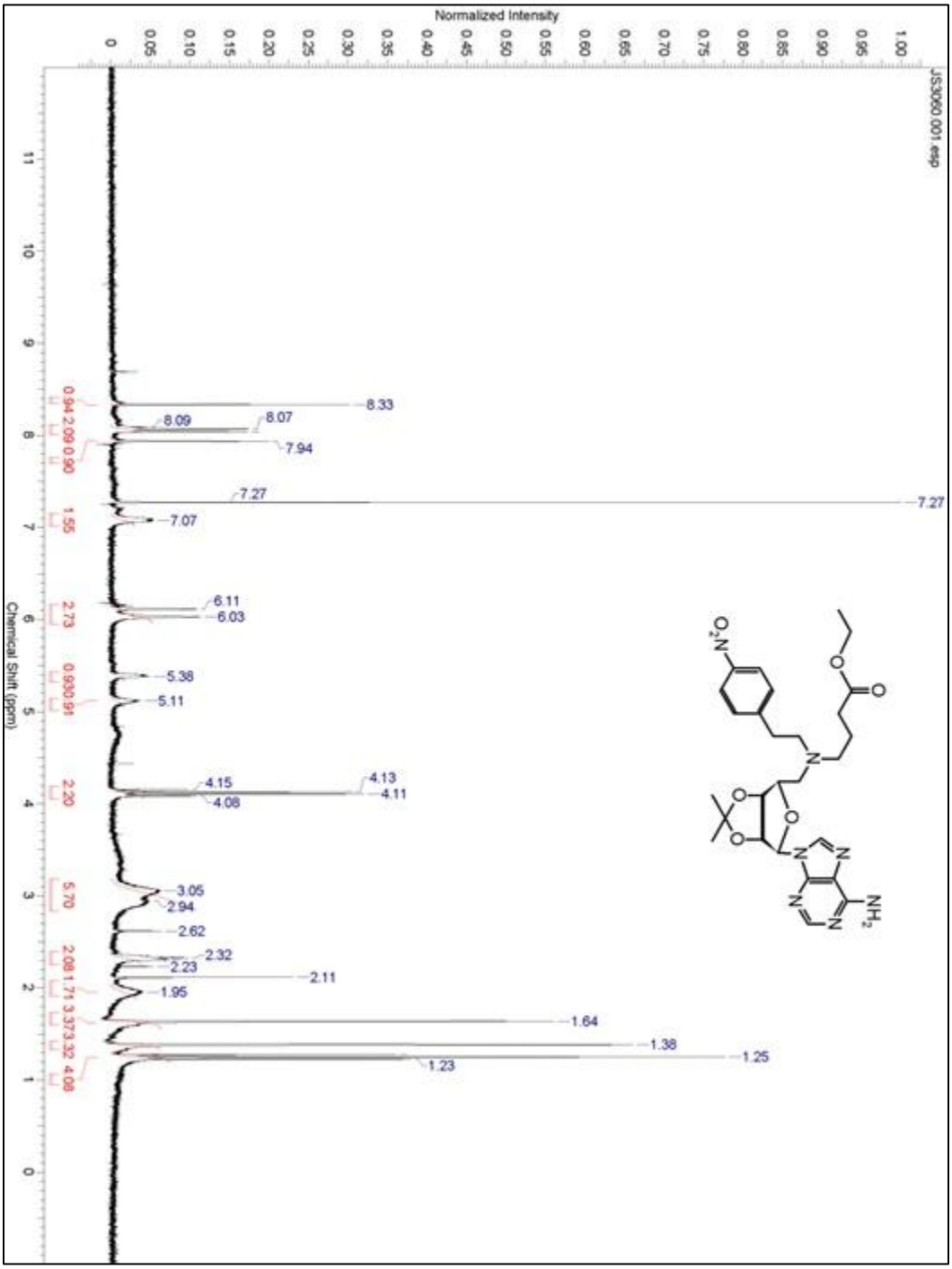
Normalized Intensity
JS3060.001.esp
Chemical Shift (ppm)
8.33
8.09
8.07
7.94
7.27
7.27
7.07
6.11
6.03
5.38
5.11
4.15
4.13
4.11
4.08
3.05
2.94
2.62
2.32
2.23
2.11
1.95
1.64
1.38
1.25
1.23
0.94 2.09 0.90
1.55
2.73
0.93 0.91
2.20
5.70
2.08 1.71 3.37 3.32 4.08
O2N
NH2

Compound 26

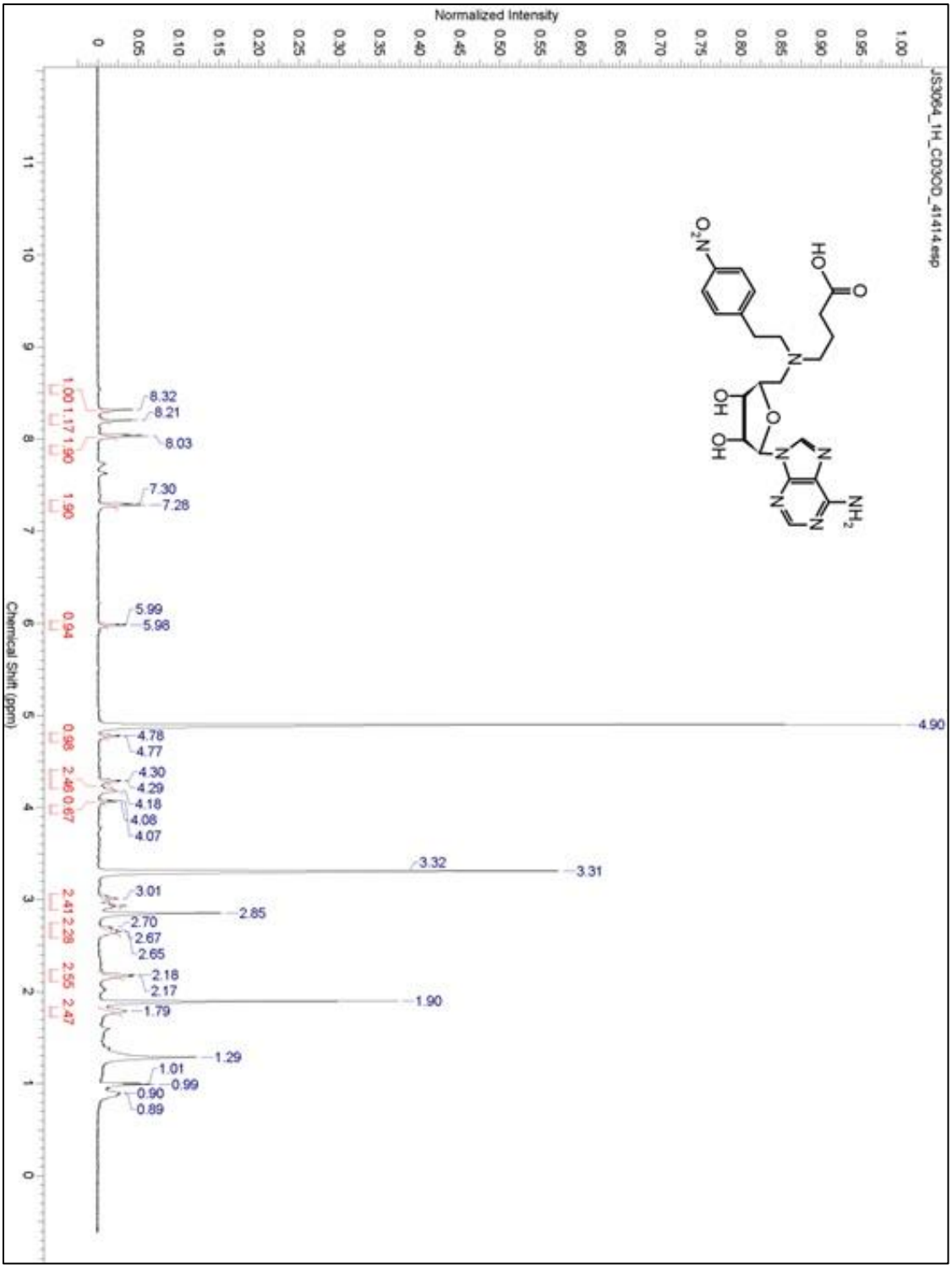
Normalized Intensity
JS3064_1H_CD3OD_41414.esp
Chemical Shift (ppm)
8.32
8.21
8.03
7.30
7.28
5.99
5.98
4.90
4.78
4.77
4.30
4.29
4.18
4.08
4.07
3.32
3.31
3.01
2.85
2.70
2.67
2.65
2.18
2.17
1.90
1.79
1.29
1.01
0.99
0.90
0.89
1.00 1.17 1.90 1.90 0.94 0.98 2.46 0.67 2.41 2.28 2.55 2.47

A.2 ^{13}C NMR Spectra

Compound 7

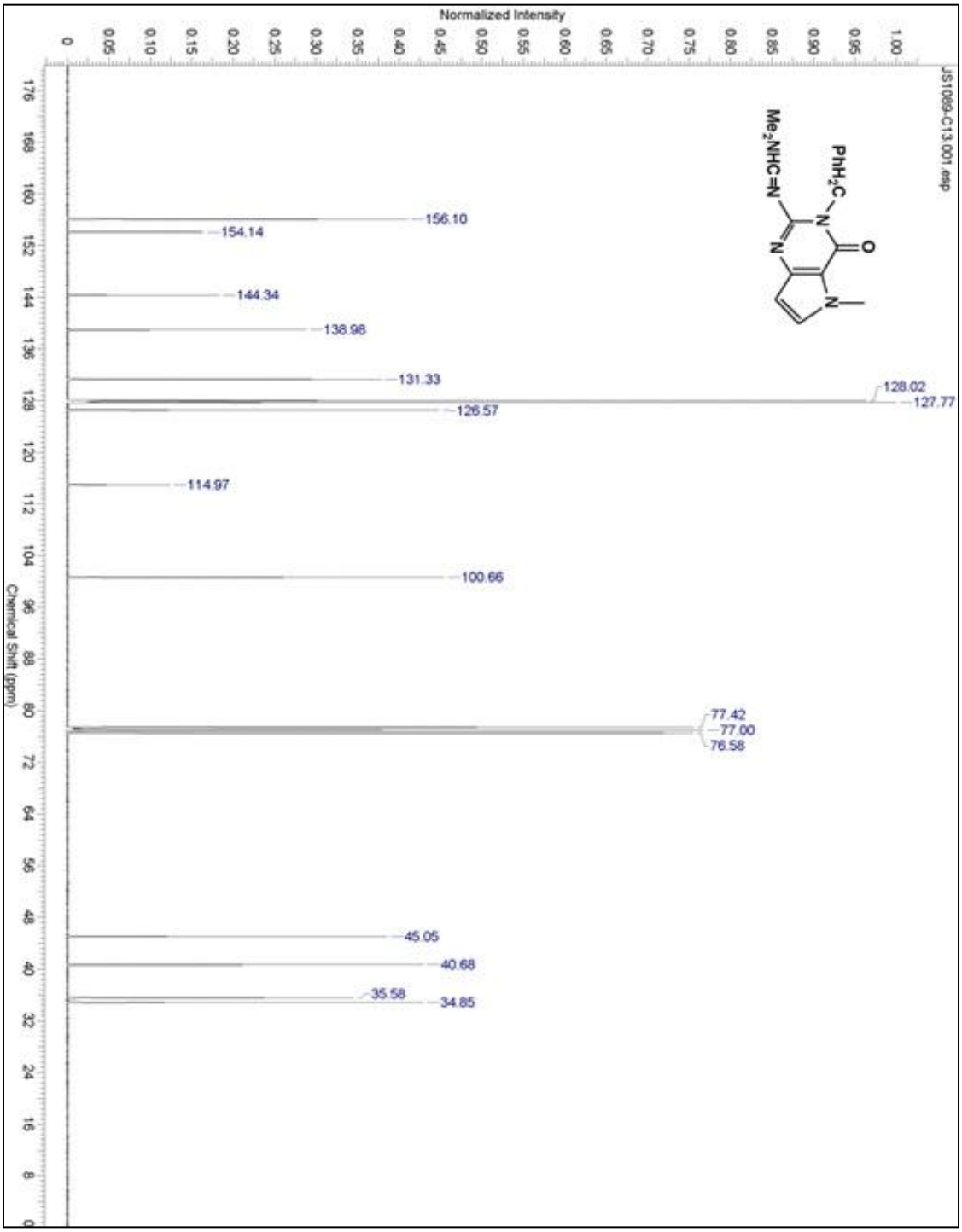

Compound 9

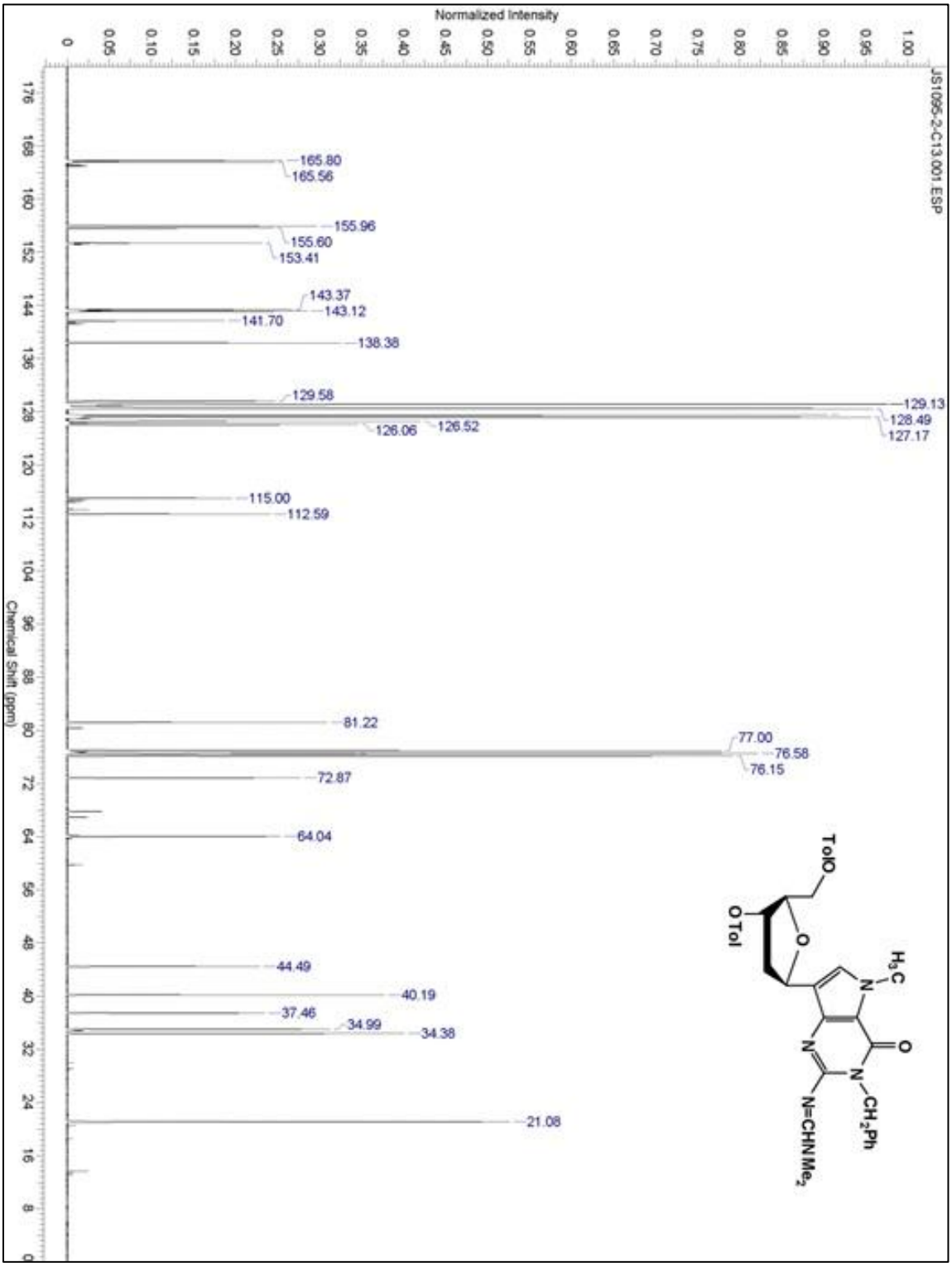
Normalized Intensity
JS1095-2-C13.001.ESP
Chemical Shift (ppm)
165.80
165.56
155.96
155.60
153.41
143.37
143.12
141.70
138.38
129.58
129.13
128.49
127.17
126.06
126.52
115.00
112.59
81.22
77.00
76.58
76.15
72.87
64.04
44.49
40.19
37.46
34.99
34.38
21.08
TolO
OTol
O
H3C
N
O
N
N
CH2Ph
N=CHNMe2

Compound 10

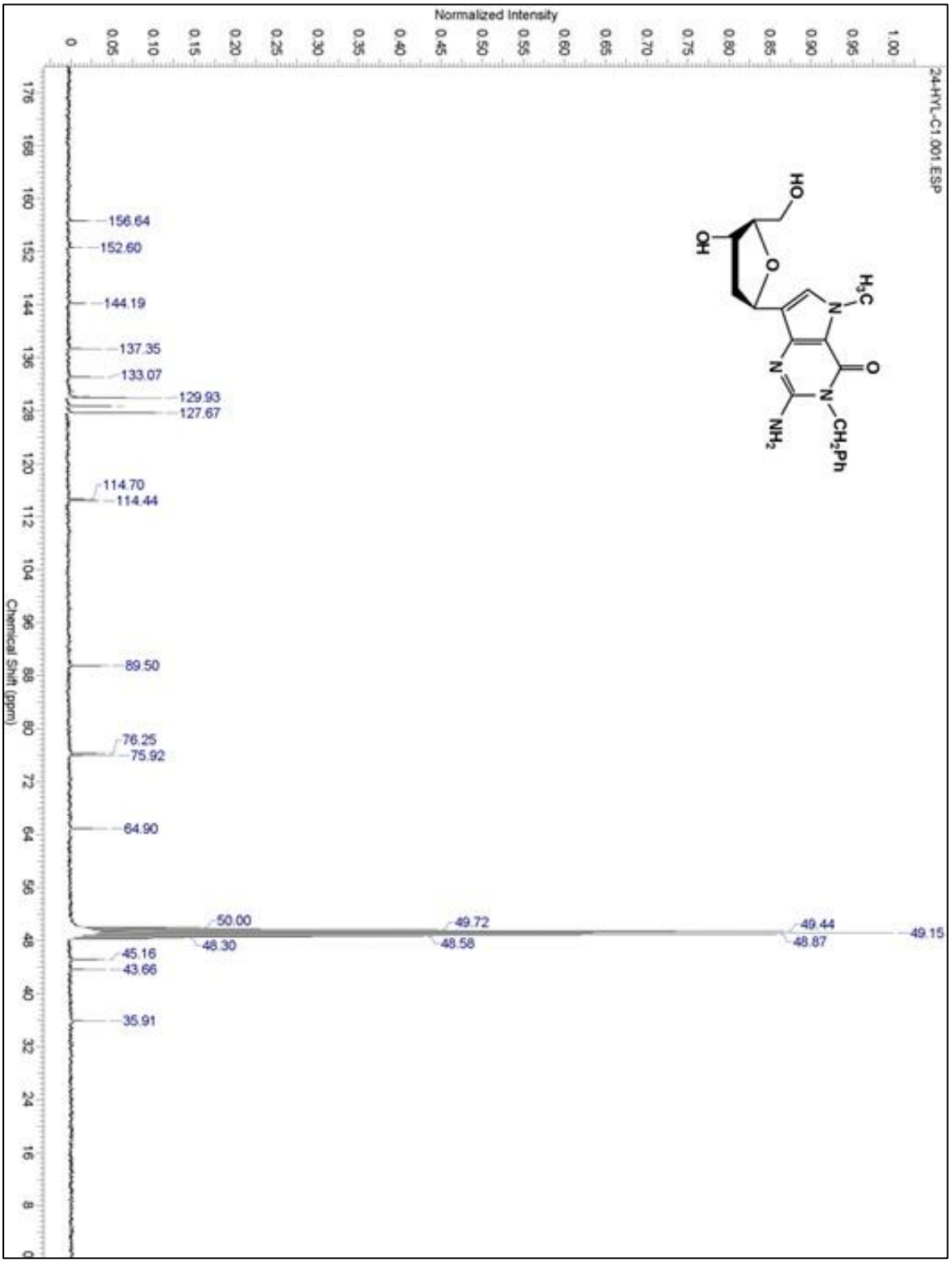
Normalized Intensity
24-HYL-C1.001.ESP
Chemical Shift (ppm)
156.64
152.60
144.19
137.35
133.07
129.93
127.67
114.70
114.44
89.50
76.25
75.92
64.90
50.00
49.72
49.44
49.15
48.30
48.58
48.87
45.16
43.66
35.91
HO
OH
O
H_3C
N
O
NH_2
CH_2Ph

Compound 12

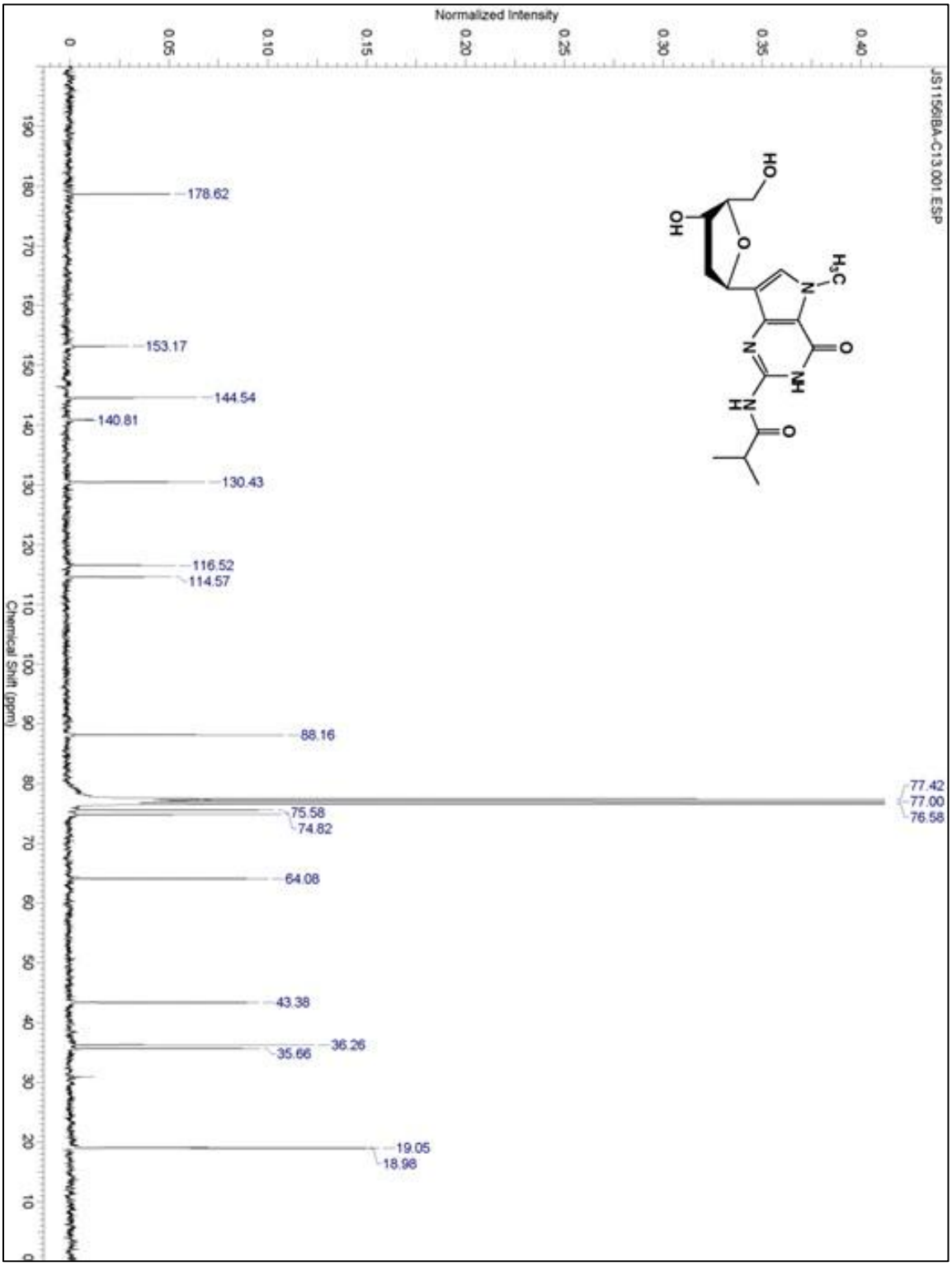
Normalized Intensity
0
0.05
0.10
0.15
0.20
0.25
0.30
0.35
0.40
JS1156IBA-C13.001.ESP
Chemical Shift (ppm)
178.62
153.17
144.54
140.81
130.43
116.52
114.57
88.16
77.42
77.00
76.58
75.58
74.82
64.08
43.38
36.26
35.66
19.05
18.98
HO
OH
O
N
H3C
N
O
NH
HN
O

Compound 13

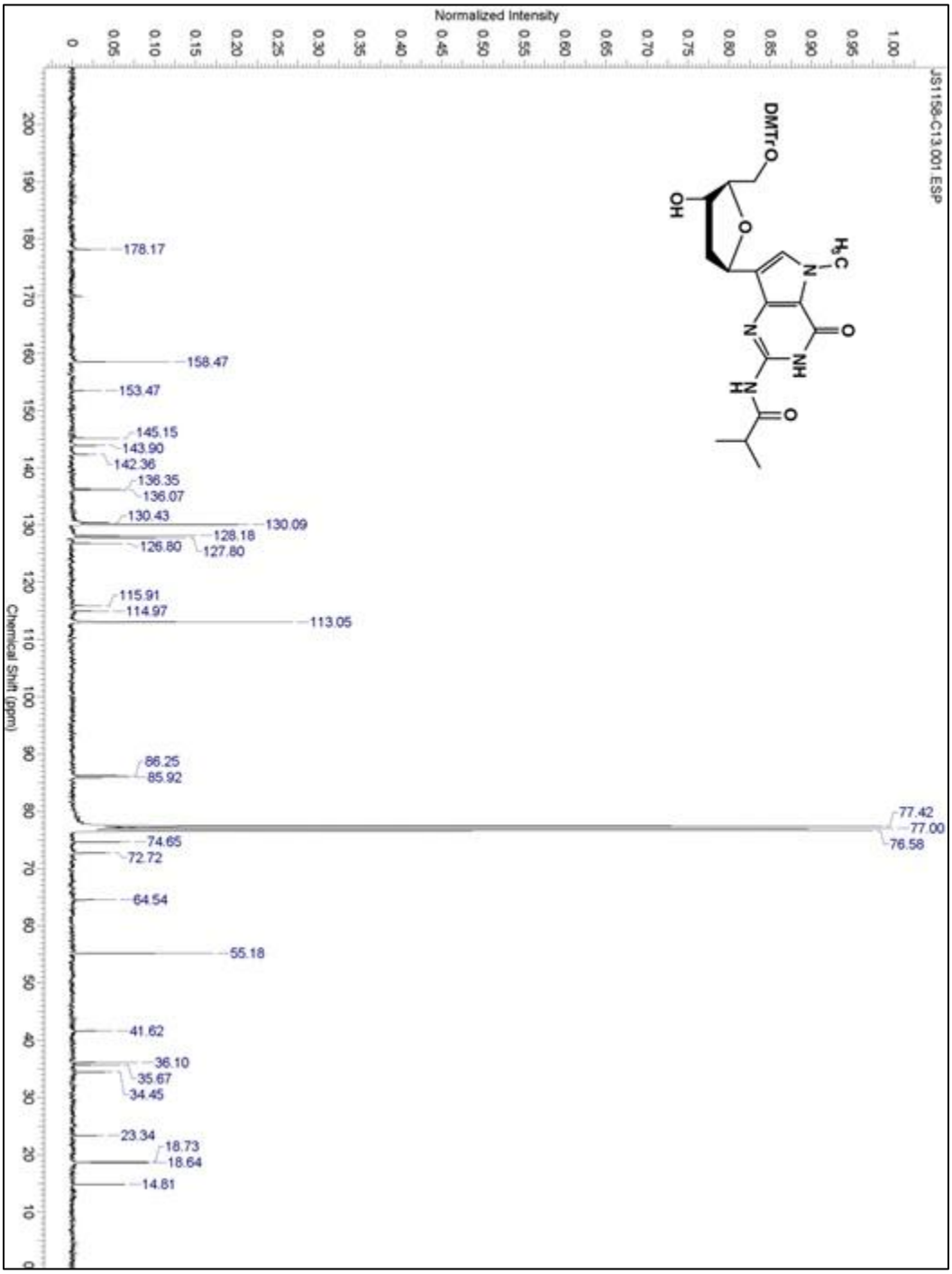
Normalized Intensity
JS1158-C13.001.ESP
Chemical Shift (ppm)
DMTrO
OH
O
N
H3C
O
N
NH
N
H
O
178.17
158.47
153.47
145.15
143.90
142.36
136.35
136.07
130.43
130.09
128.18
126.80
127.80
115.91
114.97
113.05
86.25
85.92
77.42
77.00
76.58
74.65
72.72
64.54
55.18
41.62
36.10
35.67
34.45
23.34
18.73
18.64
14.81

Compound 14 ^{31}P NMR Spectra

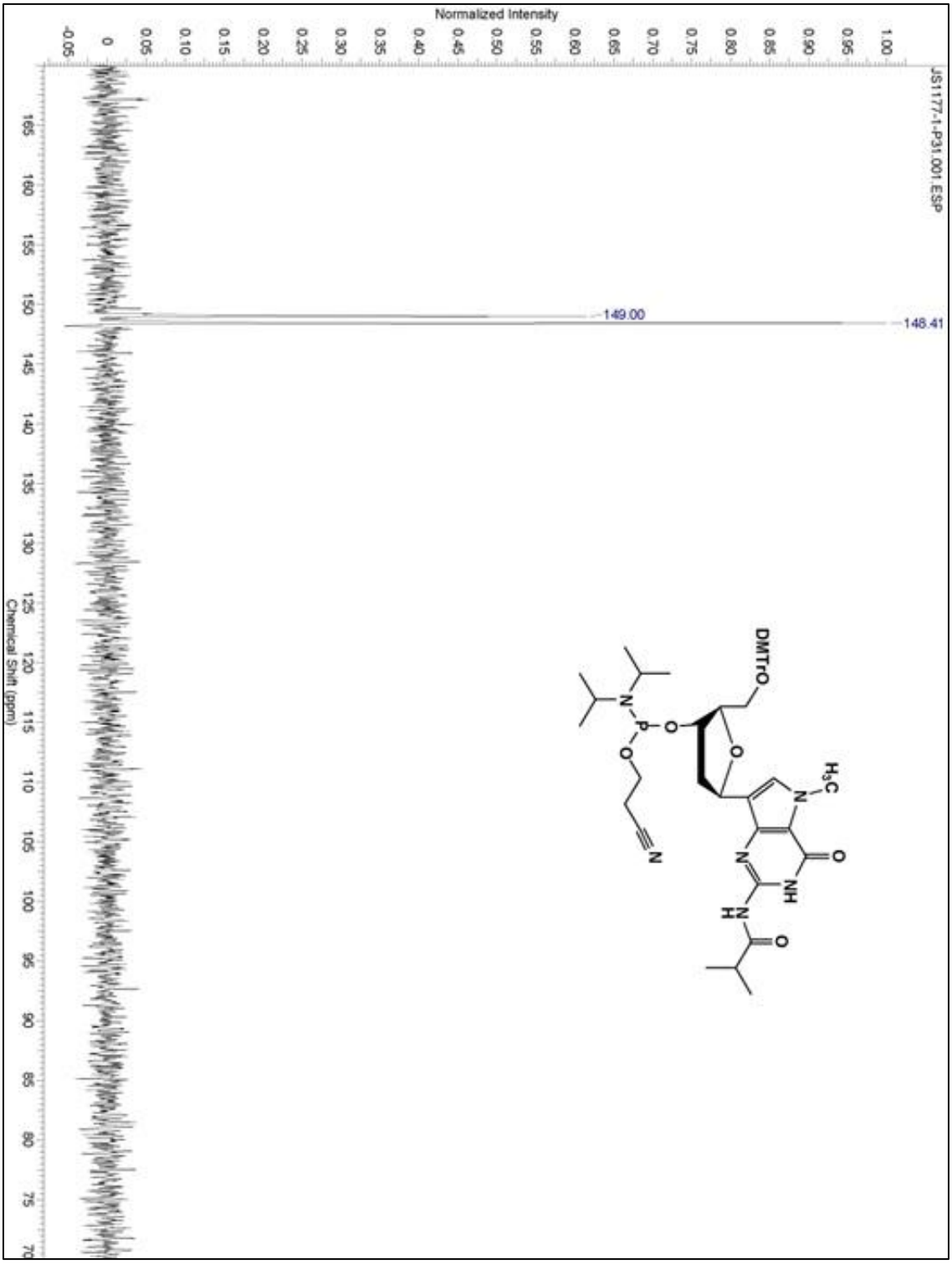

A.3 Mass Spectra

Compound 7

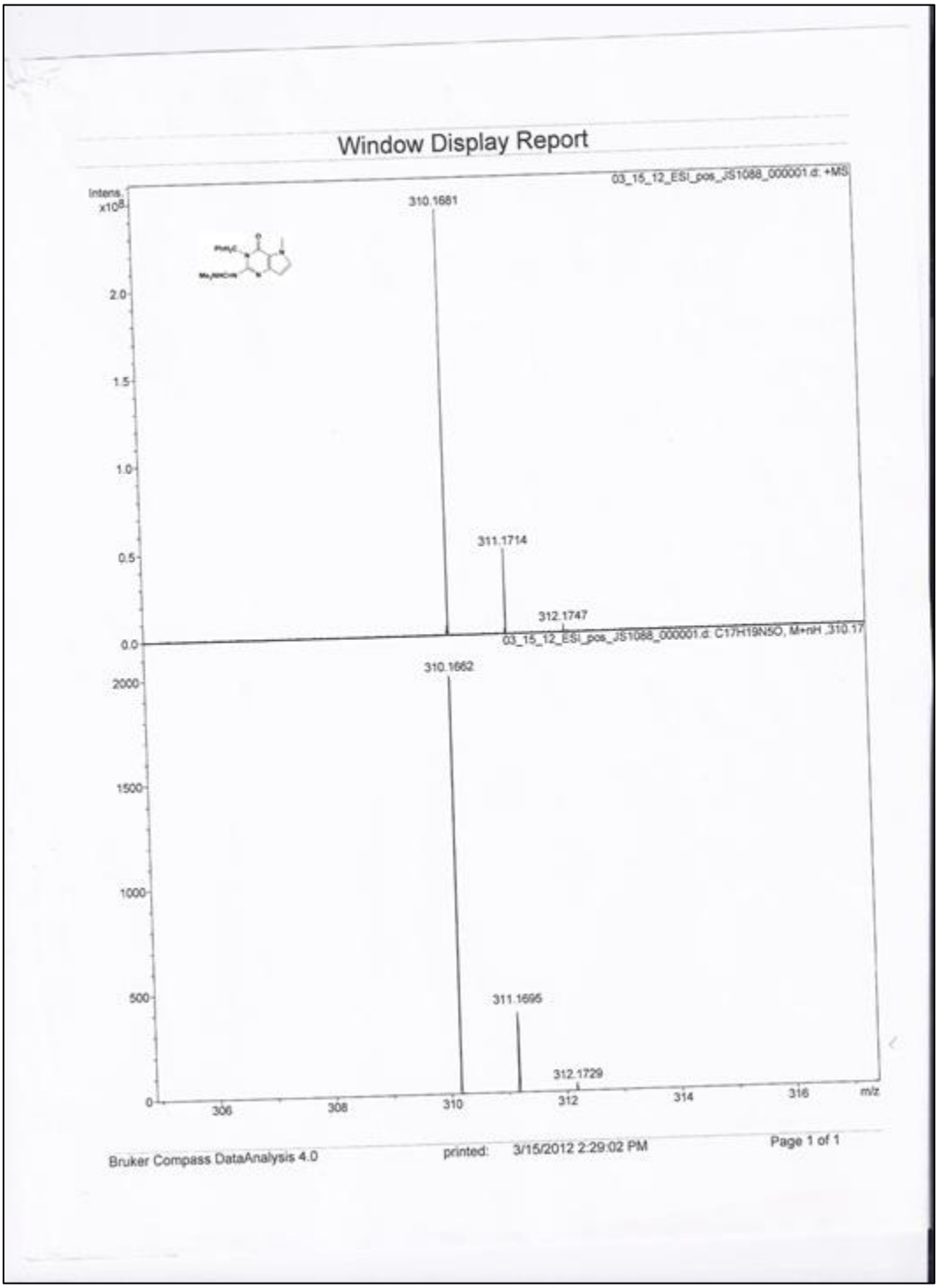

Compound 9

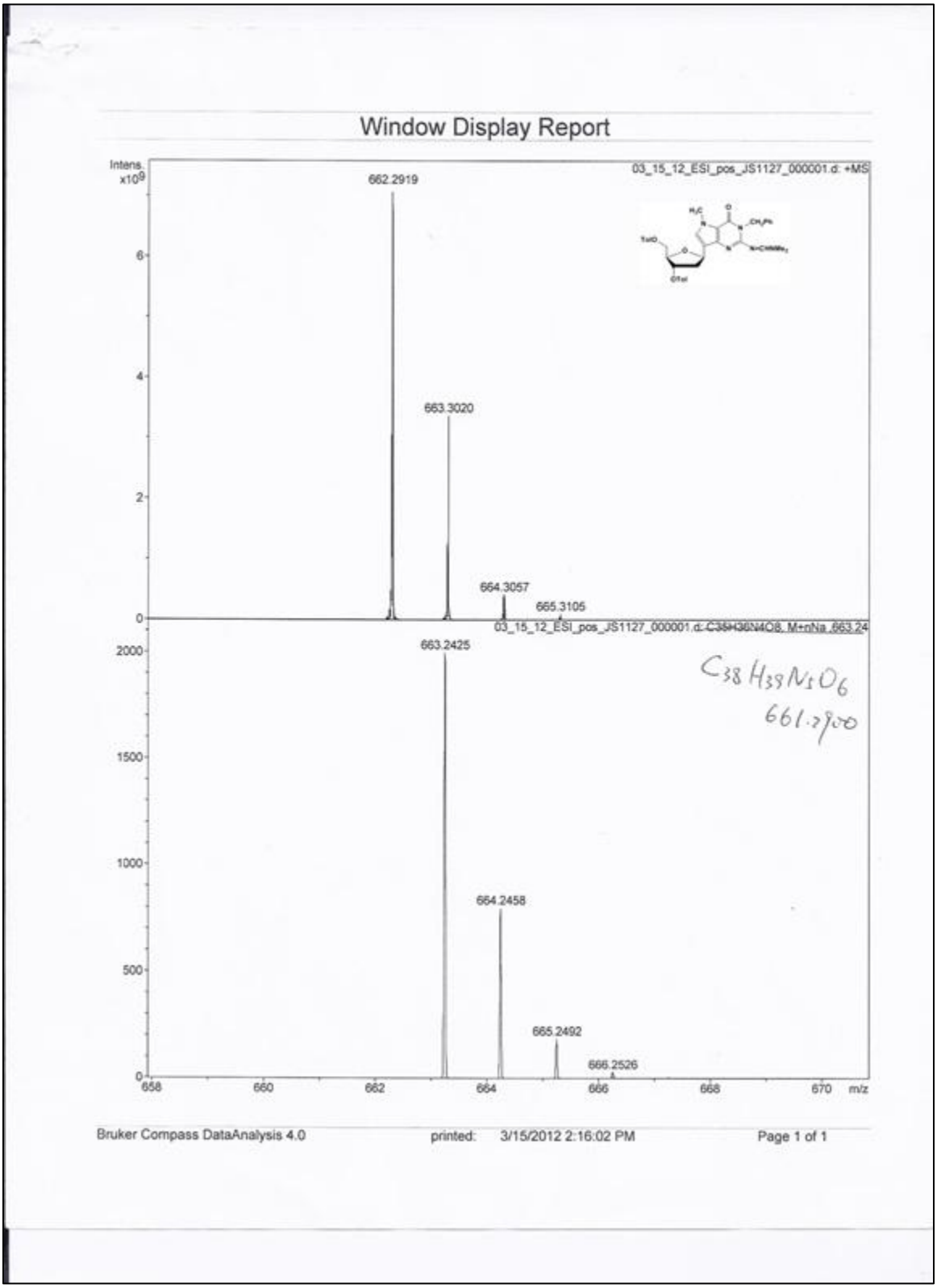
Window Display Report
Intens.
x10^9
03_15_12_ESI_pos_JS1127_000001.d: +MS
662.2919
663.3020
664.3057
665.3105
03_15_12_ESI_pos_JS1127_000001.d: C38H38N4O8, M+nNa, 663.24
663.2425
664.2458
665.2492
666.2526
C38 H38 N4 O6
661.2700
m/z
Bruker Compass DataAnalysis 4.0
printed: 3/15/2012 2:16:02 PM
Page 1 of 1

Compound 10

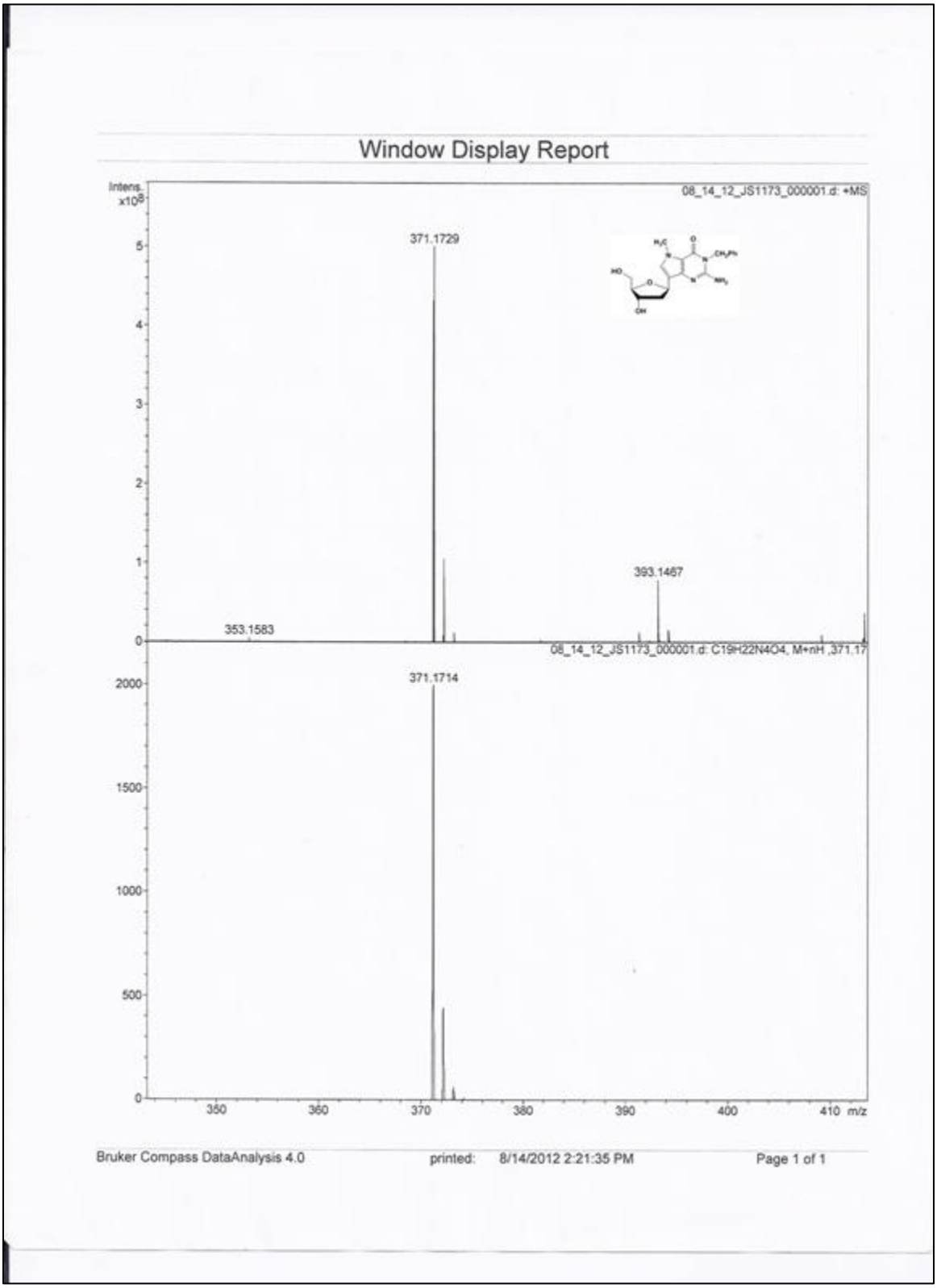
Window Display Report
Intens.
x10^8
08_14_12_JS1173_000001.d: +MS
371.1729
393.1467
353.1583
08_14_12_JS1173_000001.d: C19H22N4O4, M+nH ,371.17
371.1714
2000
1500
1000
500
0
350
360
370
380
390
400
410 m/z
Bruker Compass DataAnalysis 4.0
printed: 8/14/2012 2:21:35 PM
Page 1 of 1

Compound 12

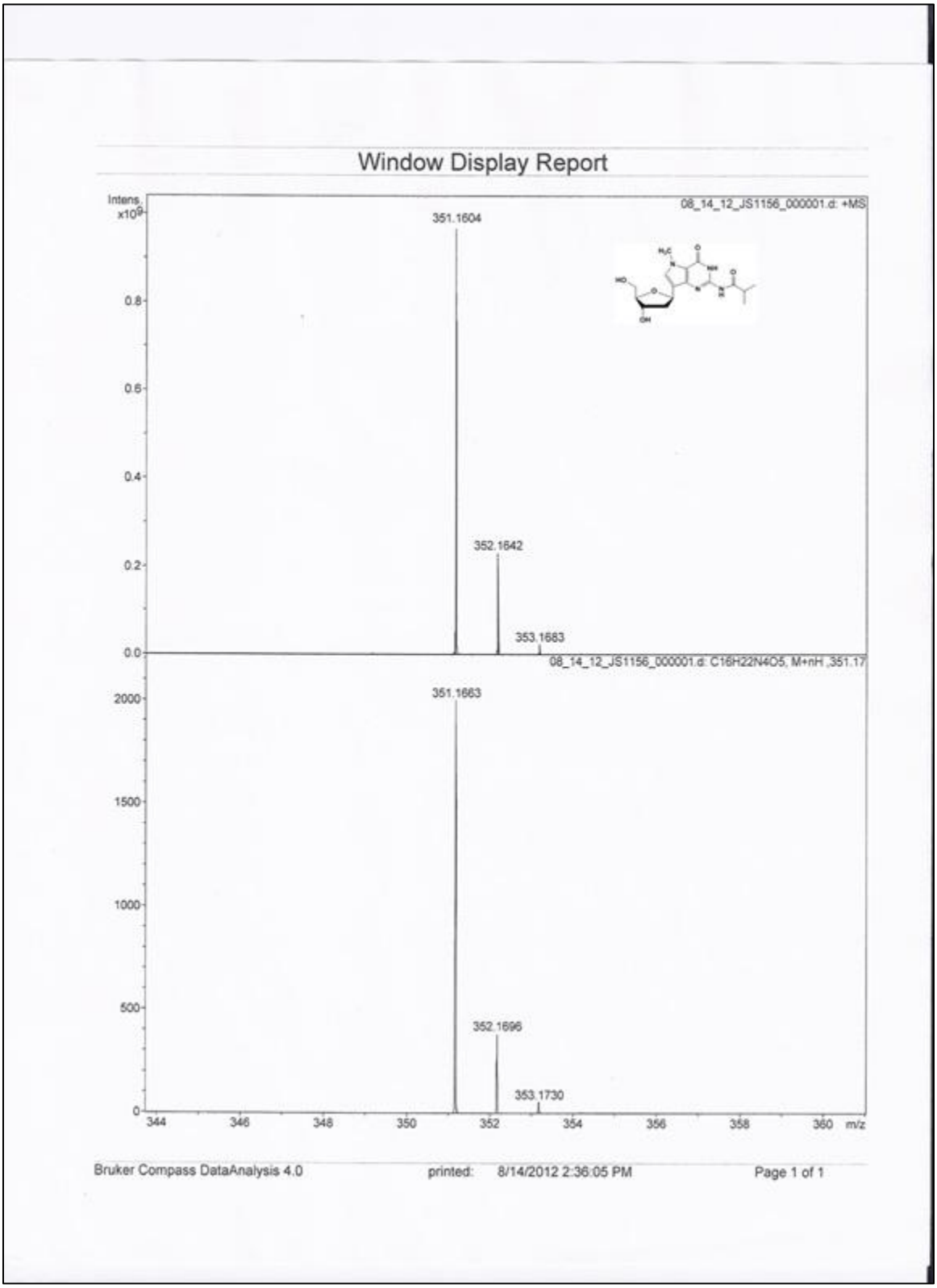
Window Display Report
Intens.
x10⁹
08_14_12_JS1156_000001.d: +MS
351.1604
352.1642
353.1683
0.8
0.6
0.4
0.2
0.0
08_14_12_JS1156_000001.d: C16H22N4O5, M+nH ,351.17
2000
1500
1000
500
0
351.1663
352.1696
353.1730
344
346
348
350
352
354
356
358
360
m/z
Bruker Compass DataAnalysis 4.0
printed: 8/14/2012 2:36:05 PM
Page 1 of 1

Compound 13

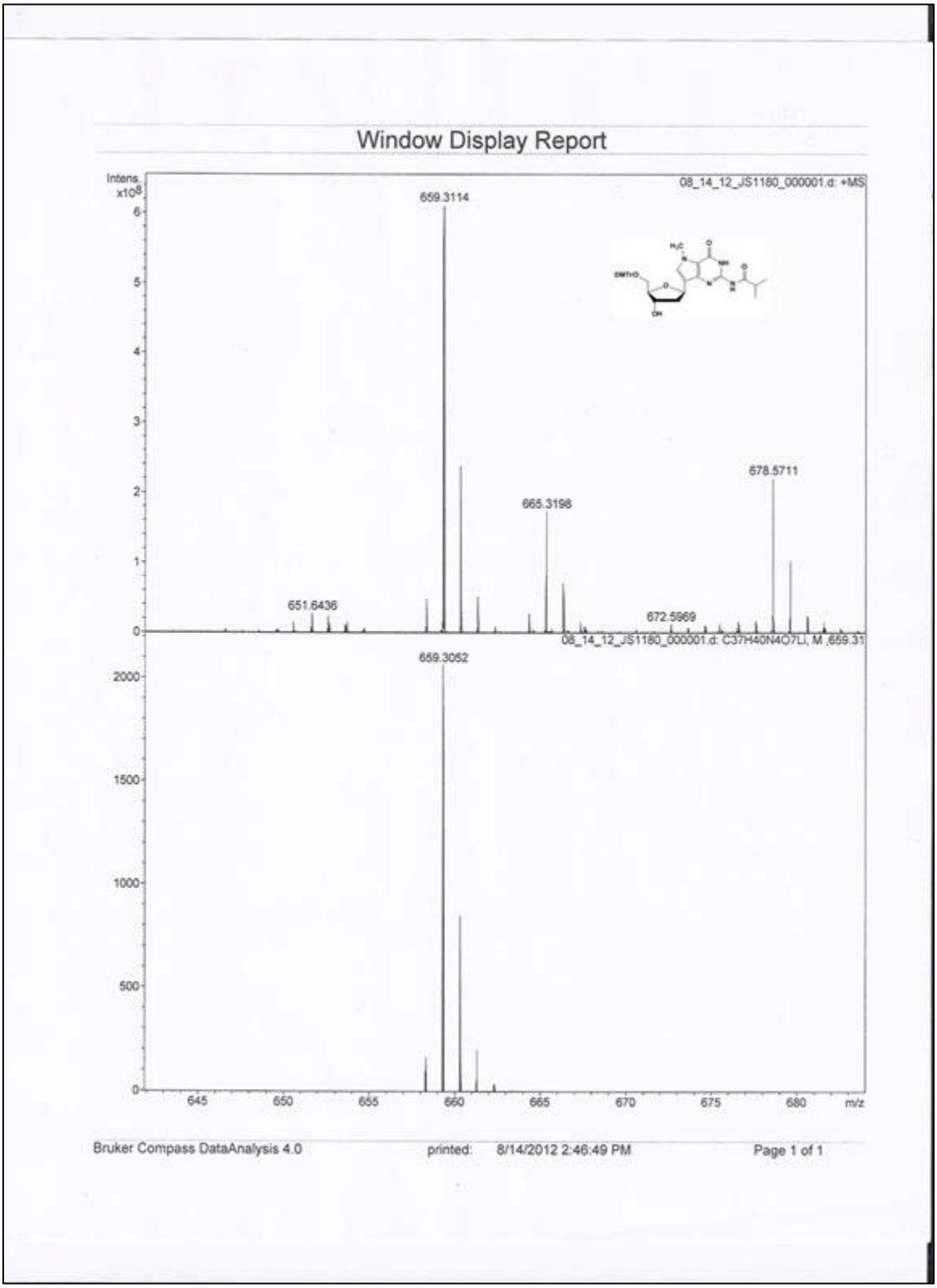
Window Display Report
Intens.
x10^8
08_14_12_JS1180_000001.d: +MS
659.3114
678.5711
665.3198
651.6436
672.5969
08_14_12_JS1180_000001.d: C37H40N4O7Li, M ,659.31
659.3052
2000
1500
1000
500
0
645
650
655
660
665
670
675
680
m/z
Bruker Compass DataAnalysis 4.0
printed: 8/14/2012 2:46:49 PM
Page 1 of 1

Compound 14

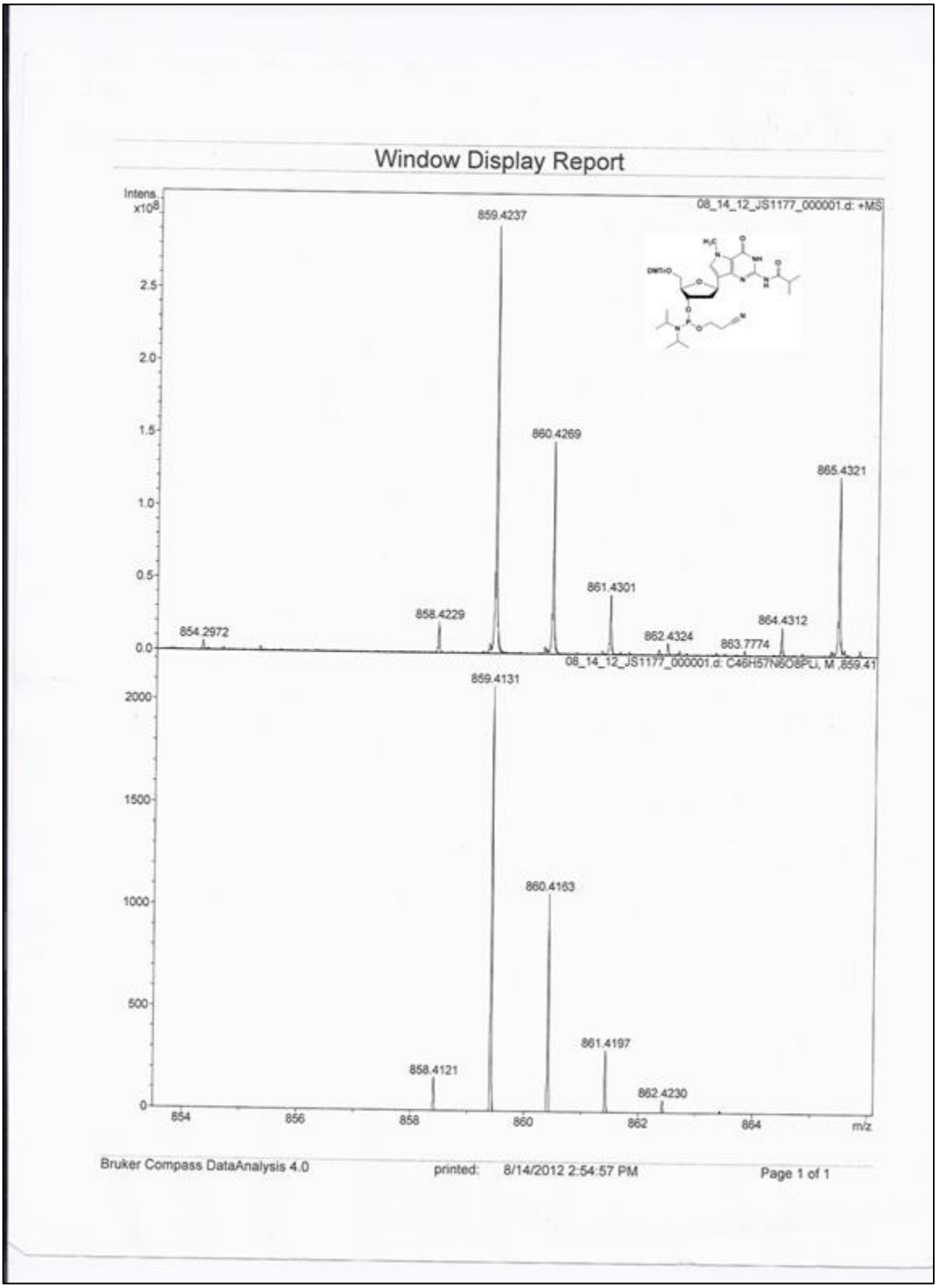
Window Display Report
Intens.
x10^8
08_14_12_JS1177_000001.d: +MS
859.4237
860.4269
865.4321
861.4301
858.4229
854.2972
862.4324
863.7774
864.4312
08_14_12_JS1177_000001.d: C46H57N6O8PLi, M ,859.41
859.4131
860.4163
861.4197
858.4121
862.4230
854
856
858
860
862
864
m/z
Bruker Compass DataAnalysis 4.0
printed: 8/14/2012 2:54:57 PM
Page 1 of 1

Oligonucleotide 16

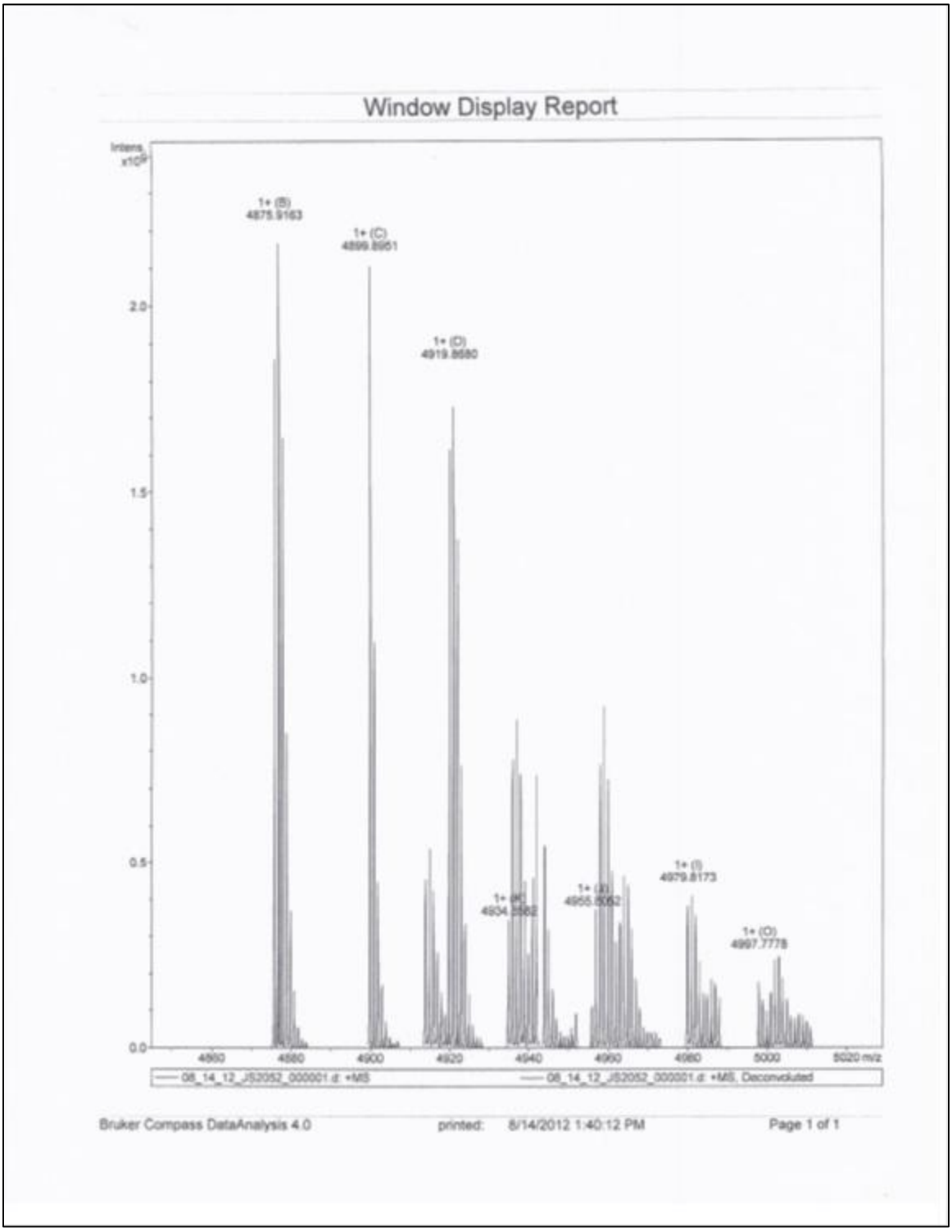

Oligonucleotide 18

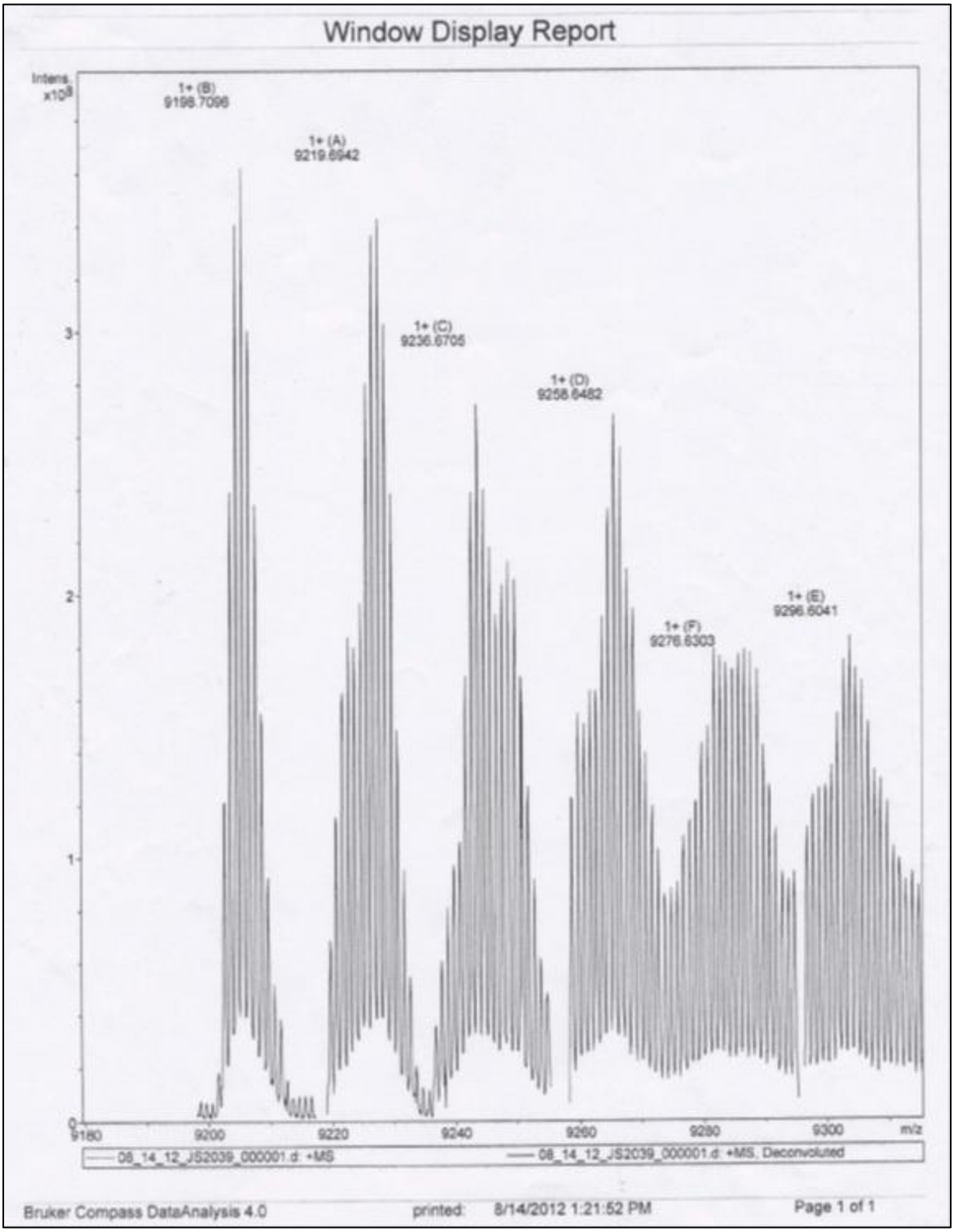

Oligonucleotide 22

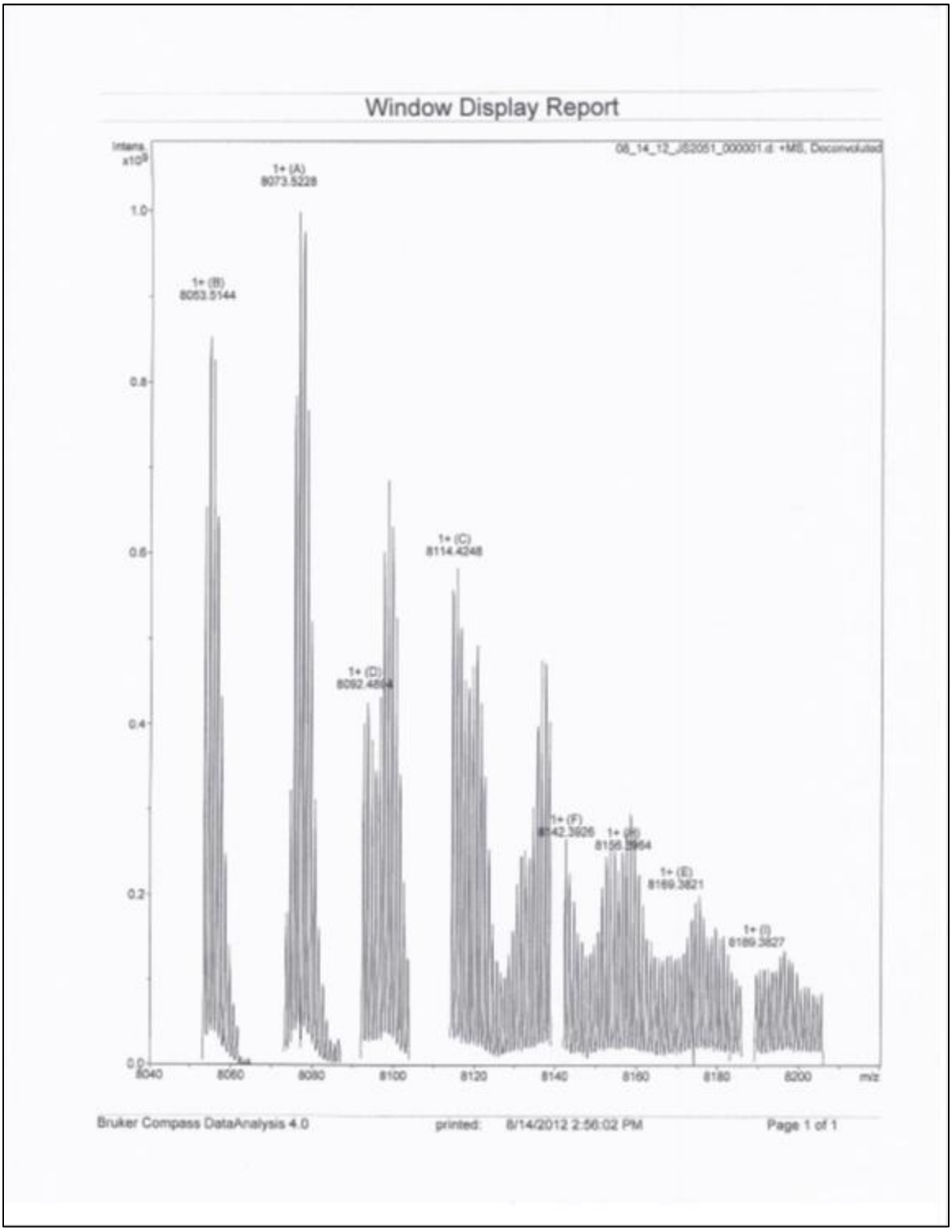

REFERENCES

1. Pletsa, V., Valavanis, C., Van Delft, J., Steenwinkel, M., and Kyrtopoulos, S. A. (1997) DNA Damage and Mutagenesis Induced by Procarbazine in Lambda Lacz Transgenic Mice: Evidence that Bone Marrow Mutations do not Arise Primarily Through Miscoding by O6-Methylguanine, *Carcinogenesis 18*, 2191-2196.

2. De Bont, R., and van Larebeke, N. (2004) Endogenous DNA Damage in Humans: A Review of Quantitative Data, *Mutagenesis 19*, 169-185.

3. O'Hagan, H. M., Mohammad, H. P., and Baylin, S. B. (2008) Double Strand Breaks can Initiate Gene Silencing and SIRT1-Dependent Onset of DNA Methylation in an Exogenous Promoter CpG Island, *PLoS Genetics 4*, e1000155.

4. Mishina, Y., Duguid, E. M., and He, C. (2006) Direct Reversal of DNA Alkylation Damage, *Chemical Reviews 106*, 215-232.

5. Gates, K. S., Nooner, T., and Dutta, S. (2004) Biologically Relevant Chemical Reactions of N7-Alkylguanine Residues in DNA, *Chemical Research in Toxicology 17*, 839-856.

6. Pullman, A., and Pullman, B. (1981) Molecular Electrostatic Potential of the Nucleic Acids, *Quarterly Reviews of Biophysics 14*, 289-380.

7. Jang, Y. H., Goddard, W. A., 3rd, Noyes, K. T., Sowers, L. C., Hwang, S., and Chung, D. S. (2002) First Principles Calculations of the Tautomers and Pk(a) Values Of 8-Oxoguanine: Implications for Mutagenicity and Repair, *Chemical Research in Toxicology 15*, 1023-1035.

8. O'Connor, P. J., Capps, M. J., Craig, A. W., Lawley, P. D., and Shah, S. A. (1972) Differences in the Patterns of Methylation in Rat Liver Ribosomal Ribonucleic Acid after Reaction In Vivo with Methyl Methanesulphonate and N,N-Dimethylnitrosamine, *Biochemical Journal 129*, 519-528.

9. Shooter, K. V., Howse, R., Shah, S. A., and Lawley, P. D. (1974) The Molecular Basis for Biological Inactivation of Nucleic Acids. The Action of Methylating Agents on the Ribonucleic Acid-Containing Bacteriophage R17, *Biochemical Journal 137*, 303-312.

10. Beranek, D. T. (1990) Distribution of Methyl and Ethyl Adducts Following Alkylation with Monofunctional Alkylating Agents, *Mutation Research 231*, 11-30.

11. Preussmann, R., and Stewart, B. W. (1984) N-Nitroso Carcinogens in Chemical Carcinogens, *ACS Monograph 182. 2*, 643-828.

12. Boysen, G., Pachkowski, B. F., Nakamura, J., and Swenberg, J. A. (2009) The Formation and Biological Significance of N7-Guanine Adducts, *Mutation Research 678*, 76-94.

13. Drabløs, F., Feyzi, E., Aas, P. A., Vaagbø, C. B., Kavli, B., Bratlie, M. S., Peña-Diaz, J., Otterlei, M., Slupphaug, G., and Krokan, H. E. (2004) Alkylation Damage in DNA and RNA Repair Mechanisms and Medical Significance, *DNA Repair 3*, 1389-1407.

14. Crick, F., and Watson, J. (1953) Molecular Structure of Nucleic Acids, *Nature 171*, 737-738.

15. Han, L., and Zhao, Z. (2009) CpG Islands or CpG Clusters: How to Identify Functional GC-Rich Regions in a Genome?, *BMC Bioinformatics 10*, 65.

16. Gavery, M. R., and Roberts, S. B. (2010) DNA Methylation Patterns Provide Insight into Epigenetic Regulation in the Pacific Oyster (Crassostrea Gigas), *BioMed Central Genomics 11*, 483.

17. Wu, H., Tao, J., Chen, P. J., Shahab, A., Ge, W., Hart, R. P., Ruan, X., Ruan, Y., and Sun, Y. E. (2010) Genome-Wide Analysis Reveals Methyl-CpG–Binding Protein 2–Dependent Regulation of MicroRNAs in a Mouse Model of Rett Syndrome, *Proceedings of the National Academy of Sciences 107*, 18161-18166.

18. Lapeyre, J.-N., and Becker, F. F. (1979) 5-Methylcytosine Content of Nuclear DNA During Chemical Hepatocarcinogenesis and in Carcinomas which Result, *Biochemical and Biophysical Research Communications 87*, 698-705.

19. Robertson, K. D. (2001) DNA Methylation, Methyltransferases, and Cancer, *Oncogene 20*, 3139-3155.

20. Okano, M., Bell, D. W., Haber, D. A., and Li, E. (1999) DNA Methyltransferases Dnmt3a and Dnmt3b are Essential for De Novo Methylation and Mammalian Development, *Cell 99*, 247-257.

21. Bestor, T., Laudano, A., Mattaliano, R., and Ingram, V. (1988) Cloning and Sequencing of a cDNA Encoding DNA Methyltransferase of Mouse Cells: The Carboxyl-Terminal Domain of the Mammalian Enzymes is Related to Bacterial Restriction Methyltransferases, *Journal of Molecular Biology 203*, 971-983.

22. Xie, S., Wang, Z., Okano, M., Nogami, M., Li, Y., He, W.-W., Okumura, K., and Li, E. (1999) Cloning, Expression and Chromosome Locations of the Human DNMT3 Gene Family, *Gene 236*, 87-95.

23. Goll, M. G., and Bestor, T. H. (2005) Eukaryotic Cytosine Methyltransferases, *Annual Review of Biochemistry 74*, 481-514.

24. Weisenberger, D. J., Velicescu, M., Cheng, J. C., Gonzales, F. A., Liang, G., and Jones, P. A. (2004) Role of the DNA Methyltransferase Variant Dnmt3b3 in DNA Methylation, *Molecular Cancer Research 2,* 62-72.

25. Hermann, A., Gowher, H., and Jeltsch, A. (2004) Biochemistry and Biology of Mammalian DNA Methyltransferases, *Cellular and Molecular Life Sciences 61,* 2571-2587.

26. Robertson, K. D., Uzvolgyi, E., Liang, G., Talmadge, C., Sumegi, J., Gonzales, F. A., and Jones, P. A. (1999) The Human DNA Methyltransferases (DNMTs) 1, 3a and 3b: Coordinate mRNA Expression in Normal Tissues and Overexpression in Tumors, *Nucleic Acids Research 27,* 2291-2298.

27. Anger, W. K., Moody, L., Burg, J., Brightwell, W. S., Taylor, B. J., Russo, J. M., Dickerson, N., Setzer, J. V., Johnson, B. L., and Hicks, K. (1986) Neurobehavioral Evaluation of Soil and Structural Fumigators Using Methyl Bromide and Sulfuryl Fluoride, *Neurotoxicology 7*, 137-156.

28. Hotchkiss, J. H. (1989) Preformed N-nitroso Compounds in Foods and Beverages, *Cancer Surveys 8,* 295-321.

29. Rydberg, B., and Lindahl, T. (1982) Nonenzymatic Methylation of DNA by the Intracellular Methyl Group Donor S-adenosyl-L-methionine is a Potentially Mutagenic Reaction., *The European Molecular Biology Organization Journal 1*, 211–216.

30. Jansen, J. G., de Groot, A. J. L., van Teijlingen, C. M. M., Tates, A. D., Vrieling, H., and van Zeeland, A. A. (1996) Induction of hprt Gene Mutations in Splenic T-lymphocytes from the Rat Exposed in vivo to DNA Methylating Agents is Correlated with Formation of O6-Methylguanine in Bone Marrow and not in the Spleen, *Carcinogenesis 17*, 2183-2191.

31. Larson, K., Sahm, J., Shenkar, R., and Strauss, B. (1985) Methylation Induced Blocks to in Vitro DNA Replication, *Mutation Research 150,* 77-84.

32. Fronza, G., and Gold, B. (2004) The Biological Effects of N3-Methyladenine, *Journal of Cellular Biochemistry 91,* 250-257.

33. Lawley, P. D., and Searle, C. E. (1984) Carcinogenesis by Alkylating Agents in Chemical Carcinogens, *ACS Monograph 182. 1*, 303–484.

34. Boiteux, S., Huisman, O., and Laval, J. (1984) 3-Methyladenine Residues in DNA Induce the SOS Function sfiA in Escherichia coli, *The European Molecular Biology Organization Journal 3,* 2569.

35. Settles, S., Wang, R.-W., Fronza, G., and Gold, B. (2010) Effect of N3-Methyladenine and an Isosteric Stable Analogue on DNA Polymerization, *Journal of Nucleic Acids 2010*, 1-14.

36. Lawley, P. D., and Brookes, P. (1961) Acidic Dissociation of 7 : 9-Dialkylguanines and its Possible Relation to Mutagenic Properties of Alkylating Agents, *Nature 192*, 1081-1082.

37. Loechler, E. L., Green, C. L., and Essigmann, J. M. (1984) In Vivo Mutagenesis by O6-Methylguanine Built into a Unique Site in a Viral Genome, *Proceedings of the National Academy of Sciences 81*, 6271-6275.

38. Citti, L., Gervasi, P. G., Turchi, G., Bellucci, G., and Bianchini, R. (1984) The Reaction of 3,4-Epoxy-1-Butene with Deoxyguanosine and DNA in Vitro: Synthesis and Characterization of the Main Adducts, *Carcinogenesis 5*, 47-52.

39. O'Connor, T. R., Boiteux, S., and Laval, J. (1988) Ring-Opened 7-Methylguanine Residues in DNA are a Block to in Vitro DNA Synthesis, *Nucleic Acids Research 16*, 5879-5894.

40. Earley, L. F., Minko, I. G., Christov, P. P., Rizzo, C. J., and Lloyd, R. S. (2013) Mutagenic Spectra Arising from Replication Bypass of the 2,6-Diamino-4-hydroxy-N5-methyl Formamidopyrimidine Adduct in Primate Cells, *Chemical Research in Toxicology 26*, 1108-1114.

41. Strauss, B. S. (1991) The 'A rule' of Mutagen Specificity: A Consequence of DNA Polymerase Bypass of Non-Instructional Lesions?, *BioEssays 13*, 79-84.

42. Armstrong, M. J., and Galloway, S. M. (1997) Mismatch Repair Provokes Chromosome Aberrations in Hamster Cells Treated with Methylating Agents or 6-Thioguanine, but not with Ethylating Agents, *Mutation Research 373*, 167-178.

43. Pauly, G. T., and Moschel, R. C. (2001) Mutagenesis by O 6-Methyl, O6-Ethyl, and O6-Benzylguanine and O4-Methylthymine in Human Cells: Effects of O6-Alkylguanine DNA Alkyltransferase and Mismatch Repair, *Chemical Research in Toxicology 14*, 894-900.

44. Delaney, J. C., and Essigmann, J. M. (2004) Mutagenesis, Genotoxicity, and Repair of 1-Methyladenine, 3-Alkylcytosines, 1-Methylguanine, and 3-Methylthymine in AlkB *Escherichia coli*, *Proceedings of the National Academy of Sciences of the United States of America 101*, 14051-14056.

45. Baertschi, S. W., Raney, K. D., Stone, M. P., and Harris, T. M. (1988) Preparation of the 8, 9-Epoxide of the Mycotoxin Aflatoxin B1: The Ultimate Carcinogenic Species, *Journal of the American Chemical Society 110*, 7929-7931.

46. Ludlum, D. B. (1970) The Properties of 7-Methylguanine-Containing Templates for Ribonucleic Acid Polymerase, *Journal of Biological Chemistry 245*, 477-482.

47. Ellison, K. S., Dogliotti, E., Connors, T. D., Basu, A. K., and Essigmann, J. M. (1989) Site-Specific Mutagenesis by O6-Alkylguanines Located in the Chromosomes of Mammalian Cells: Influence of the Mammalian O6-Alkylguanine DNA Alkyltransferase, *Proceedings of the National Academy of Sciences 86*, 8620-8624.

48. Warren, J. J., Forsberg, L. J., and Beese, L. S. (2006) The Structural Basis for the Mutagenicity of O6-Methylguanine Lesions, *Proceedings of the National Academy of Sciences 103*, 19701-19706.

49. Elder, R. H., Jansen, J. G., Weeks, R. J., Willington, M. A., Deans, B., Watson, A. J., Mynett, K. J., Bailey, J. A., Cooper, D. P., Rafferty, J. A., Heeran, M. C., Wijnhoven, S. W. P., van Zeeland, A. A., and Margison, G. P. (1998) Alkylpurine–DNA–N-Glycosylase Knockout Mice Show Increased Susceptibility to Induction of Mutations by Methyl Methanesulfonate, *Molecular and Cellular Biology 18*, 5828-5837.

50. Shrivastav, N., Li, D., and Essigmann, J. M. (2010) Chemical Biology of Mutagenesis and DNA Repair: Cellular Responses to DNA Alkylation, *Carcinogenesis 31*, 59-70.

51. Calléja, F., Jansen, J. G., Vrieling, H., Laval, F., and van Zeeland, A. A. (1999) Modulation of the Toxic and Mutagenic Effects Induced by Methyl Methanesulfonate in Chinese hamster Ovary Cells by Overexpression of the Rat N-Alkylpurine-DNA Glycosylase, *Mutation Research/Fundamental and Molecular Mechanisms of Mutagenesis 425*, 185-194.

52. Ezaz-Nikpay, K., and Verdine, G. L. (1992) Aberrantly Methylated DNA: Site-Specific Introduction of N-7-Methyl-2'-deoxyguanosine into the Dickerson/Drew dodecamer, *Journal of the American Chemical Society 114*, 6562-6563.

53. Ezaz-Nikpay, K., and Verdine, G. L. (1994) The Effects of N7-Methylguanine on Duplex DNA Structure, *Chemistry & Biology 1*, 235-240.

54. Huang, H., and Greenberg, M. M. (2008) Synthesis and Analysis of Oligonucleotides Containing Abasic Site Analogues, *The Journal of Organic Chemistry 73*, 2695-2703.

55. Lee, S., Bowman, B. R., Ueno, Y., Wang, S., and Verdine, G. L. (2008) Synthesis and Structure of Duplex DNA Containing the Genotoxic Nucleobase Lesion N7-Methylguanine, *Journal of the American Chemical Society 130*, 11570-11571.

56. Wright, G. E., and Brown, N. C. (1990) Deoxyribonucleotide Analogs As Inhibitors and Substrates of DNA Polymerases, *Pharmacology & Therapeutics 47*, 447-497.

57. Angelov, T., Guainazzi, A., and Schärer, O. D. (2009) Generation of DNA Interstrand Cross-Links by Post-Synthetic Reductive Amination, *Organic Letters 11*, 661-664.

58. Plosky, B. S., Frank, E. G., Berry, D. A., Vennall, G. P., McDonald, J. P., and Woodgate, R. (2008) Eukaryotic Y-family Polymerases Bypass a 3-Methyl-2′-deoxyadenosine Analog in Vitro and Methyl Methanesulfonate Induced DNA Damage in Vivo, *Nucleic Acids Research 36*, 2152-2162.

59. Plosky, B. S., Frank, E. G., Berry, D. A., Vennall, G. P., McDonald, J. P., and Woodgate, R. (2008) Eukaryotic Y-family polymerases bypass a 3-methyl-2′-deoxyadenosine analog in vitro and methyl methanesulfonate-induced DNA damage in vivo, *Nucleic Acids Research 36*, 2152-2162.

60. Gibson, E. S., Lesiak, K., Watanabe, K. A., Gudas, L. J., and Pankiewicz, K. W. (1999) Synthesis of a Novel C-Nucleoside, 2-Amino-7-(2-deoxy-β-D-erythro-pentofuranosyl)-3H, 5H-pyrrolo-[3, 2-d] pyrimidin-4-one (2′-Deoxy-9-deazaguanosine), *Nucleosides, Nucleotides & Nucleic Acids 18*, 363-376.

61. Hoffer, M. (1960) α-Thymidin, *Chemische Berichte 93*, 2777-2781.

62. Hamm, M. L., Parker, A. J., Steele, T. W., Carman, J. L., and Parish, C. A. (2010) Oligonucleotide Incorporation and Base Pair Stability of 9-deaza-2′-deoxyguanosine, an Analogue of 8-oxo-2′-deoxyguanosine, *The Journal of Organic Chemistry 75*, 5661-5669.

63. Liu, M. C., Luo, M. Z., Mozdziesz, D. E., Dutschman, G. E., Gullen, E. A., Cheng, Y. C., and Sartorelli, A. C. (2005) Synthesis and Biological Evaluation of 2',3'-didehydro-2',3'-dideoxy-9-deazaguanosine, a Monophosphate Prodrug and two Analogues, 2',3'-dideoxy-9-deazaguanosine and 2',3'-didehydro-2',3'-dideoxy-9-deazainosine, *Nucleosides Nucleotides Nucleic Acids 24*, 135-145.

64. Luzzio, F. A., and Menes, M. E. (1994) A Facile Route to Pyrimidine-Based Nucleoside Olefins: Application to the Synthesis of d4T (Stavudine), *The Journal of Organic Chemistry 59*, 7267-7272.

65. Johnson, D. C., and Widlanski, T. S. (2004) Facile Deprotection of O-Cbz-Protected Nucleosides by Hydrogenolysis: An Alternative to O-Benzyl Ether-Protected Nucleosides, *Organic Letters 6*, 4643-4646.

66. Pankiewicz, K. W., Krzeminski, J., Ciszewski, L. A., Ren, W. Y., and Watanabe, K. A. (1992) A synthesis of 9-(2-deoxy-2-fluoro-.beta.-D-arabinofuranosyl)adenine and -hypoxanthine. An effect of C3'-endo to C2'-endo Conformational Shift on the Reaction Course of 2'-hydroxyl Group with DAST, *The Journal of Organic Chemistry 57*, 553-559.

67. Felix, A. M., Heimer, E. P., Lambros, T. J., Tzougraki, C., and Meienhofer, J. (1978) Rapid Removal of Protecting Groups from Peptides by Catalytic Transfer Hydrogenation with 1, 4-Cyclohexadiene, *The Journal of Organic Chemistry 43*, 4194-4196.

68. Beaucage, S. L., and Caruthers, M. H. (1981) Deoxynucleoside Phosphoramidites—A New Class of key Intermediates for Deoxypolynucleotide Synthesis, *Tetrahedron Letters 22*, 1859-1862.

69. Seela, F., and Chen, Y. (1997) Methylated DNA : The Influence of 7-deaza-7-Methylguanine on the Structure and Stability of Oligonucleotides, *Helvetica Chimica Acta 80*, 1073-1086.

70. Liu, M.-C., Luo, M.-Z., Mozdziesz, D. E., and Sartorelli, A. C. (2005) Synthesis and Biological Evaluation of 2-and 7-Substituted 9-deazaadenosine Analogues, *Nucleosides, Nucleotides and Nucleic Acids 24*, 45-62.

71. Johnson, A., and O'Donnell, M. (2005) Cellular DNA Replicases: Components and Dynamics at the Replication Fork, *Annual Review of Biochemistry 74*, 283-315.

72. Steitz, T. A. (1999) DNA Polymerases: Structural Diversity and Common Mechanisms, *The Journal of Biological Chemistry 274*, 17395-17398.

73. Lehman, I. R., Bessman, M. J., Simms, E. S., and Kornberg, A. (1958) Enzymatic Synthesis of Deoxyribonucleic Acid. I. Preparation of Substrates and Partial Purification of an Enzyme from *Escherichia coli*, *The Journal of Biological Chemistry 233*, 163-170.

74. Berdis, A. J. (2009) Mechanisms of DNA Polymerases, *Chemical Reviews 109*, 2862-2879.

75. Mendelman, L. V., Petruska, J., and Goodman, M. F. (1990) Base Mispair Extension Kinetics. Comparison of DNA Polymerase Alpha And Reverse Transcriptase, *Journal of Biological Chemistry 265*, 2338-2346.

76. Ganguly, M., Wang, F., Kaushik, M., Stone, M. P., Marky, L. A., and Gold, B. (2007) AStudy of 7-deaza-2′-deoxyguanosine–2′-deoxycytidine Base Pairing in DNA, *Nucleic Acids Research 35*, 6181-6195.

77. Ganguly, M., Wang, R. W., Marky, L. A., and Gold, B. (2009) Introduction of Cationic Charge into DNA near the Major Groove Edge of a Guanine x Cytosine Base Pair: Characterization of Oligodeoxynucleotides Substituted with 7-Aminomethyl-7-deaza-2'-deoxyguanosine, *Journal of the American Chemical Society 131*, 12068-12069.

78. Davis, D. R. (1995) Stabilization of RNA Stacking by Pseudouridine, *Nucleic Acids Research 23*, 5020-5026.

79. Goodman, M. F., Creighton, S., Bloom, L. B., and Petruska, J. (1993) Biochemical Basis of DNA Replication Fidelity, *Critical Reviews in Biochemistry and Molecular Biology 28*, 83-126.

80. Weledji, Y. N., Wiederholt, C. J., Delaney, M. O., and Greenberg, M. M. (2008) DNA Polymerase Bypass in Vitro and in E. coli of a C-Nucleotide Analogue of Fapy·dG, *Bioorganic & Medicinal Chemistry 16*, 4029-4034.

81. Hamm, M. L., Gill, T. J., Nicolson, S. C., and Summers, M. R. (2007) Substrate Specificity of Fpg (MutM) and hOGG1, Two Repair Glycosylases, *Journal of the American Chemical Society 129*, 7724-7725.

82. Asaeda, A., Ide, H., Asagoshi, K., Matsuyama, S., Tano, K., Murakami, A., Takamori, Y., and Kubo, K. (2000) Substrate Specificity of Human Methylpurine DNA N-Glycosylase, *Biochemistry 39*, 1959-1965.

83. Fromme, J. C., Banerjee, A., Huang, S. J., and Verdine, G. L. (2004) Structural Basis for Removal of Adenine Mispaired with 8-Oxoguanine by MutY Adenine DNA Glycosylase, *Nature 427*, 652-656.

84. O'Brien, P. J., and Ellenberger, T. (2004) Dissecting the Broad Substrate Specificity of Human 3-Methyladenine-DNA Glycosylase, *Journal of Biological Chemistry 279*, 9750-9757.

85. Warren, J. J., Forsberg, L. J., and Beese, L. S. (2006) The Structural Basis for the Mutagenicity of O6-Methyl-Guanine Lesions, *Proceedings of the National Academy of Sciences 103*, 19701-19706.

86. Fromme, J. C., Banerjee, A., and Verdine, G. L. (2004) DNA Glycosylase Recognition and Catalysis, *Current Opinion in Structural Biology 14*, 43-49.

87. Stivers, J. T., and Jiang, Y. L. (2003) A Mechanistic Perspective on the Chemistry of DNA Repair Glycosylases, *Chemical Reviews 103*, 2729-2760.

88. Fromme, J. C., and Verdine, G. L. (2003) DNA Lesion Recognition by the Bacterial Repair Enzyme MutM, *The Journal of Biological Chemistry 278*, 51543-51548.

89. O'Brien, P. J., and Ellenberger, T. (2004) Dissecting the Broad Substrate Specificity of Human 3-Methyladenine-DNA Glycosylase, *The Journal of Biological Chemistry 279*, 9750-9757.

90. Vilkaitis, G., Merkiene˙, E., Serva, S., Weinhold, E., and Klimašauskas, S. (2001) The Mechanism of DNA Cytosine-5 Methylation: Kinetic and Mutational Dissection of HhaI Methyltransferase, *Journal of Biological Chemistry 276*, 20924-20934.

91. Jurkowska, R. Z., Jurkowski, T. P., and Jeltsch, A. (2011) Structure and Function of Mammalian DNA Methyltransferases, *Chembiochem 12*, 206-222.

92. Gros, C., Fahy, J., Halby, L., Dufau, I., Erdmann, A., Gregoire, J.-M., Ausseil, F., Vispé, S., and Arimondo, P. B. (2012) DNA Methylation Inhibitors in Cancer: Recent and Future Approaches, *Biochimie 94*, 2280-2296.

93. Okano, M., Bell, D. W., Haber, D. A., and Li, E. (1999) DNA Methyltransferases Dnmt3a and Dnmt3b are Essential for de novo Methylation and Mammalian Development, *Cell 99*, 247-257.

94. Szyf, M. (1994) DNA Methylation Properties: Consequences for Pharmacology, *Trends in Pharmacological Sciences 15*, 233-238.

95. Medina-Franco, J. L., and Caulfield, T. (2011) Advances in the Computational Development of DNA Methyltransferase Inhibitors, *Drug Discovery Today 16*, 418-425.

96. Fandy, T. E. (2009) Development of DNA Methyltransferase Inhibitors for the Treatment of Neoplastic Diseases, *Current Medicinal Chemistry 16*, 2075-2085.

97. Cheng, J. C., Yoo, C. B., Weisenberger, D. J., Chuang, J., Wozniak, C., Liang, G., Marquez, V. E., Greer, S., Orntoft, T. F., Thykjaer, T., and Jones, P. A. (2004) Preferential Response of Cancer Cells to Zebularine, *Cancer Cell 6*, 151-158.

98. Villar-Garea, A., Fraga, M. F., Espada, J., and Esteller, M. (2003) Procaine is a DNA Demethylating Agent with Growth Inhibitory Effects in Human Cancer Cells, *Cancer Research 63*, 4984-4989.

99. Suzuki, T., Tanaka, R., Hamada, S., Nakagawa, H., and Miyata, N. (2010) Design, Synthesis, Inhibitory Activity, and Binding Mode Study of Novel DNA Methyltransferase 1 Inhibitors, *Bioorganic & Medicinal Chemistry Letters 20*, 1124-1127.

100. Brueckner, B., Garcia Boy, R., Siedlecki, P., Musch, T., Kliem, H. C., Zielenkiewicz, P., Suhai, S., Wiessler, M., and Lyko, F. (2005) Epigenetic Reactivation of Tumor Suppressor Genes by A Novel Small-Molecule Inhibitor of Human DNA Methyltransferases, *Cancer Research 65*, 6305-6311.

101. Holloway, A. F., and Oakford, P. C. (2007) Targeting Epigenetic Modifiers in Cancer, *Current Medicinal Chemistry 14*, 2540-2547.

102. Amato, R. J. Inhibition of DNA Methylation by Antisense Oligonucleotide MG98 as Cancer Therapy, *Clinical Genitourinary Cancer 5*, 422-426.

103. Plummer, R., Vidal, L., Griffin, M., Lesley, M., de Bono, J., Coulthard, S., Sludden, J., Siu, L. L., Chen, E. X., Oza, A. M., Reid, G. K., McLeod, A. R., Besterman, J. M., Lee, C., Judson, I., Calvert, H., and Boddy, A. V. (2009) Phase I study of MG98, An Oligonucleotide Antisense Inhibitor of Human DNA Methyltransferase 1, Given as a 7-Day Infusion In Patients With Advanced Solid Tumors, *Clinical Cancer Research 15*, 3177-3183.

104. Datta, J., Ghoshal, K., Denny, W. A., Gamage, S. A., Brooke, D. G., Phiasivongsa, P., Redkar, S., and Jacob, S. T. (2009) A New Class of Quinoline-Based DNA Hypomethylating Agents Reactivates Tumor Suppressor Genes by Blocking DNA Methyltransferase 1 Activity and Inducing its Degradation, *Cancer Research 69*, 4277-4285.

105. Valente, S., Liu, Y., Schnekenburger, M., Zwergel, C., Cosconati, S., Gros, C., Tardugno, M., Labella, D., Florean, C., Minden, S., Hashimoto, H., Chang, Y., Zhang, X., Kirsch, G., Novellino, E., Arimondo, P. B., Miele, E., Ferretti, E., Gulino, A., Diederich, M., Cheng, X., and Mai, A. (2014) Selective Non-nucleoside Inhibitors of Human DNA Methyltransferases Active in Cancer Including in Cancer Stem Cells, *Journal of Medicinal Chemistry 57*, 701-713.

106. Meeran, S. M., Ahmed, A., and Tollefsbol, T. O. (2010) Epigenetic Targets of Bioactive Dietary Components for Cancer Prevention and Therapy, *Clinical Epigenetics 1*, 101-116.

107. Li, Y., and Tollefsbol, T. O. (2010) Impact on DNA Methylation in Cancer Prevention and Therapy by Bioactive Dietary Components, *Current Medicinal Chemistry 17*, 2141.

108. Isakovic, L., Saavedra, O. M., Llewellyn, D. B., Claridge, S., Zhan, L., Bernstein, N., Vaisburg, A., Elowe, N., Petschner, A. J., and Rahil, J. (2009) Constrained S-adenosyl-l-homocysteine (SAH) Analogues as DNA Methyltransferase Inhibitors, *Bioorganic & Medicinal Chemistry Letters 19*, 2742-2746.

109. Kumar, R., Srivastava, R., Singh, R. K., Surolia, A., and Rao, D. N. (2008) Activation and Inhibition of DNA Methyltransferases by S-Adenosyl-L-Homocysteine Analogues, *Bioorganic & Medicinal Chemistry 16*, 2276-2285.

110. Reich, N. O., and Everett, E. A. (1990) Identification of Peptides Involved in S-Adenosylmethionine Binding in the EcoRI DNA Methylase. Photoaffinity Laveling with 8-Azido-S-Adenosylmethionine, *The Journal of Biological Chemistry 265*, 8929-8934.

111. Wu, S. (2012) Design and Synthesis Studies of New S-Adenosyl-L-Methionine Analogues, Master Thesis, New Jersey Institute of Technology.

112. Song, J., Teplova, M., Ishibe-Murakami, S., and Patel, D. J. (2012) Structure-Based Mechanistic Insights into DNMT1-Mediated Maintenance DNA Methylation, *Science 335*, 709-712.

113. Debnath, J., Dasgupta, S., and Pathak, T. (2010) Comparative Inhibitory Activity of 3′-And 5′-Functionalized Nucleosides on Ribonuclease A, *Bioorganic & Medicinal Chemistry 18*, 8257-8263.

114. Enomoto, K., Nagasaki, T., Yamauchi, A., Onoda, J., Sakai, K., Yoshida, T., Maekawa, K., Kinoshita, Y., Nishino, I., and Kikuoka, S. (2006) Development of High-Throughput Spermidine Synthase Activity Assay Using Homogeneous Time-Resolved Fluorescence, *Analytical Biochemistry 351*, 229-240.

115. Ireland, R. E., and Liu, L. (1993) An Improved Procedure for the Preparation of the Dess-Martin Periodinane, *The Journal of Organic Chemistry 58*, 2899-2899.

116. Revelant, G., Dunand, S., Hesse, S., and Kirsch, G. (2011) Microwave-Assisted Synthesis of 5-Substituted 2-Aminothiophenes Starting from Arylacetaldehydes, *Synthesis 2011*, 2935-2940.

117. Feely, W., Lehn, W., and Boekelheide, V. (1957) Communications-Alkaline Decomposition of Quaternary Salts of Amine Oxides, *The Journal of Organic Chemistry 22*, 1135-1135.

118. Ley, S. V., Norman, J., Griffith, W. P., and Marsden, S. P. (1994) Tetrapropylammonium Perruthenate, $Pr4N^{+}RuO4^{-}$, TPAP: A Catalytic Oxidant for Organic Synthesis, *Synthesis 1994*, 639-666.

119. Kokatla, H. P., Thomson, P. F., Bae, S., Doddi, V. R., and Lakshman, M. K. (2011) Reduction of Amine N-Oxides by Diboron Reagents, *The Journal of Organic Chemistry 76*, 7842-7848.

120. Rawalay, S. S., and Shechter, H. (1967) Oxidation of Primary, Secondary, and Tertiary Amines with Neutral Permanganate. Simple Method for Degrading Amines to Aldehydes and Ketones, *The Journal of Organic Chemistry 32*, 3129-3131.

121. Srivastava, S. K., Chauhan, P. M. S., and Bhaduri, A. P. (1999) A Novel Strategy for N-Alkylation of Primary Amines, *Synthetic Communications 29*, 2085-2091.

122. Chesworth, R., Kuntz, K. W., Olhava, E. J., and Patane, M. A. (2013) Modulators of Histone Methyltransferase, and Methods of Use Thereof, Google Patents,US2013/0310333 A1.

123. Mai, V., and Comstock, L. R. (2011) Synthesis of an Azide-Bearing N-Mustard Analogue of S-Adenosyl-l-methionine, *The Journal of Organic Chemistry 76*, 10319-10324.

124. Wang, F., Yang, Z.-J., Jin, H.-W., Zhang, L.-R., and Zhang, L.-H. (2007) A Concise Synthesis of 4,6-dideoxy-4-base-6-amino-2,5-anhydro-l-mannitols, *Tetrahedron: Asymmetry 18*, 2139-2146.